RÉPUBLIQUE ALGÉRIENNE DÉMOCRATIQUE ET POPULAIRE
MINISTÈRE DE L'ENSEIGNEMENT SUPÈRIEUR ET DE LA RECHERCHE SCIENTIFIQUE

UNIVERSITE MENTOURI - CONSTANTINE
FACULTE DES SCIENCES EXACTES
DEPARTEMENT DE PHYSIQUE

N° d'ordre: .....
Sèrie: .....

Thèse
Présentée pour obtenir le diplôme de Doctorat
Troisième Cycle LMD en physique
Spécialité:
Physique Fondamentale et Applications

Théme:

La physique au-delà du modèle Standard

par: Meriem DJOUALA

Soutenu le : 13/07/2021

♦ Devant le jury:

Président:	*Mr.*	**BENSLAMA Achour**	***Prof.***	*Univ. Frères Mentouri-Constantine 1*
Rapporteur:	*Mr.*	***MEBARKI Noureddine***	***Prof.***	*Univ. Frères Mentouri-Constantine 1*
Examinateurs:	*Mr.*	**AISSAOUI Habib**	***Prof.***	*Univ. Frères Mentouri-Constantine 1*
	Mr.	**DELENDA Yazid**	***Prof.***	*Univ. Hadj Lakhdar-Batna 1*
	Mr.	**AOUACHRIA Mekki**	***Prof.***	*Univ. Hadj Lakhdar-Batna 1*
	Mr.	**ZAIM Slimane**	***Prof.***	*Univ. Hadj Lakhdar-Batna 1*

PEOPLE'S DEMOCRATIC REPUBLIC OF ALGERIA MINISTRY OF HIGHER EDUCATION AND SCIENTIFIC RESEARCH

MENTOURI UNIVERSITY-CONSTANTINE
FACULTY OF EXACT SCIENCES
PHYSICS DEPARTMENT

N° order: .....
Serie: .....

Thesis

Presented to obtain the Doctorate degree
Third Cycle LMD in Physics
Speciality:
Fondamentale Physics and Applications

Theme:

Physics beyond the Standard Model

by: Meriem DJOUALA

Thesis defense on 13/07/2021

♦ Thesis jury:

President:	*Mr.*	**BENSLAMA Achour**	***Prof.***	*Univ. Frères Mentouri-Constantine 1*
Supervisor:	*Mr.*	***MEBARKI Noureddine***	***Prof.***	*Univ. Frères Mentouri-Constantine 1*
Examiners:	*Mr.*	**AISSAOUI Habib**	***Prof.***	*Univ. Frères Mentouri-Constantine 1*
	Mr.	**DELENDA Yazid**	***Prof.***	*Univ. Hadj Lakhdar-Batna 1*
	Mr.	**AOUACHRIA Mekki**	***Prof.***	*Univ. Hadj Lakhdar-Batna 1*
	Mr.	**ZAIM Slimane**	***Prof.***	*Univ. Hadj Lakhdar-Batna 1*

Acknowledgments

I would like to thank my supervisor Prof.Mebarki Noureddine for all the effort he made to ensure the success of the work presented in this thesis.

I would like to thank Prof. Aissaoui Habib, Prof. Benslama Achour, Prof.Delenda Yazid, Prof. Aouachria Mekki and Prof Zaim Slimane who accepted to judged the value of this work.

I would like to thank Renato M.Fonseca for all his fruitful discussion.

My gratitude goes also to Garv Chauhan and Uladzimir Khasianevich for the interesting discussions and their support that they give me to complete this thesis.

Thanks to all my friends and colleagues.

Dedication

I would like to thank my parents, my brothers, my sister and my husband, to whom I dedicate this thesis.

Contents

List of Figures

List of Tables

Introduction

The Standard Model of particle physics is a free chiral anomaly model based on the gauge group $SU(3)_C \otimes SU(2)_L \otimes U(1)_Y$ [1–3], it represents the unification of all forces of the universe (except the gravitation force). Furthermore, it describes all the known elementary particles which are:

- Three fermion generations (Quarks and leptons),
- Four gauge bosons of the electroweak theory $W^{\mp}$, γ and Z.
- Eight gauge bosons of the strong interactions that called the gluons.

as we show in figure 0.1.

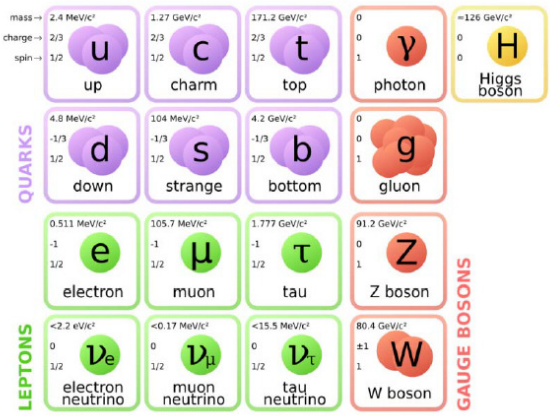

Figure 0.1: The elementary particles in the Standard Model (SM)

Besides the fermions and gauge bosons, Brout, Englert and Higgs in 1964 were proposed a new neutral scalar boson called the Standard Model Higgs boson and its field (Higgs filed) (Figure 0.1) with a special theoretical formalism to can explain how all particles gain their masses through the Higgs mechanism which based on the interactions of the particles with the Higgs field [4–6]. The Higgs search took a big interest from both theoretical and

experimental physicist to precise the fundamental properties of it and to determine the experimental scale in which the Standard Model Higgs boson will appear. Its experimental discover faced many straggles and hard tries, it started over many years ago at the Large Electron Positron (LEP) Collider [7–9]. The main production mechanism in e^+e^- collisions is through an intermediate (above mass-shell) Z-boson production, which then decays into a Higgs and a lower energy Z-boson. No signal was observed at LEP. Next try was in the Tevatron [10], proton-antiproton Collider. The dominant production mechanisms were via gluon fusion or vector boson fusion from a W-boson. The shut down of this collider was in 2011 after ten years of collecting data. No signal of a Higgs was observed but an excess of events in the bottom- quark decay-channel led to a mass range between 115 GeV and 135 GeV [11]. The next try to detect a Higgs boson was at the Large Hadron Collider (LHC) [12–15], proton proton Collider. The main Higgs production mechanism at the LHC was through gluon fusion because of the high energies at LHC. The most expected decay of the Higgs boson was the decay into two energetic photons. This decay only happens 2 out of every 1000 times, but is relatively easy to detect due to the zero contributions of the background.

On July 4, 2012, the mystery has been solved, a Higgs-like particle was observed [16, 17] Combined searches from ALTAS and CMS led to an observed mass of $m_H = 125,09$ GeV.

After the discovery of a new scalar resonance with a mass around 125 GeV (the Higgs boson) in the Large Hadron Collider (LHC) [18–24] and the compatibility of the theoretical predictions with the experimental results such as all decay and production modes are in good agreement with the Standard Model as we show in figure 0.2 and the masses are compatible in all decay modes as it has been shown in figure 0.3. the Standard Model has been remarkably successful.

In spite of all the successes, the SM is unable to address the answers of many outstanding questions like gravity (why it is weak?), the SM can not explain why there are 3 generations of quarks and leptons, How are neutrino masses generated?, also there are questions about why is not there the same amount of antimatter as matter in the Universe ?, dark and energy matter mastery, quantization charges...etc. Thus, theoretical physicist are widely believed that the SM is incomplete theory.

To answer those fundamental questions and to understand the nature of the unknown particles. Many models Beyond the Standard Model have been proposed many years ago such as Two-Higgs Doublet Models (THDM) [26, 27], left-right symmetric models [28], supersymmetric models [29], left-right supersymmetric models [30], 331 models [31–35], 341 models [35–39], little Higgs models [40, 41], extra dimension models [42] and many others, those theories BSM have paved the way for new directions in high energy particle physics.

Among many beyond Standard Model theories, we focus on models based on the gauge

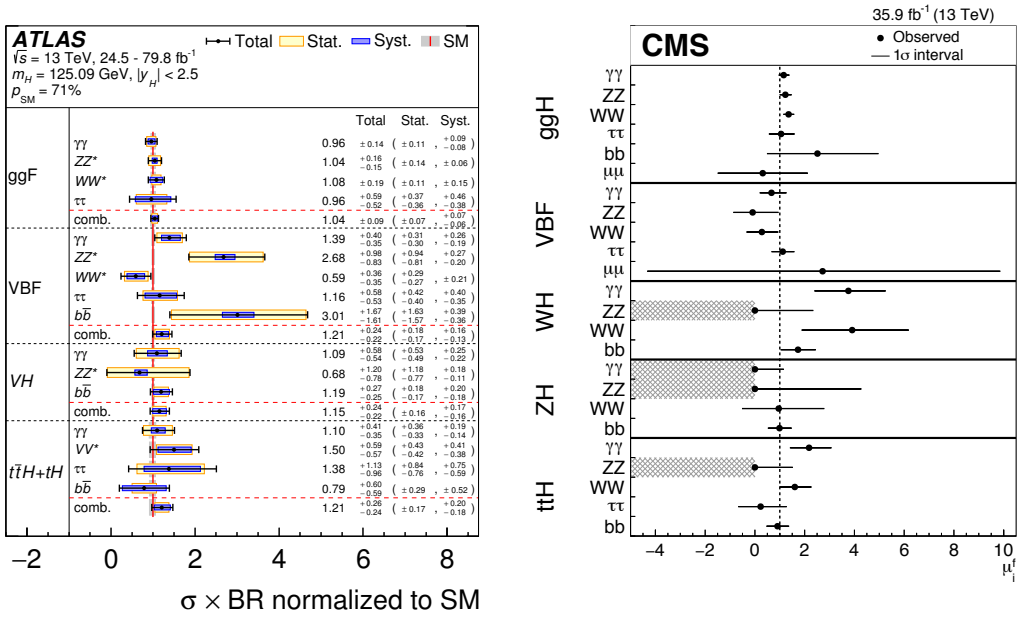

Figure 0.2: Combined measurements of the products $\sigma.BR$, normalised to the SM predictions, for the five main production and five main decay modes [25].

group $SU(3)_C \otimes SU(4)_L \otimes U(1)_X$ (341 models for short). Those models have new features such as the existence of new exotic fermions (leptons and quarks) which are produced because of the arrangements of the fermions in the group SU(4). Moreover, besides $W^{\mp}$, Z and γ, those kind of models predict the existence of new charged and neutral gauge bosons. Furthermore, the 341 models have extra bosons in the scalar sector, some of them have simply electric charge, others are double charged $h^{\mp\mp}$ and there are the neutral ones.

In the literature, there are many classifications of those models depending on the existence or not of fermions with exotic charges, structure of the scalar potential and spontaneous symmetry breaking of the gauge group. These models are usually parameterized by two parameters β and γ [37–39, 43–46].

The 341 models have many versions, we distinguish them based on the parameters β and γ which the electric charge expression has been written as a function of them, the exotic electric charges and based on the number of the scalar fields [37, 38, 44].

The most fundamental feature of all the 341 model versions except the flipped model is the arrangement of the fermion families, two of the quark generations have arranged in conjugate fundamental representation $\bar{4}$, while, the third one with the three lepton generations lie in the fundamental representation of the group SU(4) (or vice versa). This arrangement makes the models free from the $(SU(4))^3_L$ anomaly and makes them the most attractive models to explain theoretically why they do exist three quark families.

This thesis is organized as five chapters, we start with a general introduction, the first

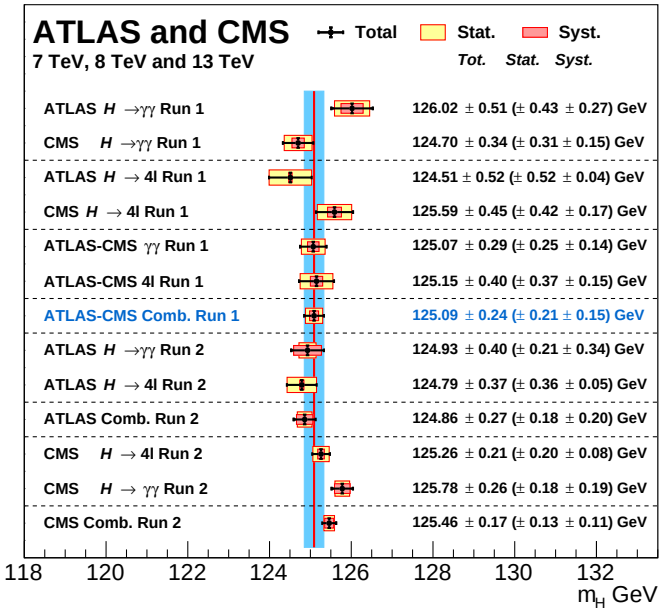

Figure 0.3: Summary of the Higgs boson mass measurements from the individual analyses (Run 1 measurement) performed by ATLAS and CMS [25].

chapter ,1 is about the Standard Model, we summarized the most fundamental features, the particle content of the SM and we discussed how particles gain their mass through the Higgs mechanism. In the chapter 2, the fundamental features of the 341 models are reviewed, we discuss the constituents: fermion, gauge boson and scalar sectors and how the chiral anomalies have been canceled. Furthermore, we reviewed four different 341 model versions. In the second part of the chapter 2, we use the compact 341 version as an example to explain how to get the electric charges of the particles (fermions, scalar and gauge bosons) and how they gain their masses through the Higgs mechanism, in the end, we showed the full Lagrangian of the compact 341 model. In chapter 3, theoretical constraints on the scalar potential of the compact 341 model with three quadruplets scalar fields are discussed. It is shown that, in order to ensure the good behaviour of the scalar potential and the validity of the model, the criteria such as copositivity, minimization, perturbative unitarity, perturbativity of the scalar couplings and no ghost scalar bosons (scalar bosons masses positivity) are imposed and bounds on the scalar couplings are obtained. Moreover, the existence of the Landau pole in the model imposes stringent limits.

The Higgs physics has an important role on the LHC and it is an open window to discover new physics, that motivate us to discuss the Higgs physics in the compact 341 model.

In chapter 4, the neutral scalar bosons(the SM-like Higgs boson h_1 besides the other heavy scalar bosons h_2 and h_3 that are predicted by the compact 341 model) decays using only three scalar fields with additional extra Lagrangian called the effective Lagrangian

are studied. The starting point was with the calculation of the partial width decays for many individual channels $b\bar{b}$,$\ell\ell$,$\gamma\gamma$,γZ,W^*W and Z^*Z taking into account the contributions of news fermions, new gauge bosons and news scalars bosons, notice that all the scalar parameters $\lambda_{1..9}$ in our model are constrained by the theoretical conditions. Using those partial widths expressions, we studied both the signal strength and the branching ratios. The signal strength for h_1 has confronted with the results reported at ATLAS, CMS and ATLAS+CMS combination to determine the deviation of the compact 341 model from the Standard Model. Whereas, the computation of the branching ratio for the other heavy neutral scalars bosons h_2 and h_3 are discussed to determine their theoretical properties.

The chapter 5, we have introduced for the first time a new anomaly free model without exotic electric charge which is different from the ordinary 341 versions in the arrangement of the particle content. It turns out that the previous quarks and leptons replication is not the only way to have models free from the $SU(4)_L \otimes U(1)_X$ gauge anomalies. In this work, we build a new unique gauge anomaly free model without exotic electric charges baptized the flipped 341 model as an extension of where the previous scheme of construction is reversed that is all the quarks generations transform under the same representation while leptons are not. Thus, a flavor changing neutral current (FCNC) is expected at the tree level in the lepton sector through the exchange of new neutral gauge bosons Z' and Z'' of the model like in the rare leptonic decays of the form $\ell_i \longrightarrow \ell_i\ell_k\bar{\ell}_k$ and $\ell_i \longrightarrow \ell_k\gamma$ $(i \neq k)$. The FCNC and mixing in the leptonic sector are explored via the study of the rare processes $\mu \longrightarrow ee\bar{e}$ and $\mu \longrightarrow e\gamma$ and stringent inequalities and bounds on the Z' and Z'' masses are obtained. The cancellation of the triangle gauge anomalies leads to the introduction of new extra exotic leptons ψ_e that is lie in the fundamental representation 10 with X=0 and a quadruplet $\widetilde{\psi}$ which belongs to the conjugate representation $\bar{4}$ with $X = \frac{-1}{2}$. Furthermore, Fermions mixing as well as masses have discussed at both the tree and one loop levels in both charged and neutral fermions using four scalar fields and two scalar matrices S and S'.

We draw all our fundamental results in conclusion. Finally, the appendices summarize the principle expressions and additional information that we have used during the calculations.

Chapter 1

The Standard Model of particle physics and Beyond

1.1 Introduction

The Standard Model (SM) of the elementary particle physics developed in the 1970s [47–50], it is a quantum field theory based on the gauge group $SU(3)_C \otimes SU(2)_L \otimes U(1)_Y$ where C, L and Y refer to the color charge, left-handed and a new quantum number called the hypercharge respectively. This model describes all the known particles and all forces of the universe except the gravitation force. The Standard Model is built as a combination of the quantum chromodynamics (QCD) [51–64] and the electroweak theory (EW), this model got a great success when the missing piece has discovered at the LHC in 2012, the Higgs boson which is produced after the spontaneous symmetry breaking (SSB) during the Higgs mechanism to give masses to all the known particles of the universe.

In this chapter, we discuss and review the basic details of the Standard Model (both the QCD and the EW theories), the fundamental constituents and its total Lagrangian, we review how particles gain their masses through the Higgs mechanism in both abelian U(1) and non-abelian $SU(2) \otimes U(1)$ theories. in the last part of this chapter, we review the problem of the SM and we discuss why going beyond it became mandatory.

1.2 The quantum chromodynamics theory

The quantum chromodynamics theory (QCD) is a non-abelian gauge field theory which based on the gauge group SU(3). It is described the strong interactions between the familiar six quarks (Up, Down, Charm, Strange, Beauty, Top), which have mediated by eight gluons ($N^2 - 1$ the number of generations of the SU(3) group). The strong interactions have

described by the following Lagrangian:

$$\mathcal{L} = \sum \bar{q}(i\gamma^{\mu}\partial_{\mu} + g_s\gamma^{\mu}A_{\mu} - m_f)q\delta_{ij} - \frac{1}{4}G_{\mu\nu}G^{\mu\nu} \tag{1.2.1}$$

where γ^{μ} is the Dirac matrices, m_f is the quarks masses, q represents the quarks fields, $A_{\mu} = A^a_{\mu}t^a_{ij}$ are the gauge bosons (the gluons in the case of the strong interactions), the sum runs over flavors, i and j are color indices that run over colors and $G_{\mu\nu}$ is the field strength tensor which determines the kinetic term of the gluons, its expression has the following form:

$$G_{\mu\nu} = \partial_{\mu}G^a_{\nu} - \partial_{\nu}G^a_{\mu} - g_s\epsilon_{abc}G^b_{\mu}G^c_{\nu}, \tag{1.2.2}$$

with g_s is the coupling constant of the strong interaction, its expression has taken the following form:

$$g_s = 4\pi\alpha_s, \tag{1.2.3}$$

where α_s is the strong coupling. According to this coupling, two regions have been disguised as we show in Figure 1.1. The first region is the asymptotic freedom where at high energy scales the quarks and gluons become free without interactions, the coupling becomes small and perturbations calculations are valid, while, the second region is about the confinement where at low energy scales the Parton (quarks and gluons) are confined in hadrons with colorless where the fort coupling diverges and perturbations calculations are not valid anymore.

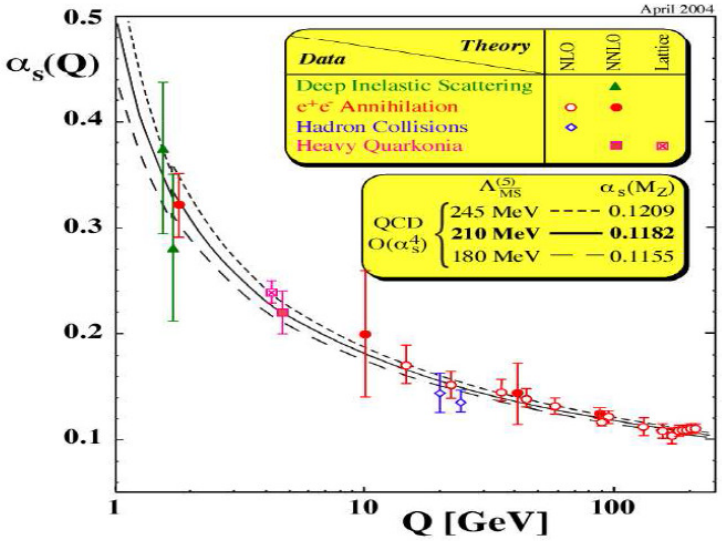

Figure 1.1: The evaluation of $\alpha_s(Q)$ as a function of the energy Q(GeV) [25].

1.3 The electroweak theory

The electroweak theory represents the second part of the Standard Model, it is also a non-abelian theory that based on the gauge group $SU(2)_L \otimes U(1)_Y$ proposed by Glashow, Salam and Weinberg, it unified the weak and electrometric interactions, this theory is mediated by 4 gauge bosons $W^{\mp}$, Z and γ (Photon) [25, 65]. It describes the interactions of all quarks and leptons with two conserved quantum numbers: isospin and hypercharge.

In the next subsections, we discuss all the particle content and their interactions.

1.3.1 Fermion sector

In the electroweak theory, the representation of the fermions is composed of two spinors: the felt helicity P_L and the right helicity P_R where the ψ is written as a combination between them:

$$\psi = P_R\psi + P_L\psi = \psi_R + \psi_L, \tag{1.3.1}$$

where

$$\psi_L = \frac{1}{2}(1 - \gamma_5)\psi, \tag{1.3.2}$$

$$\psi_R = \frac{1}{2}(1 + \gamma_5)\psi. \tag{1.3.3}$$

The left-handed fermions have the weak isospin I equals to $\frac{1}{2}$, that makes the third component of weak isospin I_3 equals to $\mp\frac{1}{2}$, as a result of this, the felt- handed fermions are arranged in doublets multiplies in the $SU(2)_L$, whereas, the right-handed fermions have I=0, that makes the third component of the weak isospin I_3 has the value 0 that force the right handed fermions to arrange as singlets multiplies in $SU(2)_L$. Moreover, a new quantum number has introduced which associated with the group $U(1)_Y$, it is called the hypercharge Y, it has a direct relationship with both the electric charge Q and the third component of weak isospin I_3 through the Gell-Mann-Nishijima formula [66]:

$$Q = I_3 + \frac{Y}{2}. \tag{1.3.4}$$

Thus, the fermion sector in the electroweak theory (under the $SU(2)_L \otimes U(1)_Y$ theory) are presented as follows:

- For the left-handed quarks:

We have three generations of quarks arranged in doublets multiplies:

$$\begin{pmatrix} u \\ d \end{pmatrix}, \begin{pmatrix} c \\ s \end{pmatrix}, \begin{pmatrix} t \\ b \end{pmatrix}, \tag{1.3.5}$$

with weak isospin $I = \frac{1}{2}$ and $Y = \frac{1}{3}$.

- For the left-handed leptons:

We get also three lepton generations arranged as doublets, each lepton has its partner neutrino:

$$\begin{pmatrix} \nu_e \\ e \end{pmatrix}, \begin{pmatrix} \nu_\mu \\ \mu \end{pmatrix}, \begin{pmatrix} \nu_\tau \\ \tau \end{pmatrix}, \tag{1.3.6}$$

with weak isospin $I = \frac{1}{2}$ and $Y = -1$. For the right-handed fermions, they are presented as singlets fermions: u_R, d_R, c_R, s_R, t_R, b_R, e_R, μ_R and τ_R, notice that for the right handed neutrinos, they do not exist in the Standard Model.

Concerning the anti-particles, each fermion has its own anti-particle which has the same masse and spin but with opposite electric charge. The following table (1.1) summaries all the fermion content of the Standard Model.

Multiplet	Particles generations	$SU(3)_C \otimes SU(2)_L \otimes U(1)_Y$
L_L	$\begin{pmatrix} \nu_e \\ e \end{pmatrix}, \begin{pmatrix} \nu_\mu \\ \mu \end{pmatrix}, \begin{pmatrix} \tau_\tau \\ \tau \end{pmatrix}$	(1,2,-1)
E_R	e_R, μ_R, τ_R	(1,1,-2)
Q_L	$\begin{pmatrix} u \\ d \end{pmatrix}, \begin{pmatrix} c \\ s \end{pmatrix}, \begin{pmatrix} t \\ b \end{pmatrix}$	(3,2,$\frac{1}{3}$)
U_R	u_R, c_R, t_R	(3,1,$\frac{4}{3}$)
D_R	d_R, s_R, b_R	(3,1,$\frac{-2}{3}$)

Table 1.1: Fermions content of the Standard Model.

1.3.2 Interaction sector

The interactions in the electroweak theory are mediated by gauge bosons of spin 1, based on the number of the generators $(N^2 - 1)$, we get three gauge bosons $W_\mu^{1,2,3}$ for $SU(2)_L$ and another field B_μ corresponds to the group $U(1)_Y$. The mixing between the last fields introduces the physical fields of the electroweak theory $W^\mp$, Z and γ. Those mixings have presented in the following transformations:

$$\begin{aligned} W^\mp &= \frac{W^1 \pm iW^2}{\sqrt{2}}, \\ B_\mu &= Z\cos\theta_W + \gamma\sin\theta_W, \\ W_\mu^3 &= Z\cos\theta_W - \gamma\sin\theta_W, \end{aligned} \tag{1.3.7}$$

where θ_W is a mixing angle called the Weinberg angle.

1.3.3 Scalar sector

The scalar sector (Higgs field) is a field that has a non-zero value ϕ_0 in the vacuum, this scalar has used to break the symmetry (the spontaneous symmetry breaking), it is presented as a doublet under $SU(2)_L$:

$$\begin{pmatrix} \Phi^+ \\ \Phi^0 \end{pmatrix} \tag{1.3.8}$$

The scalar potential is given by the following expression:

$$V(\Phi) = -\mu^2 \Phi^\dagger \Phi + \lambda (\Phi^\dagger \Phi)^2, \tag{1.3.9}$$

where λ and μ^2 are the Higgs self coupling and a mass dimension parameters respectively.

1.4 The Standard Model Lagrangian

The renormalizable Lagrangian of the Standard model which is invariant under the gauge group $SU(3)_C \otimes SU(2)_L \otimes U(1)_Y$ has taken the following form:

$$\mathcal{L}_{SM} = \mathcal{L}_{Fermions} + \mathcal{L}_{Gauge} + \mathcal{L}_{Higgs} + \mathcal{L}_{Yukawa} + \mathcal{L}_{SI} \tag{1.4.1}$$

The term $\mathcal{L}_{SI}$ represents the Lagrangian of the strong interactions that is presented in Eq.(1.2.1).

1.4.1 Fermions Lagrangian

The first term in the Lagrangian of the Standard model represents the fermions Lagrangian which has the form:

$$\mathcal{L}_{Fermions} = i\bar{\Psi}_R \gamma^\mu D_\mu \Psi_R + i\bar{\Psi}_L \gamma^\mu D_\mu \Psi_L, \tag{1.4.2}$$

where Ψ represents both leptons and quarks and the covariant derivative D_μ for left and right handed fields are given respectively by:

$$D_\mu \Psi_L = (\partial_\mu + \frac{i}{2} g' Y B_\mu + \frac{i}{2} t_a W_\mu^a) \Psi_L, \tag{1.4.3}$$

$$D_\mu \Psi_R = (\partial_\mu + \frac{i}{2} g' Y B_\mu) \Psi_R. \tag{1.4.4}$$

The $t_a (a = 1..3)$ represents the generators of the $SU(2)$ giving by the three Pauli matrix, g and g' are the couplings constants associated with the groups SU(2) and U(1) respectively.

1.4.2 Yung-Mills Lagrangian

The second term in $\mathcal{L}_{SM}$ represents the Lagrangian of gauge bosons (Yung-Mills Lagrangian [67]), it takes the form:

$$\mathcal{L}_{Gauge \quad Bosons} = -\frac{1}{4}W_{\mu\nu}W^{\mu\nu} - \frac{1}{4}F_{\mu\nu}F^{\mu\nu}, \tag{1.4.5}$$

this Lagrangian represents the kinematics of the gauge bosons. The strength tensors $F_{\mu\nu}$ and $B_{\mu\nu}$ are given by:

$$W_{\mu\nu} = \partial_\mu W^a_\nu - \partial_\nu W^a_\mu + g f^{abc} W^b_\mu W^c_\nu. \tag{1.4.6}$$

$$F_{\mu\nu} = \partial_\mu F_\nu - \partial_\nu F_\mu, \tag{1.4.7}$$

where f_{abc} is the structure constant of the group SU(2) and a,b and c run from 1 to 3.

1.4.3 Higgs Lagrangian

The term $\mathcal{L}_{Higgs}$ presents the Higgs Lagrangian which is responsible for giving masses to all particles in the SM:

$$\mathcal{L} = \left|\partial_\mu\phi + \frac{i}{2}g' y B_\mu \phi + \frac{i}{2}g T_a W^a_\mu \Phi\right|^2 - V(\Phi). \tag{1.4.8}$$

The first part represents the kinematic of the Higgs, while, the second one determines the scalar potential $V(\Phi)$ that is given in Eq.(1.3.9).

From the Lagrangian (1.4.8) and after SSB, we derived the Higgs mass m_h and the Feynman rules for the Higgs self interaction vertices g_{hhh} and g_{hhhh}:

$$m_h^2 = 2\lambda\upsilon^2 = -2\mu^2, \tag{1.4.9}$$

$$g_{hhh} = 3i\lambda\upsilon = 3\frac{i}{2}\frac{m_h}{\upsilon}, \tag{1.4.10}$$

$$g_{hhhh} = 4i\frac{\lambda}{4} = 3\frac{m_h^2}{\upsilon^2}. \tag{1.4.11}$$

The value of υ was determined from the following relation:

$$\upsilon = \frac{2M_W}{g} = \sqrt{\frac{1}{\sqrt{2}G_F}} = 246 \;\; GeV, \tag{1.4.12}$$

where $G_F = 1.1663787 \times 10^{-5}$ GeV^{-2} is the Fermi constant.

1.4.4 Yukawa Lagrangian

The term $\mathcal{L}_{Yukawa}$ presents the Yukawa lagrangian, it describes the interactions between fermions and the Higgs field, its expression is:

$$\mathcal{L}_Y = \sum_{i,j=1}^{3} \Big(-\lambda_u^{ij} \overline{Q}_L^i \Phi^c u_R^j - \lambda_d^{ij} \overline{Q}_L^i \Phi d_R^j - \lambda_e^{ij} \overline{L}_L^i \Phi \ell_R^j \Big) + h.c \tag{1.4.13}$$

Where λ_f is the Yukawa coupling, L_L^i and ℓ_R^i are the left-handed and right-handed fermions (leptons, quarks) respectively, whereas, $\Phi^c = -i\tau^2 \Phi^*$.

To find physical field u and d, we introduce unitary matrix V, it transforms u and d as follows:

$$u_L = V_{uL} u'_L, \qquad u_R = V_{uL} u'_R, \tag{1.4.14}$$

$$d_L = V_{dL} d'_L, \qquad d_R = V_{dL} d'_R. \tag{1.4.15}$$

The matrix V is called the Cabibbo-Kobayashi-Maskawa (CKM) matrix, it is defined as [68, 69]:

$$\begin{pmatrix} V_{ud} & V_{us} & V_{ub} \\ V_{cd} & V_{cs} & V_{cb} \\ V_{td} & V_{ts} & V_{tb} \end{pmatrix} \tag{1.4.16}$$

For completeness, it should be mentioned that, in order to get the total quantum Lagrangian of the Standard Model it is necessary to add a gauge-fixing Lagrangian, $\mathcal{L}_{GF}$, as well as a ghost Lagrangian $\mathcal{L}_{ghost}$. Therefore, the complete Standard Model Lagrangian is:

$$\mathcal{L}_{SM} = \mathcal{L}_{Fermions} + \mathcal{L}_{Gauge} + \mathcal{L}_{Higgs} + \mathcal{L}_{Yukawa} + \mathcal{L}_{SI} + \mathcal{L}_{GF} + \mathcal{L}_{ghost}. \tag{1.4.17}$$

The expressions of $\mathcal{L}_{GF}$ and $\mathcal{L}_{ghost}$ take the following relations:

$$\mathcal{L}_{GF} = \frac{-1}{2\xi} (\partial_\mu A^\mu)^2 \tag{1.4.18}$$

And

$$\mathcal{L}_{ghost} = -\overline{c}^a \partial^\mu D_\mu c^a \tag{1.4.19}$$

Where c and $\overline{c}$ represent the ghost and anti-ghost fields respectively, they are scalars fields satisfied the Fermi's statistic.

1.5 The Higgs mechanism

Adding the term $m^2 M^\mu M_\mu$ to the Standard Model Lagrangian (1.4.1) leads to the violation of the local $SU(2) \otimes U(1)$ gauge invariance while due to its absence the gauge bosons remain

massless. But in fact the $W^{\mp}$ and Z of the electroweak interactions have a rang which proved that those gauge bosons are massive, therefore, a fundamental question was asked, how the physical gauge bosons gain their masses? The same question was asked in the fermions sector because the fermions are massive particles but the term $m\overline{\phi}_L\phi_R$ (the term which is responsible to generate fermions masses) violates the invariance of the Yukawa Lagrangian because of the two chiralities are in different representations of SU(2). To answer this question and to explain the original source of the masses in the physical spectrum. The Higgs mechanism has been proposed by Higgs-Brout-Englert in 1964 to generate masses to all particles in the Standard Model (both the gauge bosons and all fermions leaving the photon massless) by applying the spontaneous symmetry breaking (SSB) in the electroweak sector, it works only when we give a non-vanishing vacuum expectation value.

In this section, we apply this mechanism to both abelian U(1) and non-abelian SU(2) theories.

1.5.1 The SSB in the global continues symetry U(1)

The density Lagrangian for a complex scalar field $\Phi = \frac{\Phi_1 + i\Phi_2}{\sqrt{2}}$ is given by:

$$\mathcal{L} = \frac{-1}{4} F_{\mu\nu}F^{\mu\nu} + (\partial_\mu \Phi)^\dagger(\partial^\mu \Phi) - V(\Phi). \tag{1.5.1}$$

The first term represents the kinematic term of Φ, while the second one is the Higgs potential:

$$V(\Phi) = -\mu^2 \Phi^\dagger \Phi + \lambda(\Phi^\dagger \Phi)^2. \tag{1.5.2}$$

Eq.(1.5.1) represents an invariant Lagrangian under the following global transformation U(1):

$$\Phi = U\Phi = e^{i\alpha}\Phi. \tag{1.5.3}$$

According to the parameter μ^2, two regions are distinguished:

- For $\mu^2 < 0$:

To minimize the potential $V(\Phi)$, we have derived it as follows:

$$\frac{\partial V(\Phi)}{\partial \Phi} = \Phi^\dagger(-\mu^2 + 2\lambda\Phi^2) = 0, \tag{1.5.4}$$

we get:

$$\Phi^\dagger(-\mu^2 + 2\lambda\Phi^2) = 0. \tag{1.5.5}$$

For $\lambda > 0$ and $\mu^2 < 0$, we get only one solution $\Phi = 0$.

- For $\mu^2 > 0$:

For $\lambda > 0$ and $\mu^2 > 0$, we get two solutions $\Phi = 0$ and $\Phi = \frac{\upsilon}{\sqrt{2}}$ where $\upsilon = \sqrt{\frac{\mu^2}{\lambda}} e^{i\theta}$.
The solution $\Phi = 0$ corresponds to a maximum whereas the solution $\Phi = \frac{\upsilon}{\sqrt{2}}$ represents a minimum of the potential, a graphic representation to those solutions has been presented it the following Figure:

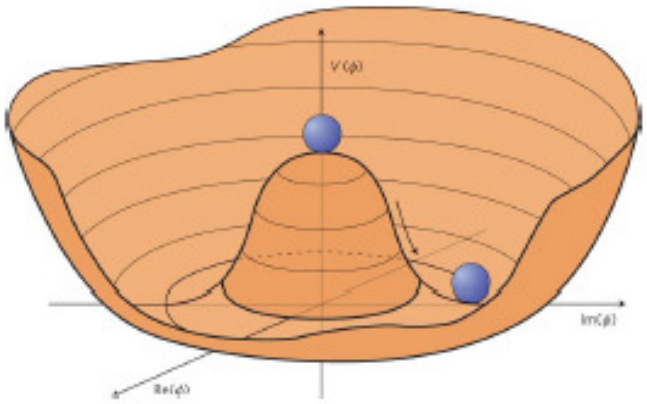

Figure 1.2: The graphic representation of the scalar potential where $\mu^2 > 0$.

In the minimum, the complex scalar field Φ has a non-null value $< \psi >= \upsilon$.
The perturbation around the minimum can be parameterized by: $\frac{h}{\sqrt{2}} = \Phi_1 - \frac{\upsilon}{\sqrt{2}}$ and $\Phi_2 = \frac{\xi}{\sqrt{2}}$, thus, a new scalar field has introduced:

$$\Phi(x) = \frac{1}{\sqrt{2}}(\upsilon + h + i\xi) = e^{\frac{i\xi}{\upsilon}}(\frac{\upsilon + h}{\sqrt{2}}), \tag{1.5.6}$$

where both ξ and h are real fields. We have developed the potential using the expression (1.5.6), we get:

$$V(\Phi) = V(\frac{\upsilon}{\sqrt{2}}) + \frac{1}{2}(2\mu^2 h^2) + ... \tag{1.5.7}$$

After some steps in the calculations, we get a real scalar field h that has a mass $\sqrt{2\mu^2}$ with no Goldstone bosons appear in the theory.

1.5.2 The SSB in the abelian gauge theory

In this section, the Higgs mechanism in the abelian gauge theory is discussed using the local transformation where $\alpha(x)$ is an arbitrary function of space-time, this transformation get the following form:

$$\Phi = U\Phi = e^{i\alpha(x)}\Phi = e^{iq\theta(x)}\Phi, \tag{1.5.8}$$

where q is the Noether's charge, $\theta(x)$ is a local transformation parameter. Lagrangian is variant under this transformation, to take its invariance back, that requires to replace ∂_μ

by D_μ. The introduction of D_μ leads to the appearance of a new vector field A_μ called the gauge field. The expression of the covariant derivative in the abelian group U(1) is given by:

$$D_\mu = \partial_\mu + iqA_\mu, \tag{1.5.9}$$

where A_μ has the following transformation:

$$A'_\mu = A_\mu - \partial_\mu \theta. \tag{1.5.10}$$

The propagation of the field A_μ is described by the following tensor:

$$F_{\mu\nu} = \partial_\mu F_\nu - \partial_\nu F_\mu. \tag{1.5.11}$$

The resulted invariant Lagrangian has the following form:

$$\mathcal{L} = \frac{-1}{4} F_{\mu\nu}F^{\mu\nu} + (D_\mu \Phi)^\dagger (D^\mu \Phi) + \mu^2 \Phi^\dagger \Phi - \lambda(\Phi^\dagger \Phi)^2. \tag{1.5.12}$$

As we reported before, if we add the term $m^2 A^\mu A_\mu$ to the Lagrangian (1.5.12), that will break the invariance, therefore, to get the mass of A_μ we use $\lambda > 0$ and $\mu^2 > 0$. According to (1.5.6), we get:

$$\Phi(x) = \frac{1}{\sqrt{2}}(\upsilon + h + i\xi) \tag{1.5.13}$$

Using the Eq.(1.5.13) and after the development of the Lagrangian (1.5.12), we get:

$$\begin{aligned} \mathcal{L} &= -\frac{1}{4}F_{\mu\nu}F^{\mu\nu} + \frac{1}{2}(\partial_\mu h)^2 + \frac{1}{2}(\partial_\mu \xi)^2 \\ &- \upsilon^2 \lambda h^2 + \frac{1}{2}e^2\upsilon^2 A_\mu A^\mu - e\upsilon A_\mu \partial^\mu \xi \end{aligned} \tag{1.5.14}$$

From the Eq.(1.5.14), we get a mass term for the scalar field h given by $m_h = \sqrt{2\mu^2}$, the field ξ remains massless and the boson A_μ get a mass $m_A = e\upsilon$.
To get a pure theory the Goldstone field ξ has to disappear, we do that by using the following transformations that called "the unitary gauge":

$$A_\mu \rightarrow A_\mu - \frac{\partial_\mu \xi}{e\upsilon}, \tag{1.5.15}$$

$$\Phi' \rightarrow e^{\frac{-i\xi}{\upsilon}} e^{\frac{i\xi}{\upsilon}} \frac{1}{\sqrt{2}}(\upsilon + h), \tag{1.5.16}$$

Using the conditions (1.5.15) and (1.5.16), we get the final form of the Lagrangian:

$$\mathcal{L} = -\frac{1}{4}F_{\mu\nu}F^{\mu\nu} + \frac{1}{2}(\partial_\mu h)^2 + \frac{1}{2}q^2(\upsilon + h)^2 A^\mu A_\mu - \lambda\upsilon^2 h^2 - \lambda\upsilon h^3 - \frac{1}{4}\lambda h^4 + ... \tag{1.5.17}$$

This Lagrangian describes the kinematic part of the scalar boson with its mass $m_h = \sqrt{2\mu^2}$, the kinematics of the field A_μ with its mass expression $m_A = q\upsilon$. Notice that the Goldstone boson was eaten by the gauge field to can acquire its mass.

In the next section, we discuss this mechanism in the non-abelian theory $SU(2) \otimes U(1)$ (electroweak sector).

1.5.3 The SSB in the non-abelian theory

In the case of the non-abelian theory (electroweak sector), we introduce a doublet complex scalar field under the group $SU(2)$:

$$\frac{1}{\sqrt{2}}\begin{pmatrix}\Phi_1+i\Phi_2\\ \Phi_3+i\Phi_4\end{pmatrix} \tag{1.5.18}$$

The local transformation in the electroweak theory has the following expression:

$$\Phi = \exp(i\alpha_i\frac{\sigma_i}{2})\Phi \tag{1.5.19}$$

The Lagrangian under the group $SU(2)\otimes U(1)$ is written as:

$$\mathcal{L} = (D_\mu\Phi)^\dagger D^\mu\Phi + \mu^2\Phi^\dagger\Phi - \lambda(\Phi^\dagger\Phi)^2 - \frac{1}{4}F_{\mu\nu}F^{\mu\nu} \tag{1.5.20}$$

In the case $\mu^2>0$ and $\lambda>0$, the product $\Phi^\dagger\Phi$ can be expressed as:

$$\Phi^\dagger\Phi = \frac{-\mu^2}{2\lambda} = \frac{1}{2}(\Phi_1^2+\Phi_2^2+\Phi_3^2+\Phi_4^2) \tag{1.5.21}$$

To break the symmetry SU(2), we choose Φ to take the following form:

$$\Phi = e^{i\theta_a(x)\frac{\tau^a}{\upsilon}}\begin{pmatrix}0\\ \frac{1}{\sqrt{2}}(\upsilon+h)\end{pmatrix}, \tag{1.5.22}$$

where h represents a reel scalar field, we proceed as in the previous section, we perform an $SU(2)_L$ scalar field:

$$\Phi = \begin{pmatrix}0\\ \frac{1}{\sqrt{2}}(\upsilon+h)\end{pmatrix}, \tag{1.5.23}$$

using the previous field with the product (1.5.21) and after some steps of calculations, we get the term $|D_\mu\Phi|^2$:

$$\begin{aligned}
|D_\mu\Phi|^2 &= \left|(\partial_\mu+\frac{i}{2}g'yB_\mu+\frac{i}{2}gT_aW_\mu^a)\Phi\right|^2\\
&= \frac{1}{2}\left|\begin{pmatrix}\partial_\mu-\frac{i}{2}(gW_\mu^3+g'B_\mu) & \frac{-i}{2}g(W_\mu^1-iW_\mu^2)\\ \frac{-i}{2}g(W_\mu^1+iW_\mu^2) & \partial_\mu+\frac{i}{2}(gW_\mu^3-g'B_\mu)\end{pmatrix}\Phi\right|^2\\
&= \frac{1}{2}(\partial_\mu H)^2+\frac{1}{8}g^2(\upsilon+H)^2|W_\mu^1+W_\mu^2|^2\\
&+ \frac{1}{8}(\upsilon+H)^2|gW_\mu^3-g'B_\mu|^2,
\end{aligned} \tag{1.5.24}$$

Substitute the following mixing angles:

$$\cos\theta_W = \frac{g}{\sqrt{g^2+g'^2}}, \tag{1.5.25}$$

$$\sin\theta_W = \frac{g'}{\sqrt{g^2+g'^2}}, \tag{1.5.26}$$

$$\tan\theta_W = \frac{g'}{g}, \tag{1.5.27}$$

with the expressions (1.3.7) in the expression (1.5.24), we get the following result:

$$(D_\mu\Phi)^\dagger(D^\mu\psi) = \frac{1}{2}(\partial_\mu h)^2 + \frac{1}{4}g^2(\upsilon+h)^2W_\mu^+W_\mu^- + \frac{1}{8}(g'^2+g^2)(\upsilon+h)^2Z_\mu^2 + ... \tag{1.5.28}$$

From the expression (1.5.28), we find the masses of the gauge bosons:

$$m_W = \frac{g}{2}\upsilon, \tag{1.5.29}$$

$$m_Z = \frac{1}{2}\sqrt{g^2+g'^2}, \tag{1.5.30}$$

$$m_A = 0, \tag{1.5.31}$$

where we have used the following definitions during the development of the Lagrangian:

$$Z^\mu = \frac{gW_\mu^3 - g'B^\mu}{\sqrt{g^2+g'^2}} \tag{1.5.32}$$

And

$$A^\mu = \frac{gW_\mu^3 + g'B^\mu}{\sqrt{g^2+g'^2}} \tag{1.5.33}$$

In the SM, g and g' are free parameters which have a linear relationship with the gauge bosons masses m_W and m_Z. Experimentally we have got $m_W = 80.40$ GeV and $m_Z = 91.19$ GeV, that help us to determine the values of both $\cos^2\theta_W$ and $\sin^2\theta_W$ that have taken 0.778 and 0.232 respectively.

Thus, after we apply the spontaneously symmetry breaking in the electroweak theory and by using the local transformations, we found that the gauge bosons $W^\mp$ and Z have absorbed the Goldstone bosons to gain their masses $m_{W^\mp}$ and m_Z, leaving the $U(1)_Q$ unbroken (the photon remains massless) and from all that, we get:

$$SU(2)_L \otimes U(1)_Y \longrightarrow U(1)_{QED}. \tag{1.5.34}$$

From the same expression (1.5.24), we get the Higgs boson coupling to the gauge bosons:

$$g_{hVV} = \frac{-2im_V^2}{\upsilon}, \tag{1.5.35}$$

$$g_{hhVV} = \frac{-2im_V^2}{\upsilon^2}, \tag{1.5.36}$$

$$\tag{1.5.37}$$

where V represents the gauge bosons $W^\mp$ or Z.

1.5.4 The Higgs mechanism for fermions

In this section, we discuss how fermions gain their masses through the Yukawa Lagrangian by using the Higgs mechanism.
The expression of the Yukawa Lagrangian as we reported before is:

$$\mathcal{L}_Y = \sum_{i,j=1}^{3} \Big(-\lambda_u^{ij} \overline{Q}_L^i \Phi^c u_R^j - \lambda_d^{ij} \overline{Q}_L^i \Phi d_R^j - \lambda_e^{ij} \overline{L}_L^i \Phi^c \ell_R^j \Big) + h.c \tag{1.5.38}$$

For electrons, we have:

$$\mathcal{L}_Y = -\lambda_e \overline{e}_L \Phi^c e_R + h.c \tag{1.5.39}$$

Substituting the same doublet scalar field

$$\Phi = \begin{pmatrix} 0 \\ \frac{1}{\sqrt{2}}(\upsilon + h(x)) \end{pmatrix} \tag{1.5.40}$$

in the Lagrangian (1.5.39), we get:

$$\mathcal{L}_Y = -\frac{\lambda_e}{\sqrt{2}} \upsilon \overline{e}_L e_R - \frac{\lambda_e}{\sqrt{2}} h \overline{e}_L e_R. \tag{1.5.41}$$

Therefore, the electron mass is:

$$m_e = \frac{\lambda_e}{\sqrt{2}} \upsilon. \tag{1.5.42}$$

From the same Lagrangian (1.5.41), we found the coupling of the Higgs boson with electrons:

$$g_{he^-e^+} = \frac{i m_e}{\upsilon} \tag{1.5.43}$$

Applying the same method, we can get the remaining lepton masses (m_μ and m_τ) and the other couplings $g_{h\mu\mu}$ and $g_{h\tau\tau}$

1.6 Neutrinos masses

Neutrinos are assumed to be massless in the Standard Model (SM). The absence of the right handed neutrinos in SM particle content makes the following Lagrangian:

$$-\mathcal{L} = ... + Y_{ij}^{\nu} \overline{\nu}_{Ri} L_j H + h.c. \tag{1.6.1}$$

which represents the Dirac neutrinos mass term is not allowed. But the experiments indicated the existence of neutrino oscillations which can happen only if the neutrinos are massive and lepton flavors are mixed, thus, a new physics appears but Beyond the Standard Model.

In 1979, Weinberg extended the SM to generate non-zero tiny neutrino masses by introducing some higher-dimension operators in terms of the fields of the SM itself [71, 72]:

$$\mathcal{L}_{eff} = \mathcal{L}_{SM} + \frac{\mathcal{L}_{d=5}}{\Lambda} + \frac{\mathcal{L}_{d=6}}{\Lambda} + ..., \tag{1.6.2}$$

where Λ denotes the cut-off scale of this effective theory. The lowest dimension operator that violates the lepton number (L) is the dimension 5 Weinberg effective operator [72]:

$$\frac{C_{ij}}{2}\left(\epsilon_{\alpha\gamma}\epsilon_{\beta\sigma}L^T_{\alpha i}\mathrm{C}L_{\beta j}H_\gamma H_\sigma\right) + h.c. \tag{1.6.3}$$

where the Greek and Roman indices denote $SU(2)_L$ and flavor components, respectively. After spontaneous gauge symmetry breaking (EWSB), this Weinberg operator yields to neutrinos masses:

$$\frac{C_{ij}}{2}\langle H^0\rangle^2\nu^T_{Li}\mathrm{C}\nu_{Lj} + h.c, \tag{1.6.4}$$

where the coefficients C^{ij} are of the order Λ^{-1} where Λ is a mass scale which generates the effective Weinberg operator. The neutrino masses can be sufficiently small ≤ 1 eV only if Λ is not far away from the scale of grand unified theories ($\Lambda \sim 10^{13}$ GeV for $\langle H\rangle \sim 10^2$ GeV).

In fact, there are other ways to generate the Weinberg operator at tree level (indeed it can also be generated radiatively [73–76]), the so called seesaw mechanism.

There ought to be two vertices with L's, H's and some mediator field. If the two H's are in the same vertex, HH must be in a triplet representation of $SU(2)_L$ (because the singlet combination is antisymmetric), so the mediator must be a scalar triplet $\triangle$=($\triangle^{++}, \triangle^{+}, \triangle^{0}$) (type-II seesaw [77]). If, on the other hand, each vertex contains both an L and an H, then the LH combination can be either in an invariant or in a triplet representation of $SU(2)_L$, so the mediator field must be a fermion singlet ν_R (type-I seesaw [77]) or a fermion triplet $\Sigma = (\Sigma^+, \Sigma^0, \Sigma^-)$ (type-III seesaw [77]).

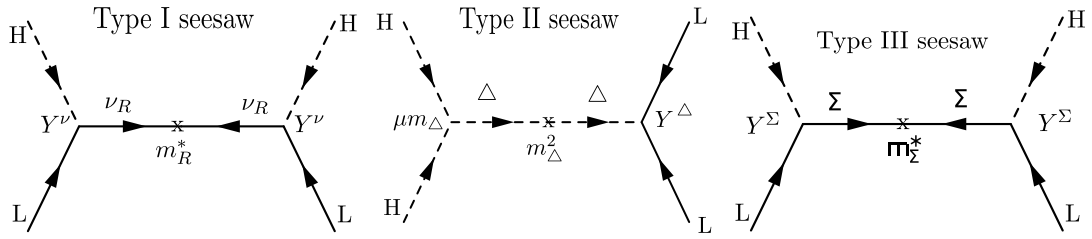

Figure 1.3: Diagrams which generate the different seesaw mechanisms. The mediator field might be a fermionic singlet (type-I seesaw), a scalar triplet (type-II seesaw), or a fermionic triplet (type-III seesaw).

1)-The type-I seesaw mechanism: The simplest way to give mass to neutrinos in the SM is to introduce right-handed neutrinos ν_R (seesaw mechanism type-I), through the following

Lagrangian:

$$-\mathcal{L} = ... + Y^{\nu}_{ij}\overline{\nu}_{Ri}L_j H + h.c. \tag{1.6.5}$$

After spontaneous gauge symmetry breaking, we get the Dirac neutrino mass $\frac{Y_\nu v}{\sqrt{2}}$ In this case, the smallness of three neutrino masses m_i (for i = 1, 2, 3) is attributed to the smallness of three eigenvalues of Y_ν denoted as y_i for i= 1,2,3 (the Yukawa matrix Y_ν must be of the order of 10^{-12} because of the neutrinos have masses smaller than the electronvolt) . Then we encounter a transparent hierarchy problem:

$$\frac{y_i}{y_e} = \frac{m_i}{m_e} \leq \frac{0.5\text{eV}}{0.5\text{MeV}} \sim 10^{-6}, \tag{1.6.6}$$

why is y_i so small?
There is no explanation at all in this Dirac-mass picture.

The question of why three known neutrinos have tiny masses can be explained at the tree level by introducing another extra renormalizable term that is allowed by the symmetries:

$$-\mathcal{L} = ... + \frac{1}{2}\overline{\nu}^T_R m^*_R \text{C}\nu_R + h.c. \tag{1.6.7}$$

Where $\text{C} = i\gamma^2\gamma^0$. Together with the Dirac mass term shown in Eq.(1.6.5), this Majorana mass term for the right-handed neutrinos generates a Majorana mass for the light, mostly left-handed neutrinos, at tree level:

$$-\mathcal{L} = ... + \frac{1}{2}\nu^T_L m^I_\nu \text{C}\nu_L + h.c, \qquad m^I_\nu = -Y^{\nu T} m_R^{-1} Y^\nu \langle H^0\rangle^2. \tag{1.6.8}$$

To derive this expression, one assumes that right-handed Majorana neutrino masses are much heavier than Dirac masses, in such a way that for practical purposes the states ν_R become non-dynamical and can be integrated out. As such, Eq.(1.6.8) is to be seen as the ν_L mass generated at tree level by the exchange of heavy ν_R states, after electroweak symmetry breaking (EWSB). This scenario, where the heavy mediators are fermions which are singlets under the Standard Model gauge group, is known as seesaw type-I. In the basis where both m_R and the light neutrino mass matrix m^I_ν are diagonal, the Yukawa matrix Y^ν has the form [77]

$$Y^\nu = \frac{i}{\langle H^0\rangle}\sqrt{m_R}\mathcal{O}\sqrt{m^I_\nu}U^\dagger, \tag{1.6.9}$$

where $\mathcal{O}$ is some orthogonal matrix which accounts for the mixing involving the heavy neutrino states.

2)- In type-II seesaw, the heavy scalar triplet $\triangle$ is added into the Standard Model, it has

the following mass and interaction terms with leptons and the SM Higgs doublet H:

$$\begin{aligned} -\mathcal{L}^{II} &= Y_{ij}^{\triangle}\Big[\triangle^{++}e_{Li}^{T}Ce_{Lj} - \frac{1}{2}\triangle^{+}(e_{Li}^{T}C\nu_{Lj} + i - j) + \triangle^{0}(\nu_{Li}^{T}C\nu_{Lj}\Big] \\ &- \mu^{*}m_{\triangle}^{*}\Big[\triangle^{++}(H^{+*})^{2} + \sqrt{2}\triangle^{+}H^{+*}H^{0*} + \triangle^{0}(H^{0*})^{2}\Big] \\ &+ \frac{m_{\triangle}^{2}}{2}\Big[|\triangle^{++}|^{2} + |\triangle^{+}|^{2} + |\triangle^{0}|^{2}\Big] + h.c., \end{aligned} \tag{1.6.10}$$

leading to an effective neutrino mass matrix of the form

$$m_{\nu}^{II} = \frac{\mu\langle H^{0}\rangle^{2}Y^{\triangle}}{m_{\triangle}}. \tag{1.6.11}$$

3)- In type-III seesaw, two or more fermionic triplets $\Sigma_i = (\Sigma_i^{+}, \Sigma_i^{0}, \Sigma_i^{-})$ are necessary to reproduce neutrino oscillation data:

$$\begin{aligned} -\mathcal{L}^{III} &= Y_{ij}^{\Sigma}\Big(\sqrt{2}H^{+}\overline{\Sigma}_{i}^{+}\nu_{Lj} + H^{+}\overline{\Sigma}_{i}^{0}e_{Lj} + H^{0}\overline{\Sigma}_{i}^{0}\nu_{Lj} - \sqrt{2}H^{0}\overline{\Sigma}_{i}^{-}e_{Lj}\Big) \\ &+ \frac{1}{2}(m_{\Sigma}^{*})_{ij}\Big(\Sigma_{i}^{+T}C\Sigma_{j}^{-} + \Sigma_{i}^{-T}C\Sigma_{j}^{+} + \Sigma_{i}^{0T}C\Sigma_{j}^{0} + h.c. \end{aligned} \tag{1.6.12}$$

Here, we used $\overline{\Sigma_i}^{\mp} \equiv \overline{(\Sigma_i^{\mp})}$. The neutral component of triplets plays an analogous role to the one of ν_R in a type-I seesaw. As such, the effective neutrino mass matrix is given by:

$$m_{\nu}^{III} = -Y^{\Sigma T}m_{\Sigma}^{-1}Y^{\Sigma}\langle H^{0}\rangle^{2}. \tag{1.6.13}$$

As a result, for each of the seesaw pictures, one may arrive at the unique dimension-5 Weinberg operator of neutrino masses after integrating out the corresponding heavy degrees of freedom [71]:

$$\frac{\mathcal{L}_{d=5}}{\Lambda} = \begin{cases} \frac{1}{2}(Y_{\nu}M_{R}^{-1}Y_{\nu}^{T})_{\alpha\beta}\overline{L}_{\alpha L}HH^{T}\ell_{L\beta}^{c} + h.c, \\ -\frac{\lambda_{\triangle}}{M_{\triangle}}(Y_{\triangle})_{\alpha\beta}\overline{L}_{\alpha L}HH^{T}\ell_{L\beta}^{c} + h.c, \\ \frac{1}{2}(Y_{\Sigma}M_{\Sigma}^{-1}Y_{\Sigma}^{T})_{\alpha\beta}\overline{L}_{\alpha L}HH^{T}\ell_{L\beta}^{c} + h.c, \end{cases} \tag{1.6.14}$$

corresponding to type-I, type-II and type- III seesaws. After spontaneous gauge symmetry breaking, H achieves its vacuum expectation value $\langle H\rangle = \frac{v}{2}$ with v= 246 GeV. Then we are left with the effective Majorana neutrino mass term for three known neutrinos,

$$-\mathcal{L}_{\text{mass}} = \frac{1}{2}\overline{\nu}_{L}M_{\nu}\nu_{L}^{c} + h.c. \tag{1.6.15}$$

where at the tree level the Majorana mass matrix M_ν is given by [71]:

$$M_{\nu} = \begin{cases} -\frac{1}{2}Y_{\nu}\frac{v^{2}}{M_{R}}Y_{\nu}^{T} & \text{(Type-I)}, \\ \lambda_{\triangle}Y_{\triangle}\frac{v^{2}}{M_{\triangle}} & \text{(Type-II)}, \\ -\frac{1}{2}Y_{\Sigma}\frac{v^{2}}{M_{\Sigma}}Y_{\Sigma}^{T} & \text{(Type-III)}. \end{cases} \tag{1.6.16}$$

It becomes obvious that the smallness of M_ν can be attributed to the largeness of M_R, $M_\triangle$ or M_Σ in the seesaw mechanism.

In the end, we have to mention that there are also other, more complex tree level seesaw realizations. We shall mention here the inverse [78] and linear [79] seesaws.

1.7 The parameters in the Standard Model

The Standard Model contains several physical parameters:

1. The constants μ and λ which the scalar potential has written as a function of them.
2. The vacuum expectation value v.
3. The couplings constants $\alpha = \frac{e^2}{4\pi}$, $\alpha_W = \frac{e^2}{4\pi \sin\theta_W}$ and $\alpha_S = \frac{g_S}{4\pi}$ of the electromagnetic interactions, the weak interactions and of the strong interactions respectively .
4. The Cabibbo-Kobayashi-Maskawa (CKM) matrix elements.
5. 12 fermions masses (quarks and leptons).
6. The electric charge e which equals to:
$$e = g \sin\theta_W = g' \cos\theta_W. \tag{1.7.1}$$
7. The parameter ρ (Veltman):
$$\rho = \frac{m_W^2}{m_Z^2 \cos^2\theta_W} = 1, \tag{1.7.2}$$
where the Weinberg angle is defined by this relation:
$$\tan\theta_W = \frac{g'}{g}, \tag{1.7.3}$$
or by:
$$\cos\theta_W = \frac{m_W}{m_Z}, \tag{1.7.4}$$
where m_W and m_Z are the masses of the gauge bosons W and Z respectively.

1.8 Theoretical constraints on the mass of the Higgs boson

In the previous sections 1.5 and 1.6, we discussed how all particles in the Standard Model gain their masses, between all of them we found out that the expression of the Higgs mass

has written as a function of the unknown parameter λ. To can detect the Higgs boson experimentally many constraints have proposed to determine the upper and lower bounds on its mass. To constrain the parameter λ, the perturbative unitarity, the stability of the potential and the triviality conditions are discussed.

1.8.1 Unitarity condition

Limiting the divergences which appear in the elastic scattering of the gauge bosons (e.g $W^+W^- \longrightarrow W^+W^-$) by adding the contributions of the scalar particles (the Higgs boson) determines the upper limit on the mass of the Higgs boson.

In order to derive unitarity constraint one needs to look at the tree level scattering processes: scalar-scalar scattering, gauge boson-gauge boson scattering, and scalar-gauge boson scattering [27]. Applying the equivalence theorem [80, 82, 83], the unitarity constraint at the tree level can be implemented by considering only scalar-scalar scattering processes dominated by quartic interactions.

The scattering amplitude of $W^+W^- \longrightarrow W^+W^-$ can be written in term of the partial waves as follows [84] :

$$\mathcal{M}(s,t,u) = 16\pi \sum_{l=0}^{\infty} (2l+1) P_l(\cos\theta) a_l(s), \tag{1.8.1}$$

where s,t,u are the Mandelston variables, $a_l(s)$ is the spin l partial wave, P_l are the Legendre polynomial of order l. The differential cross section of the process $W^+W^- \longrightarrow W^+W^-$ is given by [84]:

$$\frac{d\sigma}{d\Omega} = \frac{1}{64\pi^2 s} |\mathcal{M}|^2. \tag{1.8.2}$$

The expression of the cross section is found to be:

$$\sigma = \frac{16\pi}{s} \sum_{l=0}^{\infty} (2l+1) |a_l|^2. \tag{1.8.3}$$

From the expression of the total cross section and using the optical theorem, we get the following unitarity constraint [84]:

$$|a_l|^2 = Im(a_l) = |R(a_l)|^2 + |Im(a_l)|^2, \tag{1.8.4}$$

for all l, the expression (1.8.4) is nothing more than an equation for a circle in the plane $(R(a_l), Im(a_l))$ with the radius $\frac{1}{2}$ and the center $(0, \frac{1}{2})$. It can be shown from the graphical representation of this circle that:

$$|R(a_l)| < \frac{1}{2} \qquad \text{for all l.} \tag{1.8.5}$$

The partial wave a_l can be extracted from (1.8.1), then we get:

$$a_l = \frac{1}{32}\int_{-1}^{1} d(\cos\theta) P_l(\cos\theta)\mathcal{M}(s,t,u). \tag{1.8.6}$$

The expression of the largest amplitude of the process $W^+W^- \longrightarrow W^+W^-$ is given by [89]:

$$a_0^{max} = \frac{-3G_F m_h^2}{8\pi\sqrt{2}}. \tag{1.8.7}$$

From the condition (1.8.5), we get:

$$m_h < 700GeV, \tag{1.8.8}$$

where we have used $G_F = \frac{1}{\sqrt{2}v^2}$ and $v^2 = 246$ GeV. The expression (1.8.8) is an upper limit condition on the Higgs boson mass. Thus for the case where $m_h > 700GeV$ we lose the perturbativity of the theory, therefore the unitarity condition will break down.

The other constraints (the triviality and the vacuum stability) comes from the running of the Higgs self-coupling λ with the energy as we discuss in the next subsections.

1.8.2 Triviality and stability conditions

The second condition which constraints the Higgs mass is coming from the triviality condition. The coupling λ which runs with the energy has described by the following relation:

$$\frac{d\lambda}{dt} = \beta_\lambda, \tag{1.8.9}$$

where $t = \ln Q^2$. At one loop, the scalar contributions of the quartic coupling are shown in the following diagrams:

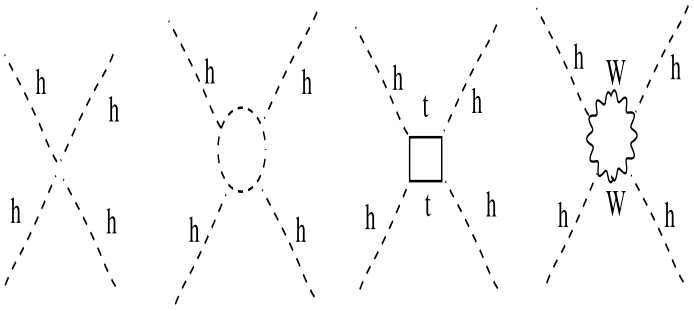

Figure 1.4: Diagrams contribute to the loop.

Those diagrams represent the quartic coupling which are run with the renormalization scale as [90]:

$$\frac{d\lambda}{dt} = \beta_\lambda = \frac{3}{4\pi^2}\left(\lambda^2 + \frac{\lambda h_t^2}{2} - \frac{\lambda h_t^4}{4} + \mathcal{B}(g,g')\right), \tag{1.8.10}$$

where h_t is the top Yukawa coupling, λ is the Higgs self coupling and $\mathcal{B}(g, g')$ describes the contribution of the gauge bosons, this contribution is given by the following relation:

$$\mathcal{B}(g, g') = \frac{-1}{8}\lambda(3g^2 + g'^2) + \frac{1}{64}(3g^4 + 2gg'^2 + g'^4). \tag{1.8.11}$$

To can find the constraints on the parameter λ, two regions are distinguished:

- $\lambda >> g, g', h_t$.
- $\lambda << g, g', h_t$.

The region where $\lambda >> g, g', h_t$

For large values of λ, the contributions of the Higgs top quark coupling and gauge bosons are negligible, so Eq. (1.8.10) becomes:

$$\frac{d\lambda}{dt} = \frac{3}{4\pi^2}\lambda^2, \tag{1.8.12}$$

Eq.(1.8.12) gives the following solution:

$$\lambda(\Lambda) = \frac{\lambda(v)}{1 - \frac{3\lambda(v)}{4\pi^2}\ln\left(\frac{\Lambda^2}{v^2}\right)}. \tag{1.8.13}$$

According to Eq.(1.8.13), we notice that whenever Λ grows, $\lambda(\Lambda)$ grows until it exists a scale Λ at which $\lambda(\Lambda)$ is infinite, the $\lambda(\Lambda)$ keeps increasing until it arrives at a singularity:

$$\frac{3\lambda(v)}{4\pi^2}\ln\left(\frac{\Lambda^2}{v^2}\right) = 1, \tag{1.8.14}$$

at a scale, we get:

$$\Lambda = v\exp(\frac{2\pi^2}{3\lambda(v)}). \tag{1.8.15}$$

The expression (1.8.15) is known as the Landau pole. If we require $\lambda(Q) < \Lambda$ for all $Q < \Lambda$ this puts a constraint on the value of the Higgs self coupling at the electroweak scale v:

$$\lambda(v)^{max} = \frac{4\pi^2}{3\ln(\frac{\Lambda^2}{v^2})}. \tag{1.8.16}$$

That leads to an upper limit on the Higgs mass which is:

$$m_h < \sqrt{\frac{8v^2\pi^2}{3\ln(\frac{\Lambda^2}{v^2})}} \Longrightarrow m_h < 160 \text{ GeV}, \tag{1.8.17}$$

where we have used the fact that the maximum Higgs mass has this relation:

$$m_h^{max} = \sqrt{2\lambda(v)^{max}v^2}. \tag{1.8.18}$$

The region where $\lambda << g, g', h_t$

In this region, the dominant contribution comes from the gauge bosons and from the Higgs top quark Yukawa coupling, so in this case Eq.(1.8.10) takes the following form:

$$\beta_\lambda = \frac{1}{16\pi^2}\left[-3h_t^4 + \frac{3}{16}(2g^4 + (g^2 + g'^2)\right] \tag{1.8.19}$$

$$= \frac{2}{16\pi^2 \upsilon^4}\left[2M_W^4 + M_Z^2 - 4m_t^2\right] < 0. \tag{1.8.20}$$

Since this result is negative, there is a scale Λ for which $\lambda(\Lambda)$ becomes negative with this kind of solution no theory is constructed because when $\lambda(\Lambda) < 0$ the potential is unbounded from below. To make the potential bounded from below it should turn λ up to be positive at a scale. This condition puts a lower limit on $\lambda(\Lambda)$, therefore:

$$\frac{d\lambda}{dt} = \beta_\lambda \Longrightarrow \lambda(\Lambda) - \lambda(\upsilon) = \beta\lambda \ln\left(\frac{\Lambda^2}{\upsilon^2}\right). \tag{1.8.21}$$

To ensure the stability of the potential a condition has proposed on $\lambda(\Lambda)$ ($\lambda(\Lambda) > 0$) together with Eq.(1.8.21), we get:

$$m_h^2 > \frac{3\upsilon^2 y_t^2}{2\pi^2} \ln(\frac{\Lambda^2}{\upsilon^2}). \tag{1.8.22}$$

The condition (1.8.22) leads to a lower limit on the Higgs mass.

1.9 The Higgs Boson of the Standard Model

After we break the symmetry, all the particles of the Standard Model gain their masses, in addition, we get a new degree of freedom which represents a new elementary particle called the Higgs boson.

In 4 July 2012, ATLAS and CMS collaborations in the LHC at CERN have announced the discovery of a new CP-even scalar particle with 5σ of the confidence that ensures the existence of the Higgs boson. This missing particle has a mass around 125-126 GeV, the combined measured at ATLAS has precise its mass from a resonance which appears as a narrow peak in the mass spectra of its decay into $\gamma\gamma$ or to 4 leptons as it indicated in the Figure 1.5 to be $m_h = 125.09 \mp 0.24$ GeV, all the experiment results indicate that this boson has $J^p = 0^+$ with no electric charge, no color charge with weak isospin equal to $\frac{-1}{2}$ and hypercharge equal to 1. The production of the Higgs boson comes from many channels but the most dominant process is the gluon-gluon fusion because of the fact that the density of gluons is more important than the density of quarks in the proton whereas it can decay to any allowed finale states since it is an unstable particle, moreover since its coupling with

particles is proportional to the particle mass, the Higgs boson prefers to decay into heavy particles as we show in the next section.

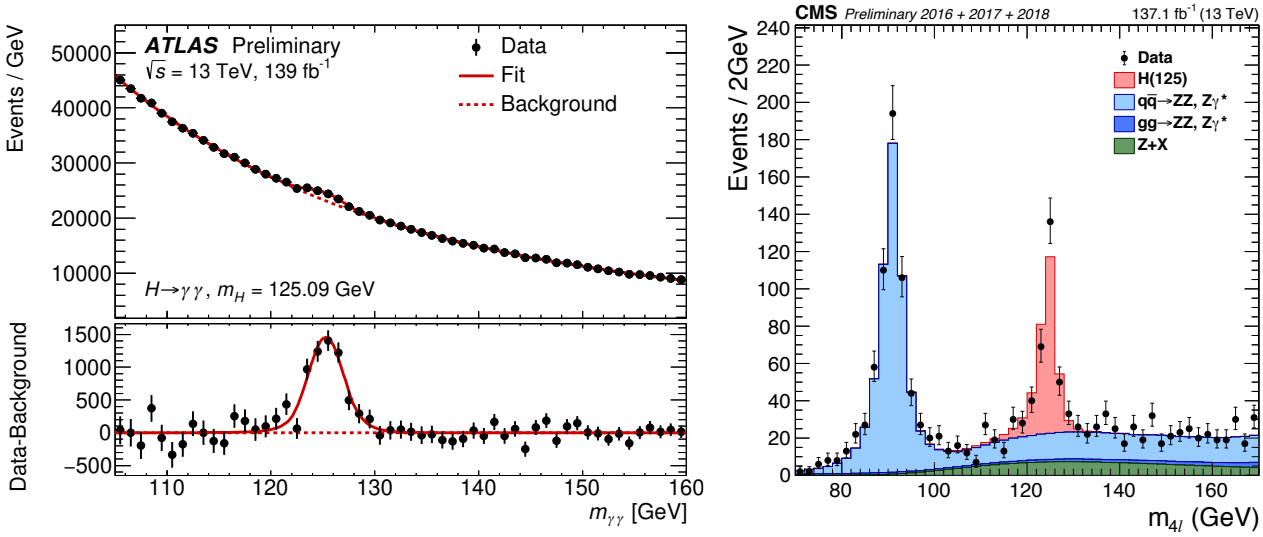

Figure 1.5: SM Higgs boson mass measurements at ATLAS and CMS [25].

Another experimental evidence that prove the existence of the Higgs boson is a parameter called the coupling modifier, it represents the ratio between the experimental and the theoretical cross section [91]:

$$\kappa_j^2 = \frac{\sigma_j}{\sigma_j^{SM}}, \tag{1.9.1}$$

it can take this form [91]:

$$\kappa_j^2 = \frac{\Gamma_j}{\Gamma_j^{SM}}. \tag{1.9.2}$$

This parameter is used to determine the deviation of the theoretical SM Higgs coupling from the experimental measurements (if it equals to 1 that leads to the direct evidence of the existence of the Higgs boson). According to the particle which will couple with the Higgs boson at the tree level, we can get many individual parameters κ_j that are κ_Z, κ_W,κ_b, κ_τ and κ_μ. ATLAS collaboration have announced the following results [91]:

$$\kappa_V = \kappa_W = \kappa_Z \qquad \kappa_V = 1.09^{+0.07}_{-0.07} \tag{1.9.3}$$

$$\kappa_F = \kappa_t = \kappa_b = \kappa_\tau = \kappa_\mu \qquad \kappa_F = 1.11^{+0.17}_{-0.15} \tag{1.9.4}$$

Those results are consistent with the SM prediction with some errors due to statistical, systematical and theoretical uncertainties.

From section 1.5, we found that the expression of the Higgs boson couplings are proportional to the mass for the fermions and they are proportional to the quadratic mass for the

gauge bosons. Figure 1.6 represents the variation of the coupling of the SM Higgs boson with the fermions and with the gauge bosons as a function of their masses, in spite of all the errors, it behaves like a straight line which is in good agreement with the theoretical prediction. That is a strong experimental evidence of the existence of the Higgs boson.

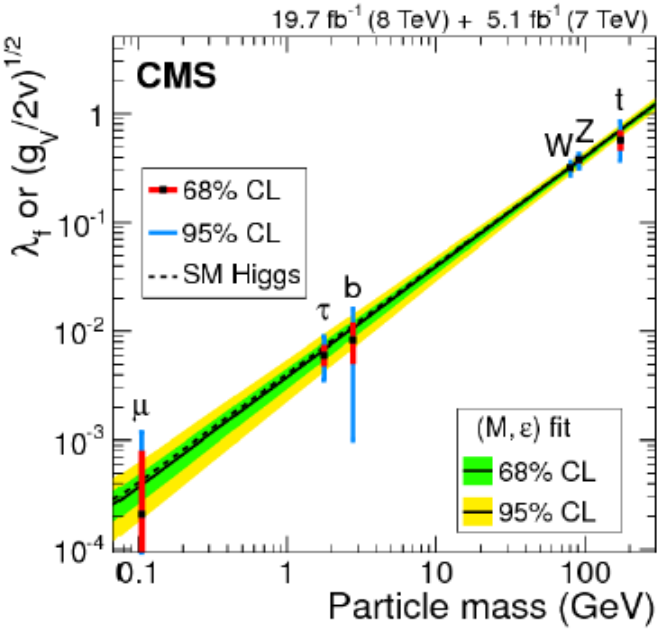

Figure 1.6: The graph shows the variation of the coupling constants of the Higgs boson to various particles. (the statistical errors are presented by the blue and red bars) [92].

1.9.1 Higgs production modes

At LHC, the four main processes to produce the Higgs boson are:

- The gluon-gluon fusion ggF ($gg \longrightarrow h$),
- The vector boson fusion VBF ($qq \longrightarrow V^*V^* \longrightarrow qqh$),
- Higgs-strahlung ($\overline{q}q \longrightarrow Wh, Zh$),
- $\overline{t}th$ production ($gg, \overline{q}q \longrightarrow \overline{t}th$).

In this section, we discuss those processes.

The gluon-gluon fusion (ggF)

The gluon-gluon fusion (ggF) is the dominant mechanism of the main Higgs production process at the LHC, in spite of the absence of any direct coupling between the Higgs and the gluons, the process $gg \longrightarrow h$ can happen in indirect manner by a loop as we show in Figure 1.7, it has a contribution comes from only massive fermions (the most dominant fermion is the top quark), since the gauge bosons are colorless, they can not couple to the gluons hence they do not have any contribution in the loop. This mode is contributing by 80 % of the total cross section of the four main Higgs production.

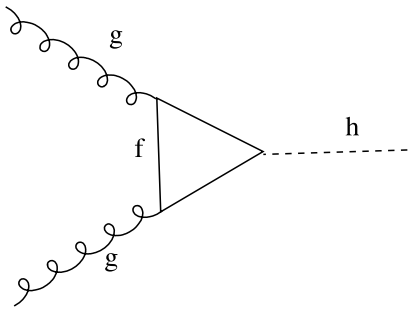

Figure 1.7: Diagram of the ggF process.

The vector boson fusion (VBF)

Higgs boson production via vector boson fusion (VBF) is the second dominant process of the main Higgs production at the LHC. It can be visualized as the inelastic scattering of two quarks (anti quarks), mediated by W or Z exchange which will combine together to produce the Higgs boson (Figure 1.8), this mode is contributing by 6.9 % of the total cross section of the four main Higgs production.

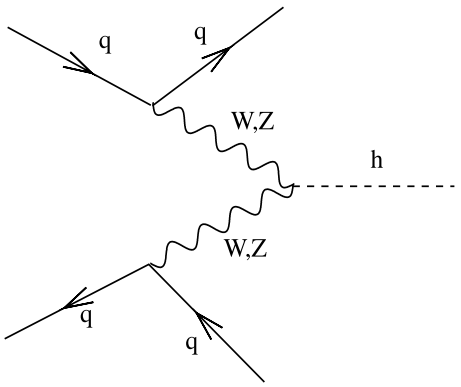

Figure 1.8: Diagram of the VBF process.

Higgs strahlung

The third dominant process in the production channel of the Standard Model Higgs boson is the Higgs strahlung (VH), it associated when a quark collides with an anti-quark to produce a massive vector bosons $W^{\mp}$, Z which they radiate a Higgs with a vector boson $W^{\mp}$, Z (Figure 1.9). This process has a much lower probability at LHC to produce the Higgs, it contributes only by 4.1 % (5.1 %) of the total cross section of the four main Higgs production.

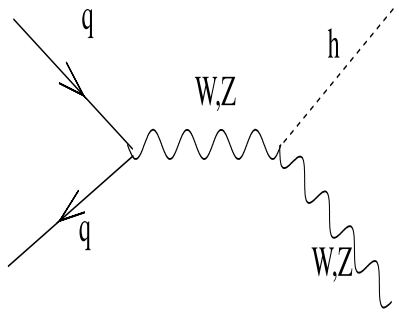

Figure 1.9: Diagram of the Higgs strahlung process.

$\bar{t}$th production

The $\bar{t}$th production has a lower probability in the Higgs production at LHC, this process happens by the scattering of two gluons to a pair of top and anti-top mediated by top quark exchange (Figure 1.10). This channel contributes only by 0.9 % of the total cross section of the four main Higgs production.

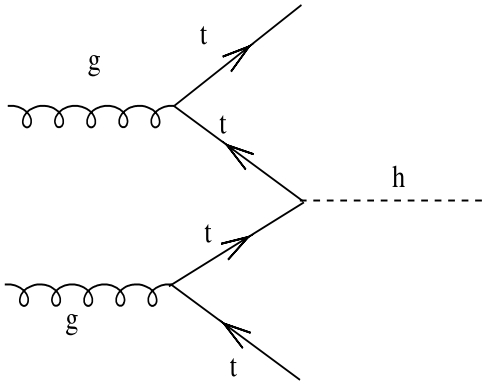

Figure 1.10: Diagram of $\bar{t}th$ production process.

1.9.2 Higgs decay modes

The Higgs boson is an unstable boson, it can decay into particles in which we have available energy. The main decay modes come from:

- Fermionic tree level decay modes $h \longrightarrow \overline{f}f$ [1],
- boson tree level decay modes $h \longrightarrow VV$,
- loop-induced decay modes $h \longrightarrow gg$ and $h \longrightarrow \gamma\gamma(Z\gamma)$.

Fermionic tree level decay modes

The Higgs coupling to fermions is proportional to the masses, therefore, the Higgs boson is likely to decay into heavy fermions (quarks,lepton), thus the most dominant Higgs decay into fermions are: $\overline{b}b$, $\overline{\tau}\tau$, $\overline{c}c$ and $\mu^-\mu^+$ (see Figure 1.11).

In the region where the mass of the Higgs is equal or smaller than 135 GeV, the most dominant decays are $\overline{b}b$ and $\overline{\tau}\tau$.

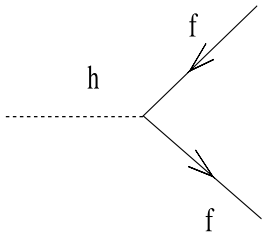

Figure 1.11: Diagram of fermionic Higgs decay.

Bosonic tree level decay modes

The Higgs boson can decay into two gauge bosons (two charged $W^{\mp}$ or two neutral bosons Z) by the following gauge vertex:

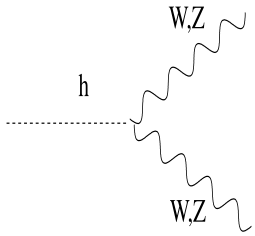

Figure 1.12: Diagram of the Higgs decay into two gauge bosons.

[1] Fermionic tree level decay modes can be $h \longrightarrow 4f$, $h \longrightarrow VV \longrightarrow 4f$.

The decay of the Higgs into two heavy gauge bosons is one of the main processes of the SM Higgs boson decay at LHC, two cases have been distinguished during the study:

- For $M_h < 2M_{W(Z)}$:

In this case, there is not enough energy to produce two real gauge bosons $W^{\mp}$ or Z, therefore, the Higgs will decay into one real gauge boson and the other will be a virtual one $h \longrightarrow V^*V$, the later V^* will decay into a pair of fermions.

- For $M_h > 2M_{W(Z)}$:

In the case where $M_h > 2M_{W(Z)}$, there is enough energy to produce two real gauge bosons, the decay $h \longrightarrow W^+W^-$ is experimentally difficult to exploit because of the high cross section of multi-jet processes in pp collisions [25].

Loop induced decay modes

The Higgs boson is a neutral scalar boson, it does not have either an electric charge or color charge, thus, there is no direct interaction between the Higgs and the photons (gluons). Therefore, all the following decays $h \longrightarrow gg$, $h \longrightarrow \gamma\gamma(Z\gamma)$ happen only by loop corrections (see Figure 1.13).

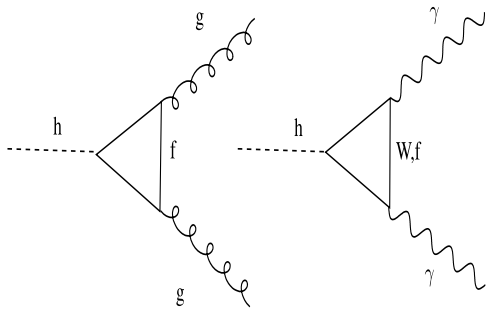

Figure 1.13: Diagram of the Higgs decay into two gauge gluons and $\gamma\gamma(Z\gamma)$.

The decay $h \longrightarrow gg$ is mediated only by massive fermions (top quark) whereas both decays $h \longrightarrow \gamma\gamma$ and $h \longrightarrow Z\gamma$ are mediated by fermions (via top quark) and via gauge bosons ($W^{\mp}$). In spite of the fact that the decay into $\gamma\gamma$ has a small branching ratio at the LHC, the diphoton channel has used to prove the existence of the Higgs boson since it has a clean signature.

1.10 Beyond Standard Model (BSM)

The Standard Model provides an extremely successful to describe the behavior of all the known elementary particle and all the forces of the universe (except the gravitation force), it can explain how particles gain their masses through the Higgs mechanism. But in spite of all the compatibility of the experimental and the theoretical results, the SM became an effective field theory which is valuable in some scale energy. It fails to address some of the most fundamental questions about the matter and forces in our universe.

1.10.1 Problems of the Standard Model

The Standard Model failed to explain many fundamental questions:

1. Gravity is a much weaker force compared to the other three forces of nature hence this force is ignored in the SM. therefore it can not explain how can gravitational interactions be described in terms of particle physics?

2. The SM can not explain why there are exactly 3 generations of quarks and leptons.

3. The oscillation neutrinos provided that the neutrinos have masses but the SM can not expect the existence of the right-handed neutrino, therefore, How we can generate neutrino masses?

4. Why is not there the same amount of antimatter as matter in the universe?

5. The SM can describe only 4% of the universe all the rest of it are dark matter and dark energy which consistent unknown particles. Thus, The SM can not explain what does dark matter in the universe consist of?

To answer all those questions, theoretical physicist proposed theories beyond the Standard Model, among those models we are interested in the extension of the electroweak sector to get models based on $SU(3) \otimes SU(N) \otimes U(1)$ where N=3,4.

1.10.2 $SU(3) \otimes SU(N) \otimes U(1)$ gauge models

Models based on the gauge group $SU(3)_C \otimes SU(N)_L \otimes U(1)_X$ (for short 3-N-1 models) are the extension of the Standard Model. where N it takes 3 for the first extensions while N=4 (the higher extension of the electro-weak theory) for the second extension. The 3N1 models have many versions according to the parameters β and γ which define the electric charges of new particles. Fermions fields in the 3N1 models are arranged in the group SU(N) that leads to the existence of new exotic fermions, depending on the exotic electric charges we

distinguish many versions, moreover we classify the 3N1 models according to the scalar sector.

For N=3, we get models based on $SU(3)_C \otimes SU(3)_L \otimes U(1)_X$ (331 models for short), they predict new particles in all the three sectors. In the fermions sector, we have additional particles in the multiplies called exotic fermions either in the lepton or in the quark generations. In the gauge boson sector, besides $W^{\mp}$, γ and Z of the SM those models predicted the existence of five new gauge bosons, some of them are doubly charged, some of them are neutral and others are singly electric charged. In the scalar sector, each scalar field is a triplet leading to the existence of new scalar bosons.

For N=4, we get models based on $SU(3) \otimes SU(4) \otimes U(1)$, the so called 341 models.
In the next chapter, we discuss the 341 models, their particle content and their fundamental features in details.

1.11 Summary

The Standard model is a pretty good theory, it can explain all the behavior and all the interactions of the known particles in the universe even it explains how particles gain their mass through the Higgs mechanism leaving no particle without mass. But in spite of all its success they still remain unanswered questions as we discuss in subsection 1.10.1. To explain the undefined phenomena and to define the unknown particles, going beyond the Standard Model becomes mandatory. Among those extensions and in our work we focus on models that based on $SU(3) \otimes SU(4) \otimes U(1)$ symmetry.

In the next chapter, we discuss what is the 341 models, we review their content particle and their fundamental features. Moreover, we show how to make those kind of models free from the gauge anomalies.

Chapter 2

The 341 models

2.1 Introduction

As we have reported in chapter 1, many unanswered questions reveal that the Standard Model is an effective field theory and going beyond it became mandatory, therefore, theories Beyond the Standard Model have been proposed many years ago. Among those theories, we are interested in models based on the gauge group $SU(3)_C \otimes SU(4)_L \otimes U(1)_X$ (hereafter the 341 just for short).

In this chapter, we review the theoretical studies of the 341 models in general then we focus on its compact version. We discuss the chiral anomalies cancellation in the compact 341 model, we show how its particle fields are composed and how they gain their masses though the Higgs mechanism using only three scalars fields. The fermion, gauge boson and the scalar sectors are discussed in detail. Moreover, Its total Lagrangian is presented.

2.2 Anomalies cancellation in the 341 models

In general, the fermion representation under $SU(3)_C \otimes SU(4)_L \otimes U(1)_X$ read:

$$\Psi_L = \begin{cases} q_L : (3, 4, X_q^L) = (3, 3, X_q^L) \oplus (3, 1, X_q^L), \\ \\ \ell_L : (1, 4, X_\ell^L) = (1, 3, X_\ell^L) \oplus (1, 1, X_\ell^L), \end{cases} \tag{2.2.1}$$

and

$$\Psi_L^* = \begin{cases} q_L^* : (3, 4^*, X_q^L) = (3, 3^*, X_q^L) \oplus (3, 1, X_q^L), \\ \\ \ell_L^* : (1, 4^*, X_\ell^L) = (1, 3^*, X_\ell^L) \oplus (1, 1, X_\ell^L), \end{cases} \tag{2.2.2}$$

while,

$$\Psi_R = \begin{cases} q_R : (3, 1, X_q^R), \\ \\ \ell_R : (1, 1, X_\ell^R). \end{cases} \tag{2.2.3}$$

where X refers to the quantum number associated with $U(1)_X$. The generator of $U(1)_X$ commutes with the matrices of $SU(4)_L$, hence, it should take the form $XI_{4\times4}$.

Our multiples (quarks or leptons) transform in the 4 or 4^* representation. In the general case, each multiplet can transform as [93]:

$$\begin{cases} q_L^{(m)}, q_L^{(m*)} : m = \underbrace{1, 2, ..., k}_{3k \quad quadreplets} ; m^* = \underbrace{k+1, k+2, ...M}_{3(M-k) \quad quadreplets}, \\ \\ \ell_L^{(n)}, \ell_L^{(n*)} : n = \underbrace{1, 2, ..., j}_{j \quad quadreplets} ; n^* = \underbrace{j+1, j+2, ...N}_{N-j \quad quadreplets}, \end{cases} \tag{2.2.4}$$

where the 3k-th multiplets of quarks are in the fundamental 4 representation while the $3(M-k)$ are in the fundamental conjugate 4^* representation for a total of $3M$ quark left-handed multiples. The factor 3 in the number of quark left-handed multiplets refers to the existence of three colors. Similarly, the first j left-handed multiplies of leptons are taken in the representation 4 and the $(N-j)$ are taken in the 4^* representation, for a total of N leptonic left-handed multiplets. To define the fermionic structures and their representations, the cancellation of the anomalies should be satisfied. Those anomalies come from a triangular diagram involves the following gauge interactions structures: $[SU(3)_C]^2 \otimes U(1)_X$, $SU(4)_L \otimes [U(1)_X]^2$, $SU(3)_C \otimes [U(1)_X]^2$,$[SU(3)_L]^3$, $[U(1)_X]^3$, $SU(3)_C \otimes SU(4)_L \otimes U(1)_X$,$[Grav]^2 \otimes U(1)_X$, $[SU(4)_L]^2 \otimes U(1)_X$, $[SU(4)_L]^2 \otimes SU(3)_C$, $[SU(3)_C]^2 \otimes SU(4)_L$, $[SU(3)_C]^3$, $SU(3)_C \otimes [Grav]^2$.

Since $\mathrm{Tr}[T^a] = 0$ and $\mathrm{Tr}[\tau^a] = 0$, all the diagrams which are proportional to $\mathrm{Tr}[T^a]$ and $\mathrm{Tr}[\tau^a]$ respectively are automatically cancel.

The remaining anomalies: $[SU(3)_C]^2 \otimes U(1)_X$, $[SU(3)_L]^3$, $[U(1)_X]^3$, $[Grav]^2 \otimes U(1)_X$, $[SU(3)_C]^3$, and $[SU(4)_L]^2 \otimes U(1)_X$ are non-trivial.

- The $[SU(4)_L]^3$ anomaly:

The total contribution of the $[SU(4)_L]^3$ anomaly comes from [94]:

$$\mathcal{A}^{abc}(4L)\left(\sum_{Q_{mL}, f_{iL}} 4_L - \sum_{Q_{nL}} 4_L^*\right) = \mathcal{A}^{abc}(4_L)(n_{4_L} - n_{4_L^*}), \tag{2.2.5}$$

where $\mathcal{A}^{abc}(4_L) = \mathrm{Tr}(T_L^a\{T_L^b, T_L^c\})$ and $\mathcal{A}^{abc}(4_L) = -\mathcal{A}^{abc}(4_L^*)$, 4_L is a $SU(4)$ quadruplet and 4_L^* represents a SU(4) anti-quadruplets, n_{4_L} and $n_{4_L^*}$ are the number of fermions quadruplets

and anti-quadruplets respectively. This anomaly cancels only if the number of quadruplets n_{4_L} is equal to the number of anti-quadruplets $n_{4^*_L}$. Thus we must have:

$$3k + j = 3(M - k) + (N - j). \tag{2.2.6}$$

- $[SU(4)_L]^2 \otimes U(1)_X$ anomaly:

This anomaly cancels only if the sum of all $U(1)_X$ charges of the $SU(4)_L$ chiral multiples is zero:

$$\sum_{f_{iL},Q_{pL}} X_L = jX_{f_L} + (N - j)X_{f_{\overline{L}}} + 3kX_{q_L} + 3(M - k)X_{\overline{q}_L} = 0. \tag{2.2.7}$$

Here M is the number of left handed quarks families, k is the number of $SU(4)_L$ quadruplets quarks multiplets and N is the number of left handed leptons multiplets. The cancellation of this anomaly requires the satisfaction of the following condition:

$$4\sum X^L_\ell + 12\sum X^L_q - 3\sum X^R_q - \sum_{Singlet} X^R_\ell = 0. \tag{2.2.8}$$

- The $[SU(3)_C]^2 \otimes U(1)_X$ anomaly:

This anomaly is similar to the $[SU(4)_L]^2 \otimes U(1)_X$ case but with $[SU(3)_C]^2$, therefore, only quarks will contribute, hence, it will be canceled only if:

$$\sum_{Q_{mL}} 4X_{q_L} + \sum_{Q_{nL}} 4X_{\overline{q}_L} - \sum_{q_R} X_{q_R} = 0, \tag{2.2.9}$$

where X_{q_R}, X_{q_L} and $X_{\overline{q}_L}$ are the $U(1)_X$ charges of the right-handed quark, the left-handed quarks and anti-quarks respectively. Notice that $\sum_{q_R} X_{q_R} = \sum_{q_R} q_R$, since the $U(1)_X$ charges of the right handed quarks are equal to their electric charges.

- The $[Grav]^2 \otimes U(1)_X$ anomaly:

To ensure the cancellation of the $[Grav]^2 \otimes U(1)_X$ anomaly, one needs to ensure that the sum over all the $U(1)_X$ charges of all fermions (both left and right handed fermions) must equal zero:

$$\sum_{fermions} X_L - \sum_{fermions} X_R = 0. \tag{2.2.10}$$

- The $[U(1)_X]^3$ anomaly

The $[U(1)_X]^3$ anomaly cancels only if:

$$\sum_{F_L} X^3_{F_L} - \sum_{F_R} X^3_{F_R} = 0, \tag{2.2.11}$$

where F_L and F_R are the left and the right-handed fermions respectively (quarks and leptons). The expression (2.2.11) can take the following form:

$$4\sum(X_\ell^L)^3 + 12\sum(X_q^L)^3 - 3\sum_{Singlet}(X_q^R)^3 - \sum_{Singlet}(X_\ell^R)^3 = 0 \tag{2.2.12}$$

Based on the anomalies cancellation, Table (2.1) shows the general fermionic structure where we take $M = N$.

N	$0 \leq j \leq N$	$0 \leq 3k \leq 3N$	solution for $j + 3k = 2N$
1	0,1	0,3	No solution
2	0,1,2	0,3,6	$j = 1; k = 1$
3	0,1,2,3	0,3,6,9	$j = 0; k = 2 \quad j = 3; k = 1$
4	0,1,2,3,4	0,3,6,9,12	$j = 2; k = 2$
5	0,1,2,3,4,5	0,3,6,9,12,15	$j = 1; k = 3 \quad J = 4; k = 2$
6	0,1,2,3,4,5,6	0,3,6,9,12,15,18	$j = 0; k = 4 \quad j = 3; k = 3 \quad j = 6; k = 2$

Table 2.1: Possible solutions for $j + 3k = 2N$ [93].

It is important to note that there are only some possible ways to choose the number of quadruplet and antiquadruplet for a given number of multiplets [93].

According to Table (2.1), for $N = 1$, we get no solutions for the equality $j + 3k = 2N$.

For $N = 2$, we get one solution $j = 1$ and $k = 1$, which leads to the possibility of the existence of a lepton and a quark generation lies in the 4 representation and another lepton with another quark generation are in the 4^* representation.

For $N = 3$, we get two solutions either $J = 0$ and $k = 2$ or $j = 3$ and $k = 1$, for the first solution $j = 0$ and $k = 2$ we get three lepton generations with a quark generation lies in the 4 representation whereas the other two quark generations are in the 4^* representation. And for the second solution where we have $j = 3$ and $k = 1$ that leads to three leptons generations with a quark generation lie in the 4^* representation and the other two quark generations lie in the 4 representation and so on as we show in Table 2.2.

As we discussed, depending on the value of N we can figure out the possible generations and their representations.

In the next section, we focus on the case where $N = 3$, we build the fermion sector based on the idea of two quarks generations transform in the same representation while the third one lies in a different representation. Table 2.2 represents the possible representations for both leptons and quarks multiplies for any version of the 341 models [1].

[1]Except the flipped 341 model

N	Allowed representations
2	$\begin{pmatrix} \ell^1 : 4 \\ \ell^2 : 4^* \\ q^1 : 4 \\ q^2 : 4^* \end{pmatrix}$
3	$\begin{pmatrix} \ell^{(1)}, \ell^{(2)}, \ell^{(3)} : 4^* \\ q^{(1)}, q^{(2)} : 4 \\ q^{(3)} : 4^* \end{pmatrix}, \begin{pmatrix} \ell^{(1)}, \ell^{(2)}, \ell^{(3)} : 4 \\ q^{(1)}, q^{(2)} : 4^* \\ q^{(3)} : 4 \end{pmatrix}$
4	$\begin{pmatrix} \ell^{(1)}, \ell^{(2)} : 4 \\ \ell^{(3)}, \ell^{(4)} : 4^* \\ q^{(1)}, q^{(2)} : 4 \\ q^{(3)}, q^{(4)} : 4^* \end{pmatrix}$
5	$\begin{pmatrix} \ell^{(5)} : 4 \\ \ell^{(1)}, \ell^{(2)}, \ell^{(3)}, \ell^{(4)} : 4^* \\ q^{(3)}, q^{(4)}, q^{(5)} : 4 \\ q^{(1)}, q^{(2)} : 4^* \end{pmatrix}, \begin{pmatrix} \ell^{(1)}, \ell^{(2)}, \ell^{(3)}, \ell^{(4)} : 4 \\ \ell^{(5)} : 4^* \\ q^{(3)}, q^{(4)}, q^{(4)} : 4^* \\ q^{(1)}, q^{(2)} : 4 \end{pmatrix}$

Table 2.2: Possible representations according to table 2.1 [93].

2.3 Particle content in the 341 models

The 341 model is the second extension of the Standard Model which is based on the gauge group $SU(3)_C \otimes SU(4)_L \otimes U(1)_X$, in this model, the particle content is defined based on the values of the γ and β parameters which the charge operator Q is written as a linear combination of their values:

$$Q = T_3 + \beta T_8 + \gamma T_{15} + X, \tag{2.3.1}$$

Where $T_i = \frac{\lambda_i}{2}$ where λ_3, λ_8 and λ_{15} are the diagonal generators of the Gell-Mann matrices of the group SU(4) where

$$\begin{aligned} \lambda_3 &= diag(1,-1,0,0)\,, \qquad \lambda_8 = \frac{1}{\sqrt{3}} diag(1,1,-2,0)\,, \\ \lambda_{15} &= \frac{1}{\sqrt{6}} diag(1,1,1,-3)\,. \end{aligned} \tag{2.3.2}$$

2.3.1 Fermionic content

The leptonic content in the 341 models is built in the way we place the left-handed lepton doublets of the Standard Model in the SU(4) quadruplet f_{aL} with additional leptons F_a and

$\widetilde{F}_a$:

$$f_{aL} \equiv \begin{pmatrix} \nu_a \\ \ell_a \\ F_a \\ \widetilde{F}_a \end{pmatrix} \sim (1, 4, X_{4\ell}) \tag{2.3.3}$$

Where a=e, μ, τ and the symbol $\sim$ refer to the quantum numbers of the $SU(3)_C$, $SU(4)_L$, $U(1)_X$ respectively.

According to Table (2.2), two quarks generations lie in the fundamental conjugate representation 4^* while the third one lies in the fundamental representation. All the quarks generations in the 341 models contain the left-handed quarks doublets of the SM with additional new quarks called "exotic quarks". Their multiplies are arranged as follows [37]:

$$Q_{1L} \begin{pmatrix} u_1 \\ d_1 \\ U_1 \\ J_1 \end{pmatrix} \sim (3, 4, X_{4q}), \qquad Q_{iL} \begin{pmatrix} d_i \\ u_i \\ D_i \\ J_i \end{pmatrix} \sim (3, 4^*, X_{4q^*}) \tag{2.3.4}$$

Where $i = 2, 3$, U_1, J_1, D_i and J_i are exotic quarks with electric charges $\frac{2}{3}$, $\frac{5}{3}$, $\frac{-1}{3}$ and $\frac{-4}{3}$ respectively in the case of the 341 model with exotic electric charge, while, in the case of the 341 model without exotic electric charge, they have ordinary electric charge $\mp\frac{2}{3}$ or $\mp\frac{1}{3}$.

The right-handed quarks transform as singlets under $SU(4)_L \otimes U(1)_X$:
u_{1R}, d_{1R}, U_{1R}, J_{1R}, u_{iR}, d_{iR}, D_{iR}, J_{iR}.

To determine the values of the $U(1)_X$ charges X_{4q}, X_{4q^*} and $X_{4\ell}$, we have to set the following relationship $Q(\ell) = Q(F_a)$ which gives:

$$\frac{-1}{2} + \frac{\beta}{2\sqrt{3}} + \frac{\gamma}{2\sqrt{6}} + X_{4\ell} = \frac{-\beta}{\sqrt{3}} + \frac{\gamma}{2\sqrt{6}} + X_{4\ell} \tag{2.3.5}$$

Hence: $\beta = \frac{1}{\sqrt{3}}$ and to get the value of γ we impose that $Q(\ell) = Q(\widetilde{F}_a)$, thus:

$$\frac{-1}{2} + \frac{\beta}{2\sqrt{3}} + \frac{\gamma}{2\sqrt{6}} + X_{4\ell} = \frac{-3\gamma}{2\sqrt{6}} + X_{4\ell} \tag{2.3.6}$$

From the relation (2.3.6), we obtain $\gamma = \frac{1}{\sqrt{6}}$.
With those values we determine a model with $\beta = \frac{1}{\sqrt{3}}$ and $\gamma = \frac{1}{\sqrt{6}}$, the so called model A it has been studied in [45]. Another model is extracted with different value of β and γ when we impose those relations $Q(\nu_a) = Q(\widetilde{F}_a)$ and $Q(\ell) = Q(F_a)$ which they give:

$$\frac{1}{2} + \frac{\beta}{2\sqrt{3}} + \frac{\gamma}{2\sqrt{6}} + X_{4\ell} = \frac{-3\gamma}{2\sqrt{6}} + X_{4\ell}, \tag{2.3.7}$$

$$\frac{-1}{2} + \frac{\beta}{2\sqrt{3}} + \frac{\gamma}{2\sqrt{6}} + X_{4\ell} = \frac{-\beta}{\sqrt{3}} + \frac{\gamma}{2\sqrt{6}} + X_{4\ell}, \tag{2.3.8}$$

then we obtain: $\beta = \frac{1}{\sqrt{3}}$ and $\gamma = \frac{-2}{\sqrt{6}}$. The model with those values is called model E.

Beside the models A and E, they do exist many others [45, 95] called B, F, C, D, G, H and I with and without exotic electric charges. Each model has its own features with different content of the fermions multiples. Table 2.3 shows particle content in all possible 341 models parameterized by β and γ and the corresponding 331 sub-representations.

Name	341 representation	331 representation	Components	F
ψ_ℓ	$(1,4,\frac{-1}{2}-\frac{\beta}{2\sqrt{3}}-\frac{\gamma}{2\sqrt{6}})$	$(1,3,\frac{-1}{2}-\frac{\beta}{2\sqrt{3}})\oplus(1,1,\frac{-2\gamma}{\sqrt{6}}-\frac{\beta}{2\sqrt{3}}-\frac{1}{2})$	$(\nu_\ell,\ell,F_\ell^{q_1},\widetilde{F}_\ell^{q_2})$	3
ℓ^c	$(1,1,1)$	$(1,1,1)$	ℓ^c	3
ℓ_X^c	$(1,1,\frac{1}{2}+\frac{\sqrt{3}}{2}\beta)$	$(1,1,\frac{1}{2}+\frac{\sqrt{3}}{2}\beta)$	ℓ_X^c	3
$Q_i(i=1,2)$	$(3,\overline{4},\frac{1}{6}+\frac{\beta}{2\sqrt{3}}+\frac{\gamma}{2\sqrt{6}})$	$(3,\bar{3},\frac{1}{6}+\frac{\beta}{2\sqrt{3}})\oplus(1,1,\frac{1}{6}+\frac{\beta}{2\sqrt{3}}+\frac{2\gamma}{\sqrt{6}})$	$(u,d,D_i^{q_1},U_i^{q_2})$	2
Q_3	$(3,4,\frac{1}{6}-\frac{\beta}{2\sqrt{3}}-\frac{\gamma}{2\sqrt{6}})$	$(3,3,\frac{1}{6}-\frac{\beta}{2\sqrt{3}})\oplus(1,1,\frac{1}{6}-\frac{\beta}{2\sqrt{3}}-\frac{2\gamma}{\sqrt{6}})$	$(d,u,U_3^{q_1},D_3^{q_2})$	1
u^c	$(\overline{3},1,\frac{-2}{3})$	$(\overline{3},1,\frac{-2}{3})$	u^c	3
d^c	$(\overline{3},1,\frac{1}{3})$	$(\overline{3},1,\frac{1}{3})$	d^c	3
$U_{1,2}^c$	$(\overline{3},1,\frac{-1}{6}-\frac{\sqrt{3}\beta}{2})$	$(\overline{3},1,\frac{-1}{6}-\frac{\sqrt{3}\beta}{2})$	$U_{1,2}^c$	2
U_3^c	$(\overline{3},1,\frac{-1}{6}+\frac{\sqrt{3}\beta}{2})$	$(\overline{3},1,\frac{-1}{6}+\frac{\sqrt{3}\beta}{2})$	U_3^c	1
$D_{1,2}^c$	$(\overline{3},1,\frac{-1}{6}-\frac{\beta}{2\sqrt{3}}-\frac{2\gamma}{\sqrt{6}})$	$(\overline{3},1,\frac{-1}{6}-\frac{\beta}{2\sqrt{3}}-\frac{2\gamma}{\sqrt{6}})$	$D_{1,2}^c$	2
D_3^c	$(\overline{3},1,\frac{-1}{6}+\frac{\beta}{2\sqrt{3}}+\frac{2\gamma}{\sqrt{6}})$	$(\overline{3},1,\frac{-1}{6}+\frac{\beta}{2\sqrt{3}}+\frac{2\gamma}{\sqrt{6}})$	$D_{1,2}^c$	1
ϕ_1	$(1,\overline{4},\frac{-\beta}{\sqrt{3}}+\frac{\gamma}{2\sqrt{6}})$	$(1,\bar{3},\text{-}\frac{1}{2}+\frac{\beta}{2\sqrt{3}})\oplus(1,1,-\frac{\beta}{\sqrt{3}}+\frac{2\gamma}{\sqrt{6}})$	$(\phi_1^{q_1},\phi_1^{q_2},\phi_1^{q_3},\phi_1^{q_4})$	1
ϕ_2	$(1,\overline{4},\frac{-1}{2}+\frac{\beta}{2\sqrt{3}}+\frac{\gamma}{2\sqrt{6}})$	$(1,\bar{3},-\frac{\beta}{\sqrt{3}})\oplus(1,1,-\frac{1}{2}+\frac{\beta}{2\sqrt{3}}+\frac{2\gamma}{\sqrt{6}})$	$(\phi_2^{q_1},\phi_2^{q_2},\phi_2^{q_3},\phi_2^{q_4})$	1
ϕ_3	$(1,\overline{4},\frac{1}{2}+\frac{\beta}{2\sqrt{3}}+\frac{\gamma}{2\sqrt{6}})$	$(1,\bar{3},\frac{1}{2}+\frac{\beta}{2\sqrt{3}})\oplus(1,1,\frac{1}{2}+\frac{\beta}{2\sqrt{3}}+\frac{2\gamma}{\sqrt{6}})$	$(\phi_3^{q_1},\phi_3^{q_2},\phi_3^{q_3},\phi_3^{q_4})$	1
ϕ_4	$(1,\overline{4},\frac{-3\gamma}{2\sqrt{6}})$	$(1,\bar{3},\frac{1}{2}+\frac{\beta}{2\sqrt{3}})\oplus(1,1,0)$	$(\phi_4^{q_1},\phi_4^{q_2},\phi_4^{q_3},\phi_4^{q_4})$	1

Table 2.3: Particles content of the 341 models for generic β and γ parameters where F represents the number of flavors.

The 321 sub-representations embedded in the fundamental and its conjugate representations of SU(3) are given by:

$$\psi_\ell \supset (1,2,\frac{-1}{2})\oplus(1,1,\frac{-1}{2}-\frac{\sqrt{3}\beta}{2})\oplus(1,1,\frac{-2\gamma}{\sqrt{6}}-\frac{\beta}{2\sqrt{3}}-\frac{1}{2}), \tag{2.3.9}$$

$$Q_i \supset (3,2,\frac{1}{6})\oplus(3,1,\frac{1}{6}+\frac{\sqrt{3}\beta}{2})\oplus(3,1,\frac{1}{6}+\frac{\beta}{2\sqrt{3}}+\frac{2\gamma}{\sqrt{6}}), \tag{2.3.10}$$

$$Q_3 \supset (3,2,\frac{1}{6})\oplus(3,1,\frac{1}{6}-\frac{\sqrt{3}\beta}{2})\oplus(3,1,\frac{1}{6}-\frac{\beta}{2\sqrt{3}}-\frac{2\gamma}{\sqrt{6}}), \tag{2.3.11}$$

$$\phi_1 \supset (1,2,\frac{-1}{2})\oplus(1,1,\frac{-1}{2}+\frac{\sqrt{3}\beta}{2})\oplus(1,1,\frac{-\beta}{\sqrt{3}}+\frac{2\gamma}{\sqrt{6}}) \tag{2.3.12}$$

$$\phi_2 \supset (1,2,\frac{-\sqrt{3}\beta}{2})\oplus(1,1,0)\oplus(1,1,\frac{-1}{2}+\frac{\beta}{2\sqrt{3}}+\frac{2\gamma}{\sqrt{6}}) \tag{2.3.13}$$

$$\phi_3 \supset (1,2,\frac{1}{2})\oplus(1,1,\frac{1}{2}+\frac{\sqrt{3}\beta}{2})\oplus(1,1,\frac{1}{2}+\frac{\beta}{2\sqrt{3}}+\frac{2\gamma}{\sqrt{6}}) \tag{2.3.14}$$

$$\phi_4 \supset (1,2,\frac{1}{2})\oplus(1,1,\frac{1}{2}+\frac{\sqrt{3}\beta}{2})\oplus(1,1,0). \tag{2.3.15}$$

The following tables represent some 341 model versions.

1)- Model A:

Name	341 representation	331 representation	Components	F
$\psi_{L\alpha}$	$(1,\bar{4},\frac{-1}{4})$	$(1,\bar{3},\frac{-1}{3})\oplus(1,1,0)$	(e^-,ν^0,N^0,N'^0)	3
e^c	(1,1,1)	(1,1,1)	e^c	3
$Q_{iL}(i=1,2)$	$(3,4,\frac{-1}{12})$	$(3,3,0)\oplus(1,1,\frac{-1}{3})$	(u_i,d_i,D_i,D'_i)	2
Q_{3L}	$(3,\bar{4},\frac{5}{12})$	$(3,\bar{3},\frac{1}{3})\oplus(1,1,\frac{2}{3})$	(d_3,u_3,U_3,U'_3)	1
u^c	$(\bar{3},1,\frac{-2}{3})$	$(\bar{3},1,\frac{-2}{3})$	u^c	3
d^c	$(\bar{3},1,\frac{1}{3})$	$(\bar{3},1,\frac{1}{3})$	d^c	3
$D^c_{1,2}$	$(\bar{3},1,\frac{1}{3})$	$(\bar{3},1,\frac{1}{3})$	$D^c_{1,2}$	2
$D'^c_{1,2}$	$(\bar{3},1,\frac{1}{3})$	$(\bar{3},1,\frac{1}{3})$	$D'^c_{1,2}$	2
U'^c_3	$(\bar{3},1,\frac{-2}{3})$	$(\bar{3},1,\frac{-2}{3})$	U'^c_3	1
U^c_3	$(\bar{3},1,\frac{-2}{3})$	$(\bar{3},1,\frac{-2}{3})$	U^c_3	1
ϕ_1	$(1,\bar{4},-\frac{1}{4})$	$(1,\bar{3},-\frac{1}{3})\oplus(1,1,0)$	$(\phi_1^-,\phi_1^0,\phi_1'^0,\phi_1''^0)$	1
ϕ_2	$(1,\bar{4},-\frac{1}{4})$	$(1,\bar{3},-\frac{1}{3})\oplus(1,1,0)$	$(\phi_2^-,\phi_2^0,\phi_2'^0,\phi_2''^0)$	1
ϕ_3	$(1,\bar{4},\frac{3}{4})$	$(1,\bar{3},\frac{2}{3})\oplus(1,1,1)$	$(\phi_3^0,\phi_3^+,\phi_3^{+\prime},\phi_3^{+\prime\prime})$	1
ϕ_4	$(1,\bar{4},-\frac{1}{4})$	$(1,\bar{3},\frac{2}{3})\oplus(1,1,0)$	$(\phi_4^-,\phi_4^0,\phi_4'^0,\phi_4''^0)$	1

Table 2.4: Field content of the model A where $\beta=\frac{1}{\sqrt{3}}$ and $\gamma=\frac{1}{\sqrt{6}}$.

2)- Model B:

Name	341 representation	331 representation	Components	F
$\psi_{L\alpha}$	$(1,4,\frac{-3}{4})$	$(1,3,\frac{-2}{3})\oplus(1,1,\text{-}1)$	(ν^0, e^-, E^-, E'^-)	3
e^c	$(1,1,1)$	$(1,1,1)$	e^c	9
$Q_{iL}(i=1,2)$	$(3,\bar{4},\frac{5}{12})$	$(3,\bar{3},\frac{1}{3})\oplus(1,1,\frac{2}{3})$	(d_i, u_i, U_i, U_i')	2
Q_{3L}	$(3,4,\frac{-1}{12})$	$(3,3,0)\oplus(1,1,\frac{-1}{3})$	(u_3, d_3, D_3, D_3')	1
u^c	$(\overline{3},1,\frac{-2}{3})$	$(\overline{3},1,\frac{-2}{3})$	u^c	3
d^c	$(\overline{3},1,\frac{1}{3})$	$(\overline{3},1,\frac{1}{3})$	d^c	3
$U^c_{1,2}$	$(\overline{3},1,\frac{-2}{3})$	$(\overline{3},1,\frac{-2}{3})$	$U^c_{1,2}$	2
$U'^c_{1,2}$	$(\overline{3},1,\frac{-2}{3})$	$(\overline{3},1,\frac{-2}{3})$	$U'^c_{1,2}$	2
D'^c_3	$(\overline{3},1,\frac{1}{3})$	$(\overline{3},1,\frac{1}{3})$	D'^c_3	1
D^c_3	$(\overline{3},1,\frac{1}{3})$	$(\overline{3},1,\frac{1}{3})$	D^c_3	1
ϕ_1	$(1,\overline{4},-\frac{1}{4})$	$(1,\overline{3},-\frac{1}{3})\oplus(1,1,0)$	$(\phi_1^-,\phi_1^0,\phi_1'^0,\phi_1''^0)$	1
ϕ_2	$(1,\overline{4},-\frac{1}{4})$	$(1,\bar{3},-\frac{1}{3})\oplus(1,1,0)$	$(\phi_2^-,\phi_2^0,\phi_2'^0,\phi_2''^0)$	1
ϕ_3	$(1,\overline{4},\frac{3}{4})$	$(1,\bar{3},\frac{2}{3})\oplus(1,1,1)$	$(\phi_3^0,\phi_3^+,\phi_3^{+\prime},\phi_3^{+\prime\prime})$	1
ϕ_4	$(1,\overline{4},-\frac{1}{4})$	$(1,\bar{3},\frac{2}{3})\oplus(1,1,0)$	$(\phi_4^-,\phi_4^0,\phi_4'^0,\phi_4''^0)$	1

Table 2.5: Field content of the model B where $\beta=\frac{1}{\sqrt{3}}$ and $\gamma=\frac{1}{\sqrt{6}}$.

3)- Model E:

Name	341 representation	331 representation	Components	F
$\psi_{L\alpha}$	$(1,\bar{4},\frac{-1}{2})$	$(1,\bar{3},\frac{-1}{3})\oplus(1,1,\text{-}1)$	(e^-,ν^0,N^0,E^-)	3
e^c	$(1,1,1)$	$(1,1,1)$	e^c	6
$Q_{iL}(i=1,2)$	$(3,4,\frac{1}{6})$	$(3,3,0)\oplus(1,1,\frac{2}{3})$	(u_i,d_i,D_i,U_i)	2
Q_{3L}	$(3,\bar{4},\frac{1}{6})$	$(3,\bar{3},\frac{1}{3})\oplus(1,1,\frac{-1}{3})$	(d_3,u_3,U_3,D_3)	1
u^c	$(\overline{3},1,\frac{-2}{3})$	$(\overline{3},1,\frac{-2}{3})$	u^c	3
d^c	$(\overline{3},1,\frac{1}{3})$	$(\overline{3},1,\frac{1}{3})$	d^c	3
$U^c_{1,2}$	$(\overline{3},1,\frac{-2}{3})$	$(\overline{3},1,\frac{-2}{3})$	$U^c_{1,2}$	2
$D^c_{1,2}$	$(\overline{3},1,\frac{1}{3})$	$(\overline{3},1,\frac{1}{3})$	$D^c_{1,2}$	1
U^c_3	$(\overline{3},1,\frac{-2}{3})$	$(\overline{3},1,\frac{-2}{3})$	U^c_3	2
D^c_3	$(\overline{3},1,\frac{1}{3})$	$(\overline{3},1,\frac{1}{3})$	D^c_3	1
ϕ_1	$(1,\overline{4},\frac{-\beta}{\sqrt{3}}+\frac{\gamma}{2\sqrt{6}})$	$(1,\bar{3},\text{-}\frac{1}{3})\oplus(1,1,\text{-}1)$	$(\phi_1^-,\phi_1^0,\phi_1'^0,\phi_1'^-)$	1
ϕ_2	$(1,\overline{4},\frac{-1}{2}+\frac{\beta}{2\sqrt{3}}+\frac{\gamma}{2\sqrt{6}})$	$(1,\bar{3},\text{-}\frac{1}{3})\oplus(1,1,\text{-}1)$	$(\phi_2^-,\phi_2^0,\phi_2'^0,\phi_2'^-)$	1
ϕ_3	$(1,\overline{4},\frac{1}{2}+\frac{\beta}{2\sqrt{3}}+\frac{\gamma}{2\sqrt{6}})$	$(1,\bar{3},\frac{2}{3})\oplus(1,1,0)$	$(\phi_3^0,\phi_3^+,\phi_3'^+,\phi_3'^0)$	1
ϕ_4	$(1,\overline{4},\frac{-3\gamma}{2\sqrt{6}})$	$(1,\bar{3},\frac{2}{3})\oplus(1,1,0)$	$(\phi_4^0,\phi_4^+,\phi_4'^+,\phi_4'^0)$	1

Table 2.6: Field content of the model E where $\beta=\frac{1}{\sqrt{3}}$ and $\gamma=\frac{-2}{\sqrt{6}}$.

4)- Model F:

Name	341 representation	331 representation	Components	F
$\psi_{L\alpha}$	$(1,4,\frac{-1}{2})$	$(1,3,\frac{-2}{3})\oplus(1,1,0)$	(ν^0, e^-, E^-, N^0)	3
e^c	(1,1,1)	(1,1,1)	e^c	6
$Q_{iL}(i=1,2)$	$(3,\overline{4},\frac{1}{6})$	$(3,\bar{3},\frac{1}{3})\oplus(1,1,\frac{-1}{3})$	(d_i, u_i, U_i, D_i)	2
Q_{3L}	$(3,4,\frac{1}{6})$	$(3,3,0)\oplus(1,1,\frac{2}{3})$	(u_3, d_3, D_3, U_3)	1
u^c	$(\overline{3},1,\frac{-2}{3})$	$(\overline{3},1,\frac{-2}{3})$	u^c	3
d^c	$(\overline{3},1,\frac{1}{3})$	$(\overline{3},1,\frac{1}{3})$	d^c	3
$U^c_{1,2}$	$(\overline{3},1,\frac{-2}{3})$	$(\overline{3},1,\frac{-2}{3})$	$U^c_{1,2}$	2
$D^c_{1,2}$	$(\overline{3},1,\frac{1}{3})$	$(\overline{3},1,\frac{1}{3})$	$D^c_{1,2}$	1
D^c_3	$(\overline{3},1,\frac{1}{3})$	$(\overline{3},1,\frac{1}{3})$	D^c_3	2
U^c_3	$(\overline{3},1,\frac{-2}{3})$	$(\overline{3},1,\frac{-2}{3})$	U^c_3	1
ϕ_1	$(1,\overline{4},\frac{-\beta}{\sqrt{3}}+\frac{\gamma}{2\sqrt{6}})$	$(1,\bar{3},\text{-}\frac{1}{3})\oplus(1,1,\text{-}1)$	$(\phi_1^-,\phi_1^0,\phi_1'^0,\phi_1'^-)$	1
ϕ_2	$(1,\overline{4},\frac{-1}{2}+\frac{\beta}{2\sqrt{3}}+\frac{\gamma}{2\sqrt{6}})$	$(1,\bar{3},\text{-}\frac{1}{3})\oplus(1,1,\text{-}1)$	$(\phi_2^-,\phi_2^0,\phi_2'^0,\phi_2'^-)$	1
ϕ_3	$(1,\overline{4},\frac{1}{2}+\frac{\beta}{2\sqrt{3}}+\frac{\gamma}{2\sqrt{6}})$	$(1,\bar{3},\frac{2}{3})\oplus(1,1,0)$	$(\phi_3^0,\phi_3^+,\phi_3'^+,\phi_3'^0)$	1
ϕ_4	$(1,\overline{4},\frac{-3\gamma}{2\sqrt{6}})$	$(1,\bar{3},\frac{2}{3})\oplus(1,1,0)$	$(\phi_4^0,\phi_4^+,\phi_4'^+,\phi_4'^0)$	1

Table 2.7: Field content of the model F where $\beta=\frac{1}{\sqrt{3}}$ and $\gamma=\frac{-2}{\sqrt{6}}$.

5)- Model of F. Pisano and V. Pleitez:

Name	341 representation	331 representation	Components	F
$\psi_{\alpha L}$	(1,4,0)	$(1,3,\frac{-1}{3})$+(1,1,1)	$(\nu_\alpha, \ell_\alpha, \nu^c_\alpha, \ell^c_\alpha)$	3
$Q_{iL}(i=2,3)$	$(3,\overline{4},\frac{-1}{3})$	$(3,\bar{3},0)$+$(3,1,\frac{-4}{3})$	(d_i, u_i, D_i, J_i)	2
Q_{1L}	$(3,4,\frac{2}{3})$	$(3,3,\frac{1}{3})$+$(3,1,\frac{5}{3})$	(u_1, d_1, U_1, J_1)	1
u_{jR}(j=1,i)	$(\overline{3},1,\frac{2}{3})$	$(\overline{3},1,\frac{2}{3})$	u_{jR}	4
$d_{jR}(j=1,i)$	$(\overline{3},1,\frac{-1}{3})$	$(\overline{3},1,\frac{-1}{3})$	d_{jR}	5
J_{1R}	$(\overline{3},1,\frac{5}{3})$	$(\overline{3},1,\frac{5}{3})$	J_{1R}	1
$J_{iR}(i=2,3)$	$(\overline{3},1,\frac{-4}{3})$	$(\overline{3},1,\frac{-4}{3})$	J_{iR}	2
ϕ_1	$(1,\overline{4},0)$	$(1,\bar{3},\frac{1}{3})\oplus(1,1,\text{-}1)$	$(\phi_1^0,\phi_1^+,\phi_1'^0,\phi_1^-)$	1
ϕ_2	$(1,\overline{4},\text{-}1)$	$(1,\bar{3},-\frac{2}{3})\oplus(1,1,\text{-}2)$	$(\phi_2^-,\phi_2^0,\phi_2'^-,\phi_2^{--})$	1
ϕ_3	$(1,\overline{4},0)$	$(1,\bar{3},\frac{1}{3})\oplus(1,1,\text{-}1)$	$(\phi_3^0,\phi_3^+,\phi_3'^0,\phi_3^-)$	1
ϕ_4	$(1,\overline{4},1)$	$(1,\bar{3},\frac{4}{3})\oplus(1,1,0)$	$(\phi_4^+,\phi_4^{++},\phi_4'^+,\phi_4^0)$	1

Table 2.8: Field content of the model of F. Pisano and V. Pleitez where $\beta=\frac{-1}{\sqrt{3}}$ and $\gamma=\frac{-4}{\sqrt{6}}$ [96].

The scalar sector for the model F. Pisano and V. Pleitez contains four scalar fields and also it can contain an extra 10 plet scalar matrix which is:

$$\begin{pmatrix} H_1^0 & H_1^+ & H_2^0 & H_2^- \\ H_1^+ & H_1^{++} & H_3^+ & H_3^0 \\ H_2^0 & H_3^+ & H_4^0 & H_4^- \\ H_2^- & H_3^0 & H_4^- & H_2^{--} \end{pmatrix} \sim (1, 10_S, 0). \tag{2.3.16}$$

Another version of 341 models is constructed from the F. Pisano and V. Pleitez with an economical scalar fields (it has been used only three scalar fields [38]), it called the compact 341 model.

2.3.2 Gauge boson sector

In the 341 models, they do exist 4^2-1 gauge bosons. Thus, those models predict the existence of 15 gauge bosons, Some of them are neutral and the other are charged, namely $W^{\mp}$, K'^{Q_1},$K_1^{Q_3}$,X^{Q_2},V^{Q_4} and Y^{Q_5}, Z with extra neutral bosons Z' and Z''.

From the Lagrangian (2.3.17), we get the gauge bosons masses and their interactions.

$$\mathcal{L}=(D_\mu\eta)^\dagger(D^\mu\eta)+(D_\mu\rho)^\dagger(D^\mu\rho)+(D_\mu\chi)^\dagger(D^\mu\chi)+...., \tag{2.3.17}$$

where η, ρ and χ are scalar fields, D_μ is the covariant derivative, its expression in the 341 models is giving by:

$$D_\mu=\partial_\mu+ig\frac{W_\mu^a\lambda_a}{2}+iXg_XW_\mu^X, \tag{2.3.18}$$

where a=1....15, λ_a represent the Gell-Mann matrices of the group $SU(4)$ (see the appendix C).

2.3.3 Charged gauge bosons

From the Lagrangian (2.3.17), we get the following matrix which collect all the charged gauge bosons:

$$W_\mu^a\lambda^a=\begin{pmatrix} W_3+\frac{W_8}{\sqrt{3}}+\frac{W_{15}}{\sqrt{6}} & \sqrt{2}W^+ & \sqrt{2}K'^{-Q_1} & \sqrt{2}X^{-Q_2} \\ \sqrt{2}W^- & -W_3+\frac{W_8}{\sqrt{3}}+\frac{W_{15}}{\sqrt{6}} & \sqrt{2}K_1^{-Q_3} & \sqrt{2}V^{-Q_4} \\ \sqrt{2}K^{Q_1} & \sqrt{2}K_1^{Q_3} & \frac{-2W_8}{\sqrt{3}}+\frac{W_{15}}{\sqrt{6}} & \sqrt{2}Y^{-Q_5} \\ \sqrt{2}X^{Q_2} & \sqrt{2}V^{Q_4} & \sqrt{2}Y^{Q_5} & \frac{-3W_{15}}{\sqrt{6}} \end{pmatrix} \tag{2.3.19}$$

Where we use the following combinations:

$$W^{\mp} = \frac{(W_\mu^1\pm iW_\mu^2)}{\sqrt{2}}, \tag{2.3.20}$$

$$K'^{\mp Q_1},K^{\mp Q_1} = \frac{(W_\mu^4\mp iW_\mu^5)}{\sqrt{2}}, \tag{2.3.21}$$

$$K_1^{\mp Q_3} = \frac{(W_\mu^6\mp iW_\mu^7)}{\sqrt{2}}, \tag{2.3.22}$$

$$X^{\mp Q_2} = \frac{(W_\mu^9\mp iW_\mu^{10})}{\sqrt{2}}, \tag{2.3.23}$$

$$V^{\mp Q_4} = \frac{(W_\mu^{11} \mp iW_\mu^{12})}{\sqrt{2}}, \tag{2.3.24}$$

$$Y^{\mp Q_5} = \frac{(W_\mu^{13} \mp iW_\mu^{14})}{\sqrt{2}}. \tag{2.3.25}$$

Using the expression (2.3.1), we find the electric charges of the charged gauge bosons in the compact 341 model where we have used $\beta = \frac{-1}{\sqrt{3}}$ and $\gamma = \frac{-4}{\sqrt{6}}$:

$$Q_1 = \frac{-1-b}{2} = 0, \tag{2.3.26}$$

$$Q_2 = \frac{-b-3-2c}{6} = 1, \tag{2.3.27}$$

$$Q_3 = \frac{1-b}{2} = 1, \tag{2.3.28}$$

$$Q_4 = \frac{-b+3-2c}{6} = 2, \tag{2.3.29}$$

$$Q_5 = \frac{-c+b}{3} = 1. \tag{2.3.30}$$

Notice that we used b=-1 and c=-4, we replace the electric charges values in the matrix (2.3.19) to get:

$$W_\mu^a \lambda^a = \begin{pmatrix} W_3 + \frac{W_8}{\sqrt{3}} + \frac{W_{15}}{\sqrt{6}} & \sqrt{2}W^+ & \sqrt{2}K'^0 & \sqrt{2}X^- \\ \sqrt{2}W^- & -W_3 + \frac{W_8}{\sqrt{3}} + \frac{W_{15}}{\sqrt{6}} & \sqrt{2}K_1^- & \sqrt{2}V^{--} \\ \sqrt{2}K^0 & \sqrt{2}K_1^+ & \frac{-2W_8}{\sqrt{3}}\frac{W_{15}}{\sqrt{6}} & \sqrt{2}Y^- \\ \sqrt{2}X^+ & \sqrt{2}V^{++} & \sqrt{2}Y^+ & \frac{-3W_{15}}{\sqrt{6}} \end{pmatrix} \tag{2.3.31}$$

From (2.3.31), we get 15 gauge bosons, with simple, double and neutral electric charges.

During the development of the Lagrangian (2.3.17) and by using the matrix (2.3.31) with the last gauge bosons combinations (2.3.20)-(2.3.25), we get the expression of the charged gauge bosons masses:

$$M^2_{W^\mp} = \frac{g^2}{4}\upsilon_\rho^2, \tag{2.3.32}$$

$$M^2_{K'^0,K^0} = \frac{g^2}{4}\upsilon_\eta^2, \tag{2.3.33}$$

$$M^2_{K_1^\mp} = \frac{g^2}{4}(\upsilon_\eta^2 + \upsilon_\rho^2), \tag{2.3.34}$$

$$M^2_{X^\mp} = \frac{g^2}{4}\upsilon_\chi^2, \tag{2.3.35}$$

$$M^2_{V^{\mp\mp}} = \frac{g^2}{4}(\upsilon_\rho^2 + \upsilon_\chi^2), \tag{2.3.36}$$

$$M^2_{Y^\mp} = \frac{g^2}{4}(\upsilon_\eta^2 + \upsilon_\chi^2). \tag{2.3.37}$$

Where g is the coupling constant of the electroweak interactions, υ_ρ, υ_χ and υ_η are the vacuum expectation values.

2.3.4 Neutral gauge bosons

Regarding the neutral gauge bosons Z, Z' and Z'', they receive their masses from the following matrix where it has written in the basis (W^3, W^8, W^{15}, W^X) [38]:

$$\begin{pmatrix} \upsilon_\rho^2 & \frac{-1}{\sqrt{3}}\upsilon_\rho^2 & \frac{-1}{\sqrt{6}}\upsilon_\rho^2 & -2t\upsilon_\rho^2 \\ \frac{-1}{\sqrt{3}}\upsilon_\rho^2 & \frac{1}{3}(\upsilon_\rho^2+4\upsilon_\eta^2) & \frac{1}{3\sqrt{2}}(\upsilon_\rho^2-2\upsilon_\eta^2) & \frac{2t}{\sqrt{3}}\upsilon_\rho^2 \\ \frac{-1}{\sqrt{6}}\upsilon_\rho^2 & \frac{1}{3\sqrt{2}}(\upsilon_\rho^2-2\upsilon_\eta^2) & \frac{1}{6}(\upsilon_\eta^2+\upsilon_\rho^2+9\upsilon_\chi^2) & \frac{2t}{\sqrt{6}}(\upsilon_\rho^2+3\upsilon_\chi^2) \\ -2t\upsilon_\rho^2 & \frac{2t}{\sqrt{3}}\upsilon_\rho^2 & \frac{2t}{\sqrt{6}}(\upsilon_\rho^2+3\upsilon_\chi^2) & 4t^2(\upsilon_\rho^2+\upsilon_\chi^2) \end{pmatrix} \tag{2.3.38}$$

Where

$$t = \frac{g_X}{g} = \sqrt{\frac{S_W^2}{1-4S_W^2}} \tag{2.3.39}$$

Diagonalezing the matrix (2.3.38) using the simplifying (and reasonable) assumption $\upsilon_\chi \simeq \upsilon_\eta \gg \upsilon_\rho$ to get its eigenvalues which present the neutral gauges bosons masses:

$$M_A^2 = 0 \tag{2.3.40}$$

$$M_Z^2 = \frac{g^2\upsilon_\rho^2}{4C_W^2} = (91GeV)^2, \tag{2.3.41}$$

$$M_Z'^2 = \frac{g^2C_W^2\upsilon_\eta^2}{h_W^2}, \tag{2.3.42}$$

$$M_Z''^2 = \frac{g^2\upsilon_\eta^2(1-4S_W^2)+h_W^2}{8h_W^2(1-4S_W^2)}. \tag{2.3.43}$$

where $M_Z < M_{Z\prime} < M_{Z\prime\prime}$, the lightest neutral gauge boson corresponds to the Z of the Standard Model and θ is the electroweak mixing angle (Weinberg angle). Concerning the eigenvectors of (2.3.38), they are found to be:

$$A^\mu = S_W W_3^\mu + C_W\left[\frac{T_W}{\sqrt{3}}(-W_8^\mu - 2\sqrt{2}W_{15}^\mu) + \sqrt{1-3T_W^2}W_X^\mu\right], \tag{2.3.44}$$

$$Z^\mu = C_\mu W_3^\mu - S_W\left[\frac{T_w}{\sqrt{3}}(-W_8^\mu - 2\sqrt{2}W_{15}^\mu) + \sqrt{1-3T_W^2}W_X^\mu\right], \tag{2.3.45}$$

$$Z'^\mu = \frac{\sqrt{3}}{3}\frac{\sqrt{1-3T_W^2}}{\sqrt{1-4S_W^2}}\left(\sqrt{h_W}W_8^\mu - 2\sqrt{2}\frac{S_W^2}{\sqrt{h_W}}W_{15}^\mu\right), \tag{2.3.46}$$

$$Z''^\mu = \frac{\sqrt{3}\sqrt{1-4S_W^2}}{\sqrt{h_W}}W_{15}^\mu + \frac{2\sqrt{2}S_W}{\sqrt{h_W}}W_X^\mu. \tag{2.3.47}$$

We have motioned here that $C_W = \cos\theta_W$, $S_W = \sin\theta_W$, $T_W = \tan\theta_W$ and $h_W = 3-4S_W^2$.

2.3.5 Scalar sector

Scalar fields

In the 341 models, in order to break spontaneously the gauge symmetry to give masses to all particles a set of four scalars fields have been introduced $\eta \sim (1,4,X_\eta), \rho \sim (1,4,X_\rho)$, $\chi \sim (1,4,X_\chi)$ and $\xi \sim (1,4,X_\xi)$. To determine the value of the $X_{\eta,\rho,\chi,\xi}$ and to find the electric charges of the element of those fields, the electric charge annihilates the VEVs:

$$X_\xi = -\frac{1}{2} - \frac{\beta}{2\sqrt{3}} - \frac{\gamma}{2\sqrt{6}}, \tag{2.3.48}$$

$$X_\rho = \frac{1}{2} - \frac{\beta}{2\sqrt{3}} - \frac{\gamma}{2\sqrt{6}}, \tag{2.3.49}$$

$$X_\eta = \frac{\beta}{\sqrt{3}} - \frac{\gamma}{2\sqrt{6}}, \tag{2.3.50}$$

$$X_\chi = \frac{3\gamma}{2\sqrt{6}}. \tag{2.3.51}$$

which also satisfies the relationship $X_\rho + X_\eta + X_\xi + X_\chi = 0$. Table (2.9) represents the scalar fields content of the 341 models for generic β and γ parameters.

Name	341 representation	331 representation	Components	F
ϕ_1	$(1,\overline{4},\frac{-\beta}{\sqrt{3}}+\frac{\gamma}{2\sqrt{6}})$	$(1,\bar{3},\text{-}\frac{1}{2}+\frac{\beta}{2\sqrt{3}})\oplus(1,1,-\frac{\beta}{\sqrt{3}}+\frac{2\gamma}{\sqrt{6}})$	$(\phi_1^{q_1},\phi_1^{q_2},\phi_1^{q_3},\phi_1^{q_4})$	1
ϕ_2	$(1,\overline{4},\frac{-1}{2}+\frac{\beta}{2\sqrt{3}}+\frac{\gamma}{2\sqrt{6}})$	$(1,\bar{3},-\frac{\beta}{\sqrt{3}})\oplus(1,1,-\frac{1}{2}+\frac{\beta}{2\sqrt{3}}+\frac{2\gamma}{\sqrt{6}})$	$(\phi_2^{q_1},\phi_2^{q_2},\phi_2^{q_3},\phi_2^{q_4})$	1
ϕ_3	$(1,\overline{4},\frac{1}{2}+\frac{\beta}{2\sqrt{3}}+\frac{\gamma}{2\sqrt{6}})$	$(1,\bar{3},\frac{1}{2}+\frac{\beta}{2\sqrt{3}})\oplus(1,1,\frac{1}{2}+\frac{\beta}{2\sqrt{3}}+\frac{2\gamma}{\sqrt{6}})$	$(\phi_3^{q_1},\phi_3^{q_2},\phi_3^{q_3},\phi_3^{q_4})$	1
ϕ_4	$(1,\overline{4},\frac{-3\gamma}{2\sqrt{6}})$	$(1,\bar{3},\frac{1}{2}+\frac{\beta}{2\sqrt{3}})\oplus(1,1,0)$	$(\phi_4^{q_1},\phi_4^{q_2},\phi_4^{q_3},\phi_4^{q_4})$	1

Table 2.9: Scalar fields content of the 341 models for generic β and γ parameters where F represents the number of flavors.

In the compact 341 model where $\beta = \frac{-1}{\sqrt{3}}$ and $\gamma = \frac{-4}{\sqrt{6}}$, we get $X_\rho = 1$, $X_\eta = 0$, $X_\chi = -1$ and $X_\xi = 0$. To avoid the mixing between the scalars η and ξ, the later has been removed therefore the scalar sector (which are necessary to generate masses) contains only three Higgs quadruplets. The compact 341 model version contains a minimum number of the scalar fields compared to the other versions, since some of them have four scalar fields and the other have four scalar fields with an additional scalar 10-plet [31].

In the compact 341 model version, the scalar fields are presented by this content:

$$\begin{pmatrix} \eta_1^{Q_1} \\ \eta_1^{Q_2} \\ \eta_2^{Q_3} \\ \eta_2^{Q_4} \end{pmatrix}, \quad \begin{pmatrix} \rho_1^{Q_5} \\ \rho^{Q_6} \\ \rho_2^{Q_7} \\ \rho^{Q_8} \end{pmatrix}, \quad \begin{pmatrix} \chi_1^{Q_9} \\ \chi^{Q_{10}} \\ \chi_2^{Q_{11}} \\ \chi^{Q_{12}} \end{pmatrix}. \tag{2.3.52}$$

Using the expression (2.3.1) with $\beta = \frac{-1}{\sqrt{3}}$ and $\gamma = \frac{-4}{\sqrt{6}}$, we get the following fields with their electric charges entries:

$$\begin{pmatrix} \eta_1^0 \\ \eta_1^- \\ \eta_2^0 \\ \eta_2^+ \end{pmatrix} \sim (1,4,0), \qquad \begin{pmatrix} \rho_1^+ \\ \rho^0 \\ \rho_2^+ \\ \rho^{++} \end{pmatrix} \sim (1,4,1), \qquad \begin{pmatrix} \chi_1^- \\ \chi^{--} \\ \chi_2^- \\ \chi^0 \end{pmatrix} \sim (1,4,-1). \tag{2.3.53}$$

The non-trivial vacuum expectation values of the scalar fields are given by:

$$\begin{pmatrix} 0 \\ 0 \\ \frac{\upsilon_\eta}{\sqrt{2}} \\ 0 \end{pmatrix}, \qquad \begin{pmatrix} 0 \\ \frac{\upsilon_\rho}{\sqrt{2}} \\ 0 \\ 0 \end{pmatrix}, \qquad \begin{pmatrix} 0 \\ 0 \\ 0 \\ \frac{\upsilon_\chi}{\sqrt{2}} \end{pmatrix}. \tag{2.3.54}$$

The expressions of the η_1^0, η_2^0, ρ^0 and χ^0 are:

$$\eta_1^0 = \frac{1}{\sqrt{2}}(R_{\eta_1} + iI_{\eta_1}), \tag{2.3.55}$$

$$\eta_2^0 = \frac{1}{\sqrt{2}}(\upsilon_\eta + R_{\eta_2} + iI_{\eta_2}), \tag{2.3.56}$$

$$\rho^0 = \frac{1}{\sqrt{2}}(\upsilon_\rho + R_\rho + iI_\rho), \tag{2.3.57}$$

$$\chi^0 = \frac{1}{\sqrt{2}}(\upsilon_\chi + R_\chi + iI_\chi), \tag{2.3.58}$$

where R_ρ, R_{η_2} and R_χ are neutrals fields which the scalar bosons h_1, h_2 and h_3 will be written as a function of them as we mention in next section and I_ρ, I_{η_2}, I_{η_1}, I_χ and R_{η_1} are a set of Goldstone bosons.

The VEV υ_χ is responsible for the first step in breaking the 341 symmetry to 331, while υ_η breaks the 331 symmetry to 321 and the final breaking to $U(1)_{QED}$ is provided by υ_ρ:

$$\begin{gathered} SU(3)_c \otimes SU(4)_L \otimes U(1)_X \\ \Downarrow \upsilon_\chi \\ SU(3)_c \otimes SU(3)_L \otimes U(1)_{X'} \\ \Downarrow \upsilon_\eta \\ SU(3)_c \otimes SU(2)_L \otimes U(1)_Y \\ \Downarrow \upsilon_\rho \\ SU(3)_c \otimes U_{QED} \end{gathered} \tag{2.3.59}$$

In this way we can impose that $\upsilon_\chi > \upsilon_\eta > \upsilon_\rho$=246 GeV.

To build the scalar potential in this model, all the possible combinations between η, ρ and

χ have to be taken into account [2], we get the most general scalar potential in the compact 341 model which is invariant under the gauge symmetry and under the additional discrete symmetry Z_3 [38]:

$$\begin{aligned} V(\eta,\rho,\chi) &= \mu_\eta^2\eta^\dagger\eta+\mu_\rho^2\rho^\dagger\rho+\mu_\chi^2\chi^\dagger\chi+\lambda_1(\eta^\dagger\eta)^2+\lambda_2(\rho^\dagger\rho)^2+\lambda_3(\chi^\dagger\chi)^2, \\ &+ \lambda_4(\eta^\dagger\eta)(\rho^\dagger\rho)+\lambda_5(\eta^\dagger\eta)(\chi^\dagger\chi)+\lambda_6(\rho^\dagger\rho)(\chi^\dagger\chi)+\lambda_7(\rho^\dagger\eta)(\eta^\dagger\rho), \\ &+ \lambda_8(\chi^\dagger\eta)(\eta^\dagger\chi)+\lambda_9(\rho^\dagger\chi)(\chi^\dagger\rho), \end{aligned} \tag{2.3.60}$$

where $\mu^2_{\mu\rho\chi}$ are the mass dimension parameters and λ_S are dimensionless coupling constants. The scalar potential (2.3.60) is minimized to get the following minimum conditions:

$$\mu_\eta^2+\lambda_1\upsilon_\eta^2+\frac{1}{2}\lambda_4\upsilon_\rho^2+\frac{1}{2}\lambda_5\upsilon_\chi^2=0, \tag{2.3.61}$$

$$\mu_\rho^2+\lambda_2\upsilon_\rho^2+\frac{1}{2}\lambda_4\upsilon_\eta^2+\frac{1}{2}\lambda_6\upsilon_\chi^2=0, \tag{2.3.62}$$

$$\mu_\chi^2+\lambda_3\upsilon_\chi^2+\frac{1}{2}\lambda_5\upsilon_\eta^2+\frac{1}{2}\lambda_6\upsilon_\rho^2=0. \tag{2.3.63}$$

Scalar bosons

In the compact 341 model, the scalar sector contains 09 scalars bosons, three neutral h_1, h_2 and h_3, four singly $h_1^\mp$ and $h_2^\mp$ and two doubly charged $h^{\mp\mp}$ scalar bosons.

From the scalar potential and by using the minimum conditions (2.3.61)-(2.3.63), in the basis (R_η, R_ρ, R_χ) we found the following mass matrix:

$$\frac{1}{2}\begin{pmatrix} 2\lambda_1\upsilon_\eta^2 & \lambda_4\upsilon_\eta\upsilon_\rho & \lambda_5\upsilon_\eta\upsilon_\chi, \\ \lambda_4\upsilon_\eta\upsilon_\rho & 2\lambda_2\upsilon_\rho^2 & \lambda_6\upsilon_\rho\upsilon_\chi^2, \\ \lambda_5\upsilon_\eta\upsilon_\chi & \lambda_6\upsilon_\rho^2\upsilon_\chi^2 & 2\lambda_3\upsilon_\chi^2. \end{pmatrix} \tag{2.3.64}$$

The eigenvalues of this matrix are:

$$m_{h_1}^2 = \lambda_2\upsilon_\rho^2+\frac{\lambda_3\lambda_4^2+\lambda_6(\lambda_1\lambda_6-\lambda_4\lambda_5)}{\lambda_5^2-4\lambda_1\lambda_3}\upsilon_\rho^2, \tag{2.3.65}$$

$$m_{h_2}^2 = c_1\upsilon_\chi^2+c_2\upsilon_\rho^2, \tag{2.3.66}$$

$$m_{h_3}^2 = c_3\upsilon_\chi^2+c_4\upsilon_\rho^2, \tag{2.3.67}$$

where the expression of c_1, c_2 are c_3 are given by:

$$c_1 = \frac{1}{2}\left(\lambda_1+\lambda_3-\sqrt{(\lambda_1-\lambda_3)^2+\lambda_5^2}\right). \tag{2.3.68}$$

[2] It exists another term $\lambda_{10}(\eta^\dagger\chi)(\eta^\dagger\rho)$+h.c but it is forbidden under the discrete symmetry Z_3.

$$c_2 = \frac{\left[\lambda_4(\lambda_1-\lambda_3-\sqrt{(\lambda_1-\lambda_3)^2+\lambda_5^2})+\lambda_5\lambda_6\right]^2}{4c_1\left[\lambda_5^2-(\lambda_1-\lambda_3)(\lambda_3-\lambda_1+\sqrt{(\lambda_1-\lambda_3)^2+\lambda_5^2}\right]}. \tag{2.3.69}$$

$$c_3 = \frac{1}{2}\left(\lambda_1+\lambda_3+\sqrt{(\lambda_1-\lambda_3)^2+\lambda_5^2}\right). \tag{2.3.70}$$

The three expressions (2.3.65)-(2.3.67) represent the masses of the CP even neutral scalars h_1, h_2 and h_3 respectively. The lightest neutral scalar h_1 is identified as the SM Higgs like-boson. The matrix (2.3.64) has the following eigenvectors:

$$h_1 = R_\rho. \tag{2.3.71}$$

$$h_2 = aR_{\eta_2}+bR_\chi. \tag{2.3.72}$$

$$h_3 = cR_{\eta_2}+dR_\chi. \tag{2.3.73}$$

Those eigenvectors represent the physical neutral scalars h_1, h_2 and h_3 respectively where:

$$a = \frac{\lambda_1-\lambda_3-\sqrt{(\lambda_1-\lambda_3)^2+\lambda_5^2}}{\lambda_5^2+(\lambda_1-\lambda_3-\sqrt{(\lambda_1-\lambda_3)^2+\lambda_5^2})} \tag{2.3.74}$$

$$b = \frac{\lambda_5}{\lambda_5^2+(\lambda_1-\lambda_3-\sqrt{(\lambda_1-\lambda_3)^2+\lambda_5^2})} \tag{2.3.75}$$

$$c = \frac{\lambda_1-\lambda_3+\sqrt{(\lambda_1-\lambda_3)^2+\lambda_5^2}}{\lambda_5^2+(\lambda_1-\lambda_3+\sqrt{(\lambda_1-\lambda_3)^2+\lambda_5^2})} \tag{2.3.76}$$

$$d = \frac{\lambda_5}{\lambda_5^2+(\lambda_1-\lambda_3+\sqrt{(\lambda_1-\lambda_3)^2+\lambda_5^2})} \tag{2.3.77}$$

From the expressions of h_1, h_2 and h_3, we get the expressions of R_ρ, R_{η_2} and R_χ as follows:

$$R_\rho = h_1, \tag{2.3.78}$$

$$R_{\eta_2} = \alpha h_2+\beta h_3, \tag{2.3.79}$$

$$R_\chi = \gamma h_2+\sigma h_3, \tag{2.3.80}$$

where the parameters α, β, γ and σ are in the appendix A.
In the basis $(\rho_2^\mp, \eta_1^\mp)$, we get the following mass matrix:

$$\frac{1}{2}\begin{pmatrix}\lambda_7\upsilon_\eta^2 & \lambda_7\upsilon_\eta\upsilon_\rho\\ \lambda_7\upsilon_\eta\upsilon_\rho & \lambda_7\upsilon_\rho^2\end{pmatrix} \tag{2.3.81}$$

Its eigenvalues are:

$$m^2_{G_1^\mp} = 0 \tag{2.3.82}$$

$$m^2_{h_1^\mp} = \frac{\lambda_7}{2}(\upsilon_\eta^2+\upsilon_\rho^2) \tag{2.3.83}$$

Those eigenvalues represent the massless Goldstone boson $G^{\mp}$ and the mass of the first charged scalar boson $h_1^{\mp}$. The expression of its eigenvectors are:

$$G_1^{\mp} = \frac{-\upsilon_\eta}{\sqrt{\upsilon_\eta^2+\upsilon_\rho^2}}\eta_1^{\mp} + \frac{-\upsilon_\chi}{\sqrt{\upsilon_\eta^2+\upsilon_\rho^2}}\rho_2^{\mp}, \tag{2.3.84}$$

$$h_1^{\mp} = \frac{-\upsilon_\rho}{\sqrt{\upsilon_\eta^2+\upsilon_\rho^2}}\eta_1^{\mp} + \frac{-\upsilon_\eta}{\sqrt{\upsilon_\eta^2+\upsilon_\rho^2}}\rho_2^{\mp}, \tag{2.3.85}$$

where $G_1^{\mp}$ represents a Goldstone Boson, while $h_1^{\mp}$ is one of the charged scalars bosons in this model which will be in the physical spectrum.

Concerning the mass matrix in the basis $(\eta_2^{\mp}, \chi_2^{\mp})$, it takes the following form:

$$\frac{1}{2}\begin{pmatrix} \lambda_8\upsilon_\chi^2 & \lambda_8\upsilon_\eta\upsilon_\chi, \\ \lambda_8\upsilon_\chi\upsilon_\eta & \lambda_8\upsilon_\eta^2. \end{pmatrix} \tag{2.3.86}$$

Its eigenvalues are:

$$m^2_{G_2^{\mp}} = 0 \tag{2.3.87}$$

$$m^2_{h_2^{\mp}} = \frac{\lambda_8}{2}(\upsilon_\eta^2+\upsilon_\chi^2) \tag{2.3.88}$$

Those expressions represent a a massless Goldstone boson $G_2^{\mp}$ and the mass of the second physical charged scalar boson $h_2^{\mp}$. This matrix have the following eigenvectors:

$$G_2^{\mp} = \frac{-\upsilon_\eta}{\sqrt{\upsilon_\eta^2+\upsilon_\chi^2}}\eta_1^{\mp} + \frac{-\upsilon_\chi}{\sqrt{\upsilon_\eta^2+\upsilon_\chi^2}}\rho_2^{\mp}, \tag{2.3.89}$$

$$h_2^{\mp} = \frac{-\upsilon_\rho}{\sqrt{\upsilon_\eta^2+\upsilon_\chi^2}}\eta_1^{\mp} + \frac{-\upsilon_\eta}{\sqrt{\upsilon_\eta^2+\upsilon_\chi^2}}\rho_2^{\mp}. \tag{2.3.90}$$

Here $G_2^{\mp}$ is the Goldstone boson and $h^{\mp}$ represents the second physical charged scalar boson. Both the Goldstone bosons $G_1^{\mp}$ and $G_2^{\mp}$ together with others will be eaten by the eight simply charged gauge bosons [38].

Another mass matrix that is written in the basis $(\eta^{\mp\mp}, \chi^{\mp\mp})$ has been found:

$$\frac{1}{2}\begin{pmatrix} \lambda_9\upsilon_\chi^2 & \lambda_9\upsilon_\rho\upsilon_\chi, \\ \lambda_9\upsilon_\chi\upsilon_\rho & \lambda_9\upsilon_\rho^2. \end{pmatrix} \tag{2.3.91}$$

This matrix has the following eigenvalues:

$$m^2_{G^{\mp\mp}} = 0, \tag{2.3.92}$$

$$m^2_{h^{\mp\mp}} = \frac{\lambda_9}{2}(\upsilon_\rho^2+\upsilon_\chi^2), \tag{2.3.93}$$

with its eigenvectors:

$$G^{\mp\mp} = \frac{-\upsilon_\rho}{\sqrt{\upsilon_\rho^2+\upsilon_\chi^2}}\rho^{\mp\mp} + \frac{-\upsilon_\chi}{\sqrt{\upsilon_\rho^2+\upsilon_\chi^2}}\chi^{\mp\mp}. \tag{2.3.94}$$

$$h^{\mp\mp} = \frac{-\upsilon_\chi}{\sqrt{\upsilon_\rho^2+\upsilon_\chi^2}}\rho^{\mp\mp} + \frac{-\upsilon_\rho}{\sqrt{\upsilon_\rho^2+\upsilon_\chi^2}}\chi^{\mp\mp}. \tag{2.3.95}$$

$G^{\mp\mp}$ is another Goldstone boson which will be eaten by the double charged gauge boson $V^{\mp}$ to acquire its mass, and $h^{\mp\mp}$ is the physical double charged scalar bosons in the compact 341 model.

2.4 The Lagrangian of 341 models

The Lagrangian in the 341 models is composed by the following terms:

$$\mathcal{L}_{341} = \mathcal{L}_{SI} + \mathcal{L}_{Yukawa} + \mathcal{L}_{Gauge} + \mathcal{L}_{Higgs}, \tag{2.4.1}$$

where $\mathcal{L}_{SI}$ is the Lagrangian of the strong interactions, it has the same form of the SM since the extension only is about the electorweak theory.

2.4.1 Yukawa Lagrangian in 341 models

The interaction between fermions and the scalar bosons in the compact 341 model is described by the Yukawa Lagrangian which is composed by two parts the ordinary Yukawa Lagrangian and the effective Lagrangian:

$$\begin{aligned}
\mathcal{L}_Y &= \lambda^J_{11}\bar{Q}_{1L}\chi J_{1R} + \lambda^J_{ij}\bar{Q}_{iL}\chi^* J_{jR} + \lambda^d_{1a}\bar{Q}_{1L}\rho d_{aR} + \lambda^u_{ia}\bar{Q}_{iL}\rho^* u_{aR} \\
&+ \lambda^U_{11}\bar{Q}_{1L}\eta U_{1R} + \lambda^D_{ij}\bar{Q}_{iL}\eta^* D_{jR} + \frac{\lambda^u_{1a}}{\Lambda^2}\epsilon_{mnop}\left(\bar{Q}_{1Lm}\rho_n\chi_0\eta^*_p\right)u_{aR} \\
&+ \frac{\lambda^d_{ia}}{\Lambda^2}\epsilon_{mnop}\left(\bar{Q}_{iLm}\rho^*_m\chi^*_0\eta_p\right)d_{aR} + h.c,
\end{aligned} \tag{2.4.2}$$

where λ^J_{11}, λ^J_{ij}, λ^d_{1a}, λ^u_{ia}, λ^U_{11}, λ^D_{ij} are the Yukawa coupling constants (a=1,2,3 and i,j=2,3).

In the 341 models, the scalar sectors contain four scalar fields with an extra additional 10-plet scalar (in other versions) [37], their particles gain their masses from the ordinary Yukawa Lagrangian (no need to introduce the effective Lagrangian).

Otherwise, in the compact 341 version (where we use only three scalar fields), the minimal number of its scalar fields leaves some fermions massless, to generate the required masses we need to introduce a new Lagrangian called the effective Lagrangian. Therefore, some of the SM fermions get their masses from the non-renormalizable effective operators (the dimension-6 effective operators) [38].

Concerning the charged Leptons, the absence of the right-handed leptons (as singlets) in the compact 341 model leads to the introduction of a new effective-five operator:

$$\frac{k_\ell}{\Lambda}\left(\bar{L}^c_{aL}\rho^*\right)\left(\chi^\dagger L_{aL}\right) + h.c, \tag{2.4.3}$$

where $\ell = e, \mu, \tau$. After SSB, this operator yields to the following relation:

$$m_\ell = \frac{1}{2} K_\ell \frac{\upsilon_\rho \upsilon_\chi}{\Lambda}, \tag{2.4.4}$$

which represent the mass of the charged leptons.
The mass matrix for the Up quarks in the basis (u_1, u_2, u_3) is found to take this form [38]:

$$M_u = \frac{1}{\sqrt{2}} \begin{pmatrix} \lambda^u_{11} \frac{\upsilon_\chi \upsilon_\rho \upsilon_\eta}{2\Lambda^2} & \lambda^u_{12} \frac{\upsilon_\chi \upsilon_\rho \upsilon_\eta}{2\Lambda^2} & \lambda^u_{13} \frac{\upsilon_\chi \upsilon_\rho \upsilon_\eta}{2\Lambda^2} \\ \lambda^u_{21} \upsilon_\rho & \lambda^u_{22} \upsilon_\rho & \lambda^u_{23} \upsilon_\rho \\ \lambda^u_{31} \upsilon_\rho & \lambda^u_{32} \upsilon_\rho & \lambda^u_{33} \upsilon_\rho \end{pmatrix} \tag{2.4.5}$$

While the down quarks mass matrix in the basis (d_1, d_2, d_3) has this form:

$$M_d = \frac{1}{\sqrt{2}} \begin{pmatrix} \lambda^d_{11} \upsilon_\rho & \lambda^d_{12} \upsilon_\rho & \lambda^d_{13} \upsilon_\rho \\ \lambda^d_{21} \frac{\upsilon_\chi \upsilon_\rho \upsilon_\eta}{2\Lambda^2} & \lambda^d_{22} \frac{\upsilon_\chi \upsilon_\rho \upsilon_\eta}{2\Lambda^2} & \lambda^d_{23} \frac{\upsilon_\chi \upsilon_\rho \upsilon_\eta}{2\Lambda^2} \\ \lambda^d_{31} \frac{\upsilon_\chi \upsilon_\rho \upsilon_\eta}{2\Lambda^2} & \lambda^d_{32} \frac{\upsilon_\chi \upsilon_\rho \upsilon_\eta}{2\Lambda^2} & \lambda^d_{33} \frac{\upsilon_\chi \upsilon_\rho \upsilon_\eta}{2\Lambda^2} \end{pmatrix} \tag{2.4.6}$$

The matrix M_u and M_d contain fermions mixing, after the daigonalization, we get the ordinary quarks masses:

$$m^u = \lambda^u_{11} \frac{\upsilon_\rho \upsilon_\eta \upsilon_\chi}{2\Lambda^2 \sqrt{2}}, \quad m^c = \lambda^u_{22} \frac{\upsilon_\rho}{\sqrt{2}}, \quad m^t = \lambda^u_{33} \frac{\upsilon_\rho}{\sqrt{2}}, \tag{2.4.7}$$

$$m^d = \lambda^d_{11} \frac{\upsilon_\rho}{\sqrt{2}}, \quad m^s = \lambda^d_{22} \frac{\upsilon_\rho \upsilon_\eta \upsilon_\chi}{2\Lambda^2 \sqrt{2}}, \quad m^b = \lambda^d_{33} \frac{\upsilon_\rho \upsilon_\eta \upsilon_\chi}{2\Lambda^2 \sqrt{2}}. \tag{2.4.8}$$

For the exotic quarks J_i (i=1..3), their masses are found from this mass matrix [38]:

$$M_J = \frac{\upsilon_\chi}{\sqrt{2}} \begin{pmatrix} \lambda^J_{11} & 0 & 0 \\ 0 & \lambda^J_{22} & \lambda^J_{23} \\ 0 & \lambda^J_{32} & \lambda^J_{33} \end{pmatrix} \tag{2.4.9}$$

which it is written in the basis (J_1, J_2, J_3), while, the masses of U_i are found from a mass matrix that is written in the basis (U_1,D_2, D_3) [38]:

$$M_D = \frac{\upsilon_\eta}{\sqrt{2}} \begin{pmatrix} \lambda^U_{11} & 0 & 0 \\ 0 & \lambda^D_{22} & \lambda^D_{23} \\ 0 & \lambda^D_{32} & \lambda^D_{33} \end{pmatrix} \tag{2.4.10}$$

Therefore, the matrices M^u, M^d, M^U and M^J generate masses to all quarks in the physical spectrum in the compact 341 model.

2.4.2 The Yang-Mills Lagrangian

The Yang-Mills Lagrangian in the compact 341 model is given by this relation:

$$\mathcal{L} = \frac{-1}{4} W_{a\mu\nu} W^{a\mu\nu} + \frac{-1}{4} F_{\mu\nu} F^{\mu\nu} \tag{2.4.11}$$

The expressions of $W^{a\mu\nu}$ and $F^{\mu\nu}$ are:

$$W^{a\mu\nu} = \partial^\mu W^{a\nu} - \partial^\nu W^{a\mu} + g f^{abc} W^{b\mu} W^{c\nu}, \tag{2.4.12}$$

$$F^{\mu\nu} = \partial^\mu B_\mu - \partial^\nu B^\mu, \tag{2.4.13}$$

where $W_{a\mu}$ and B^μ represent the gauge bosons associated from $SU(4)_L$ and $U(1)_X$ respectively where a goes from 1 to 15 and f^{abc} is the structure constant of the group SU(4) (See the appendix C).

2.4.3 The scalar Lagrangian

The scalar Lagrangian in the compact 341 model composes by two parts, the kinematic Lagrangian of the scalar bosons see Eq.(2.3.17) and the scalar potential $V(\eta, \rho, \chi)$ that is given by Eq.(2.3.60).

2.5 Summary

In this chapter, we have defined models based on the gauge group $SU_C(3) \otimes SU(4)_L \otimes U(1)_X$ called the anomalies free 341 models. We discussed their particle content (the fermions, gauge and scalar sectors). We explained how all particles gain their masses in the compact version of the 341 models. Moreover, we briefly described the total Lagrangian.

In the next chapter, we will discuss the theoretical constraints that we will use to determine the allowed regions for the unknown scalar parameters in the compact 341 model.

Chapter 3

Theoretical constraints on scalar parameters in the compact 341 model

3.1 Introduction

All our final theoretical results in the chapter 4 are written in terms of the unknown scalar parameters $\lambda_{1...9}$, their values will be our input parameters in the next chapter to build our phenomenology. The only way to determine the regions of those scalar parameters is by using the theoretical constraint such as: the boundedness of the scalar potential, minimization conditions, the perturbative unitarity, the positivity of the scalar bosons masses and the perturbativity of the scalar potential together with existence of the Landau pole and a natural cut-off at a scale μ, which will ensure the perturbative limit of our model.

In this chapter, we derive the expressions of those theoretical constraints [81]. Moreover, we discuss the existence of the Landau pole and how it was used to constraint our scalar parameters.

3.2 Constraints on the parameters space

The compact 341 model has large numbers of free scalar parameters. To determine their allowed regions and in order to obtain a viable model, many theoretical constraints have to be imposed on the scalar potential.

3.2.1 Minimization conditions

The first set of the theoretical constraints on the scalar parameters comes from the minimization conditions resulted from the first and the second derivative of the scalar potential. They require general conditions to provide the vacuum configuration $\langle\rho\rangle_0$, $\langle\chi\rangle_0$ and $\langle\eta\rangle_0$ to

be a minimum of the scalar potential (2.3.60).
The first derivative $\frac{\partial V}{\partial \phi}|_{\phi=0} = 0$ are given by Eqs (2.3.61)-(2.3.63). The second derivative test $\frac{\partial^2 V}{\partial \phi_i \phi_j}\Big|_{\phi=\phi_0}$ leads to the so called the Hessian matrix H_0 evaluated at the vacuum [81]:

$$H_0 = \begin{pmatrix} 4\lambda_1 \upsilon_\eta^2 & 2\lambda_4 \upsilon_\eta \upsilon_\rho & 2\lambda_5 \upsilon_\eta \upsilon_\chi \\ 2\lambda_4 \upsilon_\eta \upsilon_\rho & 4\lambda_2 \upsilon_\rho^2 & 2\lambda_6 \upsilon_\rho \upsilon_\chi \\ 2\lambda_5 \upsilon_\eta \upsilon_\chi & 2\lambda_6 \upsilon_\rho \upsilon_\chi & 4\lambda_3 \upsilon_\chi^2 \end{pmatrix}, \tag{3.2.1}$$

where we have used the relations in (2.3.61)-(2.3.63) in order to simplify the Hessian matrix. Using Sylvester's criterion and from the positivity of the principal minors, we get the following conditions [81]:

$$\begin{aligned} \lambda_1 > 0, \qquad \lambda_2 > 0, \qquad \lambda_3 > 0, \\ -2\sqrt{\lambda_1 \lambda_2} < \lambda_4 < 2\sqrt{\lambda_1 \lambda_2}, \\ -2\sqrt{\lambda_1 \lambda_3} < \lambda_5 < 2\sqrt{\lambda_1 \lambda_3}, \\ -2\sqrt{\lambda_3 \lambda_2} < \lambda_6 < 2\sqrt{\lambda_3 \lambda_2}, \\ \det(H_0) > 0. \end{aligned} \tag{3.2.2}$$

The positivity of the CP-even scalars masses as we will discuss in the next subsection ensures the condition $\det(H_0) > 0$ without mentioning the expression of $\det(H_0)$.

3.2.2 Boundedness from below

We study the vacuum stability at the tree level, the conditions which guarantee that the scalar potential is bounded from below in all directions in the field space as the field strength approaches infinity. In our case, we face a more complicated problem even at the tree level since we have to deal with large numbers of scalar couplings (twelve couplings). Thus, we introduce a parameterztaion which greatly reduces the number of variables and make the problem even more tractable to derive the sufficient and complete constraints of the potential stability (VS) where we ignore terms with dimension $d < 4$, since in the limit of large field values, they are negligible in comparison with the quartic couplings of the scalar potential $V^4(\eta, \rho, \chi)$ [81]:

$$\begin{aligned} V^4(\eta, \rho, \chi) =& \lambda_1 (\eta^\dagger \eta)^2 + \lambda_2 (\rho^\dagger \rho)^2 + \lambda_3 (\chi^\dagger \chi)^2 + \lambda_4 (\eta^\dagger \eta)(\rho^\dagger \rho) \\ &+ \lambda_5 (\eta^\dagger \eta)(\chi^\dagger \chi) + \lambda_6 (\rho^\dagger \rho)(\chi^\dagger \chi) + \lambda_7 (\rho^\dagger \eta)(\eta^\dagger \rho) \\ &+ \lambda_8 (\chi^\dagger \eta)(\eta^\dagger \chi) + \lambda_9 (\rho^\dagger \chi)(\chi^\dagger \rho), \end{aligned} \tag{3.2.3}$$

Since we have three different field directions, we define a parametrization of the fields on a sphere [81]:

$$\begin{aligned}
r^2 &\equiv \eta^\dagger\eta + \rho^\dagger\rho + \chi^\dagger\chi,\\
\eta^\dagger\eta &\equiv r^2\cos^2\theta\sin^2\phi,\\
\rho^\dagger\rho &\equiv r^2\sin^2\theta\sin^2\phi,\\
\chi^\dagger\chi &\equiv r^2\cos^2\phi,\\
\frac{\eta^\dagger\rho}{|\eta||\rho|} &\equiv \xi_1 e^{i\psi_1}, \quad \frac{\eta\rho^\dagger}{|\eta||\rho|} \equiv \xi_1 e^{-i\psi_1},\\
\frac{\eta^\dagger\chi}{|\eta||\chi|} &\equiv \xi_2 e^{i\psi_2}, \quad \frac{\eta\chi^\dagger}{|\eta||\chi|} \equiv \xi_2 e^{-i\psi_2},\\
\frac{\rho^\dagger\chi}{|\rho||\chi|} &\equiv \xi_3 e^{i\psi_3}, \quad \frac{\rho\chi^\dagger}{|\rho||\chi|} \equiv \xi_3 e^{-i\psi_3}.
\end{aligned} \tag{3.2.4}$$

where we adopt here a parametrization similar to the one of Ref [82], The scalar fields η, χ and ρ scan all the fields space, therefore, the radius r scans the domain $[0,\infty[$, the angle $\theta \in [0,2\pi]$ and the angle $\phi \in [0,\frac{\pi}{2}]$, $\xi_i (i = 1,2,3) \in [0,1]$ [82].

Inserting this parameterztaion in the scalar potential (3.2.3), it is straightforward to write $V^4(\rho,\chi,\eta)$ in the following form:

$$\begin{aligned}
V^4(r,\cos^2\theta,\sin^2\theta,\cos^2\phi,\xi_i) = r^4\Big(&\lambda_1\cos^4\theta\sin^4\phi\\
&+\lambda_2\sin^4\theta\sin^4\phi+\lambda_3\cos^4\phi+\lambda_4\cos^2\theta\sin^2\theta\sin^4\phi\\
&+\lambda_5\cos^2\theta\cos^2\phi+\lambda_6\sin^2\theta\sin^2\phi\cos^2\phi+\lambda_7\xi_1^2\\
&\cos^2\theta\sin^2\phi\sin^4\phi+\lambda_8\xi_2^2\cos^2\theta\sin^2\phi\cos^4\phi\\
&+\lambda_9\xi_3^2\sin^2\theta\cos^2\phi\sin^2\phi\Big),
\end{aligned} \tag{3.2.5}$$

We introduce again the following variables [82]:

$$x \equiv \cos^2\theta \quad \text{and} \quad y \equiv \sin^2\phi, \tag{3.2.6}$$

Inserting (3.2.6) in the expression (3.2.5), then we get:

$$\begin{aligned}
V^4(r,\cos^2\theta,\sin^2\theta,\cos^2\phi,\xi_i) = y^2\Big(&\lambda_1x^2+\lambda_2(1-x)^2\\
&+\lambda_4x(1-x)+\lambda_7\xi_1^2x(1-x)\Big)+\lambda_3(1-y)^2\\
&+y(1-y)\Big(\lambda_5x+\lambda_6(1-x)+\lambda_8\xi_2^2x+\lambda_9\xi_3^2(1-x)\Big).
\end{aligned} \tag{3.2.7}$$

The expression (3.2.7) has the following form:

$$f(\chi) = a\chi^2 + b(1-\chi)^2 + c\chi(1-\chi), \tag{3.2.8}$$

The copositivity of the expression (3.2.8) leads to [82]:

$$a > 0, \quad b > 0 \quad \text{and} \quad c + 2\sqrt{ab} > 0. \tag{3.2.9}$$

Applying this criterion on (3.2.7), we get:

$$A \equiv \lambda_1 x^2 + \lambda_2(1-x)^2 + \lambda_4 x(1-x) + \lambda_7 \xi_1^2 x(1-x) > 0, \tag{3.2.10}$$

$$B \equiv \lambda_3 > 0 \tag{3.2.11}$$

$$C \equiv \lambda_5 x + \lambda_6(1-x) + \lambda_8 \xi_2^2 x + \lambda_9 \xi_3^2(1-x) + 2\sqrt{AB} > 0. \tag{3.2.12}$$

From the expression (3.2.10), we find:

$$\begin{aligned} &\lambda_1 > 0, \qquad \lambda_2 > 0, \\ &\lambda_4 + 2\sqrt{\lambda_1\lambda_2} > 0. \\ &\lambda_4 + \lambda_7 + 2\sqrt{\lambda_1\lambda_2} > 0. \end{aligned} \tag{3.2.13}$$

While the expression (3.2.11) leads to:

$$\lambda_3 > 0, \tag{3.2.14}$$

From the expression (3.2.12), we distinguish two cases:
If λ_6 and $\lambda_7 > 0$, one gets (3.2.13)-(3.2.14), while, if λ_5 or $\lambda_6 < 0$, we obtain the following [81]:

$$\Lambda_1(\xi_2) \equiv 4\lambda_1\lambda_3 - (\lambda_5 + \xi_2^2\lambda_8)^2 > 0, \tag{3.2.15}$$

$$\Lambda_2(\xi_3) \equiv 4\lambda_2\lambda_3 - (\lambda_6 + \xi_3^2\lambda_9)^2 > 0, \tag{3.2.16}$$

$$\begin{aligned} \Lambda_3(\xi_i) \equiv\ & 4(\lambda_4 + \lambda_7\xi_1^2)\lambda_3 - 2(\lambda_5 + \lambda_8\xi_2^2)(\lambda_6 + \lambda_9\xi_3^2) \\ +\ & 2\sqrt{\Lambda_1(\xi_2)\Lambda_2(\xi_3)} > 0. \end{aligned} \tag{3.2.17}$$

The conditions $\Lambda_1(\xi_2) > 0$ and $\Lambda_2(\xi_3) > 0$ for all ξ_2 and ξ_3 are equivalent to $\Lambda_1(0) > 0$, $\Lambda_1(1) > 0$, $\Lambda_2(0) > 0$ and $\Lambda_2(1) > 0$, thus, we obtain the following constraints [81]:

$$-2\sqrt{\lambda_1\lambda_3} < \lambda_5 < 2\sqrt{\lambda_1\lambda_3}, \tag{3.2.18}$$

$$-2\sqrt{\lambda_1\lambda_3} < \lambda_5 + \lambda_8 < 2\sqrt{\lambda_1\lambda_3},, \tag{3.2.19}$$

$$-2\sqrt{\lambda_2\lambda_3} < \lambda_6 < 2\sqrt{\lambda_2\lambda_3}, \tag{3.2.20}$$

$$-2\sqrt{\lambda_2\lambda_3} < \lambda_6 + \lambda_9 < 2\sqrt{\lambda_2\lambda_3}, \tag{3.2.21}$$

The remaining constrains are coming from $\Lambda_3(\xi_i) > 0$ for all ξ_1, ξ_2 and ξ_3 [81]:

$$\begin{aligned}
4(\lambda_4+\lambda_7)\lambda_3 &- 2(\lambda_5+\lambda_8)(\lambda_6+\lambda_9)+2\sqrt{\Lambda_4}>0,\\
4\lambda_4\lambda_3-2\lambda_5\lambda_6 &+ 2\sqrt{\Lambda_5}>0,\\
4\lambda_4\lambda_3-2\lambda_5(\lambda_6 &+ \lambda_9)+2\sqrt{\Lambda_6}>0,\\
4\lambda_4\lambda_3-2(\lambda_5 &+ \lambda_8)(\lambda_6+\lambda_9)+2\sqrt{\Lambda_7}>0,\\
4\lambda_4\lambda_3-2(\lambda_5 &+ \lambda_8)\lambda_6+2\sqrt{\Lambda_8}>0,\\
4(\lambda_4+\lambda_7)\lambda_3 &- 2\lambda_5\lambda_6+2\sqrt{\Lambda_9}>0,\\
4(\lambda_4+\lambda_7)\lambda_3 &- 2\lambda_5(\lambda_6+\lambda_9)+2\sqrt{\Lambda_{10}}>0,\\
4(\lambda_4+\lambda_7)\lambda_3 &- 2(\lambda_5+\lambda_8)\lambda_6+2\sqrt{\Lambda_{11}}>0.
\end{aligned} \tag{3.2.22}$$

Where:

$$\Lambda_4 = (4\lambda_1\lambda_3-(\lambda_5+\lambda_8)^2)(4\lambda_2\lambda_3-(\lambda_6+\lambda_9)^2), \tag{3.2.23}$$
$$\Lambda_5 = (4\lambda_1\lambda_3-\lambda_5^2)(4\lambda_2\lambda_3-\lambda_6^2), \tag{3.2.24}$$
$$\Lambda_6 = (4\lambda_1\lambda_3-\lambda_5^2)(4\lambda_2\lambda_3-(\lambda_6+\lambda_9)^2), \tag{3.2.25}$$
$$\Lambda_7 = (4\lambda_1\lambda_3-(\lambda_5+\lambda_8)^2)(4\lambda_2\lambda_3-(\lambda_6+\lambda_9)^2), \tag{3.2.26}$$
$$\Lambda_8 = (4\lambda_1\lambda_3-(\lambda_5+\lambda_8)^2)(4\lambda_2\lambda_3-\lambda_6^2), \tag{3.2.27}$$
$$\Lambda_9 = (4\lambda_1\lambda_3-\lambda_5^2)(4\lambda_2\lambda_3-\lambda_6^2), \tag{3.2.28}$$
$$\Lambda_{10} = (4\lambda_1\lambda_3-\lambda_5^2)(4\lambda_2\lambda_3-(\lambda_6+\lambda_9)^2), \tag{3.2.29}$$
$$\Lambda_{11} = (4\lambda_1\lambda_3-(\lambda_5+\lambda_8)^2)(4\lambda_2\lambda_3-\lambda_6^2). \tag{3.2.30}$$

All the previous conditions (3.2.13)-(3.2.22) ensure the necessary and sufficient conditions for the boundedness of the scalar potential from below in any direction in the field space. Together with the minimization conditions resulted from the positivity of the Hessian matrix (3.2.2), we determine the first set of the theoretical constraints.

3.2.3 Perturbative Unitarity bounds and the positivity of the scalar bosons masses

Other constraints on the scalar potential parameters are obtained from the unitarity conditions. As we discussed in chapter 1, to derive this constraint one needs to look at the tree level scattering processes: scalar-scalar scattering, gauge boson-gauge boson scattering, and scalar-gauge boson scattering [27].

By applying the equivalence theorem [82, 83]. The unitarity constraint at the tree level in the compact 341 model can be implemented by considering only scalar-scalar scattering processes dominated by quartic interactions [81].

The perturbative unitarity conditions are obtained in many BSM models [27,82] by using the S matrix for all the elastic scatterings of two body scalar boson states, the condition (1.8.5) constraints the scattering amplitude for all possible two particle states $S_1S_2 \longrightarrow S_3S_4$ processes as follows:

$$|\mathcal{M}| < 8\pi \tag{3.2.31}$$

Where the S_i (i=1,..4) represent all (pseudo) scalar bosons in the model. The unitarity constraint is found by applying the bound (3.2.31) on all possible eigenvalues of all scattering matrices [81].

In the compact 341 model, it is difficult to calculate all the eigenvalues of all possible matrices for all the elastic scatterings of two body scalar boson states since there are many scalar fields components. Fortunately, there is an alternative method used in Ref [83]. Instead of extracting the S-Matrices and calculate all the eigenvalues, we derive all possible quartic contact terms as a function of the physical scalar fields [81, 83]. In this way we can immediately find out the unitarity bounds on the quartic couplings.

The possible non-zero quartic couplings that appear in the compact 341 after expanding the full scalar potential in terms of the physical quartic couplings are [81]:

$$\begin{aligned}
h_1h_1h_1h_1 &: \frac{\lambda_2}{4},\\
h^{--}h^{++}h_2h_2 &: \lambda_3S_\alpha^2\Gamma_3^2+\lambda_4\frac{\Gamma_1^2C_\alpha^2}{2}+(\lambda_6+\lambda_9)\frac{\Gamma_3^2C_\alpha^2}{2}-\lambda_5\frac{\Gamma_1^2S_\alpha^2}{2},\\
h^{--}h^{++}h_3h_3 &: \lambda_3S_\alpha^2\Gamma_4^2+\lambda_4\frac{C_\alpha^2\beta^2}{2}+(\lambda_6+\lambda_9)\frac{C_\alpha^2\sigma^2}{2}-\lambda_5\frac{\Gamma_2^2S_\alpha^2}{2},\\
h_2^-h_2^+h_1h_1 &: \lambda_6\frac{C_\beta^2}{2}+\lambda_4\frac{S_\beta^2}{2},\\
h^{--}h^{++}h_2h_3 &: 2\lambda_3\Gamma_4\Gamma_3S_\alpha^2+C_\alpha^2\Gamma_1\Gamma_2\lambda_4+\Gamma_4\Gamma_3C_\alpha^2(\lambda_6+\lambda_9)+\Gamma_1\Gamma_2S_\alpha^2\lambda_5,\\
h_2h_2h_1h_1 &: \lambda_4(\frac{\Gamma_1^2}{4}+\frac{\Gamma_1\Gamma_2}{2})+\lambda_6\frac{\Gamma_3^2}{4},\\
h_3h_3h_1h_1 &: \lambda_6\frac{\Gamma_3^2}{4}+\lambda_4\frac{\Gamma_2^2}{4},\\
h^{--}h_2^+h_1^+h_3 &: \lambda_8(\frac{\Gamma_2}{\sqrt{2}}C_\beta S_\alpha^2+\frac{\Gamma_3}{\sqrt{2}}S_\beta S_\alpha^2)+\lambda_9\frac{C_\alpha^2S_\beta\Gamma_3}{\sqrt{2}}+\lambda_7\frac{C_\alpha^2S_\beta\Gamma_2}{\sqrt{2}},\\
h^{--}h_2^+h_1^+h_1 &: \lambda_9\frac{C_\beta C_\alpha S_\alpha}{\sqrt{2}}+\lambda_7\frac{S_\alpha C_\alpha S_\beta}{\sqrt{2}},\\
h_1^-h_2^-h_1^{++}h_2 &: \lambda_9\frac{\Gamma_3}{\sqrt{2}}C_\alpha^2C_\beta+\lambda_7\frac{\Gamma_1}{\sqrt{2}}C_\alpha^2S_\beta+\lambda_8\frac{\Gamma_1}{\sqrt{2}}S_\alpha^2C_\beta,\\
h_1^-h_2^-h_1^{++}h_3 &: \lambda_9\frac{\Gamma_3}{\sqrt{2}}C_\alpha^2C_\beta+\lambda_7\frac{\Gamma_2}{\sqrt{2}}C_\alpha^2S_\beta,
\end{aligned}$$

$$
\begin{aligned}
h^{--}h^{++}h_1h_2 &: \lambda_9\frac{\Gamma_3}{2}C_\alpha S_\alpha,\\
h^{--}h^{++}h_1h_3 &: \lambda_9\frac{\Gamma_4}{2}C_\alpha S_\alpha,\\
h^{++}h_1^-h_2^-h_1 &: \frac{\lambda_7}{\sqrt{2}}S_\beta C_\alpha S_\alpha,\\
h_1^+h_1^-h_1h_3 &: \lambda_7 C_\alpha S_\alpha\Gamma_2,\\
h_1h_1h_2h_3 &: \frac{\lambda_6\Gamma_3\Gamma_4}{2},\\
h_1^+h_1^-h_1h_2 &: \lambda_7\frac{\Gamma_1}{2}C_\alpha S_\alpha,\\
h_1^+h_1^-h_1^+h_1^- &: \lambda_1 S_\alpha^4+\lambda_2 C_\alpha^4+\lambda_4 S_\alpha^2C_\alpha^2,\\
h^{++}h_1^-h_1^-h_2 &: \frac{\lambda_8}{\sqrt{2}}S_\alpha^2S_\beta\Gamma_3,\\
h^{++}h^{--}h^{++}h^{--} &: \lambda_2C_\alpha^4+\lambda_3S_\alpha^4+\lambda_6C_\alpha^2S_\alpha^2,\\
h_1^+h_1^-h_2h_2 &: \lambda_1S_\alpha^4\Gamma_1^2+\lambda_4\frac{\Gamma_1^2}{2}C_\alpha^2+\lambda_5\frac{\Gamma_3^2}{2}S_\alpha^2+\lambda_6\frac{\Gamma_3^2}{2}C_\alpha^2+\lambda_7\frac{\Gamma_1^2}{2}C_\alpha^2,\\
h_1^+h_1^-h_3h_3 &: \lambda_1S_\alpha^2\Gamma_2^2+\lambda_4\frac{\Gamma_2^2}{2}C_\alpha^2+\lambda_5\frac{\Gamma_4^2}{2}S_\alpha^2+\lambda_6\frac{\Gamma_4^2}{2}C_\alpha^2+\lambda_7\frac{\Gamma_2^2}{2}C_\alpha^2,\\
h_1^+h_1^-h_2h_3 &: \lambda_1S_\alpha^2\Gamma_2\Gamma_1+\lambda_4\Gamma_2\Gamma_1C_\alpha^2+\lambda_5\Gamma_4\Gamma_3S_\alpha^2+\lambda_6\Gamma_4\Gamma_3C_\alpha^2+\lambda_7\Gamma_2\Gamma_1C_\alpha^2,\\
h^{++}h_1^-h_1^-h_3 &: \frac{\lambda_8}{\sqrt{2}}(\Gamma_2S_\alpha^2C_\beta+\Gamma_3S_\alpha^2S_\beta),\\
h_2^+h_2^-h_2h_2 &: \lambda_1S_\beta^2\Gamma_1^2+\lambda_3\Gamma_3^2C_\beta^2+\lambda_5(\frac{\Gamma_1^2}{2}C_\beta^2+\frac{\Gamma_3^2}{2}S_\beta^2)+\lambda_8(\frac{\Gamma_1^2}{2}C_\beta^2+\frac{\Gamma_3\Gamma_1}{2}C_\alpha S_\beta\\
&+ \frac{\Gamma_3^2}{2}S_\beta^2+\frac{\Gamma_3\Gamma_1}{2}C_\beta S_\beta),\\
h_2h_2h_2h_3 &: \lambda_1\Gamma_1^3\Gamma_2+\lambda_3\Gamma_3^3\Gamma_4+\frac{\lambda_5}{2}(\Gamma_1\Gamma_2\Gamma_3^2+\Gamma_1^2\Gamma_3\Gamma_4),\\
h_2^+h_2^-h_3h_3 &: \lambda_1S_\beta^2\Gamma_2^2+\lambda_3\Gamma_3^2C_\beta^2+\lambda_5(\frac{\Gamma_2^2}{2}C_\beta^2+\frac{\Gamma_3^2}{2}S_\beta^2)+\frac{\lambda_8}{2}(\Gamma_2^2C_\beta^2+\Gamma_4^2S_\beta^2+\Gamma_4\Gamma_2C_\beta S_\beta),\\
h_2^+h_2^-h_2h_3 &: \lambda_1S_\beta^2\Gamma_2\Gamma_1+2\lambda_3\Gamma_4\Gamma_3C_\beta^2+\lambda_5(\Gamma_2\Gamma_1C_\beta^2+\Gamma_4\Gamma_3S_\beta^2)+\frac{\lambda_8}{2}(2\Gamma_2\Gamma_1C_\beta^2\\
&+ (\Gamma_1\Gamma_4\Gamma_2)S_\beta C_\beta+\Gamma_4\Gamma_3S_\beta^2+(\Gamma_1\Gamma_4+\Gamma_2\Gamma_3)C_\beta S_\beta+\Gamma_3\Gamma_2C_\beta S_\beta),\\
h_2^+h_2^-h_2^+h_2^- &: S_\beta^4\lambda_1+\lambda_3C_\beta^4+\lambda_5C_\beta^2S_\beta^2,\\
h_2h_2h_2h_2 &: \lambda_1\frac{\Gamma_1^4}{4}+\lambda_3\frac{\Gamma_3^2}{4},\\
h_3h_3h_3h_3 &: \lambda_1\frac{\Gamma_2^4}{4}+\lambda_3\frac{\Gamma_4^4}{4}+\lambda_5\frac{\Gamma_4^2\Gamma_2^2}{4},\\
h_2h_3h_3h_3 &: \lambda_1\Gamma_1\Gamma_2^3+\lambda_3\Gamma_3\Gamma_4^3+\frac{\lambda_5}{2}(\Gamma_1\Gamma_2\Gamma_4^2+\Gamma_2^2\Gamma_3\Gamma_4),\\
h_1^+h_1^-h_1h_1 &: \lambda_2C_\alpha^2+\frac{\lambda_4}{2}S_\alpha^2+\frac{\lambda_7}{2}S_\alpha^2,
\end{aligned}
$$

$$
\begin{aligned}
h^{++}h^{--}h_1^+h_1^- &: 2\lambda_2 C_\alpha^2 + \lambda_4 S_\alpha^4 + \lambda_5 S_\alpha^4 + \lambda_6 C_\alpha^2 S_\alpha^2 + \lambda_8 S_\alpha^4,\\
h^{++}h^{--}h_2^+h_2^- &: 2\lambda_3 S_\alpha^2 C_\beta^2 + \lambda_4 S_\beta^2 C_\alpha^2 + \lambda_5 S_\alpha^2 S_\beta^2 + \lambda_6 C_\alpha^2 C_\beta^2 + \lambda_7 C_\alpha^2 S_\beta^2,\\
h_1^+h_2^+h^{--}h_2 &: \lambda_9 \frac{\Gamma_3}{\sqrt{2}} C_\alpha^2 C_\beta + \lambda_7 \frac{\Gamma_1}{\sqrt{2}} C_\alpha^2 S_\beta + \lambda_8 (\frac{\Gamma_3}{\sqrt{2}} S_\beta S_\alpha^2 + \frac{\Gamma_1}{\sqrt{2}} C_\beta S_\alpha^2),\\
h_1^+h_1^-h_1h_2 &: \frac{\lambda_7}{2} C_\alpha S_\alpha \Gamma_1,\\
h_1^+h_1^-h_2^-h_2^+ &: 2\lambda_1 S_\beta^2 S_\alpha^2 + \lambda_4 C_\alpha^2 S_\beta^2 + (\lambda_6\\
&+ \lambda_9) C_\alpha^2 C_\beta^2 + \lambda_5 S_\alpha^2 C_\beta,\\
h_2h_2h_3h_3 &: \lambda_1 \frac{3\Gamma_2^2\Gamma_1^2}{2} + \lambda_3 \frac{3\Gamma_4^2\Gamma_3^2}{2} + \lambda_5 (\Gamma_1\Gamma_2\Gamma_3\Gamma_4 + \frac{\gamma^2\alpha^2}{4} + \frac{\Gamma_3^2\Gamma_2^2}{4} + \frac{\Gamma_4^2\Gamma_1^2}{4}).\\
h^{++}h^{--}h_1h_1 &: \lambda_2 C_\alpha^2 + \frac{\lambda_9}{2} S_\alpha + \frac{\lambda_6}{2} S_\alpha^2. \qquad (3.2.32)
\end{aligned}
$$

where

$$\cos\alpha \equiv C_\alpha = \frac{\upsilon_\eta}{\sqrt{\upsilon_\eta^2+\upsilon_\rho^2}}, \qquad \sin\alpha \equiv S_\alpha = \frac{\upsilon_\rho}{\sqrt{\upsilon_\eta^2+\upsilon_\rho^2}}, \qquad (3.2.33)$$

$$\cos\alpha_1 \equiv C_{\alpha_1} = \frac{\upsilon_\chi}{\sqrt{\upsilon_\chi^2+\upsilon_\rho^2}}, \qquad \sin\alpha_1 \equiv S_{\alpha_1} = \frac{\upsilon_\rho}{\sqrt{\upsilon_\chi^2+\upsilon_\rho^2}}, \qquad (3.2.34)$$

$$\cos\beta \equiv C_\beta = \frac{\upsilon_\chi}{\sqrt{\upsilon_\eta^2+\upsilon_\chi^2}}, \qquad \sin\beta \equiv S_\beta = \frac{\upsilon_\eta}{\sqrt{\upsilon_\eta^2+\upsilon_\chi^2}}, \qquad (3.2.35)$$

Using the fact that υ_η=υ_χ, $\upsilon_\rho \ll \upsilon_\eta$ and $\upsilon_\rho \ll \upsilon_\chi$, we find $C_\alpha^2 = C_{\alpha_1}^2 = 1$, $S_\alpha^2 = S_{\alpha_1}^2 = 0$, $C_\beta^2 = S_\beta^2 = \frac{1}{2}$. The quartic couplings in four scalar scattering are bounded by 8π. Thus, the unitarity constraints on the scalar parameters are [81]:

$$
\begin{aligned}
\Gamma_1^2\lambda_4 &+ \Gamma_3^2(\lambda_6+\lambda_9) < 16\pi,\\
\Gamma_2^2\lambda_4 &+ \Gamma_4^2(\lambda_6+\lambda_9) < 16\pi,\\
\Gamma_1\Gamma_2\lambda_4 &+ \Gamma_3\Gamma_4(\lambda_6+\lambda_9) < 8\pi,\\
(\Gamma_1^2 &+ 2\Gamma_1\Gamma_2)\lambda_4 + \Gamma_3^2\lambda_6 < 32\pi,\\
\lambda_4 &+ \lambda_6 < 32\pi,\\
\Gamma_2^2\lambda_4 &+ \Gamma_4^2\lambda_6 < 32\pi,\\
\Gamma_4\lambda_9 &+ \Gamma_2\lambda_7 < 16\pi,\\
\Gamma_3\lambda_9 &+ \Gamma_1\lambda_7 < 16\pi,\\
\Gamma_3\Gamma_4\lambda_6 &< 16\pi,\\
\Gamma_1^2\lambda_4 &+ \Gamma_3^2\lambda_6 + \Gamma_1^2\lambda_7 < 16\pi,\\
\Gamma_2^2\lambda_4 &+ \Gamma_4^2\lambda_6 + \Gamma_2^2\lambda_7 < 16\pi,\\
\Gamma_1\Gamma_2\lambda_4 &+ \Gamma_4\Gamma_3\lambda_6 + \Gamma_1\Gamma_2\lambda_7 < 8\pi,\\
2\Gamma_1^2\lambda_1 &+ 2\Gamma_3^2\lambda_3 + \lambda_5(\Gamma_1^2+\Gamma_3^2) + \lambda_8(\Gamma_1^2+\Gamma_3^2+(\sqrt{2}+1)\Gamma_3\Gamma_1) < 32\pi,
\end{aligned}
$$

$$
\begin{aligned}
2\Gamma_2^2\lambda_1 &+ 2\Gamma_4^2\lambda_3 + \lambda_5(\Gamma_2^2+\Gamma_4^2) + \lambda_8(\Gamma_2^2+\Gamma_4^2+\Gamma_4\Gamma_2) < 32\pi,\\
2\Gamma_2\Gamma_1\lambda_1 &+ 4\Gamma_4\Gamma_3\lambda_3 + 2\lambda_5(\Gamma_2\Gamma_1+\Gamma_3^2) + \lambda_8(2\Gamma_2\Gamma_1+2\Gamma_4\Gamma_1\\
&+ \Gamma_2+\Gamma_4\Gamma_3+\Gamma_2\gamma+\Gamma_4\Gamma_2) < 32\pi,\\
\lambda_1 &+ \lambda_3+\lambda_5 < 32\pi,\\
\Gamma_1^4\lambda_1 &+ \Gamma_3^2\lambda_3 < 32\pi,\\
\Gamma_2^4\lambda_1 &+ \Gamma_4^4\lambda_3 + \Gamma_4^2\Gamma_2^2\lambda_5 < 32\pi,\\
6\Gamma_2^2\Gamma_1^2\lambda_1 &+ 6\Gamma_4^2\Gamma_3^2\lambda_3 + \lambda_5(4\Gamma_1\Gamma_2\Gamma_3\Gamma_4+\Gamma_3^2\Gamma_1^2+\Gamma_3^2\Gamma_2^2+\Gamma_1^2\Gamma_4^2) < 32\pi,\\
2\Gamma_1^3\Gamma_2\lambda_1 &+ 2\lambda_3\Gamma_3^3\Gamma_4 + \lambda_5(\Gamma_2\Gamma_1\Gamma_3^2+\Gamma_1^2\Gamma_3\Gamma_4) < 16\pi,\\
2\Gamma_2^3\Gamma_1\lambda_1 &+ 2\lambda_3\Gamma_4^3\Gamma_3 + \lambda_5(\Gamma_2\Gamma_1\Gamma_4^2+\Gamma_2^2\Gamma_3\Gamma_4) < 16\pi,\\
\lambda_4 &+ \lambda_6+\lambda_9 < 16\pi,\\
\lambda_2 &< 4\pi,\\
\lambda_4 &+ \lambda_6+\lambda_7 < 16\pi,
\end{aligned}
\tag{3.2.36}
$$

where $\Gamma_1 \equiv \alpha$, $\Gamma_2 \equiv \beta$, $\Gamma_3 \equiv \gamma$ and $\Gamma_4 \equiv \sigma$ [1]. Moreover, to maintain the perturbativity of the model, all the quartic couplings of the scalar potential $\lambda_i (i = 1...9)$ must satisfy this condition:

$$|\lambda_i| \leq 4\pi \tag{3.2.37}$$

In the compact 341 model, the physical scalar bosons masses are fully determined by the parameters of the scalar potential λ_i, therefore, other constraints on the scalar parameters can be found from the positivity of all scalar bosons masses. As we reported previously, the physical spectrum consists of three CP-even scalars, h_i (i=1,2,3) four charged scalars, $h_i^{\mp}$ (i=1,2) and two doubly charged scalar bosons $h^{\mp\mp}$. A complementary set of constraints on the λ_i comes from the positivity of all the masses of the scalar bosons is [81]:

$$
\begin{aligned}
&\lambda_1+\lambda_3-\sqrt{(\lambda_1-\lambda_3)^2+\lambda_5^2} > 0,\\
&\lambda_1+\lambda_3+\sqrt{(\lambda_1-\lambda_3)^2+\lambda_5^2} > 0,\\
&\lambda_2+\frac{\lambda_3\lambda_4^2+\lambda_6(\lambda_1\lambda_6-\lambda_4\lambda_5)}{\lambda_5^2-4\lambda_1\lambda_3} > 0,\\
&\lambda_7 > 0, \qquad \lambda_8 > 0, \qquad \lambda_9 > 0.
\end{aligned}
\tag{3.2.38}
$$

In addition, the scalar parameters are constrained by another strong condition by imposing that the lightest scalar boson h_1 is identical to the Standard Model Higgs like boson,

[1] we use this notation ($\Gamma_1 \equiv \alpha$, $\Gamma_2 \equiv \beta$, $\Gamma_3 \equiv \gamma$ and $\Gamma_4 \equiv \sigma$) nomenclature in Eqs.(3.2.36) and consistently in this chapter to avoid confusion with the rotation angles defined in Eqs.(3.2.33)-(3.2.35).

by talking M_{h_1}= 125.09 GeV and υ_ρ=246 GeV, therefore [81]:

$$\lambda_2 + \frac{\lambda_3\lambda_4^2 + \lambda_6(\lambda_1\lambda_6 - \lambda_4\lambda_5)}{\lambda_5^2 - 4\lambda_1\lambda_3} = \frac{m_{h_1}^2}{\upsilon_\rho^2}, \tag{3.2.39}$$

Moreover, Ref [38] reported that the compact 341 model has a Landau pole Λ around 5 TeV, that leads to a stringent constraint on the parameters. It requires that all scalar bosons masses and all VEVs are bounded to be less or equal Λ.

We generate random numbers for λ_i(i=1..9) subject with the various theoretical constraints that we discussed in the text. For example, the following benchmark point was generated [81]:

$$\lambda_1, \lambda_2, \lambda_3, \lambda_4, \lambda_5\lambda_6, \lambda_7, \lambda_8, \lambda_9 \equiv (1.24916, 1.4595, 2.08534, 0.612214, 0.544161, -2.88788, 1.20945, 0.308258, 3.64476). \tag{3.2.40}$$

3.3 Conclusion

The theoretical constraints on the parameters space are an important issue that must be imposed on the scalar potential couplings in any theory beyond the Standard Model. Thus one needs to find the necessary conditions to ensure the allowed region for the scalar couplings.

In this chapter, the corresponding theoretical constraints in the compact 341 model are derived such as the vacuum stability, minimization of the scalar potential, perturbative unitarity bounds and perturbativity of the scalar potential couplings. Moreover, other conditions coming from the positivity of the scalar bosons masses with the stringent condition of the Landau pole are also derived.

In the next chapter, we will focus on the neutral Higgs bosons h_1, h_2 and h_3 phenomenology in the compact 341 model and confrontations with the LHC results, using the previous constraints to determine the allowed regions for the scalar parameters $\lambda_{1....9}$.

Chapter 4

A New Compact 341 Model: Higgs Decay Modes

4.1 Introduction.

The main goal of this chapter is to study the decay of the neutrals scalar bosons h_1, h_2 and h_3 in the compact 341 model [39]. We calculate the partial width decay of those neutral scalar bosons into fermions $f\overline{f}$ (quarks or leptons), gauge bosons, pair of gluons (gg), diphotons ($\gamma\gamma$) and into $Z\gamma$.

To investigate the deviation of our model from the Standard Model and to know the significance of our model in the future search at the LHC, we calculate the signal strength μ for h_1 for each individual channels and confront our theoretical results to the data reported at LHC. Moreover, to search for the other heavy scalar bosons $h_i(i = 2, 3)$, we compute their branching ratios (BR).

4.2 Higgs-like boson h_1 decay

In this section, we discuss the Higgs-like boson h_1 decay into $f\overline{f}$, WW^*, ZZ^*, $\gamma\gamma$, $Z\gamma$ and gg in the compact 341 model.

4.2.1 Higgs-like boson h_1 decay into two Fermions

The partial width decay's expression of the Higgs-like boson h_1 into a pair of fermions $h_1(p_1) \longrightarrow f(p_2)\overline{f}(p_3)$ is:

$$\Gamma_{341}(h_1 \longrightarrow \overline{f}f) = \frac{1}{2m_{h_1}} \int d\Phi \sum |\mathcal{M}|^2, \tag{4.2.1}$$

where $\sum \mid \mathcal{M} \mid^2$ and $d\Phi$ represent the amplitude of the process and the invariant phase space of the decay products respectively, their expressions have the following form:

$$\sum \mid \mathcal{M} \mid^2 = \frac{2m_f^2}{v^2} m_{h_1}^2 (1 - \frac{4m_f^2}{M_{h_1}^2}), \tag{4.2.2}$$

$$d\Phi = \frac{d^3p_2}{(2\pi)^3 2E_2} \frac{d^3p_3}{(2\pi)^3 2E_3} \delta^4(p_1 - p_2 - p_3), \tag{4.2.3}$$

where in the center of mass frame the relativistic four-momenta are given by:
$p_1^\mu = (M_{h_1}, \overrightarrow{0})$, $p_2^\mu = (E_f, \overrightarrow{p})$, $p_3^\mu = (E_f, \overrightarrow{-p})$. This implies that $E_1 = E_2 = E_f$ and $M_{h_1} = 2E_f$. After the calculations, the partial width decay of the Higgs-like boson decay to fermions anti-fermions is found to be:

$$\Gamma_{341}(h_1 \longrightarrow \overline{f} f) = \frac{N_C g^2}{32\pi} \frac{m_f^2 m_{h_1}}{m_W^2} \left(1 - \frac{4m_f^2}{m_{h_1}^2}\right)^{\frac{3}{2}}. \tag{4.2.4}$$

Notice that we use the relation:

$$\delta[f(x)] = \frac{\delta(x - x_0)}{\left|\frac{\partial f}{\partial x}\right|_{x=x_0}}, \tag{4.2.5}$$

where N_C is the number of colors, it takes 1 for leptons and 3 for quarks, m_f is the fermion mass, m_{h_1} is the Higgs-like boson mass, m_W is the mass of the gauge boson W and g is the coupling constant where

$$g = \frac{\sqrt{\frac{4\pi}{137}}}{\sin\theta_W}. \tag{4.2.6}$$

The width decay of Higgs-like boson h_1 into a pair of bottom quarks is:

$$\Gamma_{341}(h_1 \longrightarrow \bar{b} b) = \frac{3g^2}{32\pi} \frac{m_b^2 m_{h_1}}{m_W^2} \left(1 - \frac{4m_b^2}{m_{h_1}^2}\right)^{\frac{3}{2}}. \tag{4.2.7}$$

Whereas the decay of h_1 into two leptons is:

$$\Gamma_{341}(h_1 \longrightarrow \bar{\ell} \ell) = \frac{g^2}{32\pi} \frac{m_l^2 m_{h_1}}{m_W^2} \left(1 - \frac{4m_l^2}{m_{h_1}^2}\right)^{\frac{3}{2}}. \tag{4.2.8}$$

4.2.2 Higgs-like boson h_1 decay into gauge bosons

Since $m_{h_1} < 2m_V$ (V=$W^\mp, Z$), there is not enough energy to produce two real (on mass shell) weak bosons V, therefore, the decay of h_1 into two gauge bosons gives a real W with a virtual W^* one which will decay into fermions $W^* \longrightarrow f\overline{f}$ (see Figure (4.1)).

The width decay expression as a function of the Higgs-like boson h_1 mass can be written as:

$$\Gamma_{341}(h_1 \longrightarrow W^*W) = \frac{3g^4 m_{h_1}}{512\pi^3} F(\frac{m_W}{m_{h_1}}). \tag{4.2.9}$$

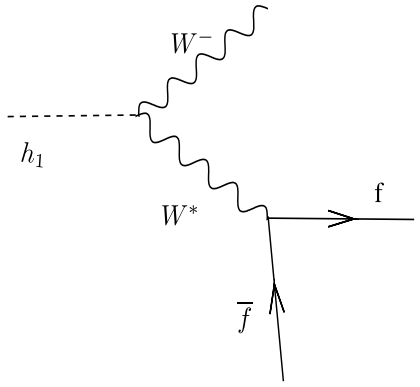

Figure 4.1: Three body Higgs decay $h_1 \longrightarrow W^- f\overline{f}$.

We consider $W^* \longrightarrow f_u f_d$, where $f_u = u, c, e, \mu, \tau$ and $f_d = d, s, b, \nu_e, \nu_\mu, \nu_\tau$, notice that the top quark is the heaviest quark, therefore, it will be the only quark that we shall not consider it as a massless particle.

Notice that we used the following Lorentz invariant kinematical variables:

$$S_{23} = (p_2 + p_3)^2 = M_W^2 + m_t^2 + 2p_3p_2, \tag{4.2.10}$$
$$S_{34} = (p_4 + p_3)^2 = m_t^2 + 2p_3p_4, \tag{4.2.11}$$
$$S_{24} = (p_4 + p_2)^2 = M_W^2 + 2p_2p_4, \tag{4.2.12}$$

with

$$p_3^2 = m_t^2 = m^2 \tag{4.2.13}$$
$$p_4^2 = m_b^2 = 0, \tag{4.2.14}$$
$$kp_3 = m^2 + p_3p_4, \tag{4.2.15}$$
$$kp_4 = p_3p_4, \tag{4.2.16}$$

where p_1, p_2, p_3 and p_4 are the impulsions of the Higgs h_1, the real gauge boson W, the fermions f and the anti-fermions $\overline{f}$ respectively and the three variables S_{23}, S_{24} and S_{34} satisfy the following relation

$$S_{23} + S_{24} + S_{34} = M_{h_1}^2 + M_W^2 + m_t^2 \tag{4.2.17}$$

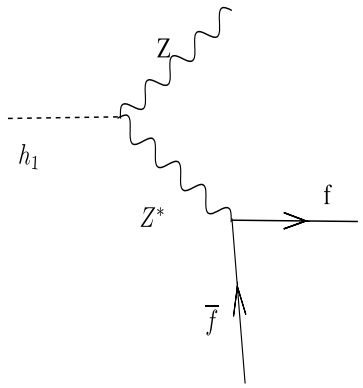

Figure 4.2: Three body Higgs decay $h_1 \longrightarrow Zf\overline{f}$.

In order to be able to express $|\mathcal{M}|^2$ as a function of S_{ij} and masses we will read the following expressions:

$$p_2p_3 = \frac{1}{2}\Big(M_{h_1^2} - S_{24} - S_{34}\Big), \tag{4.2.18}$$

$$p_2p_4 = \frac{1}{2}\Big(S_{24} - M_W^2\Big), \tag{4.2.19}$$

$$p_3p_4 = \frac{1}{2}\Big(S_{34} - m_t^2\Big). \tag{4.2.20}$$

Now, we turn our attention to the partial width of the Higgs-like boson decaying to a real neutral gauge boson Z with a virtual one Z^* ($h_1(p_1) \longrightarrow Z(p_2)f(p_3)\overline{f}(p_4)$) (see Figure 4.2). The amplitude of this process is:

$$\begin{aligned}\mathcal{M}(h_1 \longrightarrow Z\bar{t}t) &= \frac{2gM_Z^2}{\upsilon_\rho}G_{ZZh_1}\epsilon^\mu_{r_2}\Big(-g_{\mu\nu} + \frac{k_\mu k_\nu}{M_Z^2}\Big)\frac{1}{k^2 - M^2}\overline{u}_t(p_3) \\ &\cdot \gamma^\nu\Big(g_V - g_A\gamma_5\Big)v_t(p_4).\end{aligned} \tag{4.2.21}$$

Using $p_3 + p_4 = k$, then we find:

$$|\mathcal{M}|^2 = \frac{M_Z^2}{\upsilon^2}g^2\frac{T^{\beta\nu}G_{\beta\nu}}{(k^2 - M_Z^2)^2}, \tag{4.2.22}$$

where

$$T^{\beta\nu} = \mathrm{Tr}\{\gamma^\beta(g_{Vt} - g_{At}\gamma_5)(\not{p}_3 + m)\gamma^\nu(g_{Vt} - g_{At}\gamma_5)(\not{p}_4 - m)\} \tag{4.2.23}$$

After many steps of calculations, we get

$$\begin{aligned}\Gamma_{341}(h_1 \longrightarrow Z^*Z) &= \frac{g^4 m_{h_1}}{2048C_W^2\pi^3}G_{h_1ZZ}^2F(\frac{m_Z}{m_{h_1}})\Big(\sum_{j=u,d,c,s,b}(g_{jV}^2 + g_{jA}^2) + (g_{\ell V}^2 + g_{\ell A}^2) \\ &+ (g_{\nu V}^2 + g_{\nu A}^2)\Big),\end{aligned} \tag{4.2.24}$$

where $G_{ZZh_1} = \frac{4}{g^2 v_\rho} g_{ZZh_1}$ with g_{ZZh_1} represents the coupling between a pair of Z bosons and h_1 (see appendix A), g_V and g_A are real parameters, their expressions are reported in the appendix A. Concerning the kinematic factor $F(x)$, its expression is:

$$\begin{aligned} F(x) &= -|1-x^2|\left(\frac{47}{2}x^2 - \frac{13}{2} + \frac{1}{x^2}\right) - \frac{3}{2}(1-6x^2+4x^4)\ln(x) \\ &+ \frac{3(1-8x^2+20x^4)}{\sqrt{4x^2-1}} \arccos\left(\frac{3x^2-1}{2x^3}\right), \end{aligned} \tag{4.2.25}$$

where $x = \frac{m_{W(Z)}}{m_{h_1}}$.

4.2.3 Higgs-like boson h_1 decay into two photons

It is well known that the Higgs couples to the photon is induced at the loop level processes. In the Standard Model case the contributions to the diphoton decay channel comes from the top quark and the gauge boson W, therefore, its partial width decay can be written as [39]:

$$\Gamma_{SM}(h \longrightarrow \gamma\gamma) = \frac{G_F \alpha^2 m_h^3}{128\sqrt{2}\pi^3} \left| A_1(\tau_W) + N_C Q_t^2 A_{\frac{1}{2}}(\tau_t) \right|^2, \tag{4.2.26}$$

where G_F is the Fermi Constant, $N_C = 3$ the number of color, Q_t the electric charge of top quark, $A_1(\tau_W)$ and $A_{\frac{1}{2}}(\tau_t)$ are the loop functions for the W boson and the top quark respectively.

The compact 341 model contains new charged particles including fermions, scalars (the new singly and doubly charged scalar bosons) and gauge bosons that will contribute to the decay amplitudes of the decays $h_1 \longrightarrow \gamma\gamma$ and $h_1 \longrightarrow \gamma Z$ at one loop level. In the case of h_1, besides the contribution of $W^\mp$ boson and the top quark, the processes $\Gamma(h_1 \longrightarrow \gamma\gamma(\gamma Z))$ receive new contributions that come from new particles (gauge and scalar bosons) such as $V^{\mp\mp}$, $K_1^\mp$, $h_1^\mp$, $h_2^\mp$ and $h^{\mp\mp}$, Furthermore, in our model, the SM Higgs-like boson h_1 does not couple to the new heavy charged fermions, hence, the exotic quarks do not contribute to the one-loop decay amplitudes of the processes $h_{2,3} \longrightarrow (\gamma\gamma, Z\gamma, gg)$. Figure 4.3 shows the main contributions to the decay $h_i \longrightarrow \gamma\gamma$ and $Z\gamma$.

Consider a Higgs boson width four-momentum $p_{h_1} = (m_{h_1}, 0)$, decaying into two photons with four momenta: $k_1 = (E_1, k_1)$, $k_2 = (E_2, k_2)$.

$$\begin{aligned} d\Gamma(h_1 \longrightarrow \gamma\gamma) &= \frac{1}{2m_{h_1}} (2\pi)^4 \delta^4(p_{h_1} - (k_1+k_2)) \left| \mathcal{M}_{h_1} \longrightarrow \gamma\gamma \right|^2 \frac{d^3k_1}{2E_1(2\pi)^3} \\ &\cdot \frac{d^3k_2}{2E_2(2\pi)^3}. \end{aligned} \tag{4.2.27}$$

In the center of mass frame the total 3 momentum is zero thus $k_1 = -k_2$, $E_1 = E_2 = E$ and $d^3k = EdEd\Omega$, then we get:

$$d\Gamma(h_1 \longrightarrow \gamma\gamma) = \frac{1}{16\pi m_{h_1}} |\mathcal{M}_{h_1 \longrightarrow \gamma\gamma}|^2. \tag{4.2.28}$$

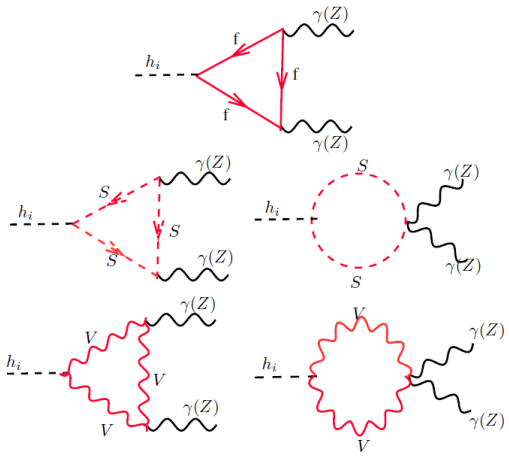

Figure 4.3: The one-Loop diagrams contributing to $h_i \longrightarrow \gamma\gamma(\gamma Z)$ decay where i=1,2 or 3.

Using the parameterizations of Feynman integrals (See appendix B) to get [39]:

$$\begin{aligned}\Gamma(h_1 \longrightarrow \gamma\gamma) &= \frac{\alpha^2 m_{h_1}^3}{1024\pi^3}\Big|\sum_V \frac{g_{h_1VV}}{m_V^2}Q_V^2\mathcal{A}_1(\tau_V)+\sum_f \frac{2g_{h_1ff}}{m_f}Q_f^2 N_{c,f}\mathcal{A}_{\frac{1}{2}}(\tau_f)\\ &+ \sum_f \frac{g_{h_1SS}}{m_S^2}Q_S^2 N_{c,S}\mathcal{A}_0(\tau_S)\Big|^2, \end{aligned} \tag{4.2.29}$$

where V, f and S refer to Spin 1, Spin $\frac{1}{2}$ and Spin 0 particles respectively, Q_V, Q_f, Q_S are electric charges of the vectors, fermions and scalars, g_{h_1SS},g_{h_1VV} and g_{h_1ff} are the couplings of the Higgs-like boson with S, V and f respectively their expressions are tabulated in tables (A.1)-(A.6) (see the appendix A), $N_{c,f}, N_{c,S}$ are the number of fermion and scalar colors respectively, $\mathcal{A}_1(\tau_V)$, $\mathcal{A}_{\frac{1}{2}}(\tau_f)$ and $\mathcal{A}_0(\tau_S)$ are the loop functions for V,f and S respectively (See the appendix B).

4.2.4 Higgs-like boson h_1 decay into photon and Z

The main contributions to the decay $h_i \longrightarrow Z\gamma$ are shown in Figure 4.3, the explicit form of the partial width for $h_1 \longrightarrow \gamma Z$ can be written down as [39]:

$$\Gamma(h_1 \longrightarrow \gamma Z) = \frac{\alpha^2 m_{h_1}^3}{512\pi^3}\left(1-\frac{M_Z^2}{M_{h_1}^2}\right)^3\left|\frac{2}{\upsilon}\frac{\mathcal{A}_{SM}}{\sin\theta_W}+\mathcal{A}\right|^2. \tag{4.2.30}$$

The factors $\mathcal{A}$ and $\mathcal{A}_{SM}$ represent the contributions of the new particles which predicted by our model and the contributions coming from the particles of the Standard Model respec-

tively, their expressions are given by [39]:

$$\begin{aligned}\mathcal{A} &= \frac{g_{h_1VV}}{m_V^2} g_{ZVV}\mathcal{A}_1(\tau_V,\lambda_V) + \widetilde{N}_{c,f}\frac{2g_{h_1ff}}{m_f}2Q_f(g_{Zll})\mathcal{A}_{\frac{1}{2}}(\tau_f,\lambda_f) \\ &- \widetilde{N}_{c,s}\frac{2g_{h_1SS}}{m_S^2}Q_S g_{ZSS}\mathcal{A}_0(\tau_S,\lambda_S), \qquad (4.2.31)\\ \mathcal{A}_{SM} &= \cos\theta_W\mathcal{A}_1(\tau_W,\lambda_W) + N_C\frac{Q_t(2T_3^t - 4Q_t\sin\theta_W^2)}{\cos\theta_W}\mathcal{A}_{\frac{1}{2}}(\tau_t,\lambda_t), \qquad (4.2.32)\end{aligned}$$

where $\tau_i = \frac{4m_i^2}{m^2_{H_1^2}}$,$\lambda_i = \frac{4m_i^2}{m^2_{Z^2}}$ and $T_3 = \frac{1}{2}$ is the weak isospin of the top quark, $\mathcal{A}_i(x,y)$ represent the loop functions (see the appendix B), $Q_t = \frac{2}{3}$ is the electric charge of the top quark, g_{Zff},g_{ZVV} and g_{ZSS} represent the couplings of the Z boson with the fermions f, gauge bosons V and scalar bosons S respectively, their expressions are tabulated in tables (A.1)-(A.6) in the appendix A.

4.3 Heavy scalar bosons decay $h_i(i = 2, 3)$

In this section, we study the heavy scalar bosons $h_i(i = 2, 3)$ decay in the compact 341 model.

4.3.1 Heavy scalar bosons decay into two Fermions

The partial widths decays of $h_i(i = 2, 3)$ into two Fermions are:

$$\begin{aligned}\Gamma(h_2 \longrightarrow \ell\ell) &= \frac{g^2}{32\pi}\frac{m_\ell^2 m_{h_2}}{m_W^2}\left(1 - \frac{4m_\ell^2}{m_{h_2}^2}\right)^{\frac{3}{2}}\left(\frac{\upsilon_\rho}{\upsilon_\chi}\gamma\right)^2, \qquad (4.3.1)\\ \Gamma(h_3 \longrightarrow \ell\ell) &= \frac{g^2}{32\pi}\frac{m_\ell^2 m_{h_3}}{m_W^2}\left(1 - \frac{4m_\ell^2}{m_{h_3}^2}\right)^{\frac{3}{2}}\left(\frac{\upsilon_\rho}{\upsilon_\chi}\sigma\right)^2, \qquad (4.3.2)\\ \Gamma(h_2 \longrightarrow \bar{b}b) &= \frac{3g^2}{32\pi}\frac{m_b^2 m_{h_2}}{m_W^2}\left(1 - \frac{4m_b^2}{m_{h_2}^2}\right)^{\frac{3}{2}}\left(\frac{\upsilon_\rho}{\upsilon_\chi}\gamma + \frac{\upsilon_\rho}{\upsilon_\eta}\alpha\right)^2, \qquad (4.3.3)\\ \Gamma(h_3 \longrightarrow \bar{b}b) &= \frac{3g^2}{32\pi}\frac{m_b^2 m_{h_3}}{m_W^2}\left(1 - \frac{4m_b^2}{m_{h_3}^2}\right)^{\frac{3}{2}}\left(\frac{\upsilon_\rho}{\upsilon_\chi}\sigma + \frac{\upsilon_\rho}{\upsilon_\eta}\beta\right)^2 \qquad (4.3.4)\end{aligned}$$

If $m_{h_i} > 2m_{U(J)}$, h_i can decay into a pair of exotic quarks $U(J)$ as follows:

$$\begin{aligned}\Gamma(h_2 \longrightarrow UU) &= \frac{3g^2}{32\pi}\frac{m_U^2 m_{h_3}}{m_W^2}\left(1 - \frac{4m_U^2}{m_{h_3}^2}\right)^{\frac{3}{2}}\left(\frac{\upsilon_\rho\alpha}{\upsilon_\eta}\right)^2, \qquad (4.3.5)\\ \Gamma(h_3 \longrightarrow UU) &= \frac{3g^2}{32\pi}\frac{m_U^2 m_{h_3}}{m_W^2}\left(1 - \frac{4m_U^2}{m_{h_3}^2}\right)^{\frac{3}{2}}\left(\frac{\upsilon_\rho\beta}{\upsilon_\eta}\right)^2, \qquad (4.3.6)\end{aligned}$$

And

$$\Gamma(h_2 \longrightarrow JJ) = \frac{3g^2}{32\pi}\frac{m_J^2 m_{h_2}}{m_W^2}\left(1-\frac{4m_J^2}{m_{h_2}^2}\right)^{\frac{3}{2}}\left(\frac{\upsilon_\rho \gamma}{\upsilon_\chi}\right)^2, \tag{4.3.7}$$

$$\Gamma(h_3 \longrightarrow JJ) = \frac{3g^2}{32\pi}\frac{m_J^2 m_{h_3}}{m_W^2}\left(1-\frac{4m_J^2}{m_{h_3}^2}\right)^{\frac{3}{2}}\left(\frac{\upsilon_\rho \sigma}{\upsilon_\chi}\right)^2, \tag{4.3.8}$$

where m_l, m_W, $m_{h_i}(i=2,3)$ and m_U, m_J are the masses of leptons, gauge boson W, the scalar bosons h_i and the exotic quarks respectively, α, β, γ, σ are real parameters (see appendix A), υ_χ is the vacuum expectation value.

4.3.2 Heavy scalar bosons decay into gauge bosons

If $m_{h_i} > 2m_{Z,V_i,Z'}$, the heavy scalar bosons h_i can decay into a pair of real Z bosons, into a pair of new gauge bosons V_i ($V_i \equiv X^{\mp}, V^{\mp\mp}, K'^0, K_1^{\mp}, Y^{\mp}$) and into a pair of Z' bosons, their partial widths decays are given respectively by:

$$\Gamma(h_i \longrightarrow ZZ) = \frac{1}{8\pi}\frac{M_Z^4}{M_{h_i}\upsilon_\rho^2}\left(1-\frac{4M_Z^2}{M_{h_i}^2}\right)^{\frac{1}{2}}\left(3+\frac{M_{h_i}^4}{M_Z^4}-\frac{M_{h_i}^2}{M_Z^2}\right)G_{ZZh_i}^2, \tag{4.3.9}$$

$$\Gamma(h_i \longrightarrow V_iV_i) = \frac{k_i}{4\pi}\frac{M_W^4}{M_{h_i}\upsilon_\rho^2}\left(1-\frac{4M_{V_i}^2}{M_{h_i}^2}\right)^{\frac{1}{2}}\left(3+\frac{1}{4}\frac{M_{h_i}^4}{M_{V_i}^4}-\frac{M_{h_i}^2}{M_{V_i}^2}\right), \tag{4.3.10}$$

$$\Gamma(h_i \longrightarrow Z'Z') = \frac{1}{8\pi}\frac{M_Z^4}{M_{h_2}\upsilon_\rho^2}\left(1-\frac{4M_{Z'}^2}{M_{h_2}^2}\right)^{\frac{1}{2}}\left(3+\frac{M_{h_2}^4}{M_{Z'}^4}-\frac{M_{h_2}^2}{M_{Z'}^2}\right)G_{Z'Z'h_i}^2, \tag{4.3.11}$$

where in the case of h_2, the coefficients k_i are given in the following table:

Higgs	$k_{X^{\mp}}$	$k_{V^{\mp\mp}}$	$k_{K'^0}$	$k_{K_1^{\mp}}$	$k_{Y^{\mp}}$
h_2	$\frac{\upsilon_\chi}{\upsilon_\rho}\gamma$	$\frac{\upsilon_\chi}{\upsilon_\rho}\gamma$	$\frac{\upsilon_\eta}{\upsilon_\rho}\alpha$	$\frac{\upsilon_\eta}{\upsilon_\rho}\alpha$	$\frac{1}{\upsilon_\rho}(\upsilon_\chi\gamma+\upsilon_\eta\alpha)$

Table 4.1: k_i coefficients in the case of h_2.

while, in the case of h_3, the coefficients k_i are given by:

Higgs	$k_{X^{\mp}}$	$k_{V^{\mp\mp}}$	$k_{K'^0}$	$k_{K_1^{\mp}}$	$k_{Y^{\mp}}$
h_3	$\frac{\upsilon_\chi}{\upsilon_\rho}\sigma$	$\frac{\upsilon_\chi}{\upsilon_\rho}\sigma$	$\frac{\upsilon_\eta}{\upsilon_\rho}\beta$	$\frac{\upsilon_\eta}{\upsilon_\rho}\beta$	$\frac{1}{\upsilon_\rho}(\upsilon_\chi\sigma+\upsilon_\eta\beta)$

Table 4.2: k_i coefficients in the case of h_3.

The expressions of G_{ZZh_i} and $G_{Z'Z'h_i}$ are given by:

$$\begin{aligned}
G_{ZZh_2} &= \frac{C_W^2}{2}\left(\frac{3}{2}\frac{\upsilon_\chi}{\upsilon_\rho}(C^{23})^2\gamma + 4(C^{24})^2\frac{S_W^2}{1-4S_W^2}\frac{\upsilon_\chi}{\upsilon_\rho}\gamma + \frac{12}{\sqrt{6}}\frac{S_W}{\sqrt{1-4S_W^2}}\frac{\upsilon_\chi}{\upsilon_\rho}C^{23}C^{24}\gamma\right. \\
&+ \left.\frac{4}{3}(C^{22})^2\frac{\upsilon_\eta}{\upsilon_\rho}\alpha + \frac{(C^{23})^2}{6}\frac{\upsilon_\eta}{\upsilon_\rho}\alpha - \frac{4}{\sqrt{18}}C^{22}C^{23}\frac{\upsilon_\eta}{\upsilon_\rho}\alpha\right), \qquad (4.3.12)\\
G_{ZZh_3} &= \frac{C_W^2}{2}\left[\frac{3}{2}\frac{\upsilon_\chi}{\upsilon_\rho}(C^{23})^2\sigma + 4(C^{24})^2\frac{S_W^2}{1-4S_W^2}\frac{\upsilon_\chi}{\upsilon_\rho}\sigma + \frac{12}{\sqrt{6}}\frac{S_W}{\sqrt{1-4S_W^2}}\frac{\upsilon_\chi}{\upsilon_\rho}C^{23}C^{24}\sigma\right. \\
&+ \left.\frac{4}{3}(C^{22})^2\frac{\upsilon_\eta}{\upsilon_\rho}\beta + \frac{(C^{23})^2}{6}\frac{\upsilon_\eta}{\upsilon_\rho}\beta - \frac{4}{\sqrt{18}}C^{22}C^{23}\frac{\upsilon_\eta}{\upsilon_\rho}\beta\right]. \qquad (4.3.13)\\
G_{Z'Z'h_2} &= \frac{C_W^2}{2}\left(\frac{3}{2}\frac{\upsilon_\chi}{\upsilon_\rho}(C^{33})^2\gamma + 4(C^{34})^2\frac{S_W^2}{1-4S_W^2}\frac{\upsilon_\chi}{\upsilon_\rho}\gamma + \frac{12}{\sqrt{6}}\frac{S_W}{\sqrt{1-4S_W^2}}\frac{\upsilon_\chi}{\upsilon_\rho}C^{33}C^{34}\gamma\right. \\
&+ \left.\frac{4}{3}(C^{32})^2\frac{\upsilon_\eta}{\upsilon_\rho}\alpha + \frac{(C^{33})^2}{6}\frac{\upsilon_\eta}{\upsilon_\rho}\alpha - \frac{4}{\sqrt{18}}C^{32}C^{33}\frac{\upsilon_\eta}{\upsilon_\rho}\alpha\right), \qquad (4.3.14)\\
G_{Z'Z'h_3} &= \frac{C_W^2}{2}\left[\frac{3}{2}\frac{\upsilon_\chi}{\upsilon_\rho}(C^{33})^2\sigma + 4(C^{34})^2\frac{S_W^2}{1-4S_W^2}\frac{\upsilon_\chi}{\upsilon_\rho}\sigma + \frac{12}{\sqrt{6}}\frac{S_W}{\sqrt{1-4S_W^2}}\frac{\upsilon_\chi}{\upsilon_\rho}C^{33}C^{34}\sigma\right. \\
&+ \left.\frac{4}{3}(C^{32})^2\frac{\upsilon_\eta}{\upsilon_\rho}\beta + \frac{(C^{33})^2}{6}\frac{\upsilon_\eta}{\upsilon_\rho}\beta - \frac{4}{\sqrt{18}}C^{32}C^{33}\frac{\upsilon_\eta}{\upsilon_\rho}\beta\right]. \qquad (4.3.15)
\end{aligned}$$

Furthermore, in the compact 341 model there is no direct coupling between the gauge boson $W^\mp$ and the heavy scalar bosons ($W^+W^-h_2 = 0$ and $W^+W^-h_3 = 0$), thus,

$$\Gamma(h_2 \longrightarrow W^+W^-) = \Gamma(h_3 \longrightarrow W^+W^-) = 0. \qquad (4.3.16)$$

Notice that we used the following relation:

$$\sum \epsilon_\mu^* \epsilon^\mu = -g^{\mu\nu} + \frac{p_\mu p_\nu}{m_{GB}^2}, \qquad (4.3.17)$$

And the following kinematics:

$$\begin{aligned}
p_1^\mu &= (m_{h_3}, \overrightarrow{p}),\\
p_3^\mu &= (E_{V_i}, \overrightarrow{-p}),\\
p_2^\mu &= (E_{V_i}, \overrightarrow{p}), \qquad (4.3.18)
\end{aligned}$$

where p_1, p_2 and p_3 are the impulsion of h_i ,gauge bosons V_i^+ and V_i^- respectively.

4.3.3 Heavy scalar bosons decay into gluon gluon

In the Standard Model, at the LHC the decay of $h \longrightarrow gg$ is mediated by a top quark. In the compact 341model, there is no direct coupling between h_i and the top quark therefore,

the one loop contribution of the decay $h_i \longrightarrow gg$ comes from the exotic quarks, thus, the partial width expressions for $h_i \longrightarrow gg$ are:

$$\Gamma(h_2 \longrightarrow gg) = \frac{\alpha_S^2 M_{h_2}^3}{128\pi^3 \upsilon_\eta^2}\alpha^2 \Big|\sum_{i=1}^{3} A_{\frac{1}{2}}(\tau_U)\Big|^2 + \frac{\alpha_S^2 M_{h_2}^3}{128\pi^3 \upsilon_\chi^2}\gamma^2 \Big|\sum_{i=1}^{3} A_{\frac{1}{2}}(\tau_J)\Big|^2, \quad (4.3.19)$$

$$\Gamma(h_3 \longrightarrow gg) = \frac{\alpha_S^2 M_{h_3}^3}{128\pi^3 \upsilon_\eta^2}\beta^2 \Big|\sum_{i=1}^{3} A_{\frac{1}{2}}(\tau_U)\Big|^2 + \frac{\alpha_S^2 M_{h_3}^3}{128\pi^3 \upsilon_\chi^2}\sigma^2 \Big|\sum_{i=1}^{3} A_{\frac{1}{2}}(\tau_J)\Big|^2, \quad (4.3.20)$$

where α_S is the strong coupling, $A_{\frac{1}{2}}(\tau_U)$ and $A_{\frac{1}{2}}(\tau_J)$ are loop functions of the exotic quarks U and J.

4.3.4 Heavy scalar bosons decay into two photons and $(Z\gamma)$

The one loop expressions for $h_{2,3}$ decays into final states including massless bosons $\gamma\gamma$ and $Z\gamma$ can be mediated by new contributions that come from the new charged particles namely $K_1^{\mp}$, K'^0, $X^{\mp}$, $Y^{\mp}$, $V^{\mp\mp}$, U, J, $h_1^{\mp}$, $h_2^{\mp}$ and $h^{\mp\mp}$, we note that the contribution of the $W^{\mp}$ boson is not included in these amplitudes since there is no direct coupling between $h_{2,3}$ and the $W^{\mp}$ boson. The interaction between h_i with the particles that run in the loop are presented in tables (A.1)-(A.6) (see the appendix A).

4.3.5 Heavy scalar boson decay into scalars bosons

It is worth pointing out that h_i may decay into a pair of scalar bosons h_1h_1, h_2h_2 and h_1h_2 . For h_2, it can decay into two identical Higgs-like bosons ($h_2 \longrightarrow h_1h_1$), while, h_3 can decay into two identical Higgs-like bosons h_1, into two identical h_2 ($h_3 \longrightarrow h_2h_2$) and into h_1h_2 ($h_3 \longrightarrow h_1h_2$).

h_2 decay into h_1h_1

The partial width decay of $h_2 \longrightarrow h_1h_1$ is:

$$\Gamma_{341}(h_2 \longrightarrow h_1h_1) = \frac{1}{2m_{h_2}}(g_{h_2h_1h_1})^2 \int d\Phi, \quad (4.3.21)$$

using the condition:

$$2E_{h_1} = m_{h_2}, \quad (4.3.22)$$

we get:

$$\Phi = \frac{m_{h_2}}{2}(1 - \frac{4m_{h_1}^2}{m_{h_2}^2})^{\frac{1}{2}} \quad (4.3.23)$$

Substitute (4.3.23) in Eq.(4.3.21), then we get:

$$\Gamma_{341}(h_2 \longrightarrow h_1 h_1) = \frac{1}{32\pi m_{h_2}}(g_{h_2 h_1 h_1})^2\left(1-\frac{4m_{h_1}^2}{m_{h_2}^2}\right)^{\frac{1}{2}}, \tag{4.3.24}$$

where the coupling $g_{h_2h_1h_1}$ represents the trilinear interaction between $h_2h_1h_1$, its expression is:

$$g_{h_2h_1h_1} = v_\chi\left(\frac{\lambda_6}{2}\gamma + \frac{\lambda_4}{2}\frac{v_\eta}{v_\chi}\alpha\right). \tag{4.3.25}$$

where λ_6, λ_4 are the scalar coupling parameters.

h_3 decay into h_1h_1

The partial width decay of $h_2 \longrightarrow h_1h_1$ is [39]:

$$\Gamma_{341}(h_3 \longrightarrow h_1 h_1) = \frac{1}{32\pi m_{h_3}}(g_{h_3 h_1 h_1})^2\left(1-\frac{4m_{h_1}^2}{m_{h_3}^2}\right)^{\frac{1}{2}}, \tag{4.3.26}$$

The coupling $g_{h_3h_1h_1}$ describes the trilinear interaction $h_3h_1h_1$, it's expression is found to be:

$$g_{h_3h_1h_1} = v_\chi\left(\frac{\lambda_6}{2}\sigma + \frac{\lambda_4}{2}\frac{v_\eta}{v_\chi}\beta\right). \tag{4.3.27}$$

h_3 decay into h_2h_2

Concerning the partial width decay of $h_3 \longrightarrow h_2h_2$, it is found to be [39]:

$$\Gamma_{341}(h_3 \longrightarrow h_2 h_2) = \frac{1}{32\pi m_{h_3}}(g_{h_3 h_2 h_2})^2\left(1-\frac{4m_{h_2}^2}{m_{h_3}^2}\right)^{\frac{1}{2}}, \tag{4.3.28}$$

where:

$$g_{h_3h_2h_2} = \frac{\lambda_5}{2}\Big(v_\chi(\alpha^2\sigma + 2\alpha\beta\gamma) + v_\eta(\beta\gamma^2 + 2\alpha\gamma\sigma)\Big). \tag{4.3.29}$$

h_3 decay into h_1h_2

Using Eq.(4.2.1) and the expression of the phase space $d\Phi$ which is:

$$d\Phi = \int \frac{d^3p_1 d^3p_2}{4E_1E_1(2\pi)^6}\delta^4(p_3-p_2-p_1)(2\pi)^4, \tag{4.3.30}$$

where p_1, p_2 and p_3 are the impulsions of h_1, h_2 and h_3 respectively, we get:

$$\Gamma_{341}(h_3 \longrightarrow h_2 h_1) = \frac{1}{8\pi m_{h_3}^2}(g_{h_3 h_2 h_1})^2 P_1^0 \tag{4.3.31}$$

where:

$$P_1^0 = \frac{1}{2}\left(\frac{m_{h_2}^4}{m_{h_3}^2} - \frac{2m_{h_1}^2 m_{h_2}^2}{m_{h_3}^2} - 2m_{h_2}^2 + \frac{m_{h_1}^4}{m_{h_3}^2} - 2m_{h_1}^2 + m_{h_3}^2\right)^{\frac{1}{2}}, \tag{4.3.32}$$

Thus, the partial width decay of h_3 into $h_2 h_1$ is [39]:

$$\Gamma_{341}(h_3 \longrightarrow h_2 h_1) = \frac{1}{16\pi m_{h_3}^2}(g_{h_3 h_2 h_1})^2\left(\frac{m_{h_2}^4}{m_{h_3}^2} - \frac{2m_{h_1}^2 m_{h_2}^2}{m_{h_3}^2} - 2m_{h_2}^2 + \frac{m_{h_1}^4}{m_{h_3}^2} - 2m_{h_1}^2 + m_{h_3}^2\right)^{\frac{1}{2}}, \tag{4.3.33}$$

where the coupling $g_{h_3 h_2 h_1}$ represents the trilinear term $h_3 h_2 h_1$, its expression is:

$$g_{h_3 h_2 h_1} = \lambda_4 \upsilon_\rho \alpha\beta + \lambda_6 \upsilon_\rho \gamma\sigma. \tag{4.3.34}$$

4.4 The signal strength

The signal strength of any process with a giving initial state i producing an Higgs h which decays to the final state f can be written as a product of the Higgs boson production cross section and its branching ratio in units of the corresponding value predicted by the SM [39]:

$$\mu_{xy} = \frac{\sigma_{341}(pp \longrightarrow h_1) BR_{341}(h_1 \longrightarrow xy)}{\sigma_{SM}(pp \longrightarrow h) BR_{SM}(h \longrightarrow xy)}, \tag{4.4.1}$$

where the superscript SM and 341 refer to the Standard Model and the compact 341 model respectively, while, x and y are any finale state, σ_i and BR$_i$ (i=341, SM) are the corresponding cross section production taking gluon-gluon fusion (ggF) is the dominant contribution of the Higgs production and the branching ratio respectively. In the compact 341 model, the coupling tth_1 is the same as tth of the Standard Model (SM), hence, the cross section of the light Higgs h_1 production process is the same as the SM at the LHC:

$$\sigma_{341}(pp \longrightarrow h_1) = \sigma_{SM}(pp \longrightarrow h), \tag{4.4.2}$$

thus, the signal strength μ_{xy} becomes the ratio between the branching ratio of the SM and of the compact 341 model:

$$\mu_{xy} = \frac{BR_{341}}{BR_{SM}} = \frac{\Gamma_{SM}(h \longrightarrow all)\Gamma_{341}(h_i \longrightarrow xy)}{\Gamma_{341}(h_i \longrightarrow all)\Gamma_{SM}(h \longrightarrow xy)}, \tag{4.4.3}$$

where the total decay width $\Gamma_{341}(h_1 \longrightarrow all)$ turns out to be the same as the one of the SM Higgs boson $\Gamma_{SM}(h \longrightarrow all)$:

$$\begin{aligned}\Gamma_{341}(h_1 \longrightarrow all) &= \Gamma_{341}(h_1 \longrightarrow b\bar{b}) + \Gamma_{341}(h_1 \longrightarrow \tau^+\tau^-) + \Gamma_{341}(h_1 \longrightarrow WW^*) \\ &+ \Gamma_{341}(h_1 \longrightarrow ZZ^*) + \Gamma_{341}(h_1 \longrightarrow \gamma\gamma) + \Gamma_{341}(h_1 \longrightarrow \gamma Z) \\ &+ \Gamma_{341}(h_1 \longrightarrow gg).\end{aligned} \tag{4.4.4}$$

In this section, we use the expression (4.4.3) to discuss the signal strength for different individual channels $\ell\bar{\ell}$, $b\bar{b}$, WW^*, ZZ^*, $\gamma\gamma$ and $Z\gamma$ in the context of the compact 341 model.

4.4.1 The signal strength of $h_1 \longrightarrow f\overline{f}$

From table (A.1), we have $(f\overline{f}h_1)_{341}$=$(f\overline{f}h)_{SM}$, thus:

$$\Gamma_{341}(h \longrightarrow f\overline{f}) = \Gamma_{SM}(h \longrightarrow f\overline{f}). \tag{4.4.5}$$

By using Eq.(4.4.3), the signal strength of the channels $h_1 \longrightarrow \ell\overline{\ell}$ and $h_1 \longrightarrow b\overline{b}$ equal to:

$$\mu_{b\overline{b}} = \mu_{\ell\overline{\ell}} = \frac{\Gamma_{SM}(h \longrightarrow all)}{\Gamma_{341}(h_1 \longrightarrow all)}. \tag{4.4.6}$$

4.4.2 The signal strength of $h_1 \longrightarrow VV^*$ $(V \equiv W \mathbf{or} Z)$

According to table (A.1), we have $(WWh_1)_{341}$=$(WWh)_{SM}$ then:

$$\Gamma_{341}(h \longrightarrow WW^*) = \Gamma_{SM}(h \longrightarrow WW^*). \tag{4.4.7}$$

The signal strength of the channel $h_1 \longrightarrow WW^*$ is:

$$\mu_{W^*W} = \frac{\Gamma_{SM}(h \longrightarrow all)}{\Gamma_{341}(h_1 \longrightarrow all)}, \tag{4.4.8}$$

while, the signal strength μ_{ZZ^*} of the process $h_1 \longrightarrow ZZ^*$ is:

$$\mu_{Z^*Z} = \frac{\Gamma_{SM}(h \longrightarrow all)\Gamma_{341}(h \longrightarrow Z^*Z)}{\Gamma_{341}(h_1 \longrightarrow all)\Gamma_{SM}(h_1 \longrightarrow Z^*Z)} \tag{4.4.9}$$

4.4.3 The signal strength of $h_1 \longrightarrow \gamma\gamma(Z\gamma)$

For the channels $\gamma\gamma$ and $Z\gamma$, we get:

$$\mu_{\gamma\gamma} = \frac{\Gamma_{SM}(h \longrightarrow all)\Gamma_{341}(h \longrightarrow \gamma\gamma)}{\Gamma_{341}(h_1 \longrightarrow all)\Gamma_{SM}(h_1 \longrightarrow \gamma\gamma)}, \tag{4.4.10}$$

$$\mu_{Z\gamma} = \frac{\Gamma_{SM}(h \longrightarrow all)\Gamma_{341}(h \longrightarrow Z\gamma)}{\Gamma_{341}(h_1 \longrightarrow all)\Gamma_{SM}(h_1 \longrightarrow Z\gamma)}. \tag{4.4.11}$$

4.5 The branching ratio

The branching ratio plays a very important role at the LHC to identified the Higgs boson mass m_h, it has been used to precise the probability of the occurrence of one mode, that motives us to use it to identified the new neutral scalar bosons predicted in our model.

The branching ratio (BR) is the fraction of the partial width decay of an individual decay over the total partial width decay:

$$\mathrm{BR} = \frac{\Gamma_i}{\Gamma_T}, \tag{4.5.1}$$

where $\Gamma_T = \sum \Gamma_i$ is the total decay rate that represents the sum of the individual decay rates. The total decay width of h_2 is determined by the following channels:

$$\begin{aligned}\Gamma_{341}(h_2 \longrightarrow all) &= \Gamma_{341}(h_2 \longrightarrow \tau^+\tau^-, b\bar{b}) + \Gamma_{341}(h_2 \longrightarrow ZZ) \\ &+ \Gamma_{341}(h_2 \longrightarrow \gamma Z) + \Gamma_{341}(h_2 \longrightarrow \gamma\gamma) + \Gamma_{341}(h_2 \longrightarrow gg) \\ &+ \Gamma_{341}(h_2 \longrightarrow h_1 h_1). \end{aligned} \tag{4.5.2}$$

Furthermore, h_2 can also decay to new charged and neutral particles F including fermions, scalar and gauge bosons, if kinematically allowed which would require $m_{h_2} > 2m_F$, therefore, in this case, $\Gamma_{341}(h_2 \longrightarrow all)$ has new contributions $\Gamma_{341}(h_2 \longrightarrow F)$ where F can be $K_1^{\mp}$, K'^0, $X^{\mp}$, $Y^{\mp}$, $V^{\mp\mp}$, Z' or exotic quarks. Regarding the other neutral scalar boson h_3, its total width decay is composed by the following decays:

$$\begin{aligned}\Gamma_{341}(h_3 \longrightarrow all) &= \Gamma_{341}(h_3 \longrightarrow \tau^+\tau^-, b\bar{b}) + \Gamma_{341}(h_3 \longrightarrow \text{exotic quarks}) \\ &+ \Gamma_{341}(h_3 \longrightarrow \gamma\gamma) + \Gamma_{341}(h_3 \longrightarrow Z\gamma) + \Gamma_{341}(h_3 \longrightarrow gg) \\ &+ \Gamma_{341}(h_3 \longrightarrow h_2 h_2) + \Gamma_{341}(h_3 \longrightarrow h_1 h_1) \\ &+ \Gamma_{341}(h_3 \longrightarrow h_2 h_1) + \Gamma_{341}(h_3 \longrightarrow VV). \end{aligned} \tag{4.5.3}$$

Where V represents gauge bosons namely $X^{\pm}$, $V^{\pm\pm}$, K_0', $K_1^{\pm}$, $Y^{\mp}$, Z and Z'.

4.6 Numerical Analysis

In this section, we discuss the phenomenology of the signal strength of h_1 and the branching ratio (BR) of the heavy scalar bosons $h_i (i = 2, 3)$.

In our work, we consider the following scenario:
υ_ρ=246 GeV, $\upsilon_\chi = \upsilon_\eta$=2 TeV, for the scalar parameters $\lambda_{1..9}$, we generate random choices subject with the various theoretical constraints that we discussed in chapter 3, in the compact 341 model, the fermion sector contains e_a, ν_a, e_a^c and ν_a^c where a can be an electron, μ or τ, the six familiar flavors Up, Down, Charm, Strange, Top and Bottom with extra six exotic quarks. Their masses are:

$$\begin{aligned} m_e &= 0.511 \ \text{MeV}, \quad m_\mu = 106 \ \text{MeV}, \quad m_\tau = 1777 \ \text{MeV}, \\ m_u &= 2.3.10^{-3} \ \text{GeV}, \quad m_d = 4.95.10^{-3} \ \text{GeV}, \quad m_c = 1.40 \ \text{GeV}, \\ m_s &= 95.10^{-3} \ \text{GeV}, \quad m_t = 172.5 \ \text{GeV}, \quad m_b = 4.75 \ \text{GeV}. \end{aligned} \tag{4.6.1}$$

Notice that ν_a^c and ν_a are massless leptons and based on the results that reported at CMS collaborations [97], the exotic quarks masses have to be bigger than 650 GeV. In our work, we take their masses equals to 700 GeV. The gauge bosons masses are given by Eqs.(2.3.32)-(2.3.37), using the fact that $g = \sqrt{\frac{4\pi}{137}}/\sin\theta_W$ and $\theta_W = 28.15°$, then we get:

Gauge boson	mass(GeV)
$m_{W^{\mp}}$	80.398
m_Z	91.1876
$m_{K_1^{\mp}}$	655
$m_{X^{\mp}}$	650
$m_{V^{\mp\mp}}$	655
$m_{K_0'}$	650
$m_{Y^{\mp}}$	920

Table 4.3: Gauge bosons masses in the compact 341 model [39].

In our model, the scalar bosons masses are:

$$\begin{aligned} m^2_{h_1} &= \lambda_2 \upsilon_\rho^2 + \frac{\lambda_3\lambda_4^2 + \lambda_6(\lambda_1\lambda_6 - \lambda_4\lambda_5)}{\lambda_5^2 - 4\lambda_1\lambda_3}\upsilon_\rho^2, \quad m^2_{h_2} = c_1\upsilon_\chi^2 + c_2\upsilon_\rho^2, \\ m^2_{h_3} &= c_3\upsilon_\chi^2 + c_4\upsilon_\rho^2, \quad m^2_{h_1^{\mp}} = \frac{\lambda_7}{2}(\upsilon_\eta^2 + \upsilon_\rho^2), \quad m^2_{h_2^{\mp}} = \frac{\lambda_8}{2}(\upsilon_\eta^2 + \upsilon_\chi^2) \\ m^2_{h^{\mp\mp}} &= \frac{\lambda_9}{2}(\upsilon_\rho^2 + \upsilon_\chi^2) \end{aligned} \tag{4.6.2}$$

Generating random numbers for the scalar parameters λ_i leads to the scalar boson masses.

4.6.1 The signal strength

In this section, we review the signal strength reported at CMS and ATLAS. Then, we discuss our results and their confrontations with the experimental data.

The signal strength μ at LHC

The SM Higgs boson is produced from the ggF fusion (the most dominant production process at LHC) and since it is an unstable boson then it will decay into different final states before its arrival to the detector, therefore, the detectors can not measure the cross section and the branching ration separately. Experimentally we can measure the so called the Signal Strength μ.

As we discussed in section 4.4, the signal strength represents the product of the Higgs boson production cross section and its branching ratio in units of the corresponding value predicted by the SM. Thus in the Standard Model, this parameter μ determiners the agreement between the theoretical expectations versus the experimental results.

Table (4.4) summaries the available experimental signal strength values from LHC Run 1 for the combination of ATLAS and CMS, and separately for each experiment, for the combined $\sqrt{s} = 7$ and 8 TeV data for different Higgs boson decay channels. The expected

uncertainties in the measurements are displayed in table 4.4. These results are obtained assuming that the Higgs boson production process cross sections at s = 7 and 8 TeV are the same as in the SM [98] of each individual channel $\ell\bar{\ell}$, $b\bar{b}$, ZZ^*, WW^* and $\gamma\gamma$.

Decay channel	ATLAS	CMS	ATLAS+CMS
$\mu^{\gamma\gamma}$	$1.14^{+0.27}_{-0.25}$	$1.11^{+0.25}_{-0.23}$	$1.14^{+0.19}_{-0.18}$
μ^{ZZ}	$1.52^{+0.40}_{-0.34}$	$1.04^{+0.32}_{-0.26}$	$1.29^{+0.26}_{-0.23}$
μ^{WW}	$1.22^{+0.23}_{-0.21}$	$0.90^{+0.23}_{-0.21}$	$1.09^{+0.18}_{-0.16}$
$\mu^{\tau\tau}$	$1.41^{+0.40}_{-0.36}$	$0.88^{+0.30}_{-0.28}$	$1.11^{+0.24}_{-0.22}$
μ^{bb}	$0.62^{+0.37}_{-0.37}$	$0.81^{+0.45}_{-0.43}$	$0.70^{+0.29}_{-0.27}$

Table 4.4: h signal strengths of the official ATLAS, CMS and ATLAS and CMS combination for Run 1 [98], based on 25 fb^{-1} of integrated luminosity.

The signal strength in the compact 341 model

Table 4.5 shows the signal strength results in our model and Figure 4.4 shows the signal strengths for the various decay modes ZZ^*, $\gamma\gamma$, WW^*, $\tau^+\tau^-$ and $b\bar{b}$ in the compact 341 model with the data reported at ATLAS, CMS and the combined ATLAS+ CMS Run1. Our results can fit the current data withing the experimental errors as we can be seen in Figure 4.4 that makes the compact 341 model in perfect agreement with the values measured by ATLAS and CMS. That ensures the viability of the compact 341 model to be an available model in the future work at the LHC.

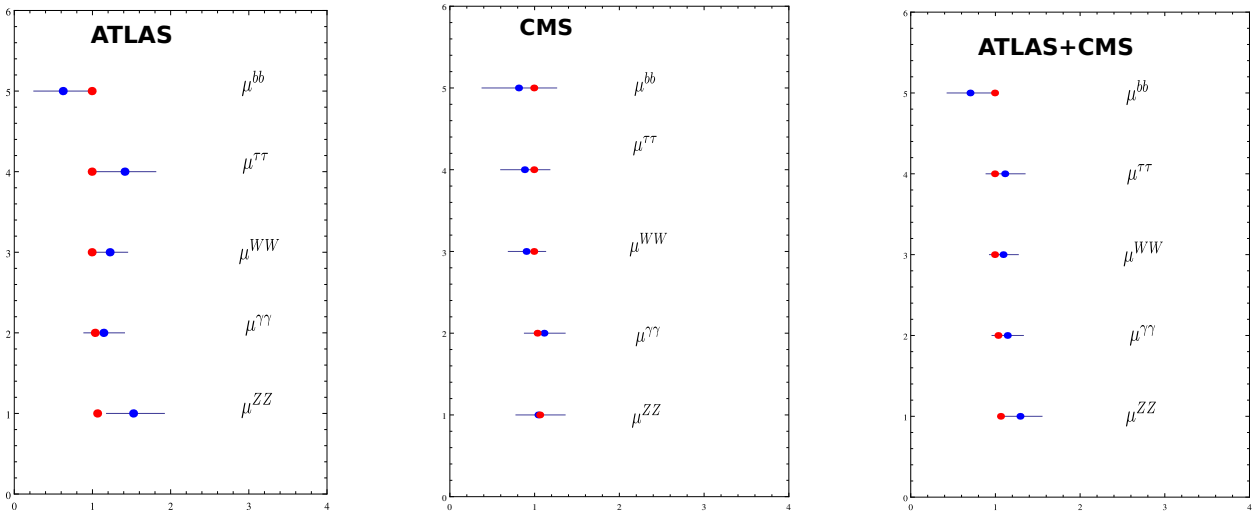

Figure 4.4: The signal strength results of h_1, the blue and the red points represent the Standard Model and the compact 341 model results respectively.

Decay channel	Our results
$\mu^{\gamma\gamma}$	1.03
μ^{ZZ}	1.06
μ^{WW}	0.99
$\mu^{\tau\tau}$	0.99
μ^{bb}	0.99

Table 4.5: The signal strengths in the compact 341 model [39].

4.6.2 The branching ratio

In this section, we discuss the BR in the SM and in the compact 341 model.

The branching ratio in the Standard Model

The left curve in Figure 4.5 represents the branching ratios of different channels of the Standard Model Higgs boson decays as function of its mass m_H, whereas the curve in the right side represents the variation of the total width decay versus the Standard Model Higgs boson mass.

Figure (4.5) shows that a light Higgs boson where $m_H < 130 - 140$ GeV behaves very

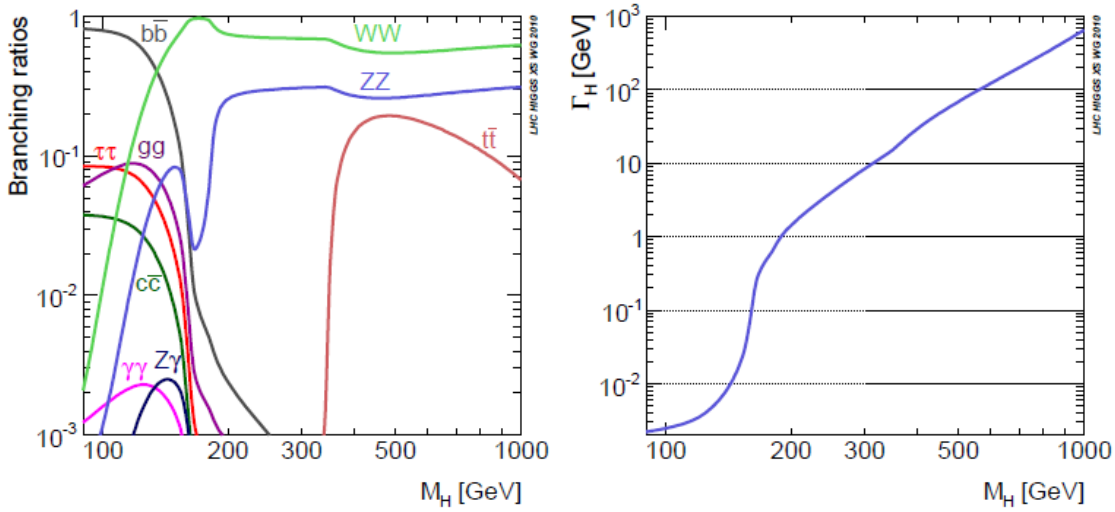

Figure 4.5: The Standard Model Higgs decay branching ratios (left) and total width decay (right) as a function of m_H [99].

differently from a heavy Higgs boson where $m_H > 130 - 140$ GeV [99].

In the region where $m_H \in (160 - 180$ GeV) the Standard Model Higgs boson prefers to

decay into a pair of electroweak gauge bosons WW or ZZ and the other decays into fermions and loop induced decays are suppressed except the decay into a pair of top quarks $t\bar{t}$.

Regarding the SM Higgs boson decay into two gauge bosons WW and ZZ, we distinguish two cases: The decay into two real gauge bosons WW and ZZ happen when $m_H > 160$ GeV, otherwise, below the WW and ZZ threshold the decay becomes into an off shell with an on shell gauge bosons WW^* and ZZ^* leading to three body decay.

On the other hand, in the region $m_H < 130$ GeV, the decay into a pair of bottom quarks $\bar{b}b$ dominates followed by the other decays into other fermions at the tree level. Additionally, in this region the decay $H \longrightarrow gg$ is the most dominant process among the loop induced decays, but Unfortunately, the SM Higgs boson decay into a pair of gg is a useless process because its huge QCD background contributions. In spite of the relatively small branching ratio value $\simeq 0.2$ of the decay $H \longrightarrow \gamma\gamma$ GeV (the SM Higgs boson does not couple to massless photons directly that makes it a rare decay), it has an important role in the SM Higgs boson searches at Large Hadron Collider (LHC), it has used as a fundamental process to identified the SM Higgs boson because of its zero QCD background contributions (clean process without hadronization).

The Standard Model predictions for the decay branching fractions for the Higgs boson with a mass of 125.09 GeV, together with their uncertainties [100] are summarized in the following table:

Decay modes	Branching fraction
$h\bar{b}b$	57.5 ∓ 1.9
hWW	21.6 ∓ 0.9
hgg	08.56 ∓ 0.86
$h\bar{t}t$	06.30 ∓ 0.36
$h\bar{c}c$	02.90 ∓ 0.35
hZZ	02.67 ∓ 0.11
$h\gamma\gamma$	0.228 ∓ 0.011
$hZ\gamma$	0.155 ∓ 0.014
$h\mu\mu$	0.022 ∓ 0.001

Table 4.6: Branching ratio of different channels in the Standard Model [93].

The total width decay of the SM Higgs boson with $m_H = 125$ GeV is $\Gamma_{tot} = 4.07.10^{-3}$ GeV as we shown in Figure 4.5 (the right curve) indicated with a relative uncertainty of $+4.0$ and -3.9.

Searches for $h_i(i = 2, 3)$

Figure 4.6 shows BR($h_2 \longrightarrow h_1h_1$) as a function of the heavy Higgs h_2 mass for $v_\chi = v_\eta$=2 TeV where in the allowed parameter space, the mass of m_{h_2} ranges from 500 GeV to 3.5 TeV. Its clear that in the region 500-1300 GeV , the decay channel $h_2 \longrightarrow h_1h_1$ is the most important one with a BR $\geq 90\%$, this happens because the trilinear coupling $h_1h_2h_2$ increases about one order of magnitude v_η. Interestingly, one can has a new production mechanism for h_2 namely $pp \longrightarrow h_2 \longrightarrow h_1h_1$. This production channel might be useful to increase the signal of the double Higgs production at the LHC.

As the mass becomes larger than 1300 GeV, we can notice that the decay modes of h_2 into the heavy gauge bosons K'^0, $K_1^\mp$, $Y^\mp$, $V^{\mp\mp}$, $X^\mp$ and Z' and into exotic quarks are kinetically allowed, in this case, the total decay width contains additional channels $h_2 \longrightarrow VV$ and $h_2 \longrightarrow Q\overline{Q}$ where $V \equiv K'^0$, $K_1^\mp$, $Y^\mp$, $V^{\mp\mp}$, $X^\mp$ and Z' and $Q \equiv$ exotic quarks. The maximum value of the branching ratio of the decay of h_2 into gauge bosons K'^0, $K_1^\mp$, $V^{\mp\mp}$ and $X^\mp$ plateaus close to $\sim$0.35, $\sim$0.26 as we shown in table 4.7, therefore, one may notice that those decays are the most significant decay channels and the decay channel $h_2 \longrightarrow h_1h_1$ becomes weak and contributing roughly $\sim 20\%$.

The branching ratios of the remaining decay modes are tabulated in the following tables:

Decay channel	BR where $m_{h_2} \in$ [500-1300](GeV)	BR where $m_{h_2} \in$ [1300-3500](GeV)
$b\bar{b}$	$\sim \mathcal{O}(10^{-5})$	$[10^{-5} - 10^{-6}]$
$\tau^+\tau^-$	$\sim \mathcal{O}(10^{-7})$	$\sim 10^{-7}$
$\gamma\gamma$	$\sim \mathcal{O}(10^{-7})$	$\sim 10^{-7}$
γZ	$\sim \mathcal{O}(10^{-3})$	$[10^{-3} - 2.6.10^{-3}]$
gg	$\sim \mathcal{O}(10^{-4})$	$[10^{-4} - 10^{-5}]$
ZZ	$\sim \mathcal{O}(10^{-32})$	$[10^{-32} - 10^{-31}]$
$Z'Z'$	$\sim \mathcal{O}(10^{-4})$	$[10^{-3} - 10^{-2}]$
$K'^0K'^0$	0	$[10^{-3}$-0.26]
Y^+Y^-	0	$[10^{-4}$-$10^{-2}]$
X^+X^-	0	$[10^{-3}$-0.35]
$V^{++}V^{--}$	0	$[10^{-3}$-0.34]
$K_1^+K_1^-$	0	$[10^{-3}$-0.26]
$U\bar{U}$	0	$[10^{-4}$-$10^{-2}]$
$J\bar{J}$	0	$[10^{-4}$-$10^{-1}]$

Table 4.7: The branching ratios (BRs) of the heavy scalar h_2 for differnet channels.

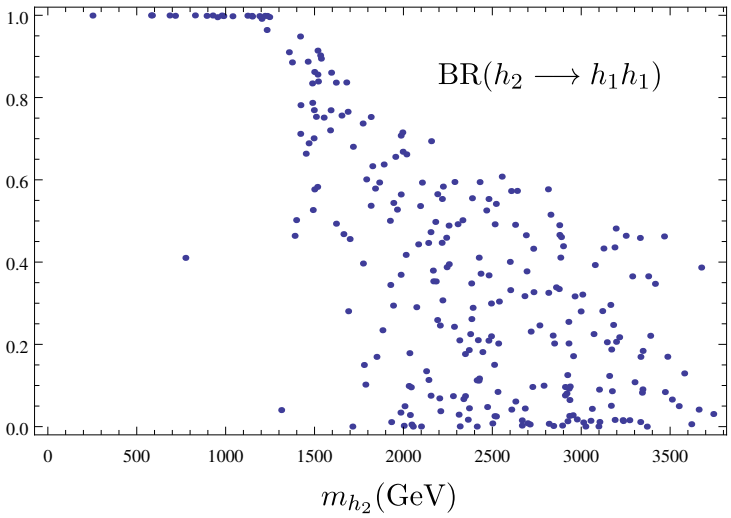

Figure 4.6: The branching ratio of $h_2 \longrightarrow h_1 h_1$ versus the heavy Higgs h_2 mass.

Now we turn our discussion to h_3, Figure 4.7 shows BR($h_3 \longrightarrow ZZ$) as a function of the heavy Higgs h_3 mass for $v_\chi = v_\eta$=2 TeV where in the allowed parameter space, the mass of m_{h_3} ranges from 3 TeV to 4 TeV. The decay channel $h_3 \longrightarrow ZZ$ is the most important one with a BR $\geq 80\%$ which is about $\sim$0.8, while, the BR in $h_1 h_1$ is the second most significant decay channel contributing roughly 20%. The lowest value of the branching ratio in that region is just below $\sim 10^{-9}$.

The branching ratios of the other decays are shown in the following tables:

Decay channel	BR where $m_{h_3} \in$ [3000-4000](GeV)
$b\bar{b}$	$\sim \mathcal{O}(10^{-5})$
$\tau^+\tau^-$	$[10^{-7} - 10^{-9}]$
$\gamma\gamma$	$[10^{-7} - 10^{-5}]$
γZ	$[10^{-3} - 10^{-2}]$
gg	$[10^{-5} - 10^{-4}]$
ZZ	~ 0.80
$Z'Z'$	$[10^{-7} - 10^{-5}]$
$K'^0 K'^0$	$[1.5.10^{-6} - 1.9.10^{-4}]$
Y^+Y^-	$[6.10^{-6} - 5.10^{-5}]$
X^+X^-	$[10^{-6} - 3.10^{-5}]$
$V^{++}V^{--}$	$[10^{-6} - 10^{-5}]$
$K_1^+ K_1^-$	$[1.5.10^{-6} - 1.9.10^{-4}]$

Table 4.8: The branching ratios (BRs) of the heavy scalar h_3 for differnet channels.

Decay channel	BR where $m_{h_3} \in$ [3000-4000](GeV)
$U\bar{U}$	$[5.10^{-2} - 0.25]$
$J\bar{J}$	$[5.10^{-2} - 10^{-3}]$
$h_1 h_1$	~ 0.20
$h_1 h_2$	$[10^{-4} - 10^{-2}]$
$h_2 h_2$	$[5.10^{-4} - 10^{-3}]$

Table 4.9: The branching ratios (BRs) of the heavy scalar h_3 for differnet channels.

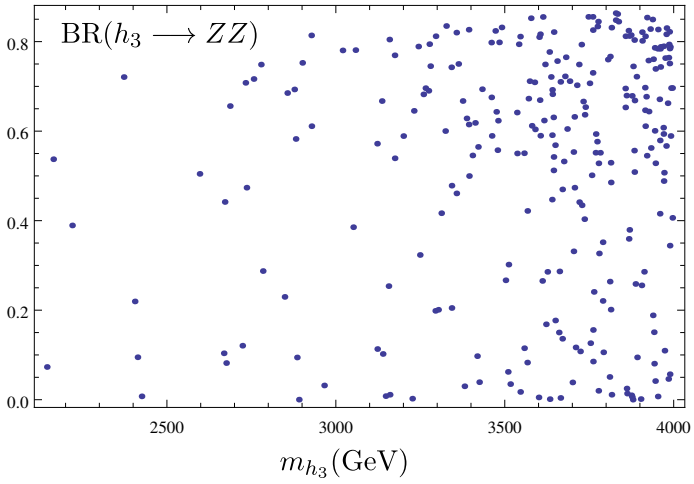

Figure 4.7: The branching ratio of $h_3 \longrightarrow ZZ$ as a function of the heavy Higgs h_3 mass.

4.6.3 Double Higgs Production

The double Higgs boson production is one of the main goal that the LHC is looking to achieve it. Its measurement leads to precise the Higgs boson coupling (the scalar potential shape) or to prove new physics.

4.6.4 Double Higgs Production at the LHC

The double Higgs production has been searched in the Run 1 and Run 2 in both resonant and non-resonant final state.

Non resonant decay

In the Standard Model, the main non-resonant production of the Higgs boson proceeds through two Feynman diagrams: Box diagram and through trilinear coupling of the Higgs boson (see Figure 4.8).

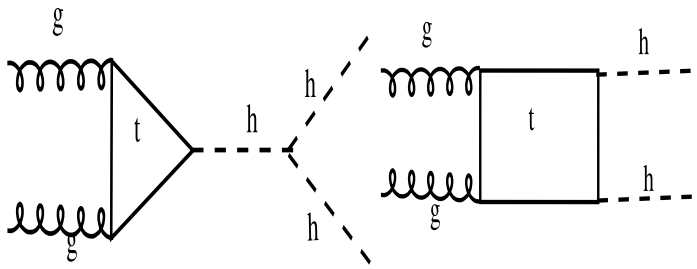

Figure 4.8: Feynam diagrams of the Higgs pair production, box diagram (right) and trilinear coupling diagram (left).

Notice that we have considered that the dominant process to produce the Higgs bosons comes from the gluon-gluon fusion mode.

At Run 1, the different possibilities final state of the SM Higgs boson decay are [101,102]:

$$hh \longrightarrow \bar{b}b\gamma\gamma, \quad hh \longrightarrow \bar{b}b\tau^-\tau^+, \quad hh \longrightarrow \bar{b}b\bar{b}b, \tag{4.6.3}$$

$$hh \longrightarrow W^*W\gamma\gamma, \quad hh \longrightarrow W^*WW^*W, \quad hh \longrightarrow W^*WZ^*Z, \tag{4.6.4}$$

$$hh \longrightarrow Z^*ZZ^*Z, \quad hh \longrightarrow W^*W\tau^-\tau^+, hh \longrightarrow ZZ^*\bar{b}b, \tag{4.6.5}$$

$$hh \longrightarrow \tau^-\tau^+\tau^-\tau^+, \tag{4.6.6}$$

whereas, at Run 2 the previous channels (Run 1) have been updated in both CMS and ATLAS collaboration:

$$hh \longrightarrow \bar{b}b\gamma\gamma, \quad hh \longrightarrow \bar{b}b\tau^-\tau^+ \tag{4.6.7}$$

$$hh \longrightarrow \bar{b}b\bar{b}b, \quad hh \longrightarrow \bar{b}bW^+W^- \tag{4.6.8}$$

$$hh \longrightarrow \gamma\gamma W^+W^- \tag{4.6.9}$$

The box diagram interferes negatively with the trilinear coupling diagram, that make the rate of this production very small, therefore, its detection becomes very difficult experimentally.

Resonant decay

Concerning the resonant Higgs pair production, it can happen via a new particle which will decay into a Higgs boson pair making this process visible even at a lower luminosity $pp \longrightarrow X \longrightarrow hh$ where h can decay into many possible final state.

In this section, we discuss the different channel decays in the resonant case.

$hh \longrightarrow \gamma\gamma\bar{b}b$

The first channel that can happen through the resonant X is the decay into $\gamma\gamma$ and a pair of $\bar{b}b$ (Figure 4.9):

$$pp \longrightarrow X \longrightarrow hh \longrightarrow \gamma\gamma\bar{b}b \tag{4.6.10}$$

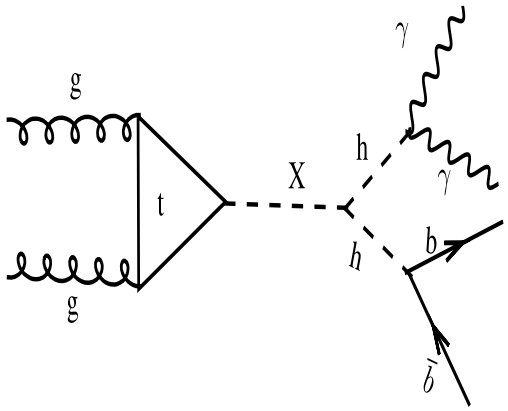

Figure 4.9: Feynman diagram of $hh \longrightarrow \gamma\gamma\bar{b}b$.

This process is a good possible way to search for the double Higgs boson production since the channel $\gamma\gamma$ is a clean channel which will help to reduce the QCD background that participate through the decay $h \longrightarrow \bar{b}b$. But, experimentally this process has a low statistic at the LHC.

$hh \longrightarrow \bar{b}b\bar{b}b$

The second possible channel can be:

$$pp \longrightarrow X \longrightarrow hh \longrightarrow \bar{b}b\bar{b}b \tag{4.6.11}$$

Figure 4.10 represents the Feynman diagram of the process (4.6.11).

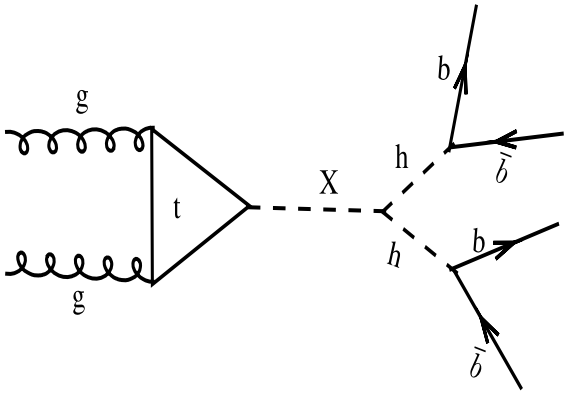

Figure 4.10: Feynman diagram of $hh \longrightarrow \bar{b}b\bar{b}b$.

This process has a high rate in its branching ratio (58%) [101, 102]. In spite of this advantage it contains a large multi-jet background.

In this case, experimental physicist expect to get a signal from a peak in the smooth diHiggs invariant mass distribution [101, 102] but according to the figure 4.11, no excess has been found.

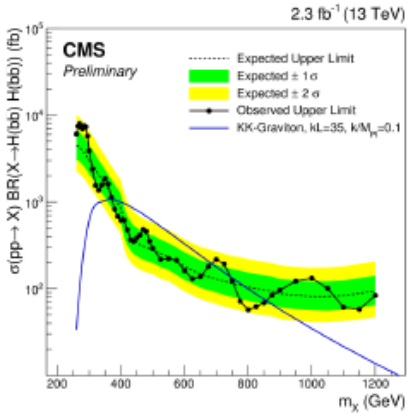

Figure 4.11: Search for the resonant $X \longrightarrow hh \longrightarrow \bar{b}b\bar{b}b$ [102].

$hh \longrightarrow b\bar{b}\ell\ell$

Another possible way to search for the double Higgs production at the LHC is from this decay:

$$pp \longrightarrow X \longrightarrow hh \longrightarrow b\bar{b}\ell\ell \tag{4.6.12}$$

Includes the following signals:

$$pp \longrightarrow X \longrightarrow hh \longrightarrow b\bar{b}W(\nu\ell)W(\nu\ell) \tag{4.6.13}$$

$$pp \longrightarrow X \longrightarrow hh \longrightarrow b\bar{b}Z(\ell\ell)Z(\nu\nu) \tag{4.6.14}$$

Those processes are presented as follows:

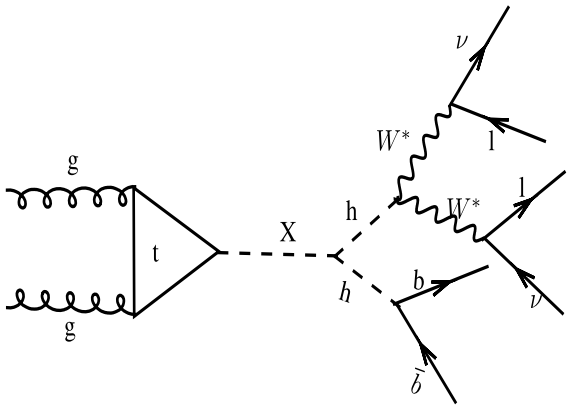

Figure 4.12: Feynman diagrams of $hh \longrightarrow \bar{b}\ell\ell$.

Due to the presence of the neutrinos in the final state, a lost of energy leads to a waste in the invariant mass resolution.

$hh \longrightarrow \bar{b}b\tau^+\tau^-$

The $pp \longrightarrow X \longrightarrow hh \longrightarrow \bar{b}b\tau^+\tau^-$ is another process that used at the LHC (see Figure 4.13). Particle physicist applied the same idea that reported in the decay $hh \longrightarrow \bar{b}b\bar{b}b$, they were looking for a peak in the $m_{\tau^-\tau^+bb}$ distribution [102], but no excess has been detected.

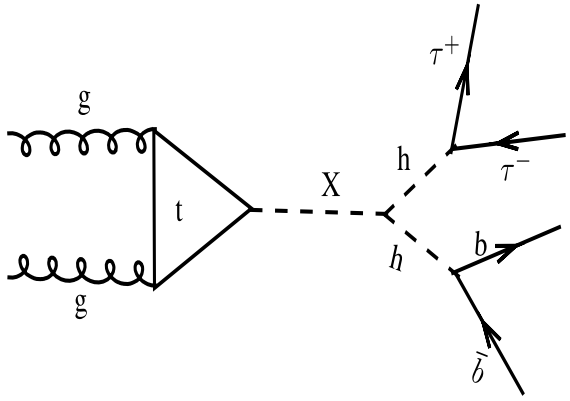

Figure 4.13: Feynman diagram of $hh \longrightarrow \bar{b}b\tau^+\tau^-$.

4.6.5 Double Higgs Production in the compact 341 model

The heavy neutral scalar bosons h_2 and h_3 in our model can be candidates to be the resonant in the pair Higgs productions process, their contributions can enhance the signal excess at the LHC to increase the probability to detect the Higgs pair productions.

Figure 4.14 represents the trilinear Feynman diagram of the Higgs pair production through the resonant $h_{2,3}$ ($pp \longrightarrow h_{2,3} \longrightarrow h_1h_1$) in the compact 341 model, this one loop

process happens through the exchange of the exotic quarks (there is no direct coupling between $h_{2,3}$ and the top quark). Notice that besides the trilinear Feynman diagram the Higgs pair productions can happen through a box diagram which is similar to the Standard Model one (the right diagram in figure 4.8).

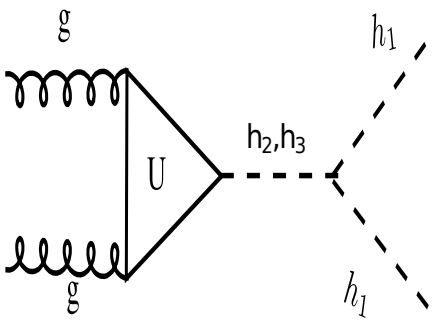

Figure 4.14: Trilinear Feynam diagram of the Higgs pair production in the compact 341 model.

4.7 Conclusion

In this chapter, we discussed the phenomenology of the neutral scalar bosons in the compact 341 model. We derived all the necessary partial decay widths where the lightest scalar h_1 is identified as the SM Higgs boson to calculate the signal strength and the branching ratios where we have used the theoretical constraints to constrain the scalar parameters such as: perturbative unitarity, boundedness from below constraints and the positivity of the scalar bosons masses.

To check the validity of the model we calculated the signal strength of the Higgs like-boson h_1 and compare our results with the experimental data that reported in ATLAS, CMS and ATLAS+CMS combination. For the other heavy scalar bosons h_2 and h_3, we calculated the branching ratio trying to discuss at which scale they will be appeared. Furthermore, We discussed the Higgs pair production in the compact 341 model trying to discuss how to increase the signal of this production using the contribution of our model.

In the next chapter, we introduced a new version of the 341 model which does not exist in the literature called the flipped 341 model. we discus its particle content : fermion, gauge and scalar sectors, we explain how all particles gain their masses using four scalar fields with two extra scalar matrices S and S' . Furthermore, we discuss the appearance of the FCNC.

Chapter 5

A new anomaly-free flipped 341 model

5.1 Introduction

In the chapter 2, we have discussed the 341 models with and without exotic electric charges, where we have reported that all the quarks families must be arranged in different representations while leptons generations are in the same representation to ensure the cancellation of the triangle gauge anomaly. But it turns out that this quarks and leptons replication is not the only way to get a model free from the $SU(4)_L^3$ anomaly. Following Ref [103] regarding the 331 model, we introduce a new unique gauge anomaly-free model where all the quark generations transform under the same representation while leptons are not. This model baptized flipped 341 model.

Since two lepton generations ψ_e and $\widetilde{\psi}$ arranged differently from the others ψ_μ and ψ_τ and all the quarks are identical under SU(4), the tree level Flavor Changing Neutral Current (FCNC) in our model is expected in the lepton sector (and it is absent in the quark sector) though the exchange of the new neutral gauge bosons Z' and Z'' such as the rare decays $\ell_i \longrightarrow \ell_i \ell_k \bar{\ell}_k$ and $\ell_i \longrightarrow \ell_j \gamma$.

In this chapter, a new model called the flipped 341 model is introduced [104, 105], its fundamental features and its particle content are discussed. The FCNC is discussed through the processes $\mu \longrightarrow ee\bar{e}$ and $\mu \longrightarrow e\gamma$. Moreover, the new physics parameter $U_{e\mu}$, $M_{Z'}$ and $M_{Z''}$ are constrained by using the experimental limits on $\mu \longrightarrow ee\bar{e}$ and $\mu \longrightarrow e\gamma$.

5.2 The flipped 341 model

In this model, the three quark generations transform under the same conjugate fundamental representation while the lepton generations lie in different representations. It is important to mention that contrary to the ordinary 341 models, a forth generation of lepton is required

in order to cancel the gauge anomaly $SU(4)_L^3$ which requires that the number of the fermion quadruplets must be equal to the number of anti-fermions quadruplets. Table 5.1 summarizes the particle content in this model where there are no fractionally electric charged different from $\mp\frac{2}{3}$ and $\mp\frac{1}{3}$ for exotic quarks and there are no integer electric charges different from 0 and ∓ 1 for femrions and gauge bosons (model without exotic electric charges). Moreover, this model is unique. The decomposition of the lepton 10-plet ψ_e contains as subgroups (1,6,X)+(1,3,X')+(1,Q), to get a real (1,6,X) representation, the value of β should be equal to $\frac{1}{\sqrt{3}}$ [103]. In the ordinary 341 models and for a giving value of β one has tow models with $\gamma = \frac{1}{\sqrt{6}}$ and $\gamma = \frac{-2}{\sqrt{6}}$. In the flipped version of the first model one has fractionally charged leptons which are forbidden.[1]. Therefore, the only acceptable flipped 341 model is the one with $\beta = \frac{1}{\sqrt{3}}$ and $\gamma = \frac{-2}{\sqrt{6}}$ [105].

The 10-plets ψ_e , S and S' contain $\Sigma^{\mp}$, Σ^0, $\triangle^+$, $\triangle'^-$, $\triangle^0$, $\triangle'^0$, $\triangle^{++}$ and $\triangle'^{--}$ which stand for triplets sub-representations, (ν_e, e), (H_S^+, H_S^0) and $(H_S'^-, H_S'^{--})$ form $SU(2)_L$ doublets, (β^+, β^0, N_e^0), (H_S^{++},H_{1S}^+,$H_{1S}'^+$) and ($H_S'^0$,H_{2S}^-,$H_{2S}'^-$) compose the triplets denoted by (1,3,$\frac{1}{3}$), (1,3,$\frac{4}{3}$) and (1,3,-$\frac{2}{3}$) respectively, while, E_e^-, σ^+, σ_S^0, ϕ_S^{++}, σ_S^{++} and ϕ_S^0 are singlets [105].

Using the tensor products and branching rules which are tabulated in the appendix D, we get the decomposition of ψ_e, S and S' where the decomposition of the sextets representation are:

$$(1, 6, \frac{-1}{3}) \supset (1, 3, 0) + (1, 2, \frac{-1}{2}) + (1, 1, -1), \tag{5.2.1}$$

$$(1, 6, \frac{2}{3}) \supset (1, 3, 1) + (1, 2, \frac{1}{2}) + (1, 1, 0), \tag{5.2.2}$$

$$(1, 6, \frac{-4}{3}) \supset (1, 3, -1) + (1, 2, \frac{-3}{2}) + (1, 1, 2). \tag{5.2.3}$$

As we showed in table 5.1, the decomposition of the 10 plet (1,10,0) representation is:

$$(1, 6, \frac{-1}{3}) + (1, 3, \frac{1}{3}) + (1, 1, 1) \tag{5.2.4}$$

where the sextet $(1, 6, \frac{-1}{3})$ of $SU(3)_L$ breaks into a triplet (1,3,0), a doublet $(1, 2, \frac{-1}{2})$ with a singlet (1,1,-1) [103]. A triplet 3 of $SU(3)_L$ breaks into a doublet 2 plus a singlet 1 of $SU(2)_L$, following Ref [106], we may simply label the components of 2 by their isospin ($\frac{1}{2}$ and $\frac{-1}{2}$), we can settle with the following identification [105, 106]:

$$4 = \begin{pmatrix} 2_{\frac{1}{2}} \\ 2_{\frac{-1}{2}} \\ 1 \\ 1' \end{pmatrix}, \qquad 3 = \begin{pmatrix} 2_{\frac{1}{2}} \\ 2_{\frac{-1}{2}} \\ 1 \end{pmatrix}. \tag{5.2.5}$$

[1]Fractionally charged leptons, produced abundantly in the early universe, would lead to an unacceptable cosmology, because there are no decay modes for the lightest of these exotic states [103].

Name	341 representation	331 representation	components	F
ψ_e	(1,10,0)	$(1,6,\frac{-1}{3})+(1,3,\frac{1}{3})+(1,1,1)$	$\begin{pmatrix} \Sigma^+ & \frac{\Sigma^0}{\sqrt{2}} & \frac{\nu_e}{\sqrt{2}} & \frac{\beta^+}{\sqrt{2}} \\ \frac{\Sigma^0}{\sqrt{2}} & \Sigma^- & \frac{e^-}{\sqrt{2}} & \frac{\beta^0}{\sqrt{2}} \\ \frac{\nu_e}{\sqrt{2}} & \frac{e^-}{\sqrt{2}} & E_e^- & \frac{N_e^0}{\sqrt{2}} \\ \frac{\beta^+}{\sqrt{2}} & \frac{\beta^0}{\sqrt{2}} & \frac{N_e^0}{\sqrt{2}} & \sigma^+ \end{pmatrix}$	1
$\psi_\alpha(\alpha=\mu,\tau)$	$(1,4,\frac{-1}{2})$	$(1,3,\frac{-2}{3})+(1,1,0)$	$(\nu_\alpha,\ell_\alpha,E_\alpha^-,N_\alpha^0)$	2
$\widetilde{\psi}$	$(1,\bar{4},\frac{-1}{2})$	$(1,\bar{3},\frac{-1}{3})+(1,1,\text{-}1)$	$(\widetilde{e}^-,\widetilde{\nu},\widetilde{N}^0,\widetilde{E}^-)$	1
ℓ_α^c	(1,1,1)	(1,1,1)	ℓ_α^c	6
Q_α	$(3,\bar{4},\frac{1}{6})$	$(3,\bar{3},\frac{1}{3})+(3,1,\frac{-1}{3})$	$(d_\alpha,u_\alpha,U_\alpha,D_\alpha)$	3
u^c	$(\bar{3},1,\frac{-2}{3})$	$(\bar{3},1,\frac{-2}{3})$	u^c	6
d^c	$(\bar{3},1,\frac{1}{3})$	$(\bar{3},1,\frac{1}{3})$	d^c	6
ϕ_1	$(1,\bar{4},\frac{-1}{2})$	$(1,\bar{3},\frac{-1}{3})+(1,1,\text{-}1)$	$(\phi_1^-,\phi_1^0,\phi_1'^0,\phi_1'^-)$	1
ϕ_2	$(1,\bar{4},\frac{-1}{2})$	$(1,\bar{3},\frac{-1}{3})+(1,1,\text{-}1)$	$(\phi_2^-,\phi_2^0,\phi_2'^0,\phi_2'^-)$	1
ϕ_3	$(1,\bar{4},\frac{1}{2})$	$(1,\bar{3},\frac{2}{3})+(1,1,0)$	$(\phi_3^0,\phi_3^+,\phi_3'^+,\phi_3'^0)$	1
ϕ_4	$(1,\bar{4},\frac{1}{2})$	$(1,\bar{3},\frac{2}{3})+(1,1,0)$	$(\phi_4^0,\phi_4^+,\phi_4'^+,\phi_4'^0)$	1
S	(1,10,1)	$(1,6,\frac{2}{3})+(1,3,\frac{4}{3})+(1,1,2)$	$\begin{pmatrix} \triangle^{++} & \frac{\triangle^+}{\sqrt{2}} & \frac{H_S^+}{\sqrt{2}} & \frac{H_S^{++}}{\sqrt{2}} \\ \frac{\triangle^+}{\sqrt{2}} & \triangle^0 & \frac{H_S^0}{\sqrt{2}} & \frac{H_{1S}^+}{\sqrt{2}} \\ \frac{H_S^+}{\sqrt{2}} & \frac{H_S^0}{\sqrt{2}} & \sigma_S^0 & \frac{H_{1S}'^+}{\sqrt{2}} \\ \frac{H_S^{++}}{\sqrt{2}} & \frac{H_{1S}^+}{\sqrt{2}} & \frac{H_{1S}'^+}{\sqrt{2}} & \phi_S^{++} \end{pmatrix}$	1
S'	(1,10,-1)	$(1,6,\frac{-4}{3})+(1,3,\frac{-2}{3})+(1,1,0)$	$\begin{pmatrix} \triangle'^0 & \frac{\triangle'^-}{\sqrt{2}} & \frac{H_S'^-}{\sqrt{2}} & \frac{H_S'^0}{\sqrt{2}} \\ \frac{\triangle'^-}{\sqrt{2}} & \triangle'^{--} & \frac{H_S'^{--}}{\sqrt{2}} & \frac{H_{2S}^-}{\sqrt{2}} \\ \frac{H_S'^-}{\sqrt{2}} & \frac{H_S'^{--}}{\sqrt{2}} & \sigma_S^{++} & \frac{H_{2S}'^-}{\sqrt{2}} \\ \frac{H_S'^0}{\sqrt{2}} & \frac{H_{2S}^-}{\sqrt{2}} & \frac{H_{2S}'^-}{\sqrt{2}} & \phi_S^0 \end{pmatrix}$	1

Table 5.1: The complete anomaly free fermions content and scalar sector in the flipped 341 model with their flavors (F).

In our case, we have $\overline{10}_{ij}4_i4'_j$ is gauge invariant, therefore, one must have the following identification [105]:

$$10=\begin{pmatrix} 3_1 & \frac{3_0}{\sqrt{2}} & \frac{1}{\sqrt{2}}2_{\frac{1}{2}} & \frac{1}{\sqrt{2}}2'_{\frac{1}{2}} \\ \frac{3_0}{\sqrt{2}} & 3_{-1} & \frac{1}{\sqrt{2}}2_{\frac{-1}{2}} & \frac{1}{\sqrt{2}}2'_{\frac{-1}{2}} \\ \frac{1}{\sqrt{2}}2_{\frac{1}{2}} & \frac{1}{\sqrt{2}}2_{\frac{-1}{2}} & 1 & 1' \\ \frac{1}{\sqrt{2}}2'_{\frac{1}{2}} & \frac{1}{\sqrt{2}}2'_{\frac{-1}{2}} & 1' & 1'' \end{pmatrix}. \tag{5.2.6}$$

Notice that the charge operator Q (Eq(2.3.1)) acts on the representations 4 and $\bar{4}$ as:

$$\begin{aligned} Q[4] &= \text{Diag}\left(\frac{1}{2}+\frac{b}{6}+\frac{c}{12}+X,\frac{-1}{2}+\frac{b}{6}+\frac{c}{12},\frac{-b}{3}+\frac{c}{12}+X,\frac{-c}{4}+X\right), \\ Q[\bar{4}] &= \text{Diag}\left(\frac{-1}{2}-\frac{b}{6}-\frac{c}{12}+X,\frac{1}{2}-\frac{b}{6}-\frac{c}{12},\frac{b}{3}-\frac{c}{12}+X,\frac{c}{4}+X\right) \end{aligned} \tag{5.2.7}$$

Thus, the electric charge for leptons in ψ_e is [105]:

$$Q = \begin{pmatrix} +1 & 0 & 0 & +1 \\ 0 & -1 & -1 & 0 \\ 0 & -1 & -1 & 0 \\ +1 & 0 & 0 & +1 \end{pmatrix}. \tag{5.2.8}$$

We also mentioned in table 5.1 that the decomposition of the scalar matrices S and S' is respectively given by [105]:

$$(1, 6, \frac{2}{3}) + (1, 3, \frac{4}{3}) + (1, 1, 2), \tag{5.2.9}$$

$$(1, 6, \frac{-4}{3}) + (1, 3, \frac{-2}{3}) + (1, 1, 0), \tag{5.2.10}$$

where the decomposition of $(1, 6, \frac{2}{3})$ and $(1, 6, \frac{-4}{3})$ has already been given in Eqs (5.2.2) and (5.2.3) respectively, while the triplets $(1, 3, \frac{4}{3})$ and $(1, 3, \frac{-2}{3})$ break respectively into:

$$(1, 2, \frac{3}{2}) + (1, 1, 1), \tag{5.2.11}$$

$$(1, 2, \frac{-1}{2}) + (1, 1, -1). \tag{5.2.12}$$

Using those decomposition with the previous identification of 10, we get the electric charge for the scalars in S [105]:

$$Q = \begin{pmatrix} +2 & +1 & +1 & +2 \\ +1 & 0 & 0 & +1 \\ +1 & 0 & 0 & +1 \\ +2 & +1 & +1 & +2 \end{pmatrix}, \tag{5.2.13}$$

and the electric charge for the scalars in S' [105]:

$$Q = \begin{pmatrix} 0 & -1 & -1 & 0 \\ -1 & -2 & -2 & -1 \\ -1 & -2 & +2 & -1 \\ 0 & -1 & -1 & 0 \end{pmatrix}. \tag{5.2.14}$$

Regarding the vector bosons, they are in the adjoint representation 15 of $SU(4)$ where the presentation (1,15,0) of $SU(4)_L \otimes U(1)_X$ breaks into (1,8,0) of $SU(3)_L \otimes U(1)_{X'}$, a triplet $(1, 3, \frac{-2}{3})$, an anti-triplet $(1, \bar{3}, \frac{2}{3})$ and a singlet (1,1,0). The identification of 15-plet will be resulted from the contraction of $15_{ij}\overline{4}_i 4_j$, but instead of using it one can write $15 = \frac{1}{\sqrt{2}}\lambda_\alpha W^\alpha_\mu$ where $\alpha = 1...15$ which represent the Gell-Mann matrices, therefore the 15 gauge bosons can

be written as [105]:

$$\frac{1}{2}\lambda_\alpha W_\mu^\alpha = \begin{pmatrix} D_{1\mu}^0 & W_\mu^+ & K_\mu^{\frac{b+1}{2}} & X_\mu^{\frac{3+b+2c}{6}} \\ W_\mu^- & D_{2\mu}^0 & K_{1\mu}^{\frac{b-1}{2}} & V_\mu^{\frac{-3+b+2c}{6}} \\ K_\mu^{\frac{-(b+1)}{2}} & K_{1\mu}^{\frac{-(b-1)}{2}} & D_{3\mu}^0 & Y_\mu^{\frac{-(b-c)}{3}} \\ X_\mu^{\frac{-(3+b+2c)}{6}} & V^{\frac{(3-b-2c)}{6}} & Y_\mu^{\frac{(b-c)}{3}} & D_{4\mu}^0 \end{pmatrix}, \tag{5.2.15}$$

where $D_{1\mu}^0 = \frac{W_\mu^3}{\sqrt{2}} + \frac{W_\mu^8}{\sqrt{6}} + \frac{W_\mu^{15}}{\sqrt{12}}$; $D_{2\mu}^0 = \frac{-W_\mu^3}{\sqrt{2}} + \frac{W_\mu^8}{\sqrt{6}} + \frac{W_\mu^{15}}{\sqrt{12}}$; $D_{3\mu}^0 = \frac{-2W_\mu^8}{\sqrt{6}} + \frac{W_\mu^{15}}{\sqrt{12}}$ and $D_{4\mu}^0 = \frac{-3W_\mu^{15}}{\sqrt{12}}$. In our model, we have b=1 and c=-2, therefore:

$$\frac{1}{2}\lambda_\alpha W_\mu^\alpha = \begin{pmatrix} D_{1\mu}^0 & W_\mu^+ & K_\mu^+ & X_\mu^0 \\ W_\mu^- & D_{2\mu}^0 & K_{1\mu}^0 & V_\mu^- \\ K_\mu^- & K_{1\mu}^0 & D_{3\mu}^0 & Y_\mu^- \\ X_\mu^0 & V_\mu^+ & Y_\mu^+ & D_{4\mu}^0 \end{pmatrix}. \tag{5.2.16}$$

Thus, the electric charge for the vector bosons is [105]:

$$Q = \begin{pmatrix} 0 & +1 & +1 & 0 \\ -1 & 0 & 0 & -1 \\ -1 & 0 & 0 & -1 \\ 0 & +1 & +1 & 0 \end{pmatrix}. \tag{5.2.17}$$

Namely, the flipped 341 model predicts the existence of $W^\mp$, $K^\mp$, $V^\mp$, $Y^\mp$, $X^0(X^{0\prime})$ and $K^0(K^{0\prime})$ besides other neutral gauge bosons Z, Z' and Z''.

5.3 Anomalies cancellations

Based on to the fact that $\mathrm{Tr}[T^a] = 0$ and $\mathrm{Tr}[\tau^a] = 0$ where T^a and τ^a are the generators of the Lie gauge groups SU(3) and SU(4) respectively, all the triangle gauge anomalies are automatically canceled expect those of the non-trivial ones: $[SU(4)_L]^3$, $[SU(3)_C]^2 \otimes U(1)_X$, $[SU(4)_L]^2 \otimes U(1)_X$, $[SU(3)_C]^3$, $[U(1)_X]^3$ and $[\mathrm{Grav}]^2 \otimes U(1)_X$. From the particles content shown in table 5.1, we notice that our flipped 341 model is free from all the gauge triangle anomalies. In fact and as we mention in chapter 2, the total contribution of the $[SU(4)_L]^3$ anomaly comes from [94]:

$$\mathcal{A}^{abc}(4_L)\left(\sum_{Q_{mL}, f_{iL}} 4_L - \sum_{Q_{nL}} \bar{4}_L\right) = \mathcal{A}^{abc}(4_L)(n_{4L} - n_{\bar{4}_L}) \tag{5.3.1}$$

where the anomaly coefficient $\mathcal{A}^{abc}(4_L) = \mathrm{Tr}(T_L^a\{T_L^b, T_L^c\})$ with $\mathcal{A}^{abc}(4_L) = -\mathcal{A}^{abc}(\bar{4}_L)$ and 4_L respectively $\bar{4}_L$ are SU(4) quadruplet and anti-quadruplets fundamental representations.

Here n_{4L} and $n_{\bar{4}_L}$ are the number of left-handed fermions quadruplets and anti-quadruplets respectively. This anomaly cancels only if the number of the quadruplets in the fundamental representation 4_L equals to the number of the quadruplets in the conjugate fundamental representation $\bar{4}_L$ as it is the case in our model (see Table 5.1). We remind that the 10-plet ψ_e contributes as much as eight quadruplets in the group SU(4) [107] ($\mathcal{A}(10) = 8\mathcal{A}(4)$), together with the remaining lepton generations ψ_μ and ψ_τ, the contribution of all lepton generations equals to $10\mathcal{A}(4)$, while, the arrangement of the three quarks families in the fundamental conjugate representation $\overline{4}$ makes their contribution equals to $9\mathcal{A}(4)$. Thus, to ensure the cancellation of the $[SU(4)_L]^3$ anomaly, a new exotic lepton $\widetilde{\psi}$ lies in the conjugate representation $\overline{4}$ must be introduced [105].

The cancellation of the $[SU(3)_C]^3$ anomaly requires the introduction of the charge conjugate of each quark field as an $SU(4)_L \otimes U(1)_X$ singlet for which the quantum number X coincides with the electric charge Q [46].

The flipped 341 model is free from the $[SU(4)_L]^2 \otimes U(1)_X$, $[SU(3)_C]^2 \otimes U(1)_X$, $[\text{Grav}]^2 \otimes U(1)_X$ and $[U(1)_X]^3$ anomalies only if its particles content satisfied the following conditions respectively [104, 105]:

$$\frac{1}{2}\left(\sum X_\ell^L + 3\sum X_q^L\right) = 0, \tag{5.3.2}$$

$$\frac{1}{2}\left(4\sum X_q^L - \sum_{Sing} X_q^R\right) = 0, \tag{5.3.3}$$

$$4\sum X_\ell^L + 12\sum X_q^L - 3\sum X_q^R - \sum X_\ell^R = 0, \tag{5.3.4}$$

$$4\sum (X_\ell^L)^3 + 12\sum (X_q^L)^3 - 3\sum_{Sing} (X_q^R)^3 - \sum_{Sing} (X_\ell^R)^3 = 0. \tag{5.3.5}$$

where $X_{\ell(q)}^L$ and $X_{\ell(q)}^R$ are the quantum numbers associated to the $U(1)_X$ group of the left (L) and right (R) handed leptons (ℓ) and quarks (q). The factor 4 appears to take into account all the components of the quadruplets and anti-quadruplets [94], the factor 3 appears because the quarks are in $SU(3)_C$ triplets [94], while, the factors 12 represents the multiplication of 3×4, the quark generations are quadruplets and triplets under the group $SU(4)$ and $SU(3)$ respectively.

The special content of the flipped 341 model ensures the cancellation of the $[\text{Grav}]^2 \otimes U(1)_X$ anomaly which requires that the sum of all the $U(1)_X$ charges yields to zero as it mentioned in Eq.(5.3.4). Table 5.2 shows the cancellation of the gauge anomalies in the flipped 341 model. Notice that the sum of all rows of each column in table 5.2 multiplied by the number of flavors (F) vanishes. Therefore, the model is gauge anomalies free.

Field	$[SU(3)_C]^3$	$[SU(4)_L]^3$	$[SU(4)_L]^2U(1)_X$	$[SU(3)_C]^2U(1)_X$	$[U(1)_X]^3$	$(Grav)^2U(1)_X$	F
ψ_e	0	4	0	0	0	0	1
ψ_α	0	$\frac{1}{2}$	$\frac{-1}{4}$	0	$\frac{-1}{2}$	-2	2
$\widetilde{\psi}$	0	$\frac{-1}{2}$	$\frac{-1}{4}$	0	$\frac{-1}{2}$	-2	1
ℓ^c_α	0	0	0	0	1	1	6
Q_α	2	$\frac{-3}{2}$	$\frac{1}{4}$	$\frac{1}{3}$	$\frac{1}{18}$	2	3
u^c_α	$\frac{-1}{2}$	0	0	$\frac{-1}{3}$	$\frac{-8}{9}$	-2	6
d^c_α	$\frac{-1}{2}$	0	0	$\frac{1}{6}$	$\frac{1}{9}$	1	6

Table 5.2: Gauge anomalies fields contributions in the flipped 341 model [105].

5.4 Fermion masses

In our flipped 341 model, in order to generate masses for particles one has to have four scalar fields ϕ_1, ϕ_2, ϕ_3, ϕ_4 and two new scalar matrices 10-plets S and S' which transform under the fundamental representation 10 of the group SU(4). Following Ref [103], we assume that there exists a stable, charge-preserving vacuum state. In this spirit, we allow all neutral scalar components in Table 5.1 to have a non-zero vacuum expectation value (VEV) [105]:

$$\langle\phi_1\rangle = \begin{pmatrix} 0 \\ k_1 \\ n_1 \\ 0 \end{pmatrix}, \quad \langle\phi_2\rangle = \begin{pmatrix} 0 \\ k_2 \\ n_2 \\ 0 \end{pmatrix}, \quad \langle\phi_3\rangle = \begin{pmatrix} k_3 \\ 0 \\ 0 \\ n_3 \end{pmatrix}, \quad \langle\phi_4\rangle = \begin{pmatrix} k_4 \\ 0 \\ 0 \\ n_4 \end{pmatrix} \tag{5.4.1}$$

,

$$\langle S\rangle = \begin{pmatrix} 0 & 0 & 0 & 0 \\ 0 & v_\triangle & \frac{v_H}{\sqrt{2}} & 0 \\ 0 & \frac{v_H}{\sqrt{2}} & v_\sigma & 0 \\ 0 & 0 & 0 & 0 \end{pmatrix}, \quad \langle S'\rangle = \begin{pmatrix} v_{\triangle'} & 0 & 0 & \frac{v_\phi}{\sqrt{2}} \\ 0 & 0 & 0 & 0 \\ 0 & 0 & 0 & 0 \\ \frac{v_\phi}{\sqrt{2}} & 0 & 0 & v_{\sigma'} \end{pmatrix} \tag{5.4.2}$$

The gauge symmetry in the flipped 341 model is broken to the Standard Model one via the following steps:

$$\begin{aligned} & SU(3)_c \otimes SU(4)_L \otimes U(1)_X \\ & \qquad \Downarrow n_3, n_4, v_\sigma, v_{\sigma'} \\ & SU(3)_c \otimes SU(3)_L \otimes U(1)_{X'} \\ & \qquad \Downarrow n_1, n_2 \\ & SU(3)_c \otimes SU(2)_L \otimes U(1)_Y \\ & \qquad \Downarrow k_1, k_2, k_3, k_4, v_\phi, v_H, v_\triangle, v_{\triangle'} \\ & SU(3)_c \otimes U_{em} \end{aligned} \tag{5.4.3}$$

Where $k_i(i=1,2,3,4), v_\phi, v_H, v_\triangle, v_{\triangle'} \ll n_1, n_2 \ll n_i(i=3,4), v_\sigma, v_{\sigma'}$.

The Yukawa Lagrangian $\mathcal{L}_Y$ that is invariant under 341 symmetry has the following form:

$$\mathcal{L}_Y = \mathcal{L}_{\text{Leptons}} + \mathcal{L}_{\text{quarks}}. \tag{5.4.4}$$

With

$$\begin{aligned}
\mathcal{L}_{\text{Leptons}} &= \sum_{i=1}^{2} y_{\alpha\beta}^{\ell(i)} \psi_\alpha \ell_\beta^c \phi_i + \lambda_\beta^{\ell'} \psi_e \ell_\beta^c S^* + \frac{y'}{\Lambda} \psi_e \psi_e S S' + y''_{\alpha\beta} \psi_\alpha \psi_\beta S'^* + \sum_{j=3}^{4} Y^{\ell(j)} \widetilde{\psi} \psi_e \phi_j \\
&+ \sum_{j=3}^{4} w_\beta^{\ell(j)} \widetilde{\psi} \ell_\beta^c \phi_j^* + \widetilde{W} \widetilde{\psi} \widetilde{\psi} S + h.c., \\
\mathcal{L}_{\text{quarks}} &= \sum_{i=1}^{2} y_{\alpha\beta}^{u(i)} Q_\alpha u_\beta^c \phi_i^* + \sum_{j=3}^{4} y_{\alpha\beta}^{d(j)} Q_\alpha d_\beta^c \phi_j^* + h.c..
\end{aligned} \tag{5.4.5}$$

where β and α stand for the flavors of the fermion fields. In the flipped 341 model, the full scalar potential $V(\phi_i, \phi_j, S, S')$ that is invariant under the gauge symmetries is:

$$\begin{aligned}
V(\phi_i, \phi_j, S, S') &= \mu_{\phi_i}^2 \phi_i^\dagger \phi_i + \mu_{\phi_j}^2 \phi_j^\dagger \phi_j + \mu_S^2 Tr[S^\dagger S] + \mu_{S'}^2 \text{Tr}[S'^\dagger S'] + \lambda_{\phi_i} (\phi_i \phi_i^\dagger)^2 \\
&+ \lambda_{\phi_j} (\phi_j \phi_j^\dagger)^2 + \lambda_S \text{Tr}[S^\dagger S]^2 + \lambda_{S'} \text{Tr}[S'^\dagger S']^2 + \lambda'_S \text{Tr}^2[S^\dagger S] \\
&+ \lambda'_{S'} \text{Tr}^2[S'^\dagger S'] + \lambda_{\phi_i\phi_j} (\phi_i^\dagger \phi_i)(\phi_j^\dagger \phi_j) + \lambda'_{\phi_i\phi_j} (\phi_i \phi_j)(\phi_i \phi_j) \\
&+ \lambda''_{\phi_i\phi_j} (\phi_i^\dagger \phi_j)(\phi_j^\dagger \phi_i) + \lambda'''_{\phi_i\phi_j} (\phi_i \phi_i)(\phi_j \phi_j) + \lambda_{\phi_i S} (\phi_i^\dagger \phi_i) \text{Tr}[S^\dagger S] \\
&+ \lambda_{\phi_j S} (\phi_j^\dagger \phi_j) \text{Tr}[S^\dagger S] + \lambda_{\phi_i S'} (\phi_i^\dagger \phi_i) \text{Tr}[S'^\dagger S'] + \lambda_{\phi_j S'} (\phi_j^\dagger \phi_j) \text{Tr}[S'^\dagger S'] \\
&+ \lambda''_{\phi_i S} (\phi_i^\dagger S)(S^\dagger \phi_i) + \lambda''_{\phi_j S} (\phi_j^\dagger S)(S^\dagger \phi_j) + \lambda''_{\phi_i S'} (\phi_i^\dagger S')(S'^\dagger \phi_i) \\
&+ \lambda''_{\phi_j S'} (\phi_j^\dagger S')(S'^\dagger \phi_j) + (f S \phi_i \phi_i + f' S' \phi_j \phi_j + h.c.),
\end{aligned} \tag{5.4.6}$$

where $i = 1, 2, j = 3, 4$, the couplings λ's are dimensionless, while the parameters μ's, f and f' have mass dimension.

It is worth to mention that the introduction of the effective term:

$$\mathcal{L}_{eff} = \frac{y'}{\Lambda} \psi_e \psi_e S S' \tag{5.4.7}$$

is necessary to generate the neutrino mass matrix where Λ represents a new physics or cutoff scale that defines the effective interaction.

Notice that the following effective Lagrangian (where $n = 1, 2, 3, 4$, $i = 1, 2$ and $j = 3, 4$):

$$\begin{aligned}
\mathcal{L}_{eff} &= \frac{y'}{\Lambda} \psi_e \psi_e \phi_i \phi_j + \frac{y'}{\Lambda} \psi_e \psi_e \phi_i \phi_i + \frac{y'}{\Lambda} \psi_e \psi_e \phi_j \phi_j + \frac{y'}{\Lambda} \psi_e \psi_e \phi_i^* \phi_j + \frac{y'}{\Lambda} \psi_e \psi_e \phi_i \phi_j^* + \frac{y'}{\Lambda} \psi_e \psi_e \phi_i^* \phi_i \\
&+ \frac{y'}{\Lambda} \psi_e \psi_e \phi_j \phi_j^* + \frac{y'}{\Lambda} \psi_e \psi_e S S + \frac{y'}{\Lambda} \psi_e \psi_e S' S' + \frac{y'}{\Lambda} \psi_e \psi_e S^* S^* + \frac{y'}{\Lambda} \psi_e \psi_e S'^* S'^* + \frac{y'}{\Lambda} \psi_e \psi_e \phi_n S' \\
&+ \frac{y'}{\Lambda} \psi_e \psi_e \phi_n^* S' + \frac{y'}{\Lambda} \psi_e \psi_e \phi_n S'^* + \frac{y'}{\Lambda} \psi_e \psi_e \phi_n S + \frac{y'}{\Lambda} \psi_e \psi_e \phi_n^* S + \frac{y'}{\Lambda} \psi_e \psi_e \phi_n S^*,
\end{aligned} \tag{5.4.8}$$

is not invariant under $SU(4)_L$ and $U(1)_X$ symmetries, therefore, it is not allowed.

Fermion masses are generated from the following interactions [103]:

$$\mathcal{L}_{\text{Fermions masses}} = m^{\ell}_{\alpha\beta}\Psi^{\ell}_{\alpha}\Psi^{\ell^c}_{\beta} + m^{\nu}_{\alpha\beta}\Psi^{\nu}_{\alpha}\Psi^{\nu}_{\beta} + m^{u}_{\alpha\beta}\Psi^{u}_{\alpha}\Psi^{u^c}_{\beta} + m^{d}_{\alpha\beta}\Psi^{d}_{\alpha}\Psi^{d^c}_{\beta} + h.c. \tag{5.4.9}$$

5.4.1 Quark masses

By substituting the VEVs into the Yukawa Lagrangian $\mathcal{L}_{\text{quarks}}$, we find the tree level masses of the up and down quarks respectively:

$$m^u = \begin{pmatrix} y^{u(1)}_{\alpha\beta}k_1 + y^{u(2)}_{\alpha\beta}k_2 \\ y^{u(1)}_{\alpha\beta}n_1 + y^{u(2)}_{\alpha\beta}n_2 \end{pmatrix} \tag{5.4.10}$$

$$m^d = \begin{pmatrix} y^{d(3)}_{\alpha\beta}k_3 + y^{d(4)}_{\alpha\beta}k_4 \\ y^{d(3)}_{\alpha\beta}n_3 + y^{d(4)}_{\alpha\beta}n_4 \end{pmatrix} \tag{5.4.11}$$

where we have written m^u (resp. m^d) in the basis (u_α, U_α) and (u^c_β) (resp.(d_α, D_α) and (d^c_β)), $y^{u(i)}_{\alpha\beta}$(i=1,2), $y^{d(j)}_{\alpha\beta}$ $(j = 3, 4)$ represent the Yukawa couplings.

In the case of only ϕ_1 and ϕ_3, the mass matrices m^u and m^d will generate massless quarks. On the other hand, with two copies of $\phi_{1,2}$ and $\phi_{3,4}$ and requiring that $\frac{k_1}{n_1} \neq \frac{k_2}{n_2}$ and $\frac{k_3}{n_3} \neq \frac{k_4}{n_4}$ [103, 105], we can generate all the quark masses at the tree level. Therefore, this leads us to consider our model with two copies of $\phi_{1,2}$ and $\phi_{3,4}$.

The admixture of u and U (d and D), it can be avoided by applying the diagonalization of the mass matrices using the perturbation theory in powers of ϵ where $\epsilon = \Lambda_{\text{EW}}/\Lambda_{\text{NP}}$ [105,108]. Or we can use an assumption which assumes that some of the Yukawa couplings in the $\mathcal{L}_{\text{Leptons}}$ are zeros [105].

5.4.2 Charged lepton masses

At the tree level, the charged lepton mass matrix m^ℓ which is written in the basis ψ^{ℓ^c}=(ℓ^c_β, Σ^+, σ^+, β^+) and ψ^{ℓ}=(ℓ_α, E_α, $(\sigma^+)^c$, $(\beta^+)^c$, E_e, ℓ_e, Σ^-) where ($\alpha = \mu, \tau$ and β=1,...6) is [105]:

$$m^\ell = \begin{pmatrix} y^{\ell(1)}_{\alpha\beta}k_1 + y^{\ell(2)}_{\alpha\beta}k_2 & 0 & 0 & 0 \\ y^{\ell(1)}_{\alpha\beta}n_1 + y^{\ell(2)}_{\alpha\beta}n_2 & 0 & 0 & 0 \\ w^{\ell(3)}_{\beta}n_3 + w^{\ell(4)}_{\beta}n_4 & 0 & Y^{\ell(3)}n_3 + Y^{\ell(4)}n_4 & Y^{\ell(3)}k_3 + Y^{\ell(4)}k_4 \\ w^{\ell(3)}_{\beta}k_3 + w^{\ell(4)}_{\beta}k_4 & Y^{\ell(3)}k_3 + Y^{\ell(4)}k_4 & 0 & Y^{\ell(3)}n_3 + Y^{\ell(4)}n_4 \\ \lambda^{\ell'}_{\beta}v_\sigma & \frac{-y'}{\Lambda}v_{\sigma'}v_\triangle & \frac{-y'}{\Lambda}v_{\triangle'}v_\triangle & \frac{y'}{\Lambda}v_\triangle v_\phi \\ \lambda^{\ell'}_{\beta}v_H & \frac{y'}{\Lambda}v_{\sigma'}v_H & \frac{y'}{\Lambda}v_H v_{\triangle'} & \frac{-y'}{\Lambda}v_H v_\phi \\ \lambda^{\ell'}_{\beta}v_\triangle & \frac{-y'}{\Lambda}v_\sigma v_{\sigma'} & \frac{-y'}{\Lambda}v_\sigma v_{\triangle'} & \frac{y'}{\Lambda}v_\sigma v_\phi \end{pmatrix}. \tag{5.4.12}$$

A striking feature of this matrix is that the combination of the last three rows in the matrix m^{ℓ} adds up to 0, hence there is a massless combination of the ψ^{ℓ} and of the ψ^{ℓ^c} [103] which corresponds to $v_H\Sigma^- + (v_\sigma - v_\triangle)\ell_e - v_H E_e$. A natural possibility, although perhaps not the only one [103], is to associate this combination to the left-handed electron, the lightest of the charged leptons [103]. Hence, the electron mass can be generated by radiative corrections to the matrix m^{ℓ} [103], the effective operator $\mathcal{O}_{\alpha}^{(ij)}\psi_e \ell_{\alpha}^c \phi_{i=1,2}\phi_{j=1,2}$ (see figure 5.1), generates a contribution, roughly of the order of [105]:

$$\text{Fig.5.1 diagram} \propto \sum_{i,j=1}^{2} \frac{F_{kj}}{16\pi^2\Lambda^2}\lambda_{\gamma}^{\ell'} y_{\sigma\gamma}^{\ell(i)*} y_{\sigma\alpha}^{\ell(k)} \ell_{\alpha}^c \Big((n_i n_j)E_e + \frac{2}{\sqrt{2}}(k_i n_j + k_j n_i)\ell_e + (k_i k_j)\Sigma^- \Big) \tag{5.4.13}$$

where F_{kj} is the coupling constants of $S\phi_j\phi_k$ $(j,k=1,2)$. Here Λ is a parameter of the order of the 341 breaking scale. We insert very roughly $n_i \sim \Lambda \sim 1$ TeV, $k_i \sim 300$ GeV and all couplings $y \sim y' \sim F_{kj} \sim 0.6$ results in a electron mass correction of the $\mathcal{O}$(MeV).

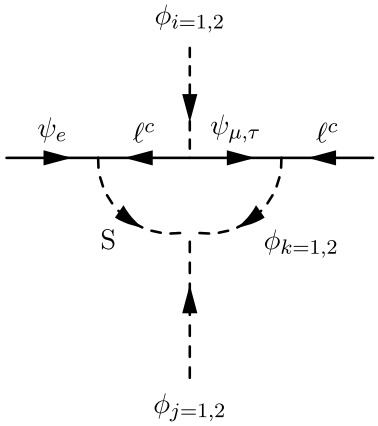

Figure 5.1: Loop diagram responsible for generating the electron mass [105].

Notice that we have identified the charged elements of $\widetilde{\psi}$ namely, $\widetilde{e}$ and $\widetilde{E}^-$ with the charge conjugated of leptons already introduced in the electron generation ψ_e which are β^+ and σ^+ respectively [105].

$$\widetilde{\psi} = \begin{pmatrix} \widetilde{e^-} \\ \widetilde{\nu} \\ \widetilde{N}^0 \\ \widetilde{E}^- \end{pmatrix} \equiv \begin{pmatrix} (\beta^+)^c \\ \widetilde{\nu} \\ \widetilde{N}^0 \\ (\sigma^+)^c \end{pmatrix}. \tag{5.4.14}$$

We have used this identification to avoid the presence of charged exotic leptons with masses of the order of the electroweak scale [108].

5.4.3 Neutral lepton masses

We turn our discussion to the neutrino masses, in our model there are 10 colorless neutral fields. From the $\mathcal{L}_{\text{leptons}}$, we get the following mass matrix in the basis ($\nu_{\alpha=\mu,\tau}, N_{\beta=\mu,\tau}$, ν_e, β_0, N_e, $\widetilde{\nu}$, Σ_0 , $\widetilde{N}$) (where $j = 3, 4$) [105]:

$$M = \begin{pmatrix} y''_{\alpha\beta}v_{\triangle'} & y''_{\alpha\beta}\frac{v_\phi}{\sqrt{2}} & 0 & 0 & 0 & 0 & 0 & 0 \\ y''_{\alpha\beta}\frac{v_\phi}{\sqrt{2}} & y''_{\alpha\beta}v_{\sigma'} & 0 & 0 & 0 & 0 & 0 & 0 \\ 0 & 0 & \frac{-y'}{2\Lambda}v_\triangle v_{\sigma'} & \frac{y'}{2\Lambda}v_H v_\phi & \frac{-y'}{\sqrt{2}\Lambda}v_\triangle v_\phi & 0 & \frac{-y'}{\sqrt{2}\Lambda}v_H v_{\sigma'} & \frac{Y^{\ell(j)}k_j}{\sqrt{2}} \\ 0 & 0 & \frac{y'}{2\Lambda}v_H v_\phi & \frac{y'}{\Lambda}v_\sigma v_{\triangle'} & \frac{-y'}{\sqrt{2}\Lambda}v_{\triangle'} v_H & \frac{Y^{\ell(j)}n_j}{\sqrt{2}} & \frac{-y'}{\sqrt{2}\Lambda}v_\phi v_\sigma & 0 \\ 0 & 0 & \frac{-y'}{\sqrt{2}\Lambda}v_\triangle v_\phi & \frac{-y'}{\sqrt{2}\Lambda}v_H v_{\triangle'} & \frac{-y'}{\Lambda}v_\triangle v_{\triangle'} & 0 & \frac{y'}{2\Lambda}v_H v_\phi & \frac{Y^{\ell(j)}n_j}{\sqrt{2}} \\ 0 & 0 & 0 & \frac{Y^{\ell(j)}}{\sqrt{2}}n_j & 0 & \widetilde{W}v_\triangle & \frac{Y^{\ell(j)}}{\sqrt{2}}k_j & \frac{2\widetilde{W}v_H}{\sqrt{2}} \\ 0 & 0 & \frac{-y'}{\sqrt{2}\Lambda}v_H v_{\sigma'} & \frac{-y'}{\sqrt{2}\Lambda}v_\phi v_\sigma & \frac{y'}{2\Lambda}v_H v_\phi & \frac{Y^{\ell(j)}}{\sqrt{2}}k_j & \frac{y'}{\Lambda}v_\sigma v_{\sigma'} & 0 \\ 0 & 0 & \frac{Y^{\ell(j)}}{\sqrt{2}}k_j & 0 & \frac{Y^{\ell(j)}}{\sqrt{2}}n_j & \frac{2\widetilde{W}}{\sqrt{2}}v_H & 0 & \widetilde{W}v_\sigma \end{pmatrix}. \tag{5.4.15}$$

The mass matrix M can be written in the following form [105]:

$$M = \begin{pmatrix} N_{\alpha\beta}^{4\times4} & 0^{4\times6} \\ 0^{6\times4} & V^{6\times6} \end{pmatrix}. \tag{5.4.16}$$

The neutrino mass matrix M can be block-diagonalized into two blocks, the sub-matrix 4×4 is in the basis (ν_α, N_β) denoted by $N_{\alpha\beta}$ and the second sub-matrix 6×6 is in the basis (ν_e, β_0, N_e, $\widetilde{\nu}$, Σ_0 , $\widetilde{N}$) denoted by V.
Where [105]:

$$N_{\alpha\beta} = \begin{pmatrix} y''_{\alpha\beta}v_{\triangle'} & y''_{\alpha\beta}\frac{v_\phi}{\sqrt{2}} \\ y''_{\alpha\beta}\frac{v_\phi}{\sqrt{2}} & y''_{\alpha\beta}v_{\sigma'} \end{pmatrix}. \tag{5.4.17}$$

Since we have $v_{\sigma'} > v_\phi, v_{\triangle'}$, in the seesaw approximation the eigenvalues take the form:

$$m^N_{\alpha\beta} \simeq y''_{\alpha\beta}v_{\sigma'}, \tag{5.4.18}$$

$$m^\nu_{\alpha\beta} \simeq y''_{\alpha\beta}v_{\triangle'} - \frac{v_\phi^2}{2v_{\sigma'}}y''_{\alpha\beta}(y''_{\alpha\beta})^{-1}(y''_{\alpha\beta})^\dagger \tag{5.4.19}$$

The light neutrinos masses $m^\nu_{\alpha\beta}$ are a mixture of a type-II and type-III seesaw mechanism contribution and the heavy neutrinos masses $m^N_{\alpha\beta}$ are proportional to the heavy VEV $v_{\sigma'}$.

Regarding the sub-matrix V, it has the form [105]:

$$V = \begin{pmatrix} \frac{-y'}{2\Lambda}v_\triangle v_{\sigma'} & \frac{y'}{2\Lambda}v_H v_\phi & \frac{-y'}{\sqrt{2}\Lambda}v_\triangle v_\phi & 0 & \frac{-y'}{\sqrt{2}\Lambda}v_H v_{\sigma'} & \frac{Y^{\ell(j)}k_j}{\sqrt{2}} \\ \frac{y'}{2\Lambda}v_H v_\phi & \frac{y'}{\Lambda}v_\sigma v_{\triangle'} & \frac{-y'}{\sqrt{2}\Lambda}v_{\triangle'} v_H & \frac{Y^{\ell(j)}n_j}{\sqrt{2}} & \frac{-y'}{\sqrt{2}\Lambda}v_\phi v_\sigma & 0 \\ \frac{-y'}{\sqrt{2}\Lambda}v_\triangle v_\phi & \frac{-y'}{\sqrt{2}\Lambda}v_H v_{\triangle'} & \frac{-y'}{\Lambda}v_\triangle v_{\triangle'} & 0 & \frac{y'}{2\Lambda}v_H v_\phi & \frac{Y^{\ell(j)}n_j}{\sqrt{2}} \\ 0 & \frac{Y^{\ell(j)}}{\sqrt{2}}n_j & 0 & \widetilde{W}v_\triangle & \frac{Y^{\ell(j)}}{\sqrt{2}}k_j & \frac{2\widetilde{W}v_H}{\sqrt{2}} \\ \frac{-y'}{\sqrt{2}\Lambda}v_H v_{\sigma'} & \frac{-y'}{\sqrt{2}\Lambda}v_\phi v_\sigma & \frac{y'}{2\Lambda}v_H v_\phi & \frac{Y^{\ell(j)}}{\sqrt{2}}k_j & \frac{y'}{\Lambda}v_\sigma v_{\sigma'} & 0 \\ \frac{Y^{\ell(j)}}{\sqrt{2}}k_j & 0 & \frac{Y^{\ell(j)}}{\sqrt{2}}n_j & \frac{2\widetilde{W}}{\sqrt{2}}v_H & 0 & \widetilde{W}v_\sigma \end{pmatrix}. \tag{5.4.20}$$

Notice that the mass matrix V can be written in the following form [105]:

$$V = \begin{pmatrix} m'^{(4\times4)} & m^{(4\times2)} \\ m^{\mathrm{T}(2\times4)} & M'^{(2\times2)} \end{pmatrix} \tag{5.4.21}$$

Since $M' > m, m'$ and using the seesaw approximation, the eigenvalues have the following form:

$$m^{\Sigma_0} \simeq \frac{y'}{\Lambda}v_\sigma v_{\sigma'}, \tag{5.4.22}$$

$$m^{\widetilde{N}} \simeq \widetilde{W}v_\sigma, \tag{5.4.23}$$

$$m^{\nu'} \simeq m' - mM'^{-1}m^T \tag{5.4.24}$$

Both Σ_0 and $\widetilde{N}$ are heavy sterile neutrinos since they are proportional to the heavy VEVs v_σ and $v_{\sigma'}$, while, the mass matrix $m^{\nu'}$ is a mixture of a type-II and type-III seesaw mechanism contribution that represents the light neutrinos.

The analytical eigenvalues and eigenstates of $m^{\nu'}$ represent the masses of ν_e, β_0, N_e, $\widetilde{\nu}$, the masses schematically take the following form: $\frac{v^2_{\text{light}}}{\Lambda}$ where $v_{\text{light}} = v_\phi, v_H, v_\triangle, v_{\triangle'}$ [105].

Ref [109] discussed the possible existence of sterile neutrinos in the eV-scale. Moreover, there are some indications from LSND and miniBoone for an eV mass sterile neutrino, in our model, β_0, N_e and $\widetilde{\nu}$ represent light sterile neutrinos .

In our case, ν_e does not mix with ν_α ($\alpha = \mu, \tau$) that makes this picture is not sufficient since oscillation neutrinos requires that ν_e mixes with the two other light neutrinos. Thus, we have to consider loops contributing to the neutrino mass matrix. We are especially interested in effective operators of the type $\mathcal{O}'^{(ij\ell)}_\alpha \psi_e \psi_\alpha \phi_i^* \phi_j^* \phi_\ell$, here i=1,2 and ℓ,j=3,4 (see figure 5.2). Since these will generate contributions mixing ν_e with ν_μ and ν_τ [103, 105].

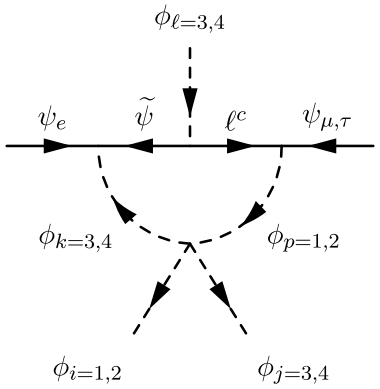

Figure 5.2: Loop diagram responsible for the mixing of ν_e with ν_μ and ν_τ [105].

A rough estimate of this diagram results in [105]:

$$\begin{aligned}
\text{Fig.5.2 diagram} \;\propto\; & \sum_{i=1}^{2} \frac{f_{ijkp}}{16\pi^2\Lambda^2} y_{\alpha\beta}^{\ell(p)} w_{\beta}^{\ell(\ell)} Y^{\ell(k)} \Bigg[\nu_\alpha \Bigg((\frac{k_i n_j k_\ell}{\sqrt{2}})\nu_e + (\frac{-n_i n_j k_\ell}{\sqrt{2}})\Sigma_0 \\
+ \; & (\frac{-n_i n_j n_\ell}{\sqrt{2}})\beta^0 + (\frac{k_i n_j n_\ell}{\sqrt{2}})N_e^0 \Bigg) + N_\alpha \Bigg((\frac{-k_i k_j k_\ell}{\sqrt{2}})\nu_e + (\frac{n_i k_j k_\ell}{\sqrt{2}})\Sigma_0 \\
+ \; & (\frac{n_i k_j n_\ell}{\sqrt{2}})\beta_0 + (\frac{-k_i k_j n_\ell}{\sqrt{2}})N_e^0 \Bigg), \\
\equiv \; & \omega_{e\mu}\nu_e\nu_\mu + \omega_{e\tau}\nu_e\nu_\tau + \omega_{\Sigma\mu}\nu_\Sigma\nu_\mu + \omega_{\Sigma\tau}\nu_\Sigma\nu_\tau + \omega_{\beta_0\mu}\nu_{\beta_0}\nu_\mu + \omega_{\beta_0\tau}\nu_{\beta_0}\nu_\tau \\
+ \; & \omega_{N_0^e\mu}\nu_{N_0^e}\nu_\mu + \omega_{N_0^e\tau}\nu_{N_0^e}\nu_\tau + \omega_{N_0^\mu e}\nu_{N_0^\mu}\nu_e + \omega_{N_0^\tau e}\nu_{N_0^\tau}\nu_e + \omega_{N_0^\mu\Sigma_0}\nu_{N_0^\mu}\nu_{\Sigma_0} \\
+ \; & \omega_{N_0^\tau\Sigma_0}\nu_{N_0^\tau}\nu_{\Sigma_0} + \omega_{N_0^\mu\beta_0}\nu_{N_0^\mu}\nu_{\beta_0} + \omega_{N_0^\tau\beta_0}\nu_{N_0^\tau}\nu_{\beta_0} + \omega_{N_0^\mu N_0^e}\nu_{N_0^\mu}\nu_{N_0^e} + \\
+ \; & \omega_{N_0^\tau N_0^e}\nu_{N_0^\tau}\nu_{N_0^e}. \qquad (5.4.25)
\end{aligned}$$

where f_{ijkp} represents the coupling constant of the quartic scalar interactions $\phi_i^*\phi_j^*\phi_k\phi_p$ ($i,p=1,2$ and $k,j,\ell=3,4$). Note that Eq.(5.4.25) does not include the corresponding loop functions and thus serves only as a rough order-of-magnitude estimate [103].

Inserting the $\omega_{\alpha\beta}$ coefficients in the mass matrix M, the full 10×10 neutrinos mass matrix in the basis (ν_e, ν_μ, ν_τ, β_0, $\widetilde{\nu}$, N_e, N_μ, N_τ, Σ_0, $\widetilde{N}$) has the following form [105]:

$$M = \begin{pmatrix} M_1^{(6\times6)} & M_2^{(6\times4)} \\ M_2^{\mathrm{T}(4\times6)} & S^{(4\times4)} \end{pmatrix}. \qquad (5.4.26)$$

Notice that N_μ,N_τ,Σ_0 and $\widetilde{N}$ are heavy neutrinos, then we should integrating them out by applying the seesaw formula, we obtain a (6×6) matrix for the active and sterile neutrinos in the basis (ν_e, ν_μ, ν_τ, β_0, $\widetilde{\nu}$, N_e) [105]:

$$\begin{aligned}
M^\nu \;&\simeq\; M_1 - M_2 S^{-1} M_2^{\mathrm{T}} \qquad (5.4.27) \\
&=\; \begin{pmatrix} m_1^{(3\times3)} & M_s^{(3\times3)} \\ M_s^{\mathrm{T}(3\times3)} & \mu_s^{(3\times3)} \end{pmatrix},
\end{aligned}$$

and (4×4) matrix for the heavy sterile neutrinos that are in the basis (N_μ,N_τ,Σ_0,$\widetilde{N}$):

$$m_1'' \simeq S. \tag{5.4.28}$$

From the matrix M^ν, there exist six light neutrinos, three of them are the active neutrinos ν_e,ν_μ and ν_τ and the others are the light sterile neutrinos β_0, $\widetilde{\nu}$ and N_e.

In the case where $\mu_s > M_s, m_1$, one may apply the seesaw formula again and find the light neutrinos mass matrix in the basis (ν_e,ν_μ,ν_τ):

$$m^\nu \simeq m_1 - M_s(\mu_s)^{-1} M_s^{\mathrm{T}}, \tag{5.4.29}$$

and the three light sterile neutrinos mass matrix in the basis $(\beta_0, \widetilde{\nu}, N_e)$:

$$m_2'' \simeq \mu_s. \tag{5.4.30}$$

Let us note that the smallness of the active neutrino masses m^ν arises from the inverse powers of the high energy cutoff Λ (where it is an upper bound depends on the Landau pole of the model (study under investigation)) and from their linear dependence on the light VEVs $v_\triangle, v_{\triangle'}, v_H, v_\phi$ [105].

5.5 PMNS matrix

Regarding the structure of the lepton mixing matrix (PMNS), in our model there are nine charged leptons and ten neutral leptons, that makes the PMNS matrix is not a square matrix, but it is a 9×10 matrix. It is given by the $W^\mp$ coupling with leptons, which is written as:

$$\frac{g}{\sqrt{2}} W_\mu^- \bar{f}_L \gamma^\mu \mathcal{U} N + h.c = \frac{g}{\sqrt{2}} W_\mu^- \bar{f}_L \gamma^\mu \begin{pmatrix} 1 & 0 & 0 & 0 & 0 & 0 & 0 & 0 & 0 & 0 \\ 0 & 1 & 0 & 0 & 0 & 0 & 0 & 0 & 0 & 0 \\ 0 & 0 & 1 & 0 & 0 & 0 & 0 & 0 & 0 & 0 \\ 0 & 0 & 0 & 0 & 0 & 0 & 0 & 0 & 0 & 0 \\ 0 & 0 & 0 & 0 & 0 & 0 & 0 & 0 & 0 & 0 \\ 0 & 0 & 0 & 0 & 0 & 0 & 0 & 0 & 0 & 0 \\ 0 & 0 & 0 & 0 & 0 & 0 & \sqrt{2} & 0 & 0 & 0 \\ 0 & 0 & 0 & 0 & 0 & 0 & 0 & 0 & 0 & 0 \\ 0 & 0 & 0 & 0 & 0 & 0 & 0 & 0 & 1 & 0 \end{pmatrix} N + h.c, \tag{5.5.1}$$

where $f = (\ell_\beta(\beta = 1...6), \Sigma^-, (\sigma^+)^c, (\beta^+)^c)$ and $N = (\nu_e, \nu_\mu, \nu_\tau, N_e, N_\mu, N_\tau, \Sigma_0, \beta_0, \widetilde{\nu}, \widetilde{N})$.

In order to go to the mass eigenstates, it is necessary to introduce the rotation matrices V_{eL} and V_ν which lead to the appearance of the lepton mixing matrix PMNS, thus:

$$\frac{g}{\sqrt{2}} W_\mu^- \bar{f}_L \gamma^\mu \mathcal{U} N + h.c = V_{mn}^{\mathrm{PMNS}} \frac{g}{\sqrt{2}} W_\mu^- \bar{f'}_{mL} \gamma^\mu N_n' + h.c. \tag{5.5.2}$$

Where the 9×10 equivalent of PMNS is:

$$V^{\text{PMNS}} = V_{eL}^{\dagger}\mathcal{U}V_{\nu} \tag{5.5.3}$$

Despite V_{eL} and V_{ν} are unitary but the presence of $\mathcal{U}$ yields a nonunitary V^{PMNS} in the flipped 341 model. If we want to adequately reproduce the SM, we should, however, recover a unitary PMNS matrix if we remain at low energies and consider only the flavor subspace of the SM particles [108]. As indicated in Ref [108], at low energies, the diagonalization of the fermion mass terms occurs in a block-diagonal way: the mixing matrices V_{eL} and V_{ν} consist in two unitary blocks, one mixing the SM particles among themselves, and the other one mixing the exotic ones among themselves. Furthermore, $\mathcal{U}$ reduces to $\mathbb{1}_{3\times3}$ in the SM flavor subspace [108] as we shown in (5.5.1). Therefore, the 3×3 SM block of V^{PMNS} is given by the product of the two unitarity 3×3 SM subspaces of V_{eL} and V_{ν}.

$$V^{\text{PMNS}} = V_{eL}^{\dagger}V_{\nu}. \tag{5.5.4}$$

This obviously does not mean that V^{PMNS} remains unitary, and our model does indeed generate small deviations of unitarity for V^{PMNS}.

Both $V_{eL}^{\dagger}$ and V_{ν} are 3×3 matrices which we can parameterize them using Euler angles θ_{ij} and phases. The parameterztaion of V_{ν} is:

$$V_{\nu} = U_{\nu}P_{\nu}, \tag{5.5.5}$$

where

$$U = \begin{pmatrix} c_{12}c_{13} & s_{12}c_{13} & s_{13}e^{-i\delta} \\ -s_{12}c_{23} - c_{12}s_{23}s_{13}e^{i\delta} & c_{12}c_{23} - s_{12}s_{13}e^{i\delta} & s_{23}c_{13} \\ s_{12}s_{23} - c_{12}c_{23}s_{13}e^{i\delta} & -c_{12}s_{23} - s_{12}c_{23}s_{13}e^{i\delta} & c_{23}c_{13} \end{pmatrix}, \tag{5.5.6}$$

and

$$P = \begin{pmatrix} 1 & 0 & 0 \\ 0 & e^{i\alpha} & 0 \\ 0 & 0 & e^{i(\beta+\delta)} \end{pmatrix}, \tag{5.5.7}$$

while V_{eL}, we parameterize it similarly as [108], s_{ij}=sin$_{\theta_{ij}}$, c_{ij}=cos$_{\theta_{ij}}$ and P is a diagonal phase matrix which contains two Majorana β, α and one Dirac δ type cp-violating phases.

The combination of the parameterztaions of $V_{eL}^{\dagger}$ and V_{ν} leads to the parametrization of the PMNS matrix, where we have to take into account the neutrino oscillation data to precise the values of all the rotation angles and phases.

5.6 Flavor Changing Neutral Current (FCNC)

The ordinary versions of the 341 models predict the existence of new heavy neutral gauge bosons Z' and Z'' which have universal couplings with leptons, while, the quarks couplings

with the new gauge bosons are non-universal. The existence of a non diagonal matrix when we rotate the flavor basis into the mass eigenstates leading to the occurrence of FCNC in the quark sector.

This scheme is reversed in the flipped 341 model, the coupling of the leptons to the photon and the Z boson are universal, while, the couplings of the leptons to Z' and Z'' are not due to the fact that two of lepton families are arranged differently from the remaining lepton generations, a mixing matrix will appear which leads to the FCNC at the tree level in the lepton sector when they are rotated to mass eigenstates [2] [81].

The aim of this section is to study the lepton flavor violation processes namely $\mu \longrightarrow ee\overline{e}$ and $\mu \longrightarrow e\gamma$ and to find some constraints on the matrix element $|U_{e\mu}|$ and the masses of the neutral gauge bosons.

The lepton neutral currents of Z' and Z'' are described by the following Lagrangian:

$$\mathcal{L}_{NC} \supset -g\overline{F}\gamma^{\mu}\Big(T_{3\mu}A_3 + T_8A_{8\mu} + T_{15}A_{15\mu} + Xg_XB_{\mu}\Big)F. \tag{5.6.1}$$

where $T_i = \lambda_i/2$ and λ_i (i=3,8,15) are the diagonal Gell-Mann matrices in the group SU(4), g and g_X represent the gauge couplings of the $SU(4)_L$ and $U(1)_X$ respectively, X is the charge associated to the group $U(1)_X$ and F runs over all fermions multiplets and

$$T_i\psi_{\alpha} = \frac{1}{2}\lambda_i\psi_{\alpha}, \tag{5.6.2}$$

and

$$T_i\psi_e = \frac{1}{2}(\lambda_i\psi_e + \psi_e\lambda_i), \tag{5.6.3}$$

where $(i = 3, 8, 15)$ and $\alpha \equiv \mu, \tau$. The right-handed leptons e_{aR} and E_{aR} do not participate in FCNC [112]. Substituting Eqs (5.6.2) and (5.6.3) in the Lagrangian (5.6.1), then we obtain [105]:

$$\begin{aligned}\mathcal{L}_{NC} \supset\ & \frac{g}{2}\left(\frac{1-t_W^2}{\sqrt{3-t_W^2}}\right)\Big(\overline{\nu}_L\gamma^{\mu}T_{\nu}\nu_L + \overline{\ell}_L\gamma^{\mu}T_{\ell}\ell_L + \overline{E}_L\gamma^{\mu}T_EE_L + \overline{N}_L\gamma^{\mu}T_{\nu}N_L\Big), Z'_{\mu} \\ +\ & \frac{g}{2}\left(\frac{-2}{\sqrt{6+4t_X^2}}\right)\Big(\overline{\nu}_L\gamma^{\mu}T'_{\nu}\nu_L + \overline{\ell}_L\gamma^{\mu}T_{\ell}\ell'_L + \overline{E}_L\gamma^{\mu}T'_EE_L + \overline{N}_L\gamma^{\mu}T'_{\nu}N_L\Big)Z''_{\mu},\end{aligned} \tag{5.6.4}$$

where $t_X^2 = s_W^2/(1-2s_W^2)$ [113], s_W, c_W and t_W are the sine, cosine and tangent of the electroweak mixing angle, while T_i and T'_i are [105]:

$$T_{\nu} = T_{\ell} = \text{diag}\Big(1, (-1-t_W^2)/(1-t_W^2), (-1-t_W^2)/(1-t_W^2)\Big), \tag{5.6.5}$$

[2] We assume that this induced FCNC is mediated by very heavy neutral scalars such as ϕ_S^0, σ_S^0, $\phi_3^{q_4}$ and $\phi_4^{q_4}$ and therefore as it was pointed out by Refs [110,111]. Its radiative loop contribution is highly suppressed and negligeable. Notice that, one can also suppress this induced FCNC by introducing some mechanisms such that Froggatt-Nelson, flavor alignement etc... [110,111].

$$T_E = \text{diag}\Big((4-2t_W^2)/(1-t_W^2),(2-2t_W^2)/(1-t_W^2),(2-2t_W^2)/(1-t_W^2)\Big), \quad (5.6.6)$$

$$T_N = \text{diag}\Big(2/(1-t_W^2),0,0\Big), \quad (5.6.7)$$

$$T'_\nu = T'_\ell = T'_E = \text{diag}\Big(1,(1-2t_X^2)/2,(1-2t_X^2)/2)\Big) \quad (5.6.8)$$

and

$$T'_N = \text{diag}\Big(-1,-(3+2t_X^2)/2,-(3+2t_X^2)/2\Big). \quad (5.6.9)$$

Changing from the flavor basis into the mass basis $\ell_L = V_{\ell L}\ell'_L$, we get the following Lagrangian:

$$\mathcal{L}_{NC} \supset \frac{g}{2}\left(\frac{1-t_W^2}{\sqrt{3-t_W^2}}\right)\overline{\ell'}_L\gamma^\mu\left(V_{\ell L}^\dagger T_\ell V_{\ell L}\right)\ell'_L Z'_\mu - \frac{g}{2}\left(\frac{-2}{\sqrt{6+4t_X^2}}\right)\overline{\ell'}_L\gamma^\mu\left(V_{\ell L}^\dagger T'_\ell V_{\ell L}\right)\ell'_L Z''_\mu. \quad (5.6.10)$$

Thus,

$$\mathcal{L}_{NC} \supset \frac{g}{2}\left(\frac{1-t_W^2}{\sqrt{3-t_W^2}}\right)\overline{\ell'}_L\gamma^\mu(V_{lL}^*)_{\alpha i}(V_{lL})_{\beta j}\ell'_L Z'_\mu + \frac{g}{2}\left(\frac{-2}{\sqrt{6+4t_X^2}}\right)\overline{\ell'}_L\gamma^\mu(V_{\ell L}^*)_{\alpha i}(V_{\ell L})_{\beta j}\ell'_L Z''_\mu. \quad (5.6.11)$$

Here ℓ' can be e,ν,E,N and $i\neq j$ for flavor changing.

The corresponding Feynman diagrams that represent the decays $\mu \longrightarrow ee\overline{e}$ and $\mu \longrightarrow e\gamma$ which are used to search for the charged lepton flavor violation are shown in figure 5.3. The first vertex in the left diagram shows the tree level FCNC coupling of $Z'(Z'')$ boson (cLF changing), whereas the right diagram represents the one loop level process where ℓ_i can be any lepton [105]. Here we consider the internal fermions line to be either μ or e, so that we will have only one FCNC $Z'\mu e$ $(Z''\mu e)$ vertex.

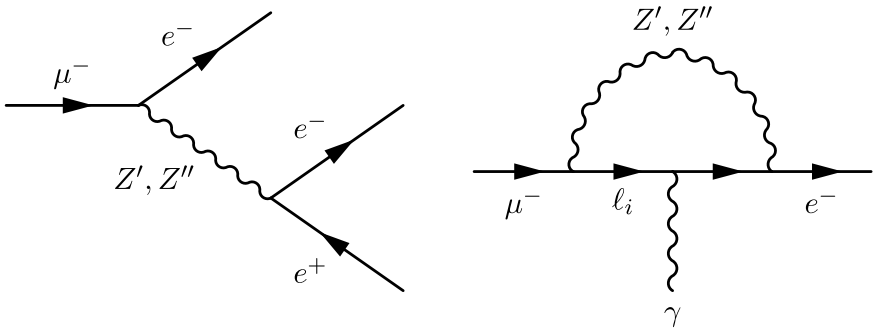

Figure 5.3: The decays $\mu \longrightarrow ee\overline{e}$ and $\mu \longrightarrow e\gamma$ via the neutral gauge bosons $Z'(Z'')$ [105].

The transferred momentum, whose maximal value is about the muon mass, is much smaller than $M_{Z'(Z'')}$ [112], therefore, the Branching ratio of the processes $\mu \longrightarrow ee\overline{e}$ and

$\mu \longrightarrow e\gamma$ through the exchange of Z' and Z'' are found to be respectively [105]:

$$Br(\mu \longrightarrow ee\overline{e}) = M_W^4 |U_{e\mu}|^2 \left(\frac{(1-t_W^2)^2}{2M_{Z'}^2(3-t_W^2)} + \frac{2}{M_{Z''}^2(6+4t_X^2)} \right)^2, \quad (5.6.12)$$

$$Br(\mu \longrightarrow e\gamma) = \frac{24\alpha}{16\pi} M_W^4 |U_{e\mu}|^2 \left(\frac{(1-t_W^2)^2}{M_{Z'}^2(3-t_W^2)} + \frac{4}{M_{Z''}^2(6+4t_X^2)} \right)^2 \quad (5.6.13)$$

where $U_{e\mu}$ is the mixing matrix. Notice that we have neglected the contribution coming from the electron internal line as it is proportional to m_e/m_μ [114] and considered the electrons as massless particles.

Using the experimental upper limit of the branching ratio $\mathrm{Br}(\mu \longrightarrow ee\overline{e}) \leq 10^{-12}$ [115] together with the current experimental limit $\mathrm{Br}(\mu \longrightarrow e\gamma) \leq 10^{-13}$ [115], we obtain, an upper limit on the lepton flavor violating matrix element $|U_{\mu e}| \leq 1.66 \times 10^{-3} \frac{M_{Z'}^2}{\mathrm{TeV}^2}$ [105] and a stringent bound on the gauge bosons masses $M_{Z'} \leq 0.597 M_{Z''}$ [105].

Figure 5.4 shows the variation of $M_{Z'}$ and $M_{Z''}$ as a function of $|U_{\mu e}|$ and the dashed areas represent the allowed region where the constraints are verified.

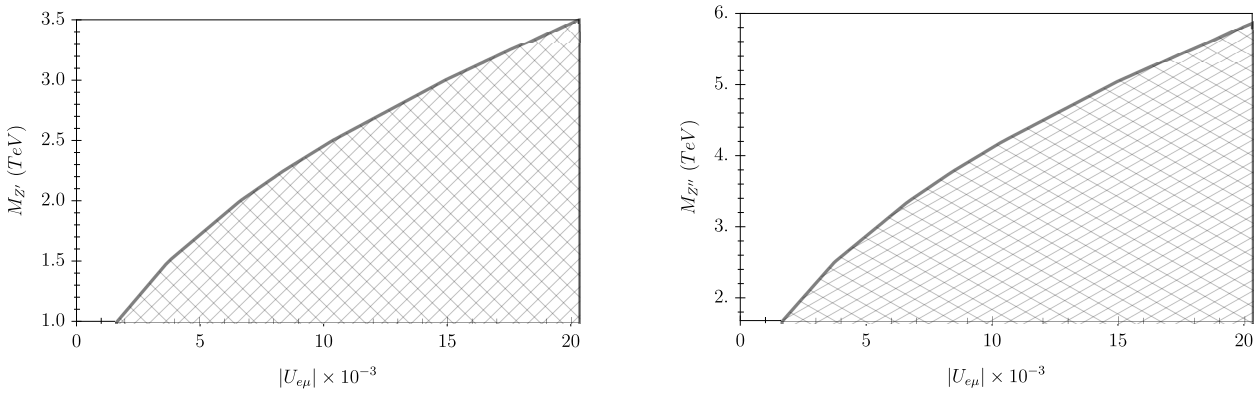

Figure 5.4: The variation of $M_{Z'}$ and $M_{Z''}$ as a function of $|U_{e\mu}|$.

5.7 Conclusion

In this chapter, we have introduced another version of the 341 models called the flipped 341 model without exotic electric charges where all the quark families are arranged in the same representations while leptons are not. The cancellation of the gauge anomalies requires the introduction of extra exotic leptons a 10-plet ψ_e which lies in the fundamental representation 10 and a quadruplet $\widetilde{\psi}$ that belongs to the conjugate fundamental representation $\bar{4}$. Using four scalar fields with two 10 plets scalar matrices, we have generated the masses of all particles at the tree and one loop levels. Furthermore, we have discussed the occurrence of the FCNC in the lepton sector through the exchange of the heavy neutral gauge bosons Z'

and Z'' in the rare decays $\mu \longrightarrow ee\overline{e}$ and $\mu \longrightarrow e\gamma$. The constraints on the masses of Z' and Z'' were discussed as well as the lepton mixing matrix $U_{e\mu}$.

Conclusion

Despite of the success of the Standard Model some fundamental questions such as matter-anti matter asymmetry, CP violation, dark matter ect....remain unsolved. Thus, going beyond the Standard Model becomes mandatory. In this thesis, we are interested in a specific BSM model called the 341 models where the $SU(3)_C \otimes SU(2)_L \otimes U(1)_Y$ gauge group of the SM is extended to $SU(3)_C \otimes SU(4)_L \otimes U(1)_X$. This provides the existence of new particles for the next step in energy scale past the SM. To assign the fermionic content of these kind of models, one has to determine the values of the two parameters β and γ.

The first chapters 1 and 2, we have summarized the fundamental feature and the particle content of the Standard model and the 341 models .

In chapter 3, we derived the theoretical constrains in the compact 341 model that are required to determine the allowed regions of the unknown scalar parameters. We have used parametrizations which allows us to find analytically the conditions which guarantee the boundedness of the scalar potential in all the directions. Together with the positivity of the Hessian matrix resulted from the first and second derivative of the scalar potential, we derive the first set of the theoretical constraints on the scalar couplings. To derive the tree level conditions for the quartic couplings of the scalar potential coming from the perturbative unitarity conditions, we express the quartic couplings in terms of the physical scalar fields instead of calculating the s-wave amplitude matrix for all possible 2 to 2 body (pseudo) scalar boson elastic scatterings in the high energy limit. Also, the positivity of all scalar bosons masses are taken into account imposing additional constraints on $\lambda_i (i = 1..9)$. Finally, We have used the fact that all quartic scalar couplings are smaller than 4π to ensure the perturbativity of the scalar potential.

The combination of all those theoretical constraints together with the emergence of the Landau pole at around 5 TeV determine the allowed regions of the parameters space which must be taken into account in our phenomenological studies (chapter 4) in the context of the compact 341 model.

In chapter 4, we discussed the neutral scalar bosons decays in the context of the compact 341 model where we used three scalar fields. To check the validity of the model we calculated the signal strength of the Higgs like-boson h_1 of different channels, we obtained

a good fit to the data as we can be seen in Figure (4.4). In particular, with υ_χ= 2 TeV, and confronted them with the ATLAS, CMS and ATLAS+CMS combination data, we have shown that the compact 341 model is achieved to a good result that are compatible to the recent measurement of LHC.

The second focus of this chapter is the computation of the branching ratio of the other heavy scalar bosons h_2 and h_3. We found that h_2 decay preferentially into a pair of Higgs-like particles with a branching ratio $\sim$ 1 a feature not easily obtained in other extensions of Standard Model, while, h_3 decay preferentially into a pair of Z boson as we shown in the Figures (4.6) and (4.7).

In conclusion, we studied the scalar sector of a new version of the compact 341 model and showed that at a scale of a few TeV this model is a compelling alternative to the SM once it is able to explain the recent measurements of LHC regarding the signal strength.

The production process $gg \longrightarrow h_{2,3}$ followed by the decays $h_{2,3} \longrightarrow h_1h_1$, h_1h_2 could be sizeable and could be an important source of the h_1 production in the case where h_1 has a large singlet component where it is rather difficult to produce it using the conventional channel of the SM.

Throughout the chapter 5, we have introduced a new and unique anomalies free model based on the gauge group $SU(3)_C \otimes SU(4)_L \otimes U(1)_X$ baptized the flipped 341 model where all the three quark families arrange in the same representation whereas lepton generations are not. The anomalies cancellation requires the introduction of new extra exotic leptons like 10 plet a ψ_e and a quadruplet $\widetilde{\psi}$..etc.

The self consistency of the model requires the introduction of an effective non renormalizable dim 5 term to the leptonic Yukawa Lagrangian. Moreover and in order to generate the leptons masses and the PMNS mixing matrix, two 10 plets as well as 4 anti quadruplets scalars are needed. As a result, we have found that the mass matrix of the neutral leptons is a mixture or a hybrid of type II and type III Seesaw. Furthermore, it turns out that the obtained mixing matrix PMNS is not unitary with the presence of eV scale sterile neutrinos. Note that in order to take into account correctly the neutrino oscillation phenomenon, we were obliged to introduce a one loop radiative correction.

Concerning the FCNC, we have argued that the most important sources contributing to the lepton flavor violation come from the gauge bosons interactions between the charged leptons and the gauge bosons Z' and Z'' while the contribution from heavy neutral scalars of the model through radiative loops is highly suppressed and using the experimental bounds of the branching ratios $\mu \longrightarrow ee\overline{e}$ and $\mu \longrightarrow e\gamma$, an upper limit on the lepton flavor violating matrix element $|U_{e\mu}|$ as well as a stringent bound between the neutral gauge bosons are obtained.

Finally, we added appendices where we have presented the Feynman rules, Parametriza-

tions of integrals that we have used through the calculation in chapter 4 and the resulted loop functions, the Gell-Man Matrices and the Non-zero structure constant of the group SU(4), The branching rules and the tensor products of the group SU(4).

Appendix A

Feynamn rules

In appendix A, we tabulated the couplings (Feynman rules in the compact 341 model) that contribute in our discussion (chapter 4) in tables (A.1), (A.2), (A.3), (A.4), (A.5) and (A.6).

Those trilinear vertices are found from Lagrangian (2.3.17) and from the scalar potential that is giving in Eq.(2.3.60). We have used also the effective Lagrangian Eq.(2.4.2) to get the interaction between quarks and the neutral scalar bosons h_i (i=1,3), while, the trilinear vertices of the gauge boson Z with the other gauge bosons that are predicted by the compact 341 model comes from the Yung-Mills Lagrangian that is given in Eq.(2.4.11).

Interactions	Couplings
$\overline{u}_i u_i h_1$	$\frac{M^{u_i}}{\upsilon_\rho}$ with $u_i \equiv u, c, t$
$\overline{d}_i d_i h_1$	$\frac{M^{d_i}}{\upsilon_\rho}$ with $d_i \equiv d, s, b$
$\overline{\ell}\ell h_1$	$\frac{m_\ell}{\upsilon_\rho}$
$W^+W^-h_1$	$\frac{g^2}{2}\upsilon_\rho$
$K_1^-K_1^+h_1$	$\frac{g^2}{2}\upsilon_\rho$
$V^{++}V^{--}h_1$	$\frac{g^2}{2}\upsilon_\rho$
$h^{++}h^{--}h_1$	$2\lambda_2\upsilon_\rho$
$h_1^+h_1^-h_1$	$2\lambda_2\upsilon_\rho$
$h_2^+h_2^-h_1$	$\frac{\upsilon_\rho}{2}(\lambda_6+\lambda_4)$
ZZh_1	$\frac{g^2\upsilon_\rho}{4}\Big((C^{21})^2 - \frac{2}{\sqrt{3}}C^{21}C^{22} - \frac{3}{\sqrt{6}}C^{21}C^{23} + \frac{(C^{22})^2}{3} + \frac{2}{\sqrt{18}}C^{22}C^{23} + \frac{(C^{23})^2}{6} + \frac{4t^2}{4}(C^{24})^2 - 4tC^{24}C^{21} + 4tC^{24}C^{22} + \frac{4t}{\sqrt{6}}C^{24}C^{23}\Big)$

Table A.1: Higgs h_1 interactions.

Interactions	Couplings
$\overline{q}qh_2$	$\frac{M^q}{\upsilon_\chi}(\gamma + \frac{\upsilon_\chi}{\upsilon_\eta}\alpha)$ with $q \equiv u, s, b$
$\overline{J}Jh_2$	$\frac{M^J}{\upsilon_\chi}\gamma$
$\overline{U}Uh_2$	$\frac{M^U}{\upsilon_\eta}\alpha$
$\overline{\ell}\ell h_2$	$\frac{m_\ell \gamma}{\upsilon_\chi}$
$X^+X^-h_2$	$\frac{g^2}{2}\upsilon_\chi\gamma$
$V^{++}V^{--}h_2$	$\frac{g^2}{2}\upsilon_\chi\gamma$
$K'^0K'^0h_2$	$\frac{g^2}{2}\upsilon_\eta\alpha$
$K_1^-K_1^+h_2$	$\frac{g^2}{2}\upsilon_\eta\alpha$
$Y^-Y^+h_2$	$\frac{g^2}{2}(\upsilon_\chi\gamma + \upsilon_\eta\alpha)$
$h^{++}h^{--}h_2$	$\lambda_4\upsilon_\eta\alpha + (\lambda_6 + \lambda_9)\upsilon_\chi\gamma$
$h_1^+h_1^-h_2$	$(\lambda_4 + \lambda_7)\upsilon_\eta\alpha + \lambda_6\upsilon_\chi\gamma$
$h_2^+h_2^-h_2$	$\frac{\upsilon_\chi\gamma}{2}(2\lambda_3 + \lambda_5 + \lambda_8) + \frac{\upsilon_\chi\alpha\lambda_8}{2} + \frac{\upsilon_\eta\alpha}{2}(\lambda_5 + \lambda_8 + 2\lambda_1) + \frac{\gamma\upsilon_\eta\lambda_8}{2}$
ZZh_2	$\frac{g^2\gamma}{4}\upsilon_\chi\left(\frac{3}{2}(C^{23})^2 + 4t^2(C^{24})^2 + \frac{12t}{\sqrt{6}}C^{23}C^{24}\right) + \frac{g^2\alpha}{4}\upsilon_\eta\left(\frac{4}{3}(C^{22})^2 + \frac{(C^{23})^2}{6} - \frac{4}{\sqrt{18}}C^{22}C^{23}\right)$
$Z'Z'h_2$	$\frac{g^2\gamma}{4}\upsilon_\chi\left(\frac{3}{2}(C^{33})^2 + 4t^2(C^{34})^2 + \frac{12t}{\sqrt{6}}C^{33}C^{34}\right) + \frac{g^2\alpha}{4}\upsilon_\eta\left(\frac{4}{3}(C^{32})^2 + \frac{(C^{33})^2}{6} - \frac{4}{\sqrt{18}}C^{32}C^{33}\right)$
$h_1h_1h_2$	$\frac{\lambda_6}{2}\upsilon_\chi\gamma + \frac{\lambda_4}{2}\upsilon_\eta\alpha$

Table A.2: Higgs h_2 interactions.

Interactions	Couplings
$\bar{q}qh_3$	$\frac{M^q}{\upsilon_\chi}(\sigma + \frac{\upsilon_\chi}{\upsilon_\eta}\beta)$ with $q \equiv u, s, b$
$\overline{J}Jh_3$	$\frac{M^J}{\upsilon_\chi}\sigma$
$\overline{U}Uh_3$	$\frac{M^U}{\upsilon_\eta}\beta$
$\bar{\ell}\ell h_3$	$\frac{m_\ell}{\upsilon_\chi}\sigma$
$X^+X^-h_3$	$\frac{g^2}{2}\upsilon_\chi\sigma$
$V^{++}V^{--}h_3$	$\frac{g^2}{2}\upsilon_\chi\sigma$
$K'^0K^{0\prime}h_3$	$\frac{g^2}{2}\upsilon_\eta\beta$
$K^-K^+h_3$	$\frac{g^2}{2}\upsilon_\eta\beta$
$Y^-Y^+h_3$	$\frac{g^2}{2}(\upsilon_\chi\sigma + \upsilon_\eta\beta)$
$h^{++}h^{--}h_3$	$\lambda_4\upsilon_\eta\beta + \upsilon_\chi\sigma(\lambda_6 + \lambda_9)$
$h_1^+h_1^-h_3$	$\upsilon_\eta\beta(\lambda_4 + \lambda_7) + \lambda_6\upsilon_\chi\sigma$
$h_2^+h_2^-h_3$	$\frac{\upsilon_\chi\sigma}{2}(2\lambda_3 + \lambda_8 + \lambda_5) + \frac{\upsilon_\chi\lambda_8}{2}\beta + \frac{\upsilon_\eta\beta}{2}(\lambda_5 + \lambda_8 + 2\lambda_1) + \frac{\upsilon_\eta\sigma\lambda_8}{2}$
ZZh_3	$\frac{g^2\upsilon_\chi\sigma}{4}\left(\frac{3}{2}(C^{23})^2 + 4t^2(C^{24})^2 + \frac{12t}{\sqrt{6}}C^{23}C^{24}\right) + \frac{g^2\upsilon_\eta\beta}{4}\left(\frac{4}{3}(C^{22})^2 + \frac{(C^{23})^2}{6} - \frac{4}{\sqrt{18}}C^{22}C^{23}\right)$
$Z'Z'h_3$	$\frac{g^2\upsilon_\chi\sigma}{4}\left(\frac{3}{2}(C^{33})^2 + 4t^2(C^{34})^2 + \frac{12t}{\sqrt{6}}C^{33}C^{34}\right) + \frac{g^2\upsilon_\eta\beta}{4}\left(\frac{4}{3}(C^{32})^2 + \frac{(C^{33})^2}{6} - \frac{4}{\sqrt{18}}C^{32}C^{33}\right)$
$h_1h_1h_3$	$\upsilon_\chi\frac{\lambda_6}{2}\sigma + \frac{\lambda_4}{2}\upsilon_\eta\beta$
$h_2h_2h_3$	$\frac{\lambda_5\upsilon_\chi}{2}(\alpha^2\sigma + 2\alpha\beta\gamma) + \frac{\lambda_5\upsilon_\eta}{2}(\beta\gamma^2 + 2\alpha\gamma\sigma)$
$h_2h_1h_3$	$\lambda_4\upsilon_\rho\alpha\beta + \lambda_6\upsilon_\rho\gamma\sigma$

Table A.3: Higgs h_3 interactions.

A.1 The vertex ZSS

The interactions of the Z boson and the charged scalar bosons are found by using Eq.(2.3.17).

Interactions	Couplings
$Zh^{++}h^{--}$	0
$Zh_1^+h_1^-$	0
$Zh_2^+h_2^-$	0

Table A.4: Couplings ZSS.

A.2 The vertex ZVV

The vertex ZVV are tabulated in the following table:

Interactions	Couplings
$W^+_\beta W^-_\alpha Z_\mu$	$igC^{21}\sum_{\alpha\beta\mu}(p,k,q)$
$K'^0_\beta K'^0_\alpha Z_\mu$	$\frac{-ig}{2}(C^{21}+\sqrt{3}C^{22})\sum_{\alpha\beta\mu}(p,k,q)$
$X^+_\beta X^-_\alpha Z_\mu$	$\frac{-ig}{2\sqrt{3}}(\sqrt{3}C^{21}+C^{22}+C^{23})\sum_{\alpha\beta\mu}(p,k,q)$
$K^+_{1\beta}K^-_{1\alpha}Z_\mu$	$\frac{-ig}{2}(\sqrt{3}C^{22}-C^{21})\sum_{\alpha\beta\mu}(p,k,q)$
$V^{++}_\beta V^{--}_\alpha Z_\mu$	$\frac{-ig}{2\sqrt{3}}(-\sqrt{3}C^{21}+C^{22}+C^{23})\sum_{\alpha\beta\mu}(p,k,q)$
$Y^+_\beta Y^-_\alpha Z_\mu$	$\frac{-ig}{2\sqrt{3}}(-C^{22}+C^{23})\sum_{\alpha\beta\mu}(p,k,q)$

Table A.5: Couplings ZVV where V is the gauge bosons $X^\mp$, $Y^\mp$, $V^{\mp\mp}$, $K^\mp_1$, K'^0 and $W^\mp$, while, $\sum_{\alpha\beta\mu}(p,k,q)=g_{\alpha\beta}(p-k)_\mu+g_{\beta\mu}(k-q)_\alpha+g_{\mu\alpha}(q-p)_\beta$.

A.3 The vertex $Zq\bar{q}$

The interactions of quarks and the Z boson, they are found from the neutral current, based on the expression of the covariance derivative:

$$D_\mu=\partial_\mu+ig\frac{W^a_\mu\lambda_a}{2}+iXg'W^X_\mu. \tag{A.3.1}$$

The interactions Zqq are in the following table:

Interactions	g_V	g_A
$\overline{u}uZ$	$\frac{-5}{3}S_WT_W+C_W$	$\frac{1}{C_W}$
$\overline{d}dZ$	$\frac{1}{3}S_WT_W-C_W$	$\frac{-1}{C_W}$
$\overline{s}sZ$	$C_W-\frac{5}{3}S_WT_W$	$C_W-3S_WT_W$
$\overline{b}bZ$	$C_W-\frac{5}{3}S_WT_W$	$C_W-3S_WT_W$
$\overline{c}cZ$	$-C_W+\frac{1}{3}S_WT_W$	$-\frac{1}{C_W}$
$\overline{t}tZ$	$-C_W+\frac{1}{3}S_WT_W$	$-\frac{1}{C_W}$
$\overline{U_1}U_1Z$	$\frac{-8}{3}S_WT_W$	0
$\overline{J_1}J_1Z$	$\frac{-20}{3}S_WT_W$	0
$\overline{D_2}D_2Z$	$\frac{4}{3}S_WT_W$	0
$\overline{D_3}D_3Z$	$\frac{4}{3}S_WT_W$	0
$\overline{J_2}J_2Z$	$\frac{16}{3}S_WT_W$	0
$\overline{J_3}J_3Z$	$\frac{16}{3}S_WT_W$	0

Table A.6: Couplings $\frac{g\gamma^\mu}{4}(g_V-\gamma_5 g_A)$ of the $Zq\overline{q}$ vertex.

We motioned that $S_W\equiv\sin\theta_W$, $C_W\equiv\cos\theta_W$, $T_W\equiv\tan\theta_W$ and $h_W=3-4S^2_W$, whereas

the parameters α, β, γ and σ are found to be:

$$\alpha = \frac{-\sqrt{X^2+(Y-\sqrt{X^2+Y^2})^2}}{\sqrt{4(X^2+Y^2)}} \tag{A.3.2}$$

$$\beta = \frac{\sqrt{X^2+(Y+\sqrt{X^2+Y^2})^2}}{\sqrt{4(X^2+Y^2)}} \tag{A.3.3}$$

$$\gamma = \frac{(Y+\sqrt{X^2+Y^2})(\sqrt{X^2+(Y-\sqrt{X^2+Y^2})^2})}{X\sqrt{4(X^2+Y^2)}} \tag{A.3.4}$$

$$\sigma = \frac{-(Y-\sqrt{X^2+Y^2})(\sqrt{X^2+(Y+\sqrt{X^2+Y^2})^2})}{X\sqrt{4(X^2+Y^2)}} \tag{A.3.5}$$

with

$$X = \lambda_5, \quad Y = \lambda_1 - \lambda_3. \tag{A.3.6}$$

Appendix B

Parameterizations of integrals and loop functions

In chapter 4, during our calculations of the partial widths decays of $h_i \longrightarrow \gamma\gamma$ and $h_i \longrightarrow Z\gamma$, we have used famous Parameterizations of integrals, their expressions are given by:

$$\int \frac{d^D p}{(2\pi)^D} \frac{1}{(p^2 - M^2)^\beta} = \frac{i(-1)^\beta}{(4\pi)^{\frac{D}{2}}} \frac{\Gamma(\beta - \frac{D}{2})}{\Gamma(\beta)} (M^2)^{\frac{D}{2}-\beta}, \tag{B.0.1}$$

$$\int \frac{d^D p}{(2\pi)^D} \frac{p^2}{(p^2 - M^2)^\beta} = \frac{i(-1)^{\beta-1}}{(4\pi)^{\frac{D}{2}}} \frac{D}{2} \frac{\Gamma(\beta - \frac{D}{2} - 1)}{\Gamma(\beta)} (M^2)^{\frac{D}{2}-\beta+1}, \tag{B.0.2}$$

$$\int \frac{d^D p}{(2\pi)^D} \frac{p^\mu p^\nu}{(p^2 - M^2)^\beta} = \frac{i(-1)^{\beta-1}}{(4\pi)^{\frac{D}{2}}} \frac{D}{2} \frac{\Gamma(\beta - \frac{g^{\mu\nu}}{2} - 1)}{\Gamma(\beta)} (M^2)^{\frac{D}{2}-\beta+1}, \tag{B.0.3}$$

where $\Gamma(\alpha)$ is the Gamma function, its fundamental properties are:

$$\Gamma(z+1) = z\Gamma(z) \tag{B.0.4}$$

$$\Gamma(n) = (n-1)! \tag{B.0.5}$$

$$\Gamma(n + \frac{1}{2}) = \frac{2n!}{4^n n!}\sqrt{\pi} \tag{B.0.6}$$

B.1 Loop Function for the Decay $h \longrightarrow \gamma\gamma$

The loop functions of the decay $h \longrightarrow \gamma\gamma$ for gauge bosons, fermions and scalar bosons respectively are given by:

$$\begin{aligned} A_1(x) &= -x^2[2x^{-2} + 3x^{-1} + 3(2x^{-1} - 1)f(x^{-1})]. \\ A_{\frac{1}{2}}(x) &= 2x^2[x^{-1} + (x^{-1} - 1)f(x^{-1})]. \\ A_0(x) &= -x^2[x^{-1} - f(x^{-1})], \end{aligned} \tag{B.1.1}$$

where

$$f(x) = \begin{cases} \arcsin^2 \sqrt{x} & \text{for} \quad x \geq 1, \\ \frac{-1}{4}\left[\ln[\frac{1+\sqrt{1-x^{-1}}}{1-\sqrt{1-x^{-1}}} - \imath\pi\right]^2 & \text{for} \quad x < 1. \end{cases} \tag{B.1.2}$$

B.2 Loop Function for the Decay $h \longrightarrow Z\gamma$

The loop functions of the decay $h \longrightarrow Z\gamma$ for gauge bosons, fermions and scalar bosons respectively are given by:

$$\begin{aligned} A_1(x,y) &= 4(3-\tan^2\theta_W)I_2(x,y) + \left[(1+2x^{-1})\tan^2\theta_W - (5+2x^{-1})\right]I_1(x,y), \\ A_{\frac{1}{2}}(x,y) &= I_1(x,y) - I_2(x,y), \\ A_0(x,y) &= I_1(x,y), \end{aligned} \tag{B.2.1}$$

where

$$I_1(x,y) = \frac{xy}{2(x-y)} + \frac{x^2y^2}{2(x-y)^2}[f(x^{-1}) - f(y^{-1})] + \frac{x^2y}{(x-y)^2}[g(x^{-1}) - g(y^{-1})], \tag{B.2.2}$$

$$I_2(x,y) = \frac{-xy}{2(x-y)}[f(x^{-1}) - f(y^{-1})]. \tag{B.2.3}$$

with

$$g(x) = \begin{cases} \sqrt{x^{-1}-1}\arcsin\sqrt{x} & \text{for} \quad x \geq 1, \\ \frac{\sqrt{1-x^{-1}}}{2}\left[\ln[\frac{1+\sqrt{1-x^{-1}}}{1-\sqrt{1-x^{-1}}} - \imath\pi\right] & \text{for} \quad x < 1. \end{cases}$$

The parameters x and y represent τ_i and λ_i that are given by $\frac{4m_i^2}{m_{h_i}^2}$ and $\frac{4m_i^2}{m_{Z_i}^2}$ respectively.

Appendix C

Gell-Man Matrices and the Non-zero structure constant of the group $SU(4)$

The 15 Gell-Man matrices of the group $SU(4)$ are [116]:

$$\lambda_1 = \begin{pmatrix} 0 & 1 & 0 & 0 \\ 1 & 0 & 0 & 0 \\ 0 & 0 & 0 & 0 \\ 0 & 0 & 0 & 0 \end{pmatrix} \quad \lambda_2 = \begin{pmatrix} 0 & -i & 0 & 0 \\ i & 0 & 0 & 0 \\ 0 & 0 & 0 & 0 \\ 0 & 0 & 0 & 0 \end{pmatrix} \quad \lambda_3 = \begin{pmatrix} 1 & 0 & 0 & 0 \\ 0 & -1 & 0 & 0 \\ 0 & 0 & 0 & 0 \\ 0 & 0 & 0 & 0 \end{pmatrix}$$

$$\lambda_4 = \begin{pmatrix} 0 & 0 & 1 & 0 \\ 0 & 0 & 0 & 0 \\ 1 & 0 & 0 & 0 \\ 0 & 0 & 0 & 0 \end{pmatrix} \quad \lambda_5 = \begin{pmatrix} 0 & 0 & -i & 0 \\ 0 & 0 & 0 & 0 \\ i & 0 & 0 & 0 \\ 0 & 0 & 0 & 0 \end{pmatrix} \quad \lambda_6 = \begin{pmatrix} 0 & 0 & 0 & 0 \\ 0 & 0 & 1 & 0 \\ 0 & 1 & 0 & 0 \\ 0 & 0 & 0 & 0 \end{pmatrix}$$

$$\lambda_7 = \begin{pmatrix} 0 & 0 & 0 & 0 \\ 0 & 0 & -i & 0 \\ 0 & i & 0 & 0 \\ 0 & 0 & 0 & 0 \end{pmatrix} \quad \lambda_8 = \frac{1}{\sqrt{3}} \begin{pmatrix} 1 & 0 & 0 & 0 \\ 0 & 1 & 0 & 0 \\ 0 & 0 & -2 & 0 \\ 0 & 0 & 0 & 0 \end{pmatrix} \quad \lambda_9 = \begin{pmatrix} 0 & 0 & 0 & 1 \\ 0 & 0 & 0 & 0 \\ 0 & 0 & 0 & 0 \\ 1 & 0 & 0 & 0 \end{pmatrix}$$

$$\lambda_{10} = \begin{pmatrix} 0 & 0 & 0 & -i \\ 0 & 0 & 0 & 0 \\ 0 & 0 & 0 & 0 \\ i & 0 & 0 & 0 \end{pmatrix} \quad \lambda_{11} = \begin{pmatrix} 0 & 0 & 0 & 0 \\ 0 & 0 & 0 & 1 \\ 0 & 0 & 0 & 0 \\ 0 & 1 & 0 & 0 \end{pmatrix} \quad \lambda_{12} = \begin{pmatrix} 0 & 0 & 0 & 0 \\ 0 & 0 & 0 & -i \\ 0 & 0 & 0 & 0 \\ 0 & i & 0 & 0 \end{pmatrix}$$

$$\lambda_{13} = \begin{pmatrix} 0 & 0 & 0 & 0 \\ 0 & 0 & 0 & 0 \\ 0 & 0 & 0 & 1 \\ 0 & 0 & 1 & 0 \end{pmatrix} \quad \lambda_{14} = \begin{pmatrix} 0 & 0 & 0 & 0 \\ 0 & 0 & 0 & 0 \\ 0 & 0 & 0 & -i \\ 0 & 0 & i & 0 \end{pmatrix} \quad \lambda_{15} = \frac{1}{\sqrt{6}} \begin{pmatrix} 1 & 0 & 0 & 0 \\ 0 & 1 & 0 & 0 \\ 0 & 0 & 1 & 0 \\ 0 & 0 & 0 & -3 \end{pmatrix}$$

APPENDIX C. GELL-MAN MATRICES AND THE NON-ZERO STRUCTURE CONSTANT OF THE GROUP $SU(4)$

The non-zero structure constants f^{abc} of SU(4) group are tabulated in the following tables [116]:

a	b	c	f^{abc}
1	9	12	$\frac{1}{2}$
1	10	11	$\frac{-1}{2}$
2	9	11	$\frac{1}{2}$
2	10	12	$\frac{1}{2}$
3	9	10	$\frac{1}{2}$
3	11	12	$\frac{-1}{2}$
4	9	14	$\frac{1}{2}$
4	10	13	$\frac{-1}{2}$
5	9	13	$\frac{1}{2}$
5	10	14	$\frac{1}{2}$
6	11	14	$\frac{1}{2}$
6	12	13	$\frac{-1}{2}$
7	11	13	$\frac{1}{2}$
7	12	14	$\frac{1}{2}$
8	9	10	$\frac{1}{\sqrt{12}}$
8	11	12	$\frac{1}{\sqrt{12}}$
8	13	14	$\frac{-1}{2\sqrt{3}}$
9	10	15	$\frac{1}{2\sqrt{3}}$
11	12	15	$\frac{1}{2\sqrt{3}}$
13	14	15	$\frac{1}{2\sqrt{3}}$

Table C.1: The structure constants f^{abc} of SU(4).

Appendix D

Properties of irreducible Representation $SU(N)$

The dimensions of the simplest representations are [117]:

Dimension	Description
N	Defining irrep
N^2	$N \otimes N$ Defining
N^2-1	$N \otimes \overline{N}$ -U(1) adjoint irrep
$\frac{N(N+1)}{2}$	Symmetric
$\frac{N(N-1)}{2}$	Anti-Symmetric
N^3	$N \otimes N \otimes N$ Defining

Table D.1: Dimensions of Irreps of SU(N).

Table (D.2) summaries the feature of representations of $A(n-1) = SU(n)(n \geq 2)$, where $SU(n)$ irrep., $d(R)$, $C_2(R)$, $T(R)$ and $A(R)$ stand for the Dynkin label of the irreducible representations of $A(n-1) = SU(n)$, their dimension, their quadratic Casimir invariant, their Dynkin index, their triangle anomaly numbe respectively, where $T(R)d(G) = C_2(R)d(R)$ and $d(G)$ is the dimension of the adjoint representation. The anomaly number of a representation is the same magnitude and its opposite sign of that of its conjugate representation: $A(R) = -A(R)$ [107].

$SU(n)$	$d(R)$	$C_2(R)$	$T(R)$	$A(R)$
(0000..0000)	1	0	0	0
(1000..0000)	n	$\frac{n^2-1}{2n}$	$\frac{1}{2}$	1
(0000..0001)	n	$\frac{n^2-1}{2n}$	$\frac{1}{2}$	-1
(1000..0000)	$\frac{n(n-1)}{2}$	$\frac{(n+1)(n-2)}{n}$	$\frac{n-2}{2}$	$n-4$
(0000..0010)	$\frac{n(n-1)}{2}$	$\frac{(n+1)(n-2)}{n}$	$\frac{n-1}{2}$	$-n+4$
(2000..0000)	$\frac{n(n+1)}{2}$	$\frac{(n-1)(n+2)}{n}$	$\frac{n+2}{2}$	$n+4$
(0000..0002)	$\frac{n(n+1)}{2}$	$\frac{(n-1)(n+2)}{n}$	$\frac{n+2}{2}$	$-n-4$
(1000..0001)	n^2-1	n	n	0
(0010..0000)	$\frac{n(n-1)(n-2)}{6}$	$\frac{(n-2)(n-3)(n-4)}{12}$	$\frac{(n-3)(n-2)}{4}$	$\frac{(n-3)(n-6)}{2}$
(0000..0100)	$\frac{n(n-1)(n-2)}{6}$	$\frac{(n-2)(n-3)(n-4)}{12}$	$\frac{(n-3)(n-2)}{4}$	$-\frac{(n-3)(n-6)}{2}$
(1100..0000)	$\frac{n(n-1)(n+1)}{3}$	$\frac{3(n^2-3)}{2n}$	$\frac{(n^2-3)}{2}$	n^2-9
(0000..0011)	$\frac{n(n-1)(n+1)}{3}$	$\frac{3(n^2-3)}{2n}$	$\frac{(n^2-3)}{2}$	$-n^2+9$
(3000..0000)	$\frac{n(n+1)(n+2)}{6}$	$\frac{(n+2)(n+3)(n+4)}{12}$	$\frac{(n+2)(n+3)}{4}$	$\frac{(n+3)(n+6)}{2}$
(0000..0003)	$\frac{n(n+1)(n+2)}{6}$	$\frac{(n+2)(n+3)(n+4)}{12}$	$\frac{(n+2)(n+3)}{4}$	$-\frac{(n+3)(n+6)}{2}$
(0200..0000)	$\frac{n^2(n+1)(n-1)}{12}$	$\frac{n(n^2-16)}{3}$	$\frac{n(n-2)(n+2)}{6}$	$\frac{n(n-4)(n+4)}{3}$
(0000..0020)	$\frac{n^2(n+1)(n-1)}{12}$	$\frac{n(n^2-16)}{3}$	$\frac{n(n-2)(n+2)}{6}$	$-\frac{n(n-4)(n+4)}{3}$

Table D.2: Representations of $SU(n)$.

-For the representation $SU(3)$:

$SU(3)$	$d(R)$	$C_2(R)$	$T(R)$	$A(R)$
(0,0)	1	0	0	0
(1,0)	3	$\frac{4}{3}$	$\frac{1}{2}$	+1
(0,1)	$\overline{3}$	$\frac{4}{3}$	$\frac{1}{2}$	-1
(0,2)	6	$\frac{10}{3}$	$\frac{5}{2}$	+7
(2,0)	$\overline{6}$	$\frac{10}{3}$	$\frac{5}{2}$	-7
(1,1)	8	3	3	0

Table D.3: $SU(3)$ representation.

-For the representation $SU(4)$

$SU(4)$	$d(R)$	$C_2(R)$	$T(R)$	$A(R)$
(0,0,0)	1	0	0	0
(1,0,0)	4	$\frac{15}{8}$	$\frac{1}{2}$	+1
(0,0,1)	$\overline{4}$	$\frac{15}{8}$	$\frac{1}{2}$	-1
(0,1,0)	6	$\frac{5}{2}$	1	0
(2,0,0)	10	$\frac{9}{2}$	3	+8
(0,0,2)	$\overline{10}$	$\frac{9}{2}$	3	-8
(1,0,1)	15	4	4	0

Table D.4: $SU(4)$ representation.

D.1 Tensor products

Tables D.5, D.6, **??** and D.7 represent some tensor products in the groups $SU(2)$, $SU(3)$ and $SU(4)$ respectively [107, 118]:

$SU(2)$ tensor products
$1 \otimes 1 = 1$
$2 \otimes 1 = 2$
$2 \otimes 2 = 3 \oplus 1$
$3 \otimes 1 = 3$
$3 \otimes 2 = 4 \oplus 2$
$3 \otimes 3 = 1 \oplus 3 \oplus 5$

Table D.5: Tensor products of SU(2).

$SU(3)$ tensor products
$3 \otimes 3 = \overline{3} \oplus 6$
$\overline{3} \otimes 3 = 8 \oplus 1$
$\overline{3} \otimes \overline{3} = \overline{6} \oplus 3$
$6 \otimes 3 = 8 \oplus 10$
$\overline{6} \otimes 6 = 1 \oplus 8 \oplus 27$
$6 \otimes \overline{3} = \overline{10} \oplus 8$

Table D.6: Tensor products of SU(3).

$SU(4)$ tensor products
$4 \otimes 4 = 10 \oplus 6$
$\overline{4} \otimes 4 = 15 \oplus 1$
$\overline{4} \otimes \overline{4} = \overline{10} \oplus \overline{6}$
$6 \otimes 4 = \overline{20} \oplus \overline{4}$
$\overline{10} \otimes 4 = \overline{4} \oplus \overline{36}$
$10 \otimes 10 = 20' \oplus 35 \oplus 45$
$10 \otimes \overline{10} = 1 \oplus 15 \oplus 84$
$10 \otimes 6 = 15 \oplus 45$
$6 \otimes 6 = 1 \oplus 15 \oplus 20'$
$20' \otimes 20' = 105 \oplus 84 \oplus 20' \oplus 1 \oplus 175 \oplus 15$

Table D.7: Tensor products of SU(4).

D.2 Branching rules

Tables D.8 and D.9 represent some branching rules of $SU(n)$ into $SU(n-1) \otimes U(1)$ (where $n = 3, 4$) [107, 118]:

$SU(3) \supset SU(2) \otimes U(1)$
$1 = (1)(0)$
$3 = (2)(1) \oplus (1)(-2)$
$\overline{3} = (2)(-1) \oplus (1)(2)$
$6 = (3)(2) \oplus (2)(-1) \oplus (1)(-4)$
$\overline{6} = (3)(-2) \oplus (2)(1) \oplus (1)(4)$
$8 = (3)(0) \oplus (2)(3) \oplus (2)(-3) \oplus (1)(0)$

Table D.8: Branching rules of $SU(3) \supset SU(2) \otimes U(1)$.

$SU(4) \supset SU(3) \otimes U(1)$
$1=(1)(0)$
$4=(3)(1)\oplus(1)(-3)$
$\overline{4}=(\overline{3})(-1)\oplus(1)(3)$
$6=(3)(-2)\oplus(\overline{3})(2)$
$10=(6)(2)\oplus(3)(-2)\oplus(1)(-6)$
$\overline{10}=(\overline{6})(-2)\oplus(\overline{3})(2)\oplus(1)(6)$
$15=(8)(0)\oplus(3)(4)\oplus(\overline{3})(-4)\oplus(1)(0)$

Table D.9: Branching rules of $SU(4) \supset SU(3) \otimes U(1)$.

Appendix E

List of Publications

-N.Mebarki, M.Djouala, J.Mimouni and H.Aissaoui, *New Compact 341 Model: Higgs Decay Modes*, *J. Phys. Conf. Ser.* **1258**, 012011 (2019), ArXiv: 2009.04242.
-M.Djouala and N.Mebarki, *A flipped* $SU(3)_C \otimes SU(4)_L \otimes U(1)_X$ *model*,*J. Phys. Conf. Ser.* **1766**, 012016 (2021).
-M.Djouala and N.Mebarki,*Theoretical constraints on scalar parameters in the compact 341 model* , *Int. J. Mod. Phys. A* **36**, 2150093 (2021), ArXiv: 2002.08758[hep-ph]
-M.Djouala, N.Mebarki and H.Aissaoui, *A new anomaly-free flipped 341 model*, *Int. J. Mod. Phys. A* **36**, 2150101 (2021), ArXiv: 1911.04887[hep-ph].

IOP Conf. Series: Journal of Physics: Conf. Series **1258** (2019) 012011 doi:10.1088/1742-6596/1258/1/012011

New Compact 341 Model: Higgs Decay Modes

N.Mebarki, M.Djouala, J.Mimouni and H.Aissaoui

Laboratoire de Physique Mathématique et Subatomique

Mentouri University, Constantine1, Algeria

jamalmimouni@yahoo.com

Abstract New developments in the anomaly free compact 341 model are discussed and the higgs bosons decay modes are studied taking into account the contributions of new fermions, gauge bosons and scalar bosons predicted by the model. It is shown from signal strengths and the branching ratios of the various decay modes analysis and the LHC constraints that there is a room for this extended BSM model and it is viable.

1. Introduction

Despite all successes of the standard model, many questions remained unsolved and not well understood like dark matter, neutrinos oscillation, matter anti-matter asymmetry etc… Trying to find a solution to those problems, one needs to extend the standard model and go beyond (BSM). The most proposed model on the literature are the ones with two-Higgs doublets (THDM)[1], supersymmetry [2], 331, extra dimensions [3] and 341 gauge models [4-11].

Among those extensions, we focus on a model which is based on the $SU(3)_c \otimes SU(4)_L \otimes U(1)_N$ gauge symmetry (denoted by 341 model for a short hand). This model has new particles like exotic quarks, new gauge bosons $K_0, K_0^{'}, K_0^{\pm}, X^{\pm}, V^{\pm\pm}$, $Y^{\pm}$, $Z_0^{'}$ and $Z_0^{''}$. Moreover, the 341 model has a very specific arrangement of the fermions into generations; for leptons, one has both right and left handed helecities arranged in the same multiplet. In order to make the model anomaly free, the second and third quarks families has to belong to the conjugate 4^* fundamental representation of the $SU(4)_L$ gauge group, while the first family transforms as a quadruplet in the 4 fundamental representation. In this compact 341 model, we have a minimum of three scalars quartets[8] and after SSB which is achieved via three steps, one ends up with three CP even neutral higgses h_1, h_2 and h_3 and eight CP odd massive higgses $h_1^{\pm}$, $h_2^{\pm}$ and $h^{\pm\pm}$.

In this paper, we focus on the analysis of the neutral Higgs decays modes and discuss the signal strengths and the branching ratios of the various decay modes as well as the LHC constraints and show that there is a room for this extended BSM model and it is viable. In section2, we present a brief review of the theoretical model. In section3, we give the various analytical expressions of the partial decays width which we have derived using the new Feynman rules of the model. Finally, in section4, we give our numerical results concerning the signal strength of the various higgses branching ratios, after imposing the self consistency and compatibility constraints on the scalar potential of the model like triviality, unitarity, vacuum stability and non-ghost conditions, make comparison with the signal strengths of the recent experimental data reported by ATLAS, CMS and combined ATLAS+CMS and draw our conclusions.

A flipped $SU(3)_C \otimes SU(4)_L \otimes U(1)_X$ model

Meriem Djouala and Noureddine Mebarki
Laboratoire de Physique Mathématique et Subatomique
Mentouri University, Constantine 1, Constantine, Algeria
E-mail: djoualameriem@gmail.com

Abstract. An anomaly free flipped 341 model where leptons and quarks generations are arranged in new different $SU(4)_L$ representations is proposed.

1. Introduction

The neutrinos oscillation phenomenon reveals that the Standard Model is an effective field theory, therefore, theories Beyond the SM (BSM) are needed to explain and answer all the remaining unsolved questions.

Among the many BSM models, we are interested in the 341 models based on the gauge group $SU(3)_C \otimes SU(4)_L \otimes U(1)_X$ for which one can distinguish different versions according to:

(i) The values of the parameters β and γ which the electric charge $\widetilde{Q}$ is written in function of them.

$$\widetilde{Q} = \frac{1}{2}\left(\lambda_3 - \frac{1}{\sqrt{3}}\lambda_8 - \frac{4}{\sqrt{6}}\lambda_{15}\right) + X, \tag{1}$$

where λ_3, λ_8 and λ_{15} are the diagonal Gell-Mann matrices of the group SU(4). Each value of β and γ lead to a model with different fermions field content.

(ii) The presence or absence of the exotic fermions (quarks and leptons) electric charge.

(iii) Moreover, we classify the 341 models according to the scalar sector content [1, 2].

The construction of any model beyond the SM must be free from the gauge anomalies [3], to ensure the cancellation of the $[SU(4)_L]^3$ anomaly (which requires that the number of multiplets lying in the fundamental representation 4 be the same as the number of anti quadruplets arranged in $\overline{4}$) in the 341 models, the three quarks generations have to be arranged in different representations: two of the three families with the three lepton generations lie in the fundamental representation 4, while, the third one have to arrange in the conjugate representation $\overline{4}$ (or vice versa). Table 1 represents the fermion content of the 341 models for generic β and γ.

2. The model

All the 341 model versions require that the quarks generations must be arranged in different representations in order to cancel the triangle gauge anomalies. It turns out that this scheme is not unique. The quarks families are arranged in the same representation while leptons are not, leading to a new version called the flipped 341 model. Table 2 shows the particle content in this model where we have used $\beta = \frac{1}{\sqrt{3}}$, $\gamma = \frac{-2}{\sqrt{6}}$ [1].

International Journal of Modern Physics A
Vol. 36, No. 16 (2021) 2150093 (17 pages)

DOI: 10.1142/S0217751X21500937

World Scientific
www.worldscientific.com

Theoretical constraints on scalar parameters in the compact 341 model

M. Djouala* and N. Mebarki†

Laboratoire de Physique Mathématique et Subatomique,
Frères Mentouri University, Constantine1, Algeria
**djoualameriem@gmail.com*
†*nnmebarki@yahoo.fr*

Received 30 December 2020
Revised 2 March 2021
Accepted 21 March 2021
Published 31 May 2021

Theoretical constraints on the scalar potential of the compact 341 model with three quadruplets scalar fields are discussed. It is shown that in order to ensure the good behavior of the potential and the viability of the model, the criteria, such as copositivity, minimization, perturbative unitarity, perturbativity of the scalar couplings and no ghost scalar bosons (scalar bosons masses positivity), are imposed and bounds on the scalar couplings are obtained. Moreover, the existence of the Landau pole in the model imposes stringent limits.

Keywords: BSM model; perturbative unitarity; boundedness from below; perturbativity; scalar masses; Landau pole.

PACS numbers: 12.60.−i, 12.90.+b

1. Introduction

Despite the success of the Standard Model, some fundamental questions such as matter–anti-matter asymmetry, CP violation, dark matter, etc. remain unsolved. Thus, going beyond the Standard Model becomes mandatory. Among the interesting proposed theories Beyond the Standard Model (BSM) is the so-called 341 model based on the Lie gauge group $SU(3)_C \otimes SU(4)_L \otimes U(1)_X$.[1–4] In the literature, there are many classifications of this model depending on the existence or not of fermions with exotic charges, structure of the scalar potential and spontaneous symmetry breaking of the gauge group. These models are usually parameterized by two parameters β and γ.[1,2,4,5] In this paper, we focus on the compact 341 model with exotic electric charges where $\beta = \frac{-1}{\sqrt{3}}$ and $\gamma = \frac{-4}{\sqrt{6}}$.[1,2] The most attractive

*Corresponding author.

International Journal of Modern Physics A
Vol. 36, No. 17 (2021) 2150101 (28 pages)

DOI: 10.1142/S0217751X21501013

World Scientific
www.worldscientific.com

A new anomaly-free flipped 341 model

M. Djouala*, N. Mebarki† and H. Aissaoui‡

Laboratoire de Physique Mathématique et Subatomique,
Frères Mentouri University, Constantine 1, Algeria
* *djoualameriem@gmail.com*
† *nnmebarki@yahoo.fr*
‡ *aissaoui_h@yahoo.com*

Received 23 December 2020
Revised 23 March 2021
Accepted 29 March 2021
Published 7 June 2021

A new flipped $\mathrm{SU}(3)_C \otimes SU(4)_L \otimes \mathrm{U}(1)_X$ model without exotic electric charges is proposed. All the quark families are arranged in the same representation while lepton generations are in different representations leading to a tree level FCNC. Moreover, it is shown that the cancellation of the triangle gauge anomalies requires new additional leptons a 10-plet and a quadruplet. All fermion masses have been also discussed. Furthermore, using the most recent experimental data of the branching ratios of $\mu \longrightarrow ee\overline{e}$ and $\mu \longrightarrow e\gamma$ rare decay modes, stringent bounds on the heavy neutral bosons masses and the muon-electron mixing matrix element are obtained.

Keywords: Beyond standard model; Gauge symmetry; neutrino physics.

PACS numbers: 12.60.−i, 14.60.Pq, 12.15.Ff

1. Introduction

Neutrinos oscillation phenomenon, dark matter, replication of quark families, charge quantization and many other fundamental questions reveal that the Standard Model (SM) is an effective gauge field theory. Thus, going beyond the Standard Model (BSM) becomes mandatory to explain these outstanding unsolved problems. In this paper, we are interested in a specific BSM model based on the Lie gauge group $\mathrm{SU}(3)_C \otimes \mathrm{SU}(4)_L \otimes \mathrm{U}(1)_X$ (denoted by 341 for short).[1–3] Much interest has been devoted to this kind of models especially those related to the LHC physics.[3–5] The most attractive feature of those models is the explanation of the family replication coming from the triangle gauge anomaly cancellation which together with QCD

*Corresponding author.

Bibliography

[1] W. Buchmüller and C. Lüdeling,*DESY-06-151* (2006), ArXiv: 0609174 [hep-ph].

[2] García Canal, C.A, *CERN Yellow Rep. School Proc.*, **4** 1–25 (2018).

[3] Boos, E., *10.5170/CERN-2015-004.1* ,1–64 (2015), 1608.02382[hep-ph].

[4] F. Englert and R. Brout, Phys. Rev. Lett. 13, 321 (1964).

[5] P. W. Higgs, Phys. Rev. Lett. 13, 508 (1964).

[6] G. S. Guralnik, C. R. Hagen and T. W. B. Kibble, Phys. Rev. Lett. 13, 585 (1964).

[7] ALEPH Collaboration, DELPHI Collaboration, L3 Collaboration, and OPAL Collaboration, *Physics Letters B* **565** (2003) 61-75.

[8] David Smith, *Third Latin American Symposium on High Energy Physics.*

[9] P. Teixeira-Dias, *J. Phys. Conf. Ser.*, **110**, 042030 (2008), arXiv:0804.4146 [hep-ex].

[10] Lidija Zivkovic, *FERMILAB-CONF-14-335-E*, 9 (2014), arXiv: 1409.4215 [hep-ph].

[11] Caterina Vernieri and CMS Collaboration, *Nuclear and Particle Physics Proceedings* **273-275**, 733-739 (2016).

[12] Particle Data Group: Review of searches for Higgs Bosons.

[13] CMS Collaboration, *Phys. Lett. B*, **716**, 30-61 (2012), arXiv: 1207.7235 [hep-ex].

[14] ATLAS Collaboration, *Phys. Lett. B*, **716**, 1–29 (2012), arXiv: 1207.7214[hep-ex].

[15] A. A.Migdal and A.M.Polyakov, *SOVIET PHYSICS JETP* **24**, 91 (1967).

[16] ATLAS Collaboration, G. Aad et al., *Phys. Lett. B* **716**, 1-29 (2012), ArXiv:1207.7214 [hep-ex].

[17] CMS Collaboration, S. Chatrchyan et al., *Phys. Lett. B* **716**, 30-61 (2012), ArXiv:1207.7235 [hep-ex]

[18] ATLAS Collaboration, *Observation of an excess of events in the search for the Standard Model Higgs boson in the gamma-gamma channel with the ATLAS detector*, July 2012.

[19] ATLAS Collaboration, *Observation of an excess of events in the search for the Standard Model Higgs boson in the $H \longrightarrow ZZ^{(*)} \longrightarrow 4\ell$ channel with the ATLAS detector*, July 2012.

[20] ATLAS Collaboration, *Phys. Lett. B* **716**, 1-29 (2012).

[21] ATLAS Collaboration, *Science* **338**, 6114 1576-158.

[22] ATLAS Collaboration, *JHEP***08**, 045 (2016).

[23] ATLAS and CMS Collaborations, *Phys. Rev. Lett.***114**, 191803 (2015), arXiv: 1503.07589 [hep-ex].

[24] The CMS Collaboration, *Phys. Rev. Lett. B***805**, 135425 (2020), arXiv: 2002.06398[hep-ex].

[25] Zyla, P.A. and others,*PTEP***2020**, 083C01 (2020).

[26] H. Haber, G. L. Kane, and T. Sterling, *Nucl.Phys. B***161**, 493 (1979).

[27] A. Arhrib, R. Benbrik, M. Chabab, G. Moultaka, M.C. Peyranere, L. Rahili, J.Ramadan, *Phys.Rev.D* **84**, 095005 (2011).

[28] R. Mohapatra and J. C. Pati, *Phys.Rev. D***11**, 2558 (1975).

[29] H. E. Haber and G. L. Kane, *Phys.Rept.* **117**, 75 (1985).

[30] C. S. Aulakh, A. Melfo, and G. Senjanovic, *Phys.Rev.D* **57**, 4174 (1998), arXiv:9707256 [hep-ph].

[31] F. Pisano and V. Pleitez, *Phys.Rev. D* **46**, 410 (1992), arXiv:hep-ph/9206242 [hep-ph].

[32] P. Frampton, *Phys.Rev.Lett.* **69**, 2889 (1992).

[33] Duong Van Loi, Phung Van Dong and Le Xuan Thuy, *JHEP*, **09**, 054 (2019), arXiv: 1906.10577 [hep-ph].

[34] P.V. Dong, H.N. Long, D.V. Soa and V. Vien, *Eur. Phys. J. C* **71**, 1544 (2011).

[35] R. Foot, H. N. Long and T. A. Tran, *Phys. Rev. D* **50**, 34-38 (1994), arXiv:9402243 [hep-ph].

[36] Guillermo Palacio, *Int. J. Mod. Phys. A*, **31**, 1650142 (2016), arXiv: 1608.08676[hep-ph].

[37] F. Pisano and V. Pleitez, *Phys. Rev. D***51**, 3865–3869 (1994), ArXiv:9401272[hep-ph].

[38] A. G. Dias, P. R. D. Pinheirob, C. A. de S. Pires and P. S. Rodrigues da Silva, *Ann.Phys.* **349**, 232 (2014), arXiv:1309.6644 [hep-ph].

[39] N. Mebarki, M. Djouala, J. Mimouni, and H. Aissaoui, *J. Phys. Conf. Ser.*, **1258**, 012011 (2019), ArXiv: 2009.04242 [hep-ph].

[40] N. Arkani-Hamed, A. G. Cohen, and H. Georgi, *Phys.Lett. B***513**, 232 (2001), arXiv:hep-ph/0105239 [hep-ph].

[41] N. Arkani-Hamed, A. Cohen, E. Katz, and A. Nelson, *JHEP* **0207**, 034 (2002), ArXiv:hep-ph/0206021 [hep-ph].

[42] L. Randall and R. Sundrum, *Phys.Rev.Lett.***83**, 3370 (1999), ArXiv:hep-ph/9905221 [hep-ph].

[43] A. Palcu, *Mod. Phys. Lett. A* **24**, 1731 (2009), ArXiv:0902.1828 [hep-ph].

[44] A.Jaramiloo and L.A.Sanchez, *Phys.Rev D.***84**.115001, (2011) ArXiv:1110.3363 [hep-ph].

[45] J.M.Cabarcas and J.A.Rodriguez, *Mod. Phys. Lett.A* **29**, 1450032 (2014), ArXiv:1303.5332 [hep-ph].

[46] William A. Ponce and Luis A. Sanchez, *Int. J. Mod. Phys. A* **22**, 435-447 (2007), ArXiv:0607175 [hep-ph].

[47] A. Salam, *Elementary Particle Theory*, eds.: Svartholm, Almquist and Wiksells, Stockholm, 1968; S. L. Glashow, J. Iliopoulos and L. Maiani, *Phys. Rev. D***2**, 1285 (1970).

[48] S. Glashow, *Nucl. Phys.* **22**, 579 (1961)..

[49] S. Weinberg, *Phys.Rev.Lett.***19**, 1264-1266 (1967).

[50] A. Salam, Proceedings of the Eighth Nobel Symposium, N. Svartholm, 367-377. Almqvist and Wiksell, (1968).

[51] M. Gell-Mann, *Phys. Lett.***8** (1964) 214.

[52] G. Zweig, CERN-Report 8182/TH401 (1964).

[53] H. Fritzsch, M. Gell-Mann and H. Leutwyler, *Phys. Lett. B***47**, 365 (1973).

[54] D. Gross and F. Wilczek, *Phys. Rev. Lett.***30**, 1343 (1973).

[55] H.D. Politzer, *Phys. Rev. Lett.***30**, 1346 (1973).

[56] G.'t Hooft, Marseille Conference on Yang-Mills fields (1972).

[57] G. Zweig, CERN-TH-412, NP-14146 (1964) .

[58] J. Bjorken, *Phys.Rev.* **179**, 1547-1553 (1969).

[59] R. P. Feynman, *Phys.Rev.Lett.***23**, 1415-1417 (1969).

[60] D. Gross and F. Wilczek, *Phys.Rev.Lett.***30**, 1343-1346 (1973).

[61] H. D. Politzer, *Phys.Rev.Lett.* **30**, 1346-1349 (1973).

[62] O. Greenberg, *Phys.Rev.Lett.***13** (1964) 598-602.

[63] M. Han and Y. Nambu, *Phys.Rev.***139**, B1006-B1010 (1965).

[64] H. Georgi and H. D. Politzer, *Phys.Rev. D***9**,416-420 (1974).
Prog. Theor. Exp. Phys. 2020, 083C01 (2020) and 2021 update.

[65] UA1 Collaboration, G. Arnison et al., *Phys.Lett. B***122**,103-116 (1983).

[66] F. Halzen and A. D. Martin. Quarks and leptons. Wiley, (1984).

[67] C.-N. Yang and R. L. Mills, *Phys.Rev.* **96**,191-195 (1954).

[68] N. Cabibbo , *Phys. Rev. Lett.***10**, 531-533 (1963).

[69] M. Kobayashi and T. Maskawa. CP-violation in the renormalizable theory of weak interaction 1973.

[70] Nicolas MERIC, *Etude théorique et expérimentale des corrections électrofaibles au processus de production inclusive de jets Développement de méthodes de détection de topologies extrèmes*, https://tel.archives-ouvertes.fr/tel-00959427.

[71] Zhi-zhong Xing,*Nuclear Physics B* (Proc. Suppl.) 203-204 (2010) 82-117.

[72] S. Weinberg, *Phys.Rev.Lett.***43** 1566-1570 (1979).

[73] A. Zee, *Phys.Lett. B***93**, 389 (1980).

[74] A. Zee, *Nucl.Phys. B***264**, 99 (1986).

[75] K. Babu, *Phys.Lett. B***203**, 132 (1988).

[76] G. Branco, W. Grimus, and L. Lavoura,*Nucl.Phys. B***312**,492 (1989).

[77] Renato Miguel Sousa da Fonseca, *Renormalization in supersymmetric models*, ArXiv:1310.1296 [hep-ph].

[78] R. Mohapatra and J. Valle, *Phys.Rev. D***34**,1642(1986).

[79] M. Malinský, J. C. Romão, and J. W. F. Valle, *Phys.Rev.Lett.***95**,161801 (2005), ArXiv:hep-ph/0506296 [hep-ph].

[80] Yao Y. P. and Yuan C. P., *Phys. Rev. D***38**, 2237 (1988); Veltman H. G. J., *Phys. Rev. D* **41**, 2294 (1990); He H. J. et al.,*Phys. Rev. Lett.***69**, 2619 (1992).

[81] M.Djouala and N.Mebarki, *Int.J. Mod. Phys. A* **36**, 2150093 (2021), ArXiv:2002.08758[hep-ph]

[82] A. Arhrib, R. Benbrik, M. EL Kacimi, L. Rahili, and S. Semlali, *Eur.Phys.J.C* **80**,13 (2020).

[83] J. Chakrabortty, J. Gluza, T. Jelinski, T. Srivastava, *Phys.Lett. B***759**,361-368 (2016).

[84] A.Arhrib in Workshop on Noncommutative Geometry, Superstrings and Particle Physics (2000),ArXiv:0012353v1 [hep-ph].

[85] Abdelhak DJOUADI, *Phys. Rept.***457**, 1–216, ArXiv: 0503172[hep-ph].

[86] Purusottam Ghosh, Abhijit Kumar Saha, Arunansu Sil, *Phys.Rev. D***97**,075034 (2018).

[87] J. Horejsi and M. Kladiva, *Eur. Phys. J.C* **46**, 81 (2006), ArXiv:0510154 [hep-ph].

[88] G. Bhattacharyya and D. Das, Pramana, *JHEP* **87**, 40 (2016).

[89] Ivan Angelozzi,Part of the Lecture Particle Physics II, UvA Particle Physics Master 2013-2014.

[90] H. Arason, D. J. Castano, B. Keszthelyi, S. Mikaelian, E. J. Piard, P. Ramond and B. D. Wright, Phys. Rev. D 46, 3945 (1992).

[91] The ATLAS and CMS Collaborations,, *ATLAS-CONF***044** (2015).

[92] Chiara Mariotti,*Int. J. Mod. Phys. A***32**, 1730003 (2017), ArXiv:1612.00269[hep-ph].

[93] Rodolfo A. Diaz, R. Martinez, F. Ochoa *Phys.Rev.D* **72**, 035018(2005), ArXiv:0411263[hep-ph].

[94] H.N.Long, L.T.Hue and D.V.Loi, *Phys.Rev.D* **94**, 015007 (2016), ArXiv:1605.07835[hep-ph].

[95] W. A. Ponce and L. A. Sanchez, *Mod. Phys. Lett. A* **22**, 435 (2007), ArXiv: 0607175 [hep-ph].

[96] F.Pisano and V.Pleitez, *Phys.Rev. D***51**, 3865(1995), ArXiv:9401272[hep-ph].

[97] J. Beringer et al., *Phys. Rev. D* **86**,010001 (2012) .

[98] The ATLAS and CMS Collaborations, *JHEP* **08** 045 (2016), ArXiv: 1606.02266[hep-ex].

[99] S. Dittmaier et al.,CERN-2011-002 (2011), ArXiv:1101.0593 [hep-ph].

[100] The ATLAS Collaboration, *Phys. Rev. D* **111** 012002 (2020), ArXiv: 1909.02845[hep-ex].

[101] Amit Adhikary, Shankha Banerjee, Rahool Kumar Barman, Biplob Bhattacherjee and Saurabh Niyogi, *JHEP* **07**, 116 (2018), ArXiv: 1712.05346[hep-ph].

[102] Cao, Qing-Hong and Li, Gang and Yan, Bin and Zhang, Dong-Ming and Zhang, Hao, *Phys. Rev. D* **96** 095031 (2017), ArXiv: 1611.09336 [hep-ph].

[103] R. M.Fonseca and M. Hirsch, *JHEP* **08**, 003 (2016), Arxiv:1606.01109 [hep-ph].

[104] M.Djouala and N.Mebarki, *J. Phys. Conf. Ser.***1766**, 012016 (2021).

[105] M.Djouala, N.Mebarki and H.Aissaoui,*Int. J. Mod. Phys. A* **36**, 2150101 (2021), ArXiv:1911.04887 [hep-ph].

[106] R.M.Fonseca, and M.Hirsch, *Phys. Rev. D***94**, 115003, (2016), ArXiv:1607.06328[hep-ph].

[107] N.Yamatsu, ArXiv:1511.08771 [hep-ph].

[108] S. Descotes-Genon, M. Moscati and G. Ricciardi, *Phys.Rev. D* **98**, 115030 (2018), ArXiv:1711.03101[hep-ph].

[109] Riazuddin and Fayyazuddin, *Eur. Phys.J.C*, **56**, 389–394 (2008), ArXiv:0803.4267[hep-ph].

[110] K.Hutchu and N.Korvunin, *JHEP* **10** (2019), 065, arXiv:1905.05278v2[hep-ph].

[111] A.Panuela and A.Pich, JHEP **12**, 084 (2017), arXiv:1710.02040 [hep-ph].

[112] D.T.Huong, D.N.Dinh, L.D.Thien, and P.Van Dong, *JHEP* **08**, 051 (2019), arXiv:1906.05240 [hep-ph].

[113] Duong Van Loi and Phung Van Dong, *JHEP* **09**, 054 (2019), arXiv:1906.10577 [hep-ph].

[114] R.Mohanta, *Eur.Phys.J.C* **71**, 1625 (2011), arXiv:1011.4184[hep-ph].

[115] M. Tanabashi et al., *Phys. Rev. D* **98**, 030001 (2018).

[116] Mahmoud A. A. Sbaih., Moeen KH. Srour, M. S. Hamada and H. M. Fayad,*EJTP***10**, 28 (2013).

[117] Marina von Steinkirch , *Introduction to Group Theory for Physicists*, 12, 2011.

[118] Robert Feger and Thomas W. Kephart, ArXiv:1206.6379 [hep-ph].

فيزياء ماوراء النموذج العياري

مريم جواله

ملخـــص

أصبح ما وراء النموذج العياري (BSM) إلزاميًا لشرح العديد من المشاكل العالقة في النموذج العياري (SM). من بين نظريات ما وراء النموذج العياري، نهتم بتمديد مجموعة قياس $SU(3)_C \otimes SU(2)_L \otimes U(1)_Y$ إلى $SU(3)_C \otimes SU(4)_L \otimes U(1)_X$ مايسمى بنماذج 341. الميزة الأكثر جاذبية لهذه النماذج هي تفسير النسخ المتماثل للعائلة الذي يأتي من إلغاء الشذوذ في مقياس المثلث والذي يتطلب أن تنتمي أجيال الكواركات الثلاثة إلى تمثيلات مختلفة من $SU(4)_L$: اثنان مع تناظر أعسر Q_{iL} يكمن في التمثيل الأساسي 4، بينما يجب أن يتم التحويل في التمثيل الأساسي الثالث Q_{3L} مع الأجيال الثلاثة من اللبتونات $\psi_{\ell L}$ تحت التمثيل الأساسي المقترن $\bar{4}$ (أو العكس).

في هذه الأطروحة، أظهرنا إصدارات مختلفة من هذه النماذج والتي تتميز بكل جيل من ليبتون بتمثيل مختلف تحت مجموعة المقاييس. في النسخة المدمجة، ندرس البوزونات العددية المحايدة من خلال دراسة الأنماط المختلفة للبوزونات العددية المحايدة. حيث قمنا بتقييد المعلمات العددية غير المعروفة باستخدام قيد الوحدوية، قيد البداهة و قيد الاستقرار. علاوة على ذلك، استنتجنا شروطًا أخرى تأتي من إيجابية كتل البوزونات العددية مع الحالة الصارمة لقطب لانداو. اتضح أن تكرار هذه الكواركات واللبتونات ليس الطريقة الوحيدة للحصول على نموذج خالٍ من شذوذ المقياس $SU(4)_L \otimes U(1)_X$ ، بناءً على ذلك نقدم نموذجًا جديدًا فريدًا من نوعه خالٍ من الشذوذ بدون شحنات كهربائية غريبة النموذج المقلوب 341 كإمتداد عكس مخطط البناء السابق، أي أن جميع أجيال الكواركات تتحول تحت نفس التمثيل بينما اللبتونات ليست كذلك وبالتالي، من المتوقع وجود تيار محايد متغير النكهة (FCNC) على مستوى الشجرة في قطاع ليبتون من خلال تبادل بوزونات قياس محايدة جديدة Z' و Z''. باستخدام الحدود التجريبية للنسب المتفرعة لاثنين من النتوءات اللبتونية النادرة، يتم الحصول على حد أعلى لنكهة اللبتون التي تنتهك عنصر المصفوفة $|U_{e\mu}|$ بالإضافة إلى القابض المرتبط على كتل البوزونات المقيسة المحايدة.

الكلمات المفتاحية : ما وراء النموذج العياري؛ فيزياء الهيغز؛ قيد البداهة؛ قيد الاستقرار؛ قيد الوحدوية؛ قطب لانداو؛ تناظر المقياس؛ فيزياء النترونات.

La physique au-delà du modèle Standard
Djouala Meriem

Résumé

Au-delà du modèle standard (BSM) devient obligatoire pour expliquer de nombreux problèmes non résolus. Parmi des théories au-delà du modèle standard, nous nous intéressons à l'extension du groupe de jauges du SM $SU(3)_C \otimes SU(2)_L \otimes U(1)_Y$ à $SU(3)_C \otimes SU(4)_L \otimes U(1)_X$ (les modèles 341). La caractéristique la plus intéressante de ces modèles est l'explication de la réplication de la famille issue de l'annulation d'anomalie de jauge triangulaire qui nécessite que les trois générations de quarks appartiennent à des représentations $SU(4)_L$ différentes: deux avec un la chiralité gauchère Q_{iL} se situe dans la représentation fondamentale 4, alors que la troisième Q_{3L} avec les trois générations de leptons $\psi_{\ell L}$ doivent se transformer sous la représentation conjugué $\bar{4}$ (ou vice versa).

Dans cette thèse, nous avons montré différentes versions de ces modèles qui sont caractérisées par chaque génération de leptons ayant une représentation différente sous le groupe de jauge. Dans le compact version, nous avons étudié les désintégrations des bosons scalaires neutres à travers l'étude des différents modes des bosons scalaires neutres. où nous avons contraint les paramètres scalaires inconnus en utilisant la stabilité, la minimisation du potentiel scalaire et la perturbativité des couplages de potentiel scalaire. De plus, nous avons dérivé d'autres conditions qui proviennent de la positivité des masses de bosons scalaires avec la condition stricte de la Landau pole. Il s'avère que cette réplication des quarks et leptons n'est pas le seul moyen de avoir un modèle exempt d'anomalies de jauge $SU(4)_L \otimes U(1)_X$, basé sur celui que nous avons introduit un nouveau modèle unique sans anomalie de jauge sans charges électriques exotiques baptisé le modèle flipped 341 comme une extension de l'endroit où le schéma de construction précédent est inversé, c'est-à-dire toutes les générations de quarks se transforment sous la même représentation alors que les leptons ne le sont pas. Ainsi, un courant neutre (FCNC) est attendu au niveau de l'arbre dans le secteur leptonique par l'échange de nouveaux bosons de jauge neutre Z' et Z''. Utilisant les limites expérimentaux des deux rares désintégrations leptoniques une limite supérieure de $|U_{e\mu}|$ ainsi qu'une borne stricte sur les bosons de jauge neutre des masses sont obtenues.

Mots clés: Au-delà du modèle standard; physique de Higgs; unitarité; perturbativité; masses scalaires; Pôle de Landau; symétrie de jauge; physique des neutrinos.

Physics Beyond the Standard Model
Djouala Meriem

Abstract

Going Beyond the Standard Model (BSM) becomes mandatory to explain many outstanding unsolved problems. Among of many theories beyond the Standard Model, we are interested in the extension of the SM $SU(3)_C \otimes SU(2)_L \otimes U(1)_Y$ gauge group to $SU(3)_C \otimes SU(4)_L \otimes U(1)_X$ the so called 341 models. The most attractive feature of those models is the explanation of the family replication coming from the triangle gauge anomaly cancellation which requires that the three quark generations belong to different $SU(4)_L$ representations: two with a left handed chirality Q_{iL} lie in the fundamental representation 4, whereas , the third one Q_{3L} together with the three lepton generations $\psi_{\ell L}$ have to transform under the conjugate fundamental representation $\bar{4}$ (or vice versa).

In this thesis, we showed various versions of these models which are characterized by each lepton generation having a different representation under the gauge group. In the compact version, we studied the neutral scalar bosons decays through the study of the various modes of the neutral scalar bosons. where we have constrained the unknown scalar parameters using the vacuum stability, minimization of the scalar potential, perturbative unitarity bounds and perturbativity of the scalar potential couplings. Moreover, we derived other conditions that come from the positivity of the scalar bosons masses with the stringent condition of the Landau pole. It turns out that this quarks and leptons replication is not the only way to have a model free from the $SU(4)_L \otimes U(1)_X$ gauge anomalies, based on that we introduced a new unique gauge anomaly free model without exotic electric charges baptized the flipped 341 model as an extension of where the previous scheme of construction is reversed that is all the quarks generations transform under the same representation while leptons are not. Thus, a flavor changing neutral current (FCNC) is expected at the tree level in the lepton sector through the exchange of new neutral gauge bosons Z' and Z''. Using the experimental bounds of the branching ratios of the two rare leptonic decays an upper limit on the lepton flavor violating matrix element $|U_{e\mu}|$ as well as a stringent bound on the neutral gauge bosons masses are obtained.

Keywords: Beyond Standard Model; Higgs physics; perturbative unitarity; boundedness from below; perturbativity; scalar masses; Landau pole; gauge symmetry; neutrino physics

Abstract

Going beyond the Standard Model (BSM) becomes mandatory to explain many outstanding unsolved problems. Among of many theories beyond the Standard Model, we are interested in the extension of the SM $SU(3)_C \otimes SU(2)_L \otimes U(1)_Y$ gauge group to $SU(3)_C \otimes SU(4)_L \otimes U(1)_X$ the so called 341 models. The most attractive feature of those models is the explanation of the family replication coming from the triangle gauge anomaly cancellation which requires that the three quark generations belong to different $SU(4)_L$ representations: two with a left handed chirality Q_{iL} lie in the fundamental representation 4, whereas , the third one Q_{3L} together with the three lepton generations $\psi_{\ell L}$ have to transform under the conjugate fundamental representation $\bar{4}$ (or vice versa).

In this thesis, we showed various versions of these models which are characterized by each lepton generation having a different representation under the gauge group. In the compact version, we studied the neutral scalar bosons decays through the study of the various modes of the neutral scalar bosons. where we have constrained the unknown scalar parameters using the vacuum stability, minimization of the scalar potential, perturbative unitarity bounds and perturbativity of the scalar potential couplings. Moreover, we derived other conditions that come from the positivity of the scalar bosons masses with the stringent condition of the Landau pole. It turns out that this quarks and leptons replication is not the only way to have a model free from the $SU(4)_L \otimes U(1)_X$ gauge anomalies, based on that we introduced a new unique gauge anomaly free model without exotic electric charges baptized the flipped 341 model as an extension of where the previous scheme of construction is reversed that is all the quarks generations transform under the same representation while leptons are not. Thus, a flavor changing neutral current (FCNC) is expected at the tree level in the lepton sector through the exchange of new neutral gauge bosons Z' and Z''. Using the experimental bounds of the branching ratios of the two rare leptonic decays an upper limit on the lepton flavor violating matrix element $|U_{e\mu}|$ as well as a stringent bound on the neutral gauge bosons masses are obtained.

Keywords: Beyond Standard Model; Higgs physics; perturbative unitarity; boundedness from below; perturbativity; scalar masses; Landau pole; gauge symmetry; neutrino physics.